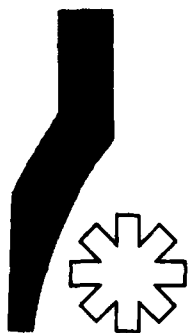


AFOSR-TR: 84-1114

⑤

Rocket Propulsion
Research Meeting

AD-A148 818



1984 AFOSR/AFRPL Rocket Propulsion Research Meeting

12-15 March 1984

Abstracts and Agenda

Approved for release:
distribution unlimited.

DTIC FILE COPY

Lancaster, California

84 12 17 062

DTIC
ELECTE
DEC 28 1984
S A D

DISCLAIMER NOTICE

**THIS DOCUMENT IS BEST QUALITY
PRACTICABLE. THE COPY FURNISHED
TO DTIC CONTAINED A SIGNIFICANT
NUMBER OF PAGES WHICH DO NOT
REPRODUCE LEGIBLY.**

UNCLASSIFIED

SECURITY CLASSIFICATION OF THIS PAGE

REPORT DOCUMENTATION PAGE

1a. REPORT SECURITY CLASSIFICATION Unclassified		1b. RESTRICTIVE MARKINGS	
2a. SECURITY CLASSIFICATION AUTHORITY		3. DISTRIBUTION/AVAILABILITY OF REPORT Approved for public release; distribution unlimited.	
2b. DECLASSIFICATION/DOWNGRADING SCHEDULE		5. MONITORING ORGANIZATION REPORT NUMBER(S) AFOSR-TR. 04-1114	
4. PERFORMING ORGANIZATION REPORT NUMBER(S)		7a. NAME OF MONITORING ORGANIZATION AFOSR/NA	
6a. NAME OF PERFORMING ORGANIZATION AIR FORCE OFFICE OF SCIENTIFIC RESEARCH	6b. OFFICE SYMBOL (If applicable) NA	7b. ADDRESS (City, State and ZIP Code) Bolling AFB, DC 20332	
6c. ADDRESS (City, State and ZIP Code) BOLLING AFB, DC 20332		9. PROCUREMENT INSTRUMENT IDENTIFICATION NUMBER In-House	
8a. NAME OF FUNDING/SPONSORING ORGANIZATION Same as #7	8b. OFFICE SYMBOL (If applicable)	10. SOURCE OF FUNDING NOS.	
8c. ADDRESS (City, State and ZIP Code)		PROGRAM ELEMENT NO. 61102F	PROJECT NO. 2308 2307; 2303
11. TITLE (Include Security Classification) AFOSR/AFRPL ROCKET RESEARCH MEETING - 1984		TASK NO. A1, A3, M1, M2, M3 M1; M1	WORK UNIT NO.
12. PERSONAL AUTHOR(S) /Editor(s) LEONARD H CAVENY ROBERT A BIGGERS*			
13a. TYPE OF REPORT INTERIM	13b. TIME COVERED FROM MAR 83 TO FEB 84	14. DATE OF REPORT (Yr., Mo., Day) 1984, February	15. PAGE COUNT 206
16. SUPPLEMENTARY NOTATION *Air Force Rocket Propulsion Laboratory Edwards AFB, CA 93534			
17. COSATI CODES		18. SUBJECT TERMS (Continue on reverse if necessary and identify by block number)	
FIELD	GROUP	ROCKETS PROPELLANTS	
		COMBUSTION CHEMICAL KINETICS	
		ENERGETIC MATERIALS THERMAL PROPERTIES	
19. ABSTRACT (Continue on reverse if necessary and identify by block number) This document contains expanded abstracts from the Air Force basic research program on rocket propulsion. The document contains the agenda for the Rocket Research Meeting held at Lancaster, CA on 12-15 March 1984. Major topics include: energetic material combustion, metal combustion, diagnostics of reacting flow, chemical kinetics, thermal properties, synthesis of new ingredients, combustion stability, acoustic interaction, plumes, beamed energy, solar propulsion, and electrical propulsion.			
20. DISTRIBUTION/AVAILABILITY OF ABSTRACT UNCLASSIFIED/UNLIMITED <input checked="" type="checkbox"/> SAME AS RPT. <input type="checkbox"/> DTIC USERS <input type="checkbox"/>		21. ABSTRACT SECURITY CLASSIFICATION UNCLASSIFIED	
22a. NAME OF RESPONSIBLE INDIVIDUAL Leonard H Caveny		22b. TELEPHONE NUMBER (Include Area Code) (202) 767-4937	22c. OFFICE SYMBOL AFOSR/NA

UNCLASSIFIED

SECURITY CLASSIFICATION OF THIS PAGE

18. SUBJECT TERMS (Cont)

EXHAUST PLUMES
COMBUSTION STABILITY
ACOUSTICS
STRUCTURAL MECHANICS

LASER HEATING
ELECTRIC PROPULSION
BEAMED ENERGY

UNCLASSIFIED

SECURITY CLASSIFICATION OF THIS PAGE

Table of Contents

Form 1473	i
Table of Contents	iii
Preface	iv
Agenda Summary	v
Agenda		

Abstracts

Appendix 1 Propulsion Research Goals

Index to Abstracts, Investigators, and Presentations

[illegible]

AIR FORCE
NOTICE
THE
L
MAY
Chief, Technical Information Division



PREFACE

This document serves dual purposes: (1) provides a status report on the Air Force's basic research program on rocket propulsion and (2) is the program for the contractors' meeting on rocket research.

Most of the abstracts follow a specific format. The text begins with a short statement of relevant scientific questions addressed by the research, followed by an explanation of the scientific approach. A statement of the uniqueness of each approach was solicited from the investigators. The major portion of the text describes the results obtained during the last twelve months. The abstracts should describe two figures: Figure 1 illustrates the main (or a representative) feature of the scientific approach and Figure 2 presents a primary accomplishment.

Hard copies of the vugraph material and collateral information are in file folders (one for each presentation) on a table at the rear of the meeting room.

Since the research on combustion instability and advanced ingredients have had adequate national forums in recent months, that research will be presented in the March 1985 Rocket Research Meeting. The abstracts of that research are included in this booklet. The research on advanced diagnostics of reacting flow is the subject of a separate meeting and abstract booklet.

A primary objective of the meeting and this booklet is to encourage the participants to interpret the technological barriers and to consider new research approaches. Since a 25 to 30 percent annual turn-over is built into the program, each year opportunities exist for new research approaches and for new principal investigators. Several of the presentations provide introductions to some of the barriers and technological challenges. Prospective principal investigators should not feel constrained by these presentations and are encouraged to look beyond the identified items. The location of the meeting (i.e., near organizations interested in the research) promotes interchanges among the investigators and those responsible for Air Force programs. Accordingly, many of the participants will be able to provide specific information on Air Force requirements. Questions concerning the meeting can be directed to either:

Leonard H Caveny
AFOSR/NA
Bolling AFB
Washington, DC 20332
Phn: (202) 767-4937
Autovon: 297-4937

or

Robert A Biggers
AFRPL/XRX
Edwards AFB, CA 93534
Phn: (805) 277-5206
Autovon: 350-5206

AGENDA SUMMARY

1984 AFOSR/AFRPL ROCKET RESEARCH MEETING

March 12 - Monday

0730 Registration
0820 Announcements
0800 Materials and Structural Mechanics
1030-1200 Combustion
1300-1430 Combustion (continued)
1500-1630 Exhaust Plumes
1630 Discussion Symposia (Snacks and Cash Bar) - Essex House

March 13 - Tuesday

0730 Registration
0800-1130 Metallized Propellants
1300 Announcements
1305 WELCOME by Don A Hart, Director, AFRPL
1315 Overview - Air Force Rocket Propulsion,
Richard R Weiss, Chief Scientist, AFRPL
1415 AFOSR Interests in Rocket Propulsion, Leonard H Caveny, AFOSR
1445 AFRPL Research Interests in Propulsion, Robert A Biggers, AFRPL
1530 Shuttle Based Experiments, William Oran and Thomas Labus, NASA
1545 Thermodynamics and Kinetics
1645-1715 Administrative Meeting for AFOSR Contractors
1645 Discussion Symposia (Snacks and Cash Bar) - Essex House

March 14 - Wednesday

0730 Late Registration
0800-1200 Beamed Energy in Flowing Media
1330-1700 Electromagnetic Acceleration of Plasmas
1700 Discussion Symposia (Snacks and Cash Bar) - Essex House

March 15 - Thursday

0800-1200 Energy Conversion
0830 NASA Sponsored Research on Nonconventional Propulsion,
Thomas H Cochran and David C Byers, NASA
1300 Working Sessions
1500 Adjourn Meeting

1984 AFOSR/AFRPL ROCKET RESEARCH MEETING

Essex House, Lancaster, CA

MONDAY (AM)

12 March 1984

0730 Registration

0820 Announcements

Session Chairman: Durwood I Thrasher, AFRPL/MKPB

Topic: Materials and Structural Mechanics

TIME NUM.

0830 1 CARBON-CARBON PROCESSING VARIABLES. W P Hoffman, AFRPL/MKBN

0900 2 STATISTICAL NATURE OF CRACK GROWTH IN SOLID PROPELLANTS. Chi T (Jimmie) Liu, AFRPL/MKPB

0930 3 PROPELLANT NONLINEAR CONSTITUTIVE THEORY EXTENSION. Gene Francis, Chemical Systems Division, United Technologies, Sunnyvale, CA

1000 4 PROPELLANT AGING RESEARCH. Douglas B Olsen, Aerochem Research Laboratories, Inc, Princeton, NJ (New Start)

1015 Break

Session Chairman: Jay N Levine, AFRPL/DYC

Topic: Combustion

1030 5 MECHANISMS FOR ACOUSTIC SUPPRESSION. Merrill W Beckstead, R I Raun, and P C Braithwaite, Brigham Young University, Provo, UT

1100 6 COMBUSTION MECHANISMS. David P Weaver and J T Edwards, AFRPL/DYP David H Campbell and Susan C Hulsizer, University of Dayton Research Institute

1130 7 THERMOPHYSICAL PROPERTY DETERMINATIONS USING TRANSIENT TECHNIQUES. Raymond E Taylor, Purdue University, West Lafayette, IN

1200 Lunch (Reconvene at 1300)

MONDAY (PM)

12 MARCH 1984

Session Chairman: Jay N Levine, AFRPL/DYC

Topic: Combustion (continued)

TIME NUM.

1300 8 CHEMICAL KINETICS OF NITRAMINE PROPELLANT COMBUSTION. Melvyn C Branch, University of Colorado, Boulder, CO (New Start)

1330 9 RAPID SCAN FTIR SPECTROSCOPY OF NITRAMINES. Thomas B. Brill, Richard J Karpowicz, and Yoshio Oyumi, University of Delaware, Newark, DE

1400 10 SOLID PROPELLANT TRANSIENT RESPONSES. Robert L Glick, Purdue University, West Lafayette, IN

11 *FUEL RICH PROPELLANT COMBUSTION BEHIND A BLUFF BODY. Warren C Strahle and Jechiel (Jeff) I Jagoda, Georgia Institute of Technology, Atlanta, GA

1430 Break

Session Chairman: David P Weaver, AFRPL/DYP

Topic: Exhaust Plumes

1500 12 SUPPRESSION OF AFTERBURNING IN SOLID ROCKET PLUMES BY POTASSIUM SALTS. Eugene Miller, University of Nevada, Reno, NV (New Start)

1530 13 AFTERBURNING SUPPRESSION KINETICS. Jay D Eversole, University of Dayton Research Institute

1600 14 COMBUSTION KINETICS OF METAL OXIDE AND HALIDE RADICALS. Arthur Fontijn, Rensselaer Polytechnic Institute, Troy, NY

1630 ADJOURN SESSION

1630 Discussion Symposia (Snacks, soft drinks, cash bar) - Essex House

*Abstract only, no presentation.

TUESDAY (AM)

13 March 1984

0730 Registration

Session Chairman: Wayne E Roe, AFRPL/DYC

Topic: Metalized Propellants

TIME	NUM.	
0800	15	WIDE DISTRIBUTION PROPELLANTS. Robert A Frederick, John C Matson, and John R Osborn, Purdue University, West Lafayette, IN
0830	16	BEHAVIOR OF ALUMINUM IN SOLID PROPELLANT COMBUSTION. Edward W Price and Robert K Sigman, Georgia Institute of Technology, Atlanta, GA
0900	17	AERODYNAMIC BREAKUP - METAL DROPLETS. James E Craig, Spectron Development Laboratory, Costa Mesa, CA
0930	18	AGGLOMERATE BREAKUP CONTROL. Kevin K Nack, AFRPL/DYC
0945		Break
1030	19	PULSED-LASER CINEMATOGRAPHY OF PROPELLANT DEFLAGRATION. Roger Becker, Univ of Dayton Research Institute.
1100	20	HOLOGRAPHIC DATA RETRIEVAL. David Netzer, U S Naval Postgraduate School, Monterey, CA
	21	*FUJI-RICH SOLID PROPELLANT BORON COMBUSTION (ANALYSIS). Merrill King, Atlantic Research Corp, Alexandria, VA
	22	*FUJI-RICH SOLID PROPELLANT BORON COMBUSTION (EXPERIMENT). James J Komar and Ronald S Fry, Atlantic Research Corp, Alexandria, VA
1130		Lunch (Reconvene at 1300)

*Abstract only, no presentation.

1984 AFOSR/AFRPL CHEMICAL ROCKET RESEARCH MEETING

Essex House, Lancaster, CA

TUESDAY (PM)

13 March 1984

Session Chairman: Leonard H Caveny, AFOSR/NA

TIME NUM.

- 1300 Announcements
- 1305 WELCOME: Don A Hart, Director, AFRPL/CC
- 1315 OVERVIEW: AIR FORCE ROCKET PROPULSION. Richard R. Weiss, Chief
Scientist, AFRPL
- 1415 23 OVERVIEW: AFOSR INTEREST IN ROCKET PROPULSION. Leonard H Caveny,
AFOSR/NA.
- 1445 OVERVIEW: AFRPL RESEARCH INTERESTS IN ROCKET PROPULSION. Robert
A Biggers, AFRPL/XRX
- 1500 Break
- 1530 Invited: SHUTTLE BASED COMBUSTION EXPERIMENTS. William Oran,
NASA Washington, DC and Thomas Labus, NASA Lewis Research Center,
Cleveland, OH

Topic: Thermodynamics and Kinetics

- 1545 24 CRITICAL EVALUATION AND COMPILATION OF THE THERMODYNAMIC
PROPERTIES OF HIGH TEMPERATURE SPECIES. Malcom W Chase, The Dow
Chemical Company, Midland, MI
- 1615 25 CRITICAL EVALUATION OF HIGH TEMPERATURE CHEMICAL KINETIC DATA.
Norman Cohen and Karl Westberg, Aerospace Corporation, Los
Angeles, CA
- 1645 ADJOURN SESSION
- 1645-1715 ADMINISTRATIVE MEETING FOR AFOSR CONTRACTORS ONLY
- 1645 Discussion Symposia (Snacks, soft drinks, cash bar) - Essex House

WEDNESDAY (AM)

14 March 1984

NONCONVENTIONAL PROPULSION

0730 Registration

Session Chairman: Clark Hawk, AFRPL/LK

Topic: Beamed Energy to Flowing Media

TIME NUM.

- 0800 26 LASER THERMAL PROPULSION. Dennis Keefer, University of Tennessee Space Institute, Tullahoma, TN
- 0830 27 LASER-INDUCED GAS BREAKDOWN IN THE VISIBLE/UV. David I Rosen and Guy M Weyl, Physical Sciences Inc, Andover, MA
- 0900 28 HIGH TEMPERATURE MOLECULAR ABSORBERS FOR CW LASER PROPULSION. David O Rosen, David O Ham, and Lauren M Cowles, Physical Sciences Inc, Andover, MA
- 0930 Break
- 1000 29 PROPAGATION OF LASER SUPPORTED PLASMAS IN FLOWING MEDIA. Charles L Merkle and Thomas M York, The Pennsylvania State University, University Park, PA
- 30 HIGH POWER Nd-GLASS LASER INSTRUMENT FOR ADVANCED PROPULSION AND DIAGNOSTICS. Charles L Merkle and Thomas M York, The Pennsylvania State University, University Park, PA
- 1030 31 PLASMA INITIATION MECHANISMS, ABSORPTION OR CW LASER ENERGY AND MIXING FLUID MECHANICS. Herman Krier, Jyoti Mazumder, and Ronald J Glumb, University of Illinois, Urbana-Champaign, IL
- 1100 32 Invited: EXPERIMENTAL STUDY OF LASER SUPPORTED HYDROGEN PLASMAS. T Dwayne McCay, D M VanZandt, and R H Eskridge, NASA/Marshall
- 1130 33 AFRPL SOLAR-THERMAL ROCKET ACTIVITIES. Curtis C Selph, AFRPL/LKCS
- 1200 LUNCH (Reconvene at 1300)

WEDNESDAY (PM)

14 March 1984

Session Chairman: Robert J Vondra, AFRPL/LKCJ

Topic: Electromagnetic Acceleration of Plasmas

TIME NUM

- 1300 34 BASIC PROCESSES IN PLASMA PROPULSION. Herbert O Schrade and Michael Kirschner, Institut fur Raumfahrtantriebe der Universitat Stuttgart
- 1330 35 MPD THRUSTER PERFORMANCE. R Joseph Cassady, Purdue University, West Lafayette, IN
Robert J Vondra and W M Schmidt, AFRPL, Edwards AFB, CA
- 1400 36 MAGNETOPLASMADYNAMIC THRUSTER EROSION RESEARCH. David Q King, Jet Propulsion Laboratory, Pasadena, CA
- 1430 37 EROSION AND ONSET MECHANISMS IN MAGNETOPLASMADYNAMIC THRUSTERS. John L Lawless, Carnegie-Mellon University, Pittsburgh, PA
- 1500 Break
- 1530 38 PERFORMANCE-LIMITATING FACTORS FOR MPD THRUSTERS. Manuel Martinez-Sanchez, Massachusetts Institute of Technology, Cambridge, MA
- 1600 39 PULSED INDUCTION ENERGY TRANSFER. Peter Mongeau and Henry Kolm, Electromagnetic Launch Research, Inc, Cambridge, MA,
- 1630 40 UNIFIED STUDY OF PLASMA-SURFACE INTERACTIONS FOR SPACE POWER AND PROPULSION. Peter Turchi, R and D Associates Washington Laboratory, Alexandria, VA
- 1700 ADVANCED DIAGNOSTICS FOR PLASMA FLOWS. Ronald K Hanson, Stanford University, Stanford, CA
- 42 *NONCONVENTIONAL ELECTROMAGNETIC PROPULSION CONCEPTS. Michael M Micci, Pennsylvania State University, University Park, PA
- 43 *CLOSED-SPACE TEMPERATURE KNUDSEN FLOW. John B McVey, Rasor Associates, Inc, Sunnyvale, CA
- 1730 Discussion Symposia (Snacks, soft drinks, cash bar) - Essex House

*Abstract only, no presentation.

THURSDAY

15 March 1984

NONCONVENTIONAL PROPULSION

Session Chairman: Frank Mead, AFRPL/LKCS

Topic: Energy Conversion

TIME NUM.

- 0800 44 VARIABLE FIELD-EFFECTS RELATED TO ROTATING FLUIDIZED BED SPACE POWER SYSTEMS. Owen C Jones, Jr, Rensselaer Polytechnic Institute, Troy, NY
- 0830 Invited: NASA SPONSORED RESEARCH ON NONCONVENTIONAL PROPULSION. Thomas H Cochran, NASA Lewis Research Center, Cleveland, OH and David C Byers, NASA/OAST, Washington, DC
- 0900 45 STABILIZED METASTABLE HELIUM. Jonas S Zmuidzinas, Jet Propulsion Laboratory, Pasadena, CA and Myron Tapper, Rockwell
- 0930 Break
- 1000 46 ELECTROSTATIC PROPULSION WITH THE ATMOSPHERE. Leik Myrabo, Rensselaer Polytechnic Institute, Troy, NY
- 1030 47 ANTI-PROTON ANNIHILATION PROPULSION. Robert L Forward, Forward Unlimited, Oxnard, CA
- 1100 48 NONCONVENTIONAL PROPULSION. Frank Mead, AFRPL/LKCS
- 1200 Lunch (Reconvene at 1300)
- 1300 WORKING SESSIONS:
- DATA SETS FOR MPD PHYSICAL MODEL VALIDATION. (Discussion leader to be determined)
- INSITUATION TO ESTABLISH PROPERTIES OF LASER SUPPORTED PLASMAS. (Discussion leader to be determined)
- 1500 Adjourn Meeting

*Abstract only, no presentation.

Topic: Internal Flows/Combustion Instability Interactions

- 49 *COUPLING BETWEEN VELOCITY OSCILLATIONS AND SOLID PROPELLANT COMBUSTION. Robert S Brown, Anthony M Blackner, and Roger Dunlap, United Technologies/Chemical Systems Division, San Jose, CA
- 50 *COMBUSTION OSCILLATIONS IN HETEROGENEOUS SYSTEMS. Moshe BenReuven and Martin Summerfield, Princeton Combustion Research Laboratory, Morristown Junction, NJ
- 51 *SOLID PROPELLANT GAS PHASE FLAME DRIVING OF AXIAL COMBUSTION INSTABILITIES. Ben T Zinn and Brady R Daniel, Georgia Institute of Technology, Atlanta, GA
- 52 *RELATION BETWEEN COMPOSITE PROPELLANT HETEROGENEITY AND NONSTEADY BURNING. Leon Strand and Norman S Cohen, Jet Propulsion Laboratory, Pasadena, CA
- 53 *INTERACTION OF MULTIDIMENSIONAL MEAN AND ACOUSTIC FIELDS IN SOLID ROCKET COMBUSTION CHAMBERS. Joseph D Baum and Jay N Levine, AFRL/DYC
- 54 *FINITE ELEMENT ANALYSIS FOR COMBUSTION INSTABILITY OF SOLID PROPELLANT ROCKET MOTORS. T J Chung, University of Alabama in Huntsville, Huntsville, AL

*Abstract only, no presentation.

Topic: Advanced Energetic Ingredients

NUM.

- 55 *ELECTROLYTIC PREPARATION OF NOVEL AZIDODINITRO COMPOUNDS. Milton B Frankel and James F Weber, Rocketdyne Division, Rockwell International, Canoga Park, CA
- 56 *SYNTHESIS AND CHEMISTRY OF ENERGETIC METALOTETRA-AZADIFENS. William C Trogler, University of California, LaJolla, CA
- 57 *HMX COMBUSTION MODIFICATIONS. Joseph E Flanagan, Milton B Frankel and Dean O Woolery, Rocketdyne Division, Rockwell International, Canoga Park, CA (Completed)
- 58 *AZIDE DECOMPOSITION AND COMBUSTION. Joseph E Flanagan and Milton B Frankel, Rocketdyne Division, Rockwell International, Canoga Park, CA (New Start)
- 59 *SYNTHESIS OF DIFLUORAMINOXY-, DIFLUORAMINO- OR FLUORODIAZONIUM-CONTAINING MATERIALS. Jean'ne M Shreeve, Univ of Idaho, Moscow, ID
- 60 *SYNTHESIS AND CHEMISTRY OF POLYNITROALKANES AND POLYNITROOLEFINS. Clifford D Bedford and Robert J Schmitt, SRI International, Menlo Park, CA
- 61 *MODIFICATION OF PROPELLANT BINDER NETWORK FOR IMPROVEMENT OF MECHANICAL PROPERTIES. C Sue Kim, California State University at Sacramento, Sacramento, CA
- 62 *INITIAL THERMOCHEMICAL DECOMPOSITION MECHANISMS OF ENERGETIC INGREDIENTS: DEUTERIUM ISOTOPE EFFECTS AND ISOTHERMAL DECOMPOSITION STUDIES. and Scott A Shackelford, Michael B Coolidge, Stephen L Rodgers, and Berge B Goshgarian, AFRPL/LKLR
- 63 *NEW SYNTHETIC TECHNIQUES FOR ADVANCED PROPELLANT INGREDIENTS: SELECTIVE CHEMICAL TRANSFORMATIONS AND NEW STRUCTURES. Scott A Shackelford, Robert D Chapman, Stephen P Herrlinger, and John L Andreshak, AFRPL/LKLR
- 64 *MECHANISTIC COMBUSTION INTERACTIONS OF ISOTOPICALLY LABELED PROPELLANT INGREDIENTS. Scott A Shackelford, AFRPL/LKLR
- 65 *POLYMERS CONTAINING AZIDE AND NITRATE ESTER GROUPS. Stan Morse, University of Dayton Research Institute, Dayton, OH

*Abstracts only, no presentation.

CARBON-CARBON PROCESSING VARIABLES INVESTIGATION

W. P. HOFFMAN

AIR FORCE ROCKET PROPULSION LABORATORY

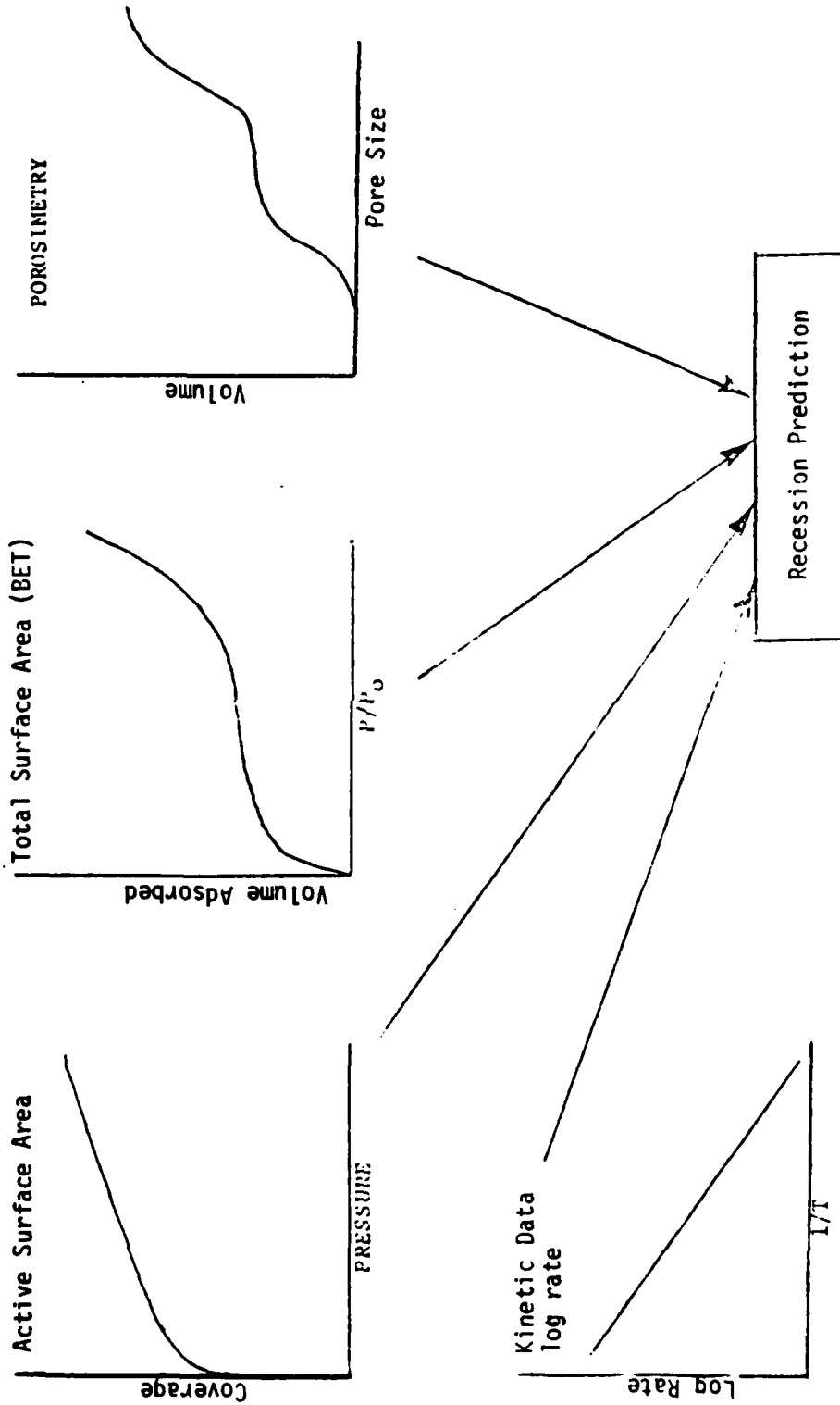
AFRPL/MKBN EDWARDS AFB, CA 93523

The chemistry and physics of carbon-carbon composites is not well understood even though they are being evaluated as nozzle materials in a number of Air Force programs. This lack of understanding includes the surface ablation kinetics of these materials. There is conjecture about the specie (s) principally responsible for recession. However, there is no definitive data available either pertaining to the principle specie (s), or to the kinetics of the heterogeneous reactions with carbon under rocket nozzle conditions. Therefore, the nozzle designer has no firm theoretical basis on which to predict the performance of his nozzle design. He is forced to make predictions based on data from actual motor firings. The nozzle and conditions used in these firings may or may not represent the composite material and operating conditions that the designer has chosen. The objective of this program is to fill this gap in our knowledge of surface reaction kinetics and their relation to carbon-carbon material construction and processing. This is being accomplished by (1) extensive surface characterization of the carbon-carbon materials and (2) by measuring the kinetics of the heterogeneous reactions between carbon-carbon materials and the various species present in the rocket motor exhaust. This will give the designer a firm basis on which to predict the performance of his nozzle.

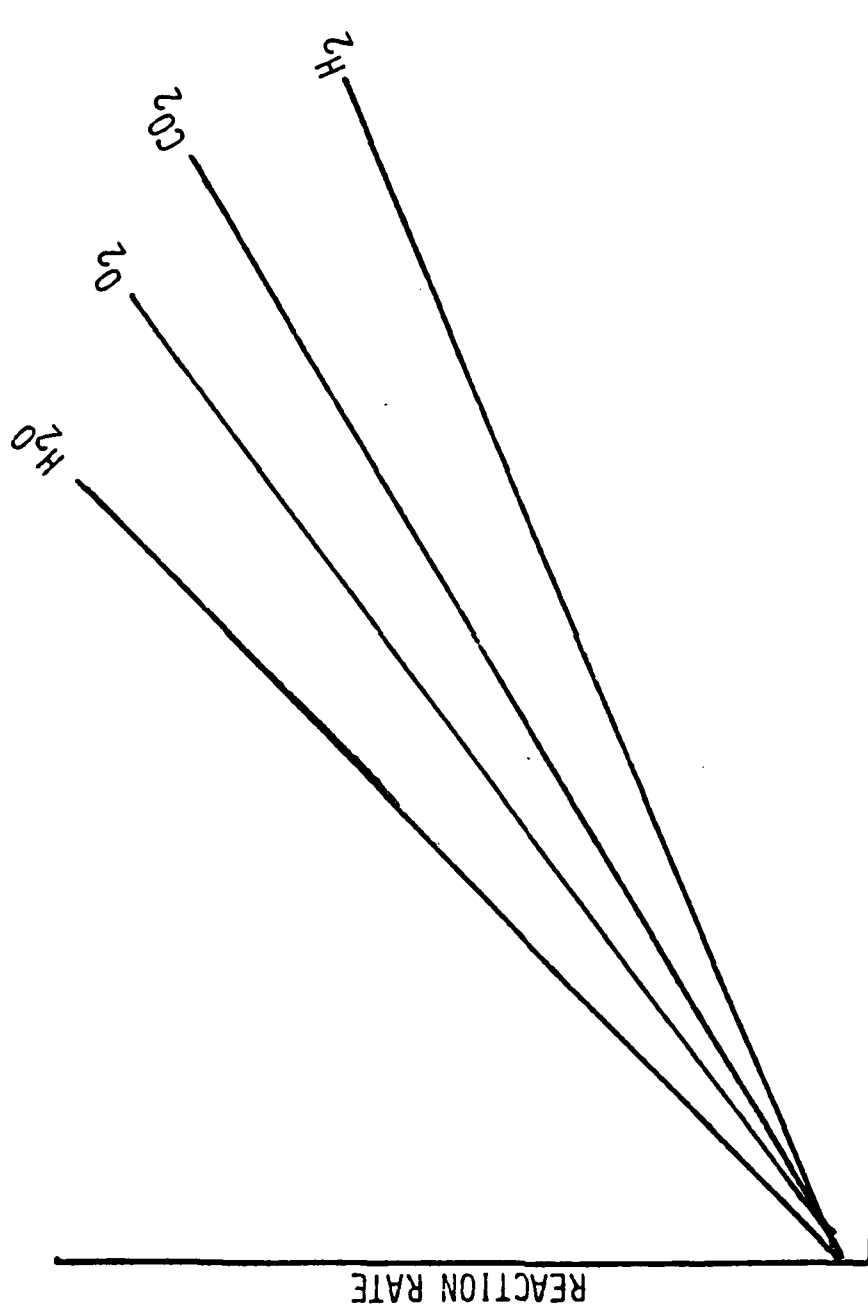
During the past year, characterization studies of two commercially prepared carbon fibers (T-300 and VSB-32) that had been heat treated to 2700°C was continued. Work has centered on gaining better understanding of fiber structure. In addition, much effort has been expended in refining the techniques developed to measure the total surface area (TSA), active surface area (ASA), and porosity of these fibers as well as composites manufactured from them. Very precise techniques are required since the parameters measured are typically very small for adsorption techniques. For instance, the TSA of these fibers is usually 0.3m²/g and the ASA is typically five percent of this value. One of the major modifications completed this year was in the automated data acquisition system. This modified the signal to noise (S/N) ratio by an order of magnitude which revealed information previously obscured. This improvement in the S/N ratio made it possible not only to confirm the microporosity of these fibers but also to quantify it. Although these fibers have been found to have similar TSA's, they have significantly different ASA's and pore size distributions. The intriguing fact however is that although there are differences between the fibers, these differences are not as significant as one would expect considering the diversity of the precursor. For the two fibers studied, the ratio of ASA's in an oxygen atmosphere was similar to the ratio of recession rates of billets manufactured from these fibers.

APPROACH

Techniques used for material characterization:



ANTICIPATED ACCOMPLISHMENT



ACTIVE SURFACE AREA

DEPENDENCE OF RECESSION RATE ON THE TYPE OF ROCKET MOTOR EXHAUST GAS.

STATISTICAL NATURE OF CRACK GROWTH IN SOLID PROPELLANTS

C. T. LIU

Air Force Rocket Propulsion Laboratory
Edwards AFB, CA 93523 (805) 277-5502

The high volume concentration of fillers of different sizes in a composite solid propellant produces a heterogeneous material. The heterogeneity of the microstructure will undoubtedly affect the material properties, as well as the failure behavior of solid propellants. Thus, depending upon the local microstructure or the local stress and strength near the crack tip, the rate of crack growth, $\frac{da}{dt}$, may show a considerable fluctuation within a specimen, or it may show considerably larger scatter among specimens even though the testing conditions remain identical. In addition to the intrinsic scatter of $\frac{da}{dt}$, due to the heterogeneity of the microstructure, the methods of the $\frac{da}{dt}$ calculation may also be a contributing factor to the scatter of the rate of crack growth due to the discrete nature of the crack growth data. Therefore, it is the purpose of this study to investigate the effect of the methods of the $\frac{da}{dt}$ calculation on the variability of the crack growth rate and the statistical characteristics of the crack growth behavior in a solid propellant.

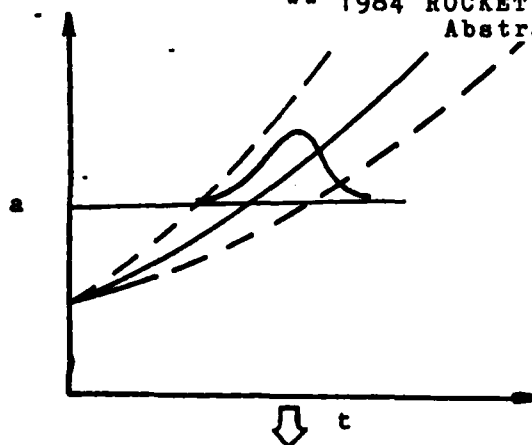
The crack growth behavior of a highly filled composite propellant under constant strain rate condition was studied through the use of centrally cracked biaxial specimens. In this study, a total of 38 replicate tests were conducted under identical conditions. The raw data (load, time, and crack length) obtained from the tests were used to calculate the instantaneous crack growth rate and the stress intensity factor for a given instantaneous crack length and the associated load. In calculating the crack growth rate, four different methods were used. The calculated crack growth rate and the stress intensity factor were analyzed statistically to determine the functional relationship between the crack growth rate and the stress intensity factor, as well as the statistical distribution function of $\frac{da}{dt}$ as a function of the stress intensity factor. A detailed discussion on the methods of $\frac{da}{dt}$ calculation and the statistical analysis was given at the 1983 Air Force Office of Scientific Research/Air Force Rocket Propulsion Laboratory (AFOSR/AFRPL) Chemical Rocket Research Meeting and subsequently shown in the meeting's report. Therefore, those subjects will not be discussed in this abstract. However, for an illustrative purpose, the schematic representation of the basic approach is reproduced and shown in Figure 1.

Based on the analysis, the following conclusions are drawn:

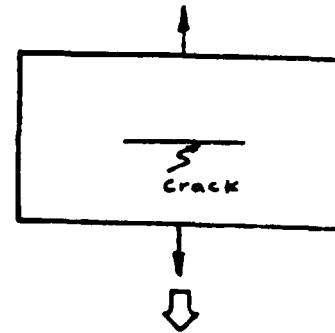
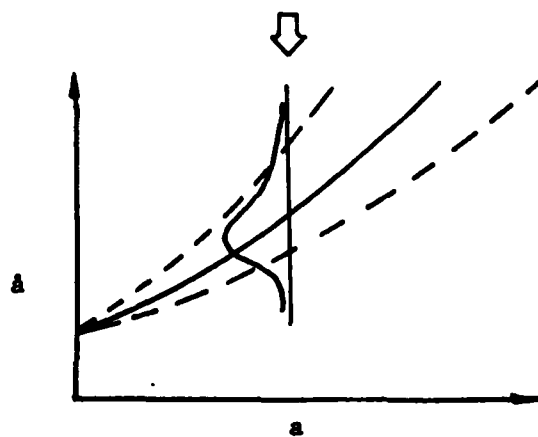
1. The method of $\frac{da}{dt}$ calculation has a significant effect on the variability of the $\frac{da}{dt}$ data.
2. The secant method introduces the least amount of error into the $\frac{da}{dt}$ data.
3. Data smoothing action introduces a large error, but less scatter, into the $\frac{da}{dt}$ data.
4. For the range of K_I considered in this study, the 2-parameter log-normal distribution provides a best fit for the $\frac{da}{dt}$ data.
5. A power law relationship exists between the crack growth rate, $\frac{da}{dt}$, and the stress intensity factors, and mathematically, it can be written as

$$\frac{da}{dt} = C_2 K_I^{C_1}$$

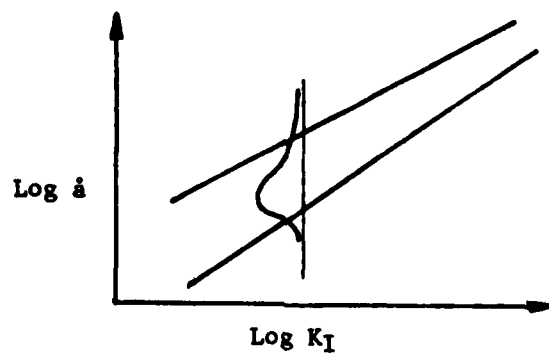
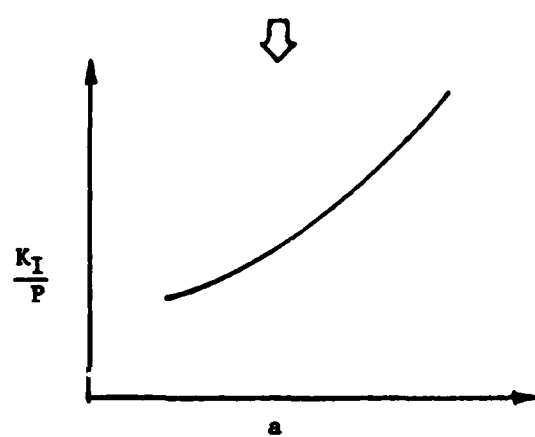
6. The parameters, C_1 and C_2 , are mutually dependent, and all the crack growth lines--plotted as $\ln \dot{a}$ vs $\ln K_I$ --tend to converge to a small region.



Data Processing
Converting a vs t Data to \dot{a} vs t Data



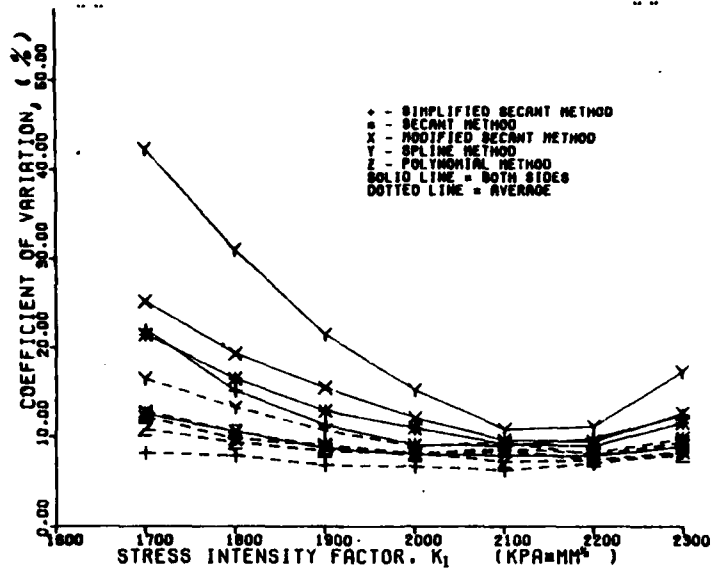
Finite Element Analysis
Generating $\frac{K_I}{P}$ vs a curve



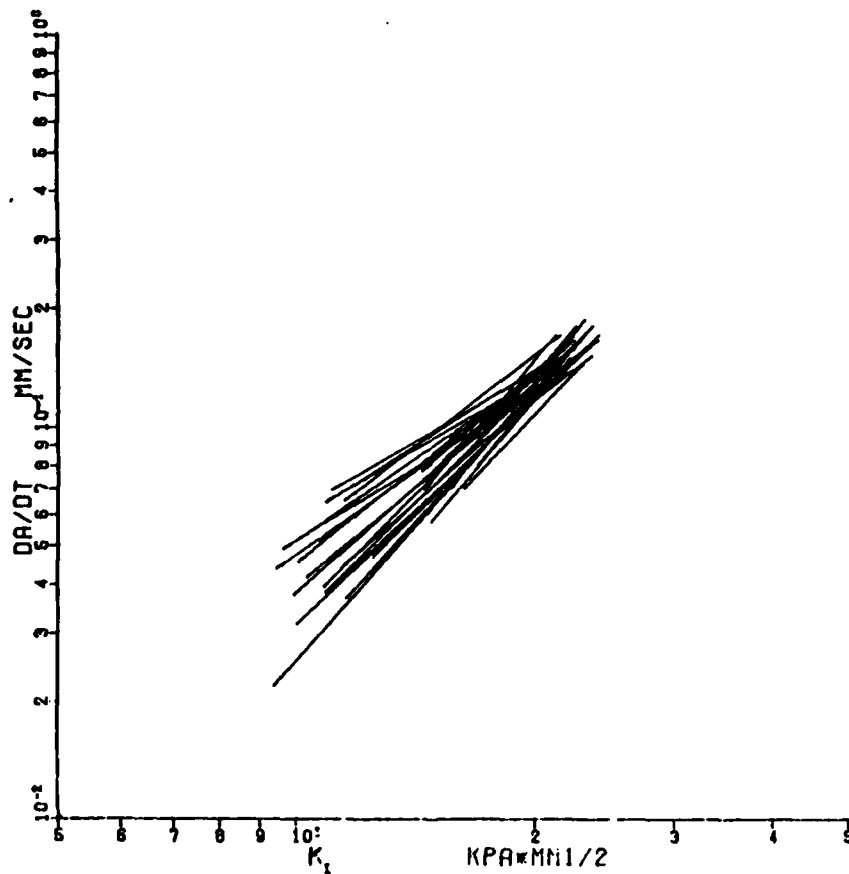
Statistical Analysis

- Statistical distribution of \dot{a} as a function of a and K_I
- Statistical model of crack growth
- Variability and statistical distribution of the parameters in the crack

Figure 1. Schematic Representation of Basic Approach



(a) Coefficient of Variation of $\frac{da}{dt}$ vs Stress Intensity Factor



(b) Log \dot{a} vs Log K_I

Figure 2. Results

PROPELLANT AGING RESEARCH

Douglas B. Olson
AeroChem Research Laboratories, Inc.
P.O. Box 12, Princeton, NJ 08542

The overall objective of this work is to gain a fundamental understanding of the chemical reaction mechanisms and kinetics of solid rocket propellant aging. If the aging chemistry of the individual propellant ingredients can be accurately modeled, then the useful lifetimes of current and improved formulations will be predictable. The approach taken (see Fig. 1) is to separately study the two main steps in the propellant aging process: the decomposition of oxidizers and plasticizers; and the attack of the highly reactive decomposition products on the binders, stabilizers, and other propellant ingredients. Mechanisms will be postulated (using the measured kinetic parameters) and the predictions of this chemical aging "model" will be compared with available data on mechanical property changes that occur from long term aging of propellants. Experiments to investigate the effects of minor ingredients, e.g., bonding agents or combustion modifiers, will be performed as needed to improve the predictive accuracy of the model.

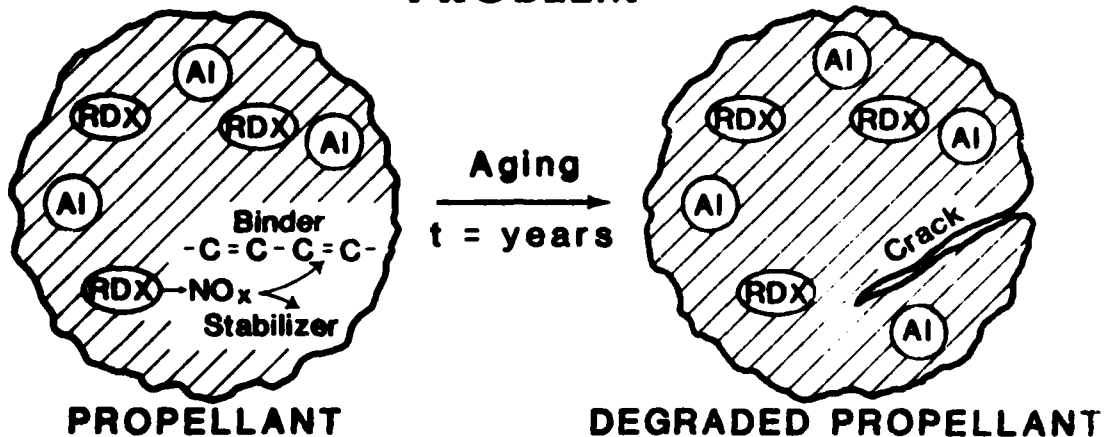
Measuring oxidizer and plasticizer decomposition rate coefficients at near ambient temperature as in this work requires ultrasensitive techniques. Gas evolution from the primary decomposition steps of several oxidizers and plasticizers (RDX, AP, and BTTN) is being investigated using the AeroChem $\text{NO}_x/\text{NH}_3 + \text{O}_2$ chemiluminescence analyzer which can measure real time decomposition rate coefficients as small as about 10^{-12} s^{-1} (half-life greater than 10^4 years), corresponding to, e.g., an NO concentration of about 1 part in 10^{10} . Obtaining data such as these at realistic propellant storage temperatures is important (see Fig. 2) because it has been found that rate coefficients obtained at higher temperatures (above $\approx 100^\circ\text{C}$) sometimes have significantly different activation energies from those at lower temperature, and give grossly incorrect estimates of compound stabilities when extrapolated to ambient temperature.

The reactivity of two propellant binders, HTPB and PEG, with and without stabilizer, toward several gaseous decomposition products from the oxidizers and plasticizers will be measured. Various techniques will be used in these studies, including measurements of gas evolution rates from binder-oxidizer or plasticizer mixtures (using the NO_x/NH_3 analyzer), binder oxidative chemiluminescence, and physical property changes (using several methods including gel permeation chromatography).

Experimental measurements on RDX decomposition are currently underway using the NO_x analyzer. Previous unpublished results (labeled AeroChem in Fig. 2) gave an activation energy of about 88 kJ mol^{-1} over the temperature range 60 to 130°C , significantly lower than the higher temperature values. The measurements in this program are being made from $\approx 60^\circ\text{C}$ down to 20°C using an improved apparatus.

PROPELLANT AGING RESEARCH

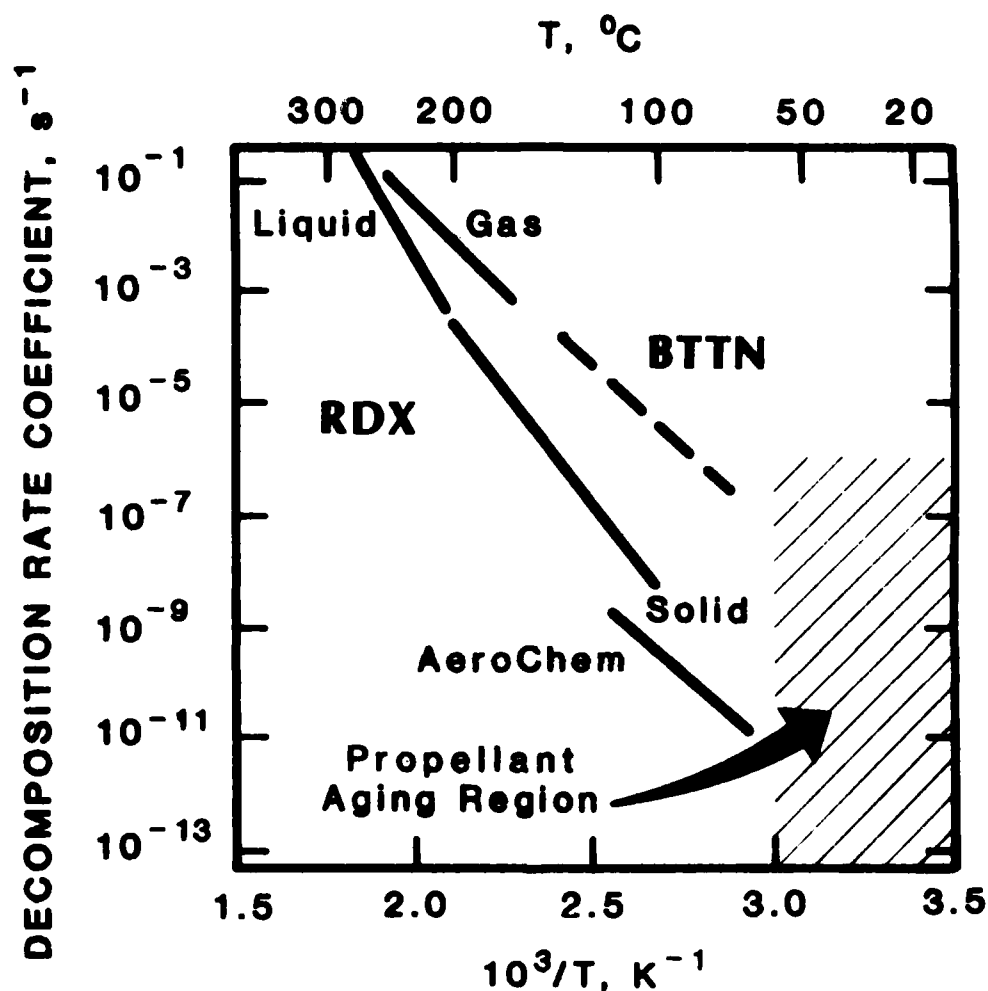
PROBLEM



APPROACH

- ★ **MEASURE OXIDIZER/PLASTICIZER DECOMPOSITION RATES**
RDX, AP, BTTN, T = 20-60°C
Use: ● NO_x/NH₃ + O₃ Analyzer
- ★ **MEASURE BINDER REACTIVITY WITH DECOMPOSITION GASES (NO, NO₂, HClO₄, ...)**
Use: ● NO_x/NH₃ + O₃ Analyzer
● Binder Chemiluminescence
● Physical Property Changes
- ★ **DEVELOP CHEMICAL AGING MODEL**
HTPB and PEG
- ★ **PREDICT PROPELLANT SERVICE LIFETIMES?**

ANTICIPATED RESULTS



RDX and BTTN Decomposition Data

ADDITIONAL DATA WILL BE OBTAINED FROM
 $T = 20$ TO $60^{\circ}C$ FOR USE IN THE
PROPELLANT AGING MODEL.

MECHANISMS FOR ACOUSTIC SUPPRESSION

Principal Investigator: Merrill W. Beckstead
Coinvestigators: R. L. Raun and P. C. Braithwaite
Brigham Young University, Provo, Utah 86402

Acoustic suppressants are commonly added to low smoke and smokeless propellants to avoid the problem of combustion instability. However, the basis for selecting the type, size, and concentration of suppressant particle for optimum performance is not well founded. Suppressants apparently work by one or more of three mechanisms:

- (1) energy loss due to viscous dissipation due to drag forces,
- (2) modification of the propellant combustion response function, or
- (3) energy interchange due to distributed combustion.

Viscous dissipation of acoustic energy by drag forces on a suspended particle is the most commonly recognized mechanism, being a direct analogy to suspended moisture in a fog. A second mechanism whereby an additive can effect acoustics occurs at the burning boundary of the system. Solid additives within the propellant can have a catalytic influence on the propellant combustion, modifying the combustion response. The best known example of this is probably Al_2O_3 . Al_2O_3 is the particulate product of aluminum combustion which provides the viscous drag dissipation previously discussed. However, Al_2O_3 is also a weak combustion catalyst in composite propellants. An additive that influences the steady burning of a propellant can also be expected to influence the transient response of the propellant. The third mechanism considered is due to the effect of a particle burning as it traverses a relatively large portion of the system. As it does so, the interchange of energy between the burning particle and the acoustic environment can result in either a driving or damping contribution to the acoustics of the system. This third mechanism is the primary area of study of the current contract.

Figure 1 is a graphic illustration of the approach, some of the technical advantages, the data to be collected and the data analysis to be performed. The experimental basis for the technical approach is the Rijke tube, a gas burner with a paddle to control (stop and start) combustion oscillations, over frequencies ranging from 500 to 1500 Hz. Advantages of this approach include allowing a separation of the three mechanisms mentioned above by testing an additive independent of the propellant burning surface, avoiding use of solid propellants, and allowing for independent control of frequency, O/F ratio, temperature and particle addition.

The principle objective of this work is to identify and develop an understanding of the mechanisms whereby acoustic suppressants modify an acoustic wave. It is expected that several mechanisms will be shown to act together to dampen acoustic oscillations, with one mechanism perhaps dominating under certain conditions and another mechanism dominating at other conditions.

Figure 2 summarizes the activities of the past year.

ACCOMPLISHMENTS

1. LITERATURE SURVEY COMPLETED

- Rijke Tube Acoustics
- Particle Damping in Solid Propellants

2. MECHANISMS FOR PARTICULATE ACOUSTIC SUPPRESSION IDENTIFIED

- Energy loss due to viscous dissipation of drag forces
- Modification of the propellant combustion response function
- Energy interchange due to distributed combustion

3. BASIC EQUATIONS OUTLINED

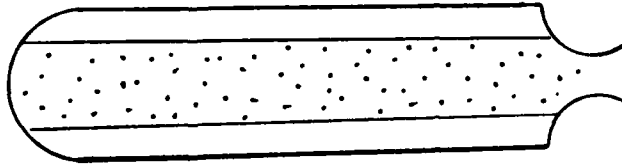
- Conservation Equations for Gas Plus Particles Defined
- Neglect: wall friction, viscous dissipation, kinetic energy terms, body forces
- Assume: one-dimensional flow, constant transport properties, constant area, small amplitude oscillations, discontinuity at flame
- Perturbation form of equations obtained

4. EXPERIMENTAL PROGRESS WITH RIJKE BURNER

- A quantitative particle feeder developed
- Improved paddle designed and constructed
- Test procedures established

MECHANISMS FOR ACOUSTIC SUPPRESSION

How Do Suppressants Work in Solid Propellant Rocket Motors?

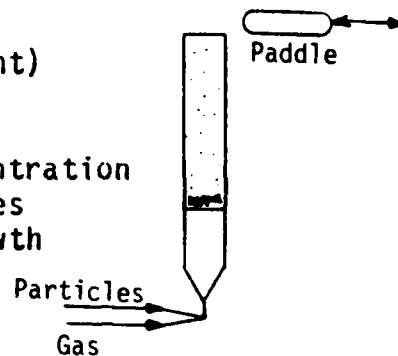


Mechanisms of Acoustic Suppressants:

Viscous dissipation due to drag forces
Modification of propellant response function
Effect of distributed combustion

CURRENT PROGRAM:

- Separate Effects of Different Mechanisms Using Unique Experiments
- The Modified Rijke burner
 - Use gas (eliminates solid propellant)
 - Evaluate acoustics w/o particles
 - Can feed particles independently
 - Vary particle type, size and concentration
 - Evaluate reactive or inert particles
 - Use paddle to control acoustic growth
- Results
 - Monitor particle combustion with high speed movies
 - Evaluate acoustic growth rates with and without particles
 - Evaluate mechanisms of reactive versus inert particles
 - Measure effect of pertinent parameter



COMBUSTION MECHANISMS

D.P. Weaver, D.H. Campbell, S.C. Hulsizer, J.T. Edwards
Air Force Rocket Propulsion Laboratory
Edwards AFB, California

The objective of all propellant development programs is the ability to tailor propellant ballistic properties and performance through the selective modification of propellant ingredients. While the influence of additives on burning rate and combustion instabilities has been well documented, as yet no detailed understanding of the specific chemical mechanisms or their influence on propellant combustion has been developed. Information on the influence of such detailed chemical kinetics changes on the overall propellant burning behavior is of fundamental importance in establishing the influence of composition variables on macroscopic properties such as performance and ballistics. The objective of this research is to provide detailed chemical kinetic mechanisms of the gas phase reacting species at or near the surface of HTPB/AP propellant samples burning at pressures typical of solid rocket motor chambers. Additionally, chemical kinetic and statistical modelling of the burning process is to be coupled to these results to aid in the interpretation of the specific chemistry of the reaction process.

On a microscopic scale, the combustion of a solid rocket motor propellant is seen to be a heterogeneous, unstable process exhibiting multiple flames, local wide variation of gas phase O/F ratios, and ignition delays of certain particles. However, the aggregate propellant sample burns at a measurable, steady rate on the macroscopic scale. This forms the basis for statistical approaches to combustion modelling and requires sufficient spatial and temporal resolution of diagnostic capability as to isolate the combustion mechanisms on the microscopic scale of the intermittent burning. Further, the information must be specific to the molecular and atomic species within such localized regions. The accumulation of such localized specific data will identify the competing mechanisms and lead to an understanding of the effect on burning rate of chemistry variation. As a first step, mechanisms leading to the localized O/F ratio variations must be specified and the affect on these ratios of specific propellant chemistry detailed. The experimental apparatus used in this study along with a representation of the resulting data is presented in Figure 1. Emphasis at this point is on coherent anti Stokes Raman scattering, laser-induced fluorescence, and emission spectroscopic surveys of HTPB/AP propellants in the pressure range 200-1000 PSI. Typical results on OH are shown in Figure 2.

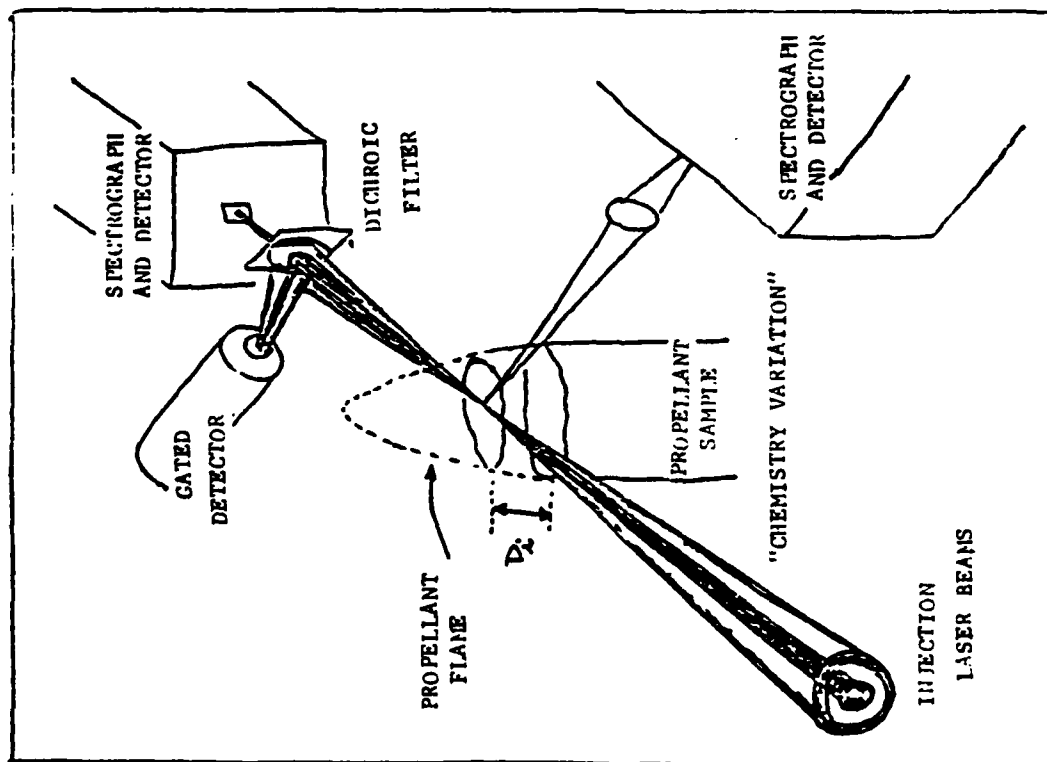
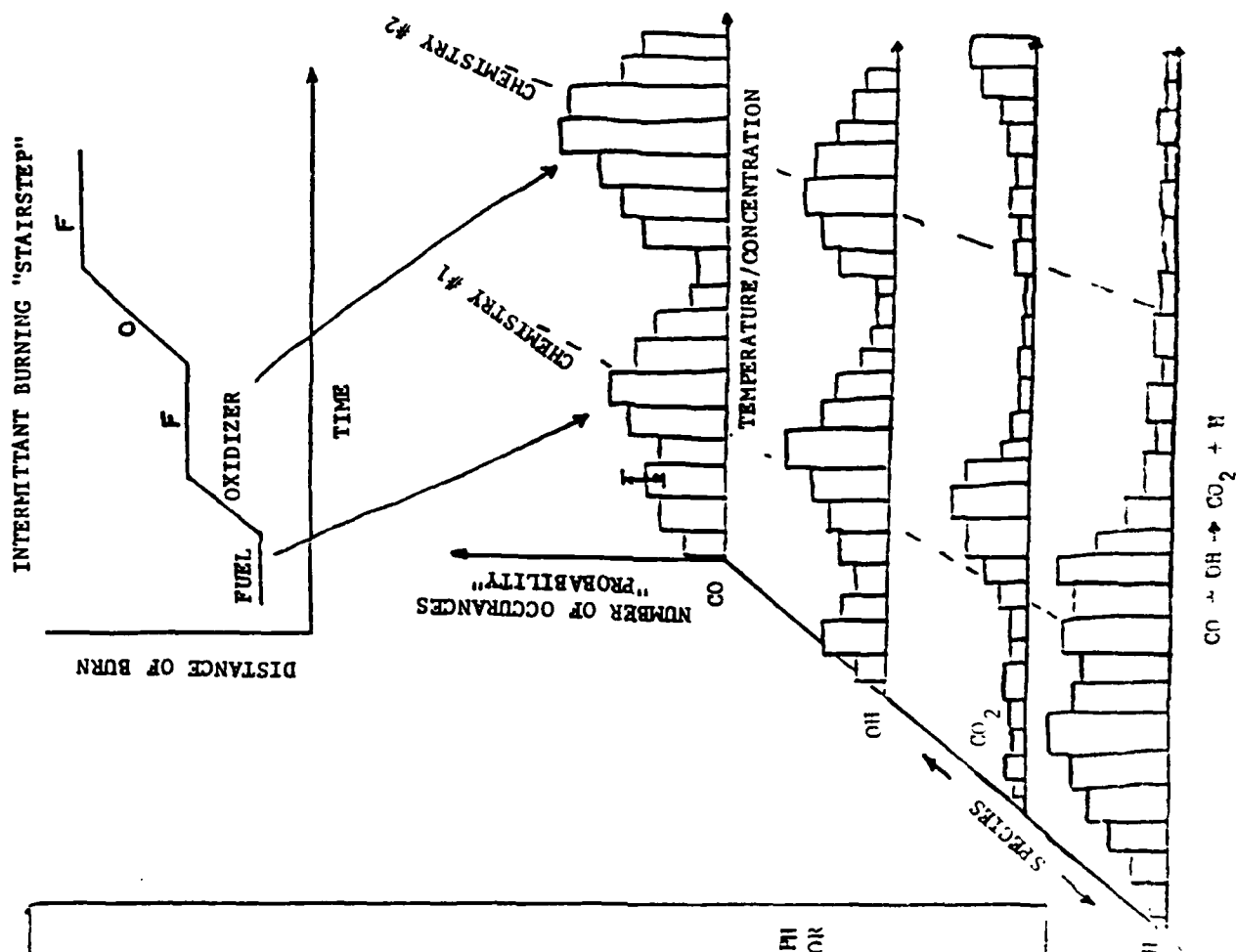


FIGURE 1: EXPERIMENTAL APPARATUS AND APPROACH

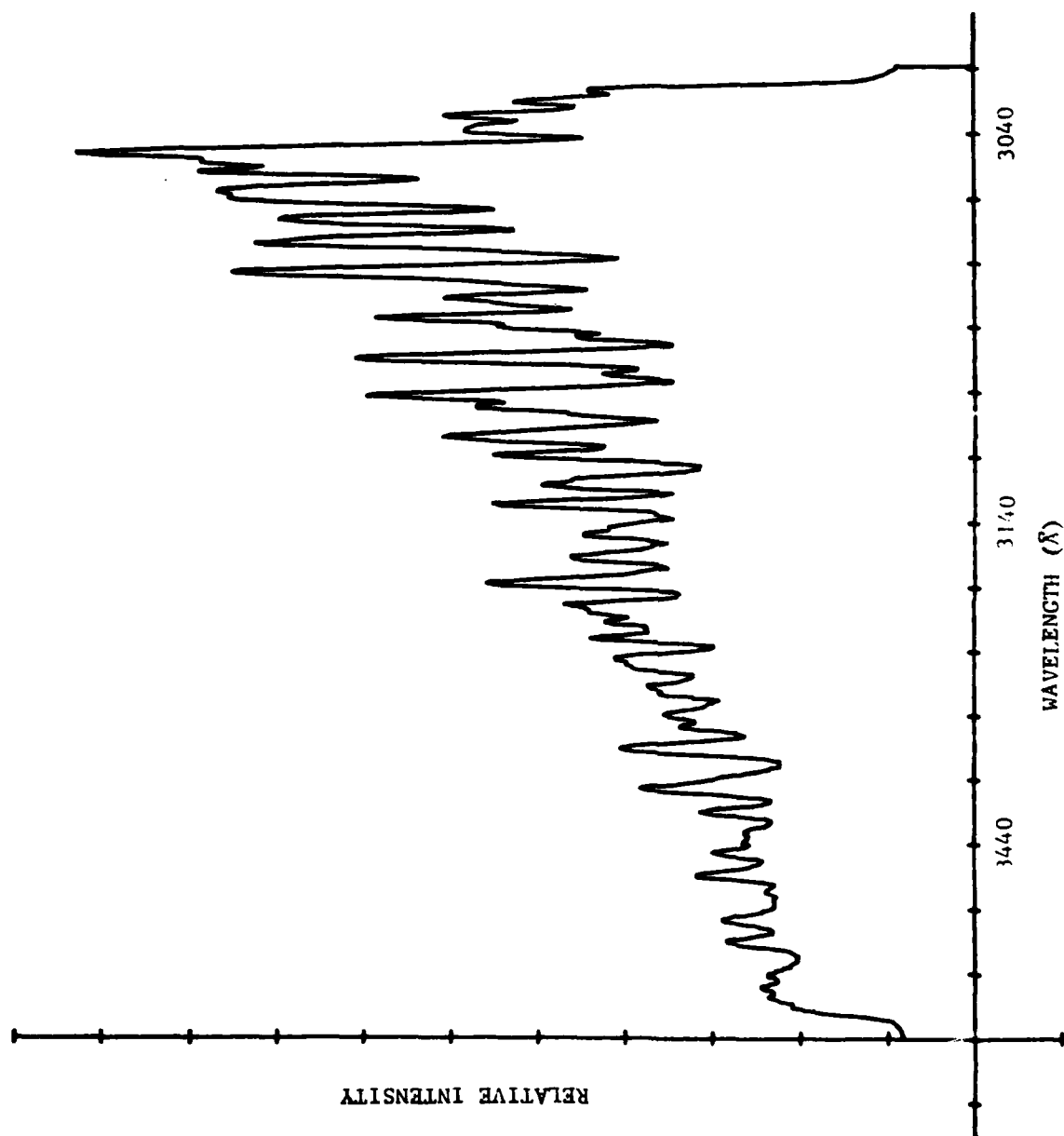


FIGURE 2: OH EMISSION FROM HTPB/AP PROPELLANT, 750 PSI

THERMOPHYSICAL PROPERTY DETERMINATIONS USING TRANSIENT TECHNIQUES

Principle Investigator: R. L. Taylor
Thermophysical Properties Research Laboratory
Purdue University
West Lafayette, Indiana

Knowledge of the thermophysical properties of rocket propellants, especially at higher temperatures where significant decomposition occurs, is necessary for understanding various physical processes which take place in the combustion of these propellants. Much effort has been put into the development of computer codes to model various aspects of rocket propellant behavior, such as combustion mechanics and BSTD. However, there is a lack of accurate thermophysical property data for the propellants being used in these models in addition to the lack of understanding of the basic heat transfer mechanisms. In this program, determinations of the thermophysical properties of AP, RDX, and HMX are being completed in an attempt to quantitatively understand heat transfer through the propellants under transient heating at temperatures near combustion.

Shown in Figure 1 is the general approach for making the thermophysical property determinations of a material when the thermal conductivity is difficult to measure directly because of sample instability. Traditional thermal conductivity measurements require large samples and steady state thermal gradients for accurate results while the pulse diffusivity method uses small samples and transient temperature rises of the order of a few degrees C. The pulse diffusivity method therefore allows the investigation of transient heat transfer in a sample while the sample is undergoing changes which more closely resembles the conditions of a burning propellant. Two thermal properties are being determined: (1) specific heat using a Perkin-Elmer model DSC-2 Differential Scanning Calorimeter, and (2) thermal diffusivity using a laser flash apparatus. All measurements are made under digital computer control for data acquisition and analysis. The product of these results and the densities of the propellants yields the thermal conductivity of the material.

Specific heat results have been obtained for all three materials. The effects of partial decomposition on the specific heat have also been studied. These results will be presented.

The rate of diffusion of heat through a material depends upon the mean free path length which in turn is a function of the crystal structure (including imperfections) and intergranular contacts. The mean free path lengths within the crystal is significantly influenced by imperfection sites due to phase changes, additives, decomposition and lattice distortion. The diffusion path length for pressed powders is dependent upon several variables: the grain size, the intergrain contact resistance, the structural integrity, the grain composition and the packing density. As a result the thermal diffusivity of a powdered propellant is highly dependent upon the propellant's composition, particle size and its structural condition. If, for example, a propellant bed has been exposed to acoustic vibrations, micro-cracking could occur which would lower the thermal diffusivity of the propellant. Therefore, knowing a propellant's composition is not sufficient to assign an accurate thermal diffusivity value to it.

The approach taken has been to determine the thermal diffusivity of pure crystals and powders of the propellants of interest. Single crystal and powdered AP samples have been measured as well as powdered samples of HMX. The thermal diffusivity along two principle crystal axes for AP were investigated. The uncorrected thermal diffusivity values along the principle axes increase as the molecular bond lengths decrease as expected. These results are plotted in Figure 2. The AP crystal is transparent to infrared light and thus it was necessary to form a layered composite by placing the sample between two opaque materials. The data presented therefore require the application of a new heat loss correction technique that is presently under development.

THERMAL DIFFUSIVITY OF ENERGETIC MATERIAL

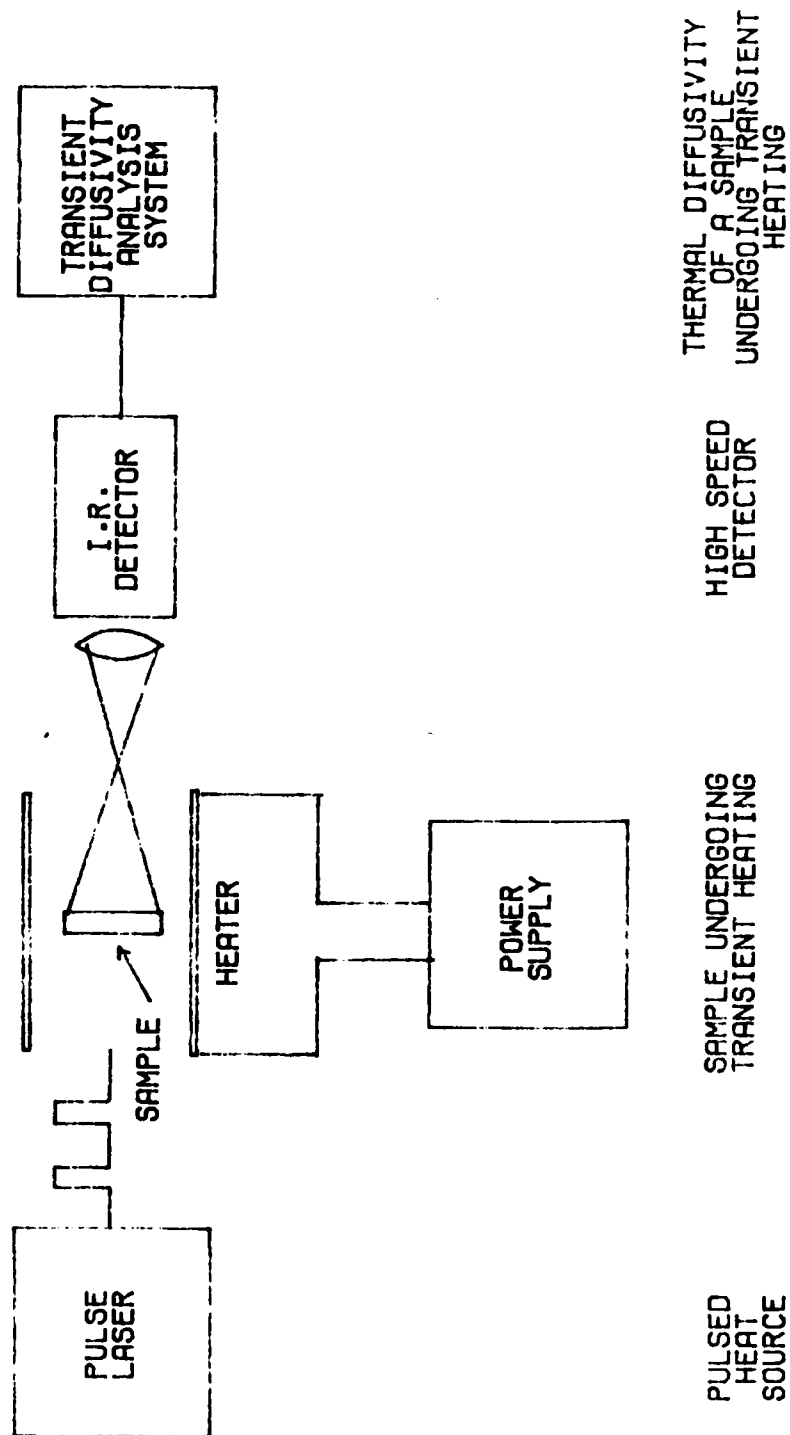


Figure 1.

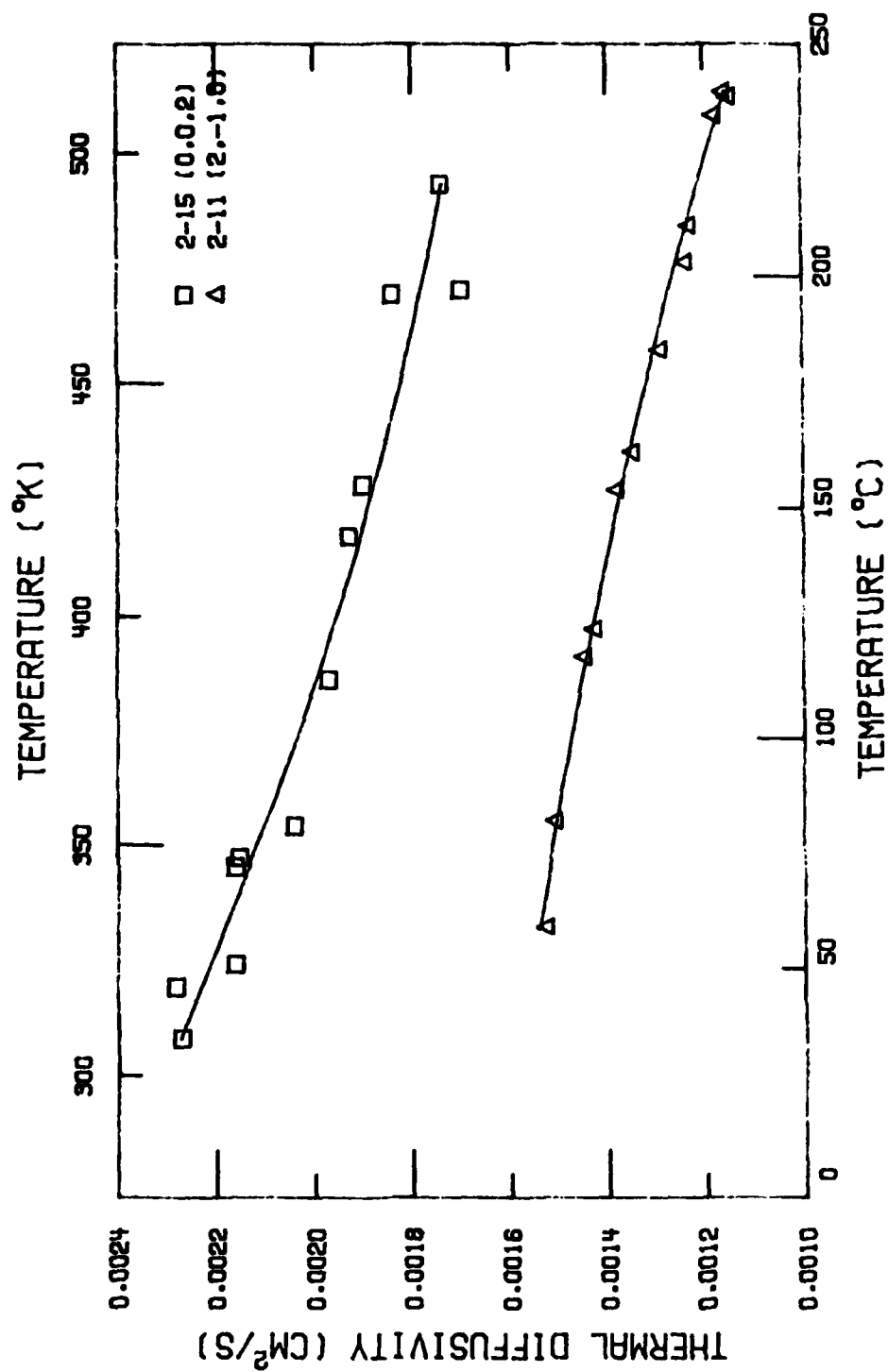


Figure 2. The Uncorrected Thermal Diffusivity
of Two Orientations of Single Crystal AP.

CHEMICAL KINETICS OF NITRAMINE PROPELLANT COMBUSTION

Melvyn C. Branch
Mechanical Engineering Department
University of Colorado
Boulder, Colorado 80309

Although nitramine solid rocket propellants have advantages of high specific impulse and low infrared and smoke emissions from their exhaust, better control of the burn rate is needed. Propellant additives have been suggested for burn rate control but the understanding of the chemical mechanism of burning is not well enough developed to predict the effects of these burn rate modifiers. The objective of the studies reported here is to describe the detailed chemistry of reactions of gas phase species which are important in the combustion of nitramine propellants and additives. Species composition, temperature and burning rate are being measured for reacting gas mixtures representative of the pyrolysis products of nitramines and nitramines with additives. The reaction is followed experimentally by precise, spatially resolved measurements of species concentration and temperature profiles above a one dimensional, laminar flat flame burner. Chemical kinetic and fluid mechanic modeling of the flame structure is also being used to correlate the experimental data and evaluate critical reaction paths and energetics and their importance in burn rate control.

Preliminary chemical kinetic modeling of the nitramine system are one dimensional, adiabatic reaction without diffusion of heat and mass. The reaction mechanism is based on existing studies of the $\text{NH}_3\text{-NO-O}_2$ reaction system (Miller, Branch and Kee, 1981). These mechanisms include reactions of the major nitrogen species NO , NO_2 , N_2O , NH_3 and N_2 and reactions in the H_2/O_2 system. The reaction mechanism also includes reactions of CH_2O , CO and CO_2 and their intermediates taken from the recent review of Westbrook and Dryer (1983). The mechanism can only be regarded as tentative and preliminary, but, nonetheless, several interesting results are derived from its use.

The reaction has a distinct two zone structure. The rapid first stage is reaction between CH_2O , NO_2 and N_2O and the intermediates H and OH . These reactions are responsible for most of the heat release of the reaction. These first stage reactions also keep the radical concentrations ($\text{H}, \text{OH}, \text{O}$) low so that second stage reactions are slow. The primary reactions in the second stage are those reducing NO . These reactions are also exothermic and increase the gas temperature. This stage of the reaction does not begin, however, until the CH_2O and NO_2 are depleted and the radicals (primarily H and OH) are able to increase in concentration. Although reactions between NH_2 and NO also deplete the NO concentration these reactions are not dominant because NH_2 is present only in low concentration. Attempts to provide sources of NH_3 or NH_2 to the propellant to accelerate this reaction process are under study (Flanagan, et al, 1982). Other calculations at lower pressures show that the sensitivity of the reaction zone thickness and reaction rate to pressure is similar to that of the burning propellant. These preliminary calculations suggest the feasibility of describing the two zone combustion and the effects of pressure on this structure by a comprehensive chemical kinetic mechanism.

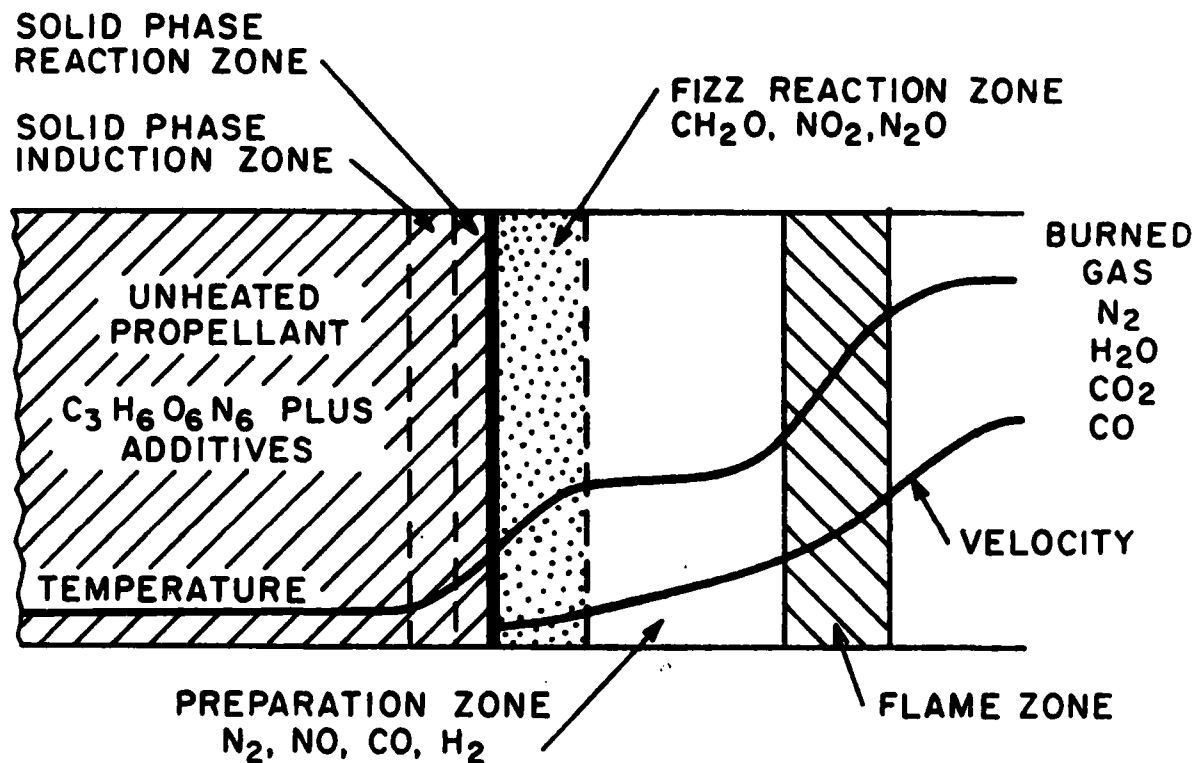


Figure 1. Schematic representation of the reaction zone near the surface (solid line) of a burning nitramine propellant. The "fizz" reaction zone in the gas phase, the gas preparation zone and gas flame zone are distinguished. This study is concerned with describing the chemistry of these regions dominated by gas reactions.

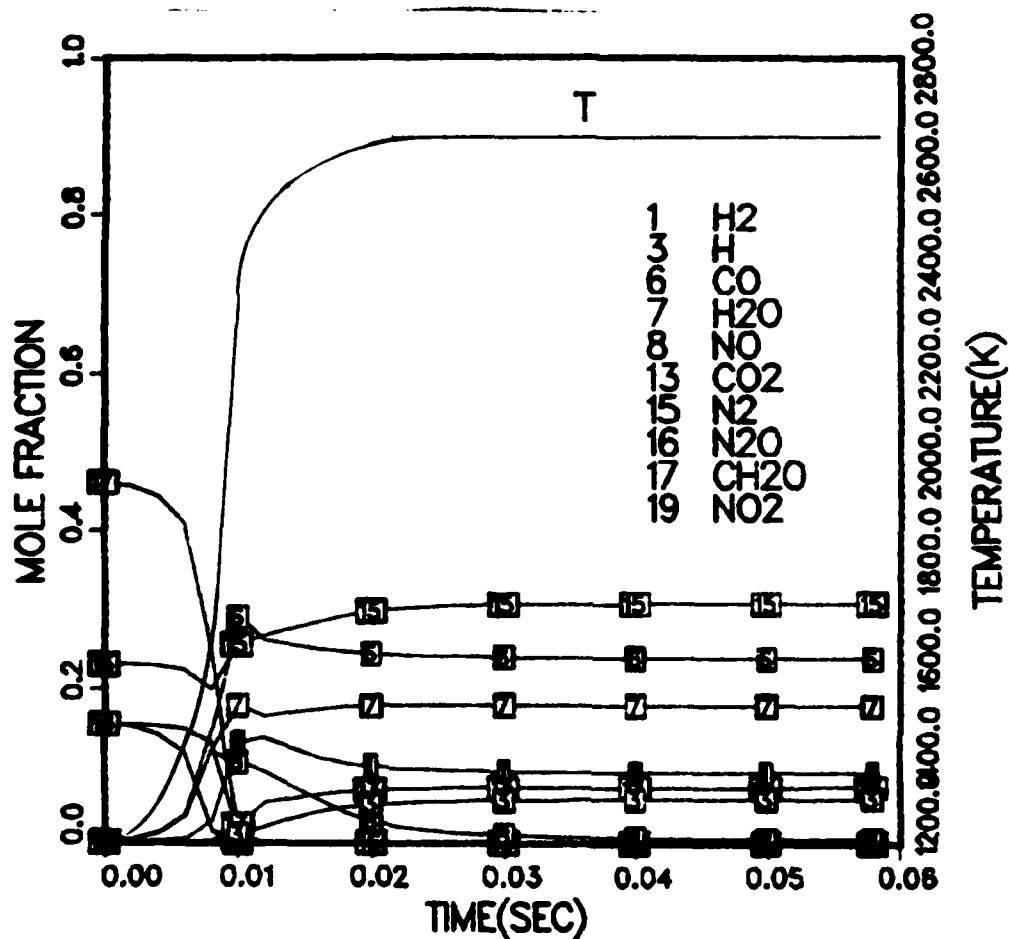


Figure 2. Products and product temperature from the one dimensional adiabatic reaction of the products of decomposition of RDX at 40 atm. Initial mixture is $3\text{CH}_2\text{O} + \text{NO}_2 + \text{N}_2\text{O} + \frac{3}{2}\text{N}_2$. A rapid first stage reaction between CH_2O , NO_2 and N_2O is shown which ends at about 0.01 sec. The second stage reaction occurs with the reduction of NO and begins at about 0.01 sec.

RAPID SCAN FTIR SPECTROSCOPY OF NITRAMINES

Thomas B. Brill, Richard J. Karpowicz, Yoshio Oyumi
Department of Chemistry, University of Delaware
Newark, Delaware 19716

The identity and structure of the chemical species in the solid and liquid phase of nitramines near their melting points are ill-defined. An experimental attack with the goal of defining the nature of condensed phase of energetic materials in real-time has been undertaken in our laboratory. Our current effort is concentrated on developing and using rapid scan FTIR spectroscopy for this role. The results have been very promising. For the first time, an answer has been provided for one of the longer-standing questions of importance in the nitramine field; *i.e.*, what is the chemical nature of RDX and HMX melts? Also for the first time, the molecular structure of RDX in the gas phase and the comparative structures of RDX and HMX in the solid, solution, melt and gas phases have been addressed. An empirical characterization of AZMTTC was accomplished by joined study using rapid-scan FTIR and X-ray crystallography.

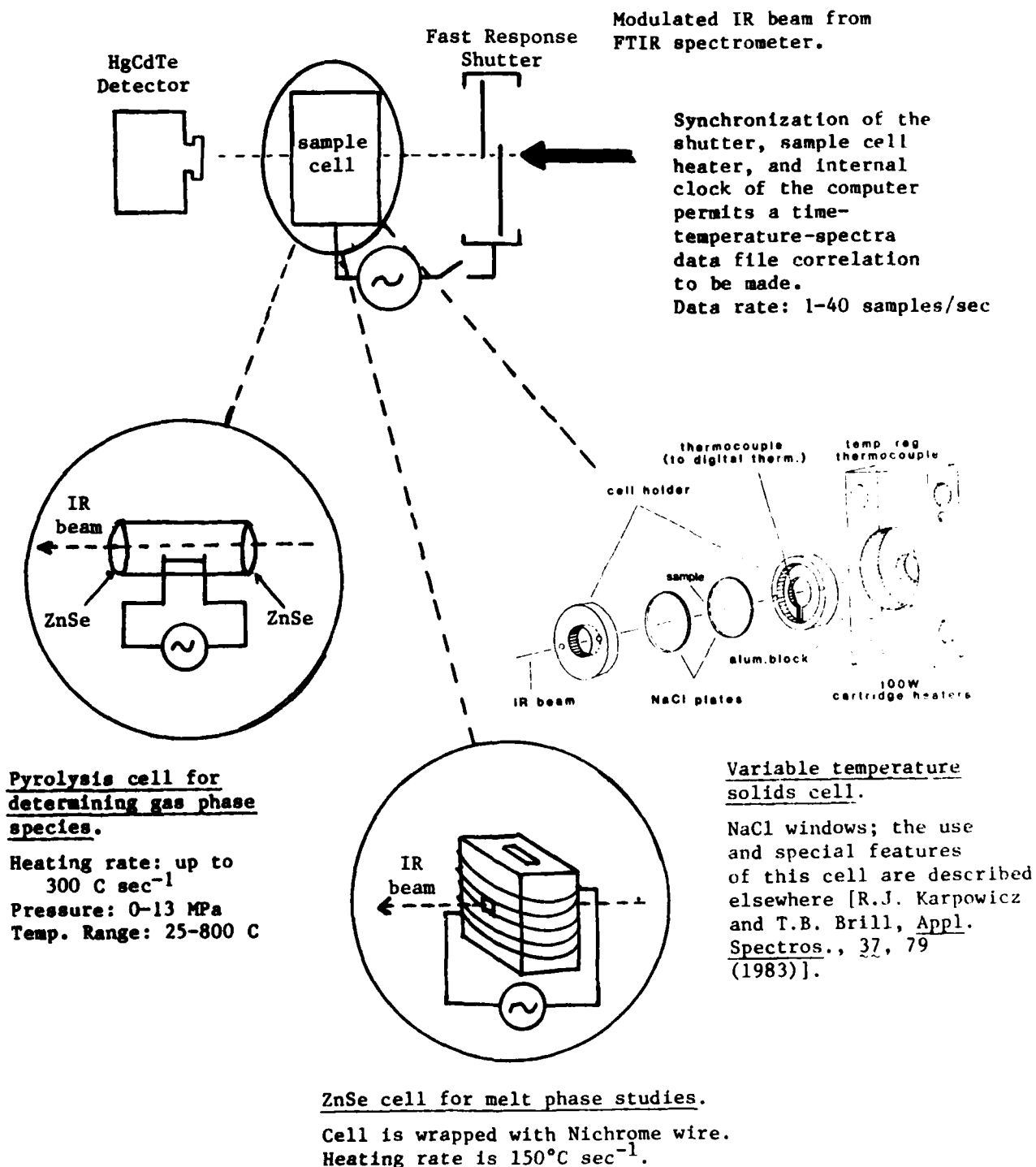
The "melt" phase of RDX and HMX was spectroscopically characterized. With a heating rate of 150 C sec^{-1} the spectra reveal that freshly melted RDX (<3 sec old) is comprised of at least 95% intact RDX. The steady-state concentrations of the intermediate degradation species in the condensed phase are below the level detectable by FTIR. The predominant liquid phase degradation product appears to be an amide such as N-hydroxymethyl-formamide. HMX decomposition occurs to some extent before the melt forms, but the fresh melt is mostly composed of intact HMX.

The molecular structure of RDX in the α and β solid phases, in solution, in the melt, and in the gas phase was determined by FTIR. No information was previously available on the β -RDX solid, the melt, and the gas phase. The molecule has essentially relaxed to C_{3v} symmetry in all phases except the α -RDX solid phase where it has C_1 symmetry. The similarity of the molecular structure of HMX in the melt to that in CD_3CN solution was established. It has mostly the chair-chair conformation.

The azidomethyl derivative of HMX, $C_4H_8N_4(NO_2)_3(CH_2N_3)$, called AZMTTC prepared by Frankel, Woolery and Flanagan (Rocketdyne) was examined by X-ray crystallography and rapid-scan FTIR. The decomposition mechanism was empirically determined. An unusually long C-N₃ bond exists. The initial gas phase decomposition product is HN₃ from cleavage of this bond, but HN₃ is rapidly eclipsed in concentration by N₂O and CH₂O formed from the nitramine portion of the molecules. The IR spectrum of the solid phase during degradation supports this observation as does the sequence of weight loss from a TGA study of AZMTTC. The decomposition is triggered by liberation of a small amount of HN₃ owing to the weak C-N₃ bond. At this point, the ring rapidly depolymerizes producing N₂O and CH₂O. The solid residue that remains then finally degrades.

Approach

Rapid Scan FTIR Studies of Nitramines



Accomplishments

Fig. A. RDX

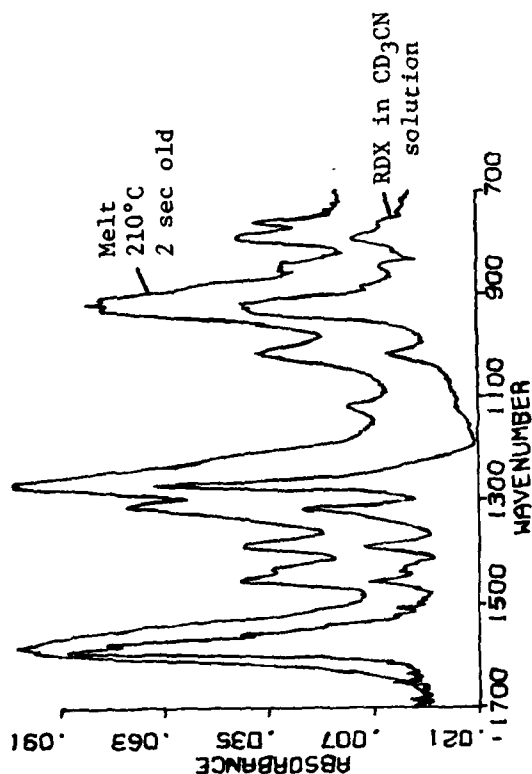


Fig. B. HMX

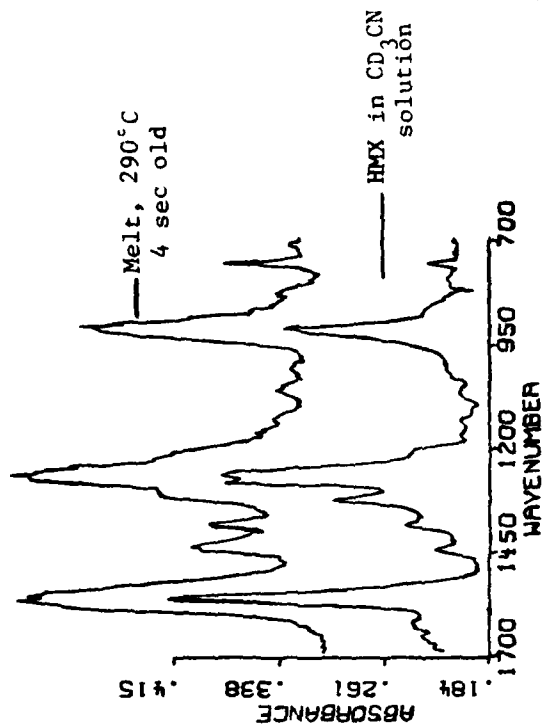
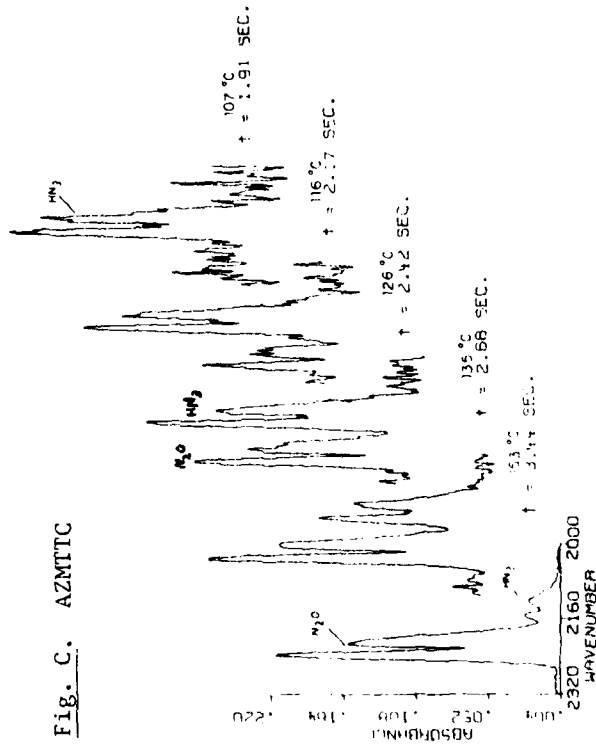


Fig. C. AZMTTC



Figures A and B show FTIR spectra of the melt phase of RDX and HMX compared to CD₃CN solutions with solvent subtraction of these nitramines. Very significant spectral similarities exist. These are the first composition studies of nitramine melts and they show that the fresh melts are >95% intact RDX and HMX molecules.

Figure C shows the rapid-scan FTIR spectra of the gas phase during pyrolysis of solid AZMTTC. Note the HN₃ initially forms, but this product is quickly dominated in concentration by N₂O. Mechanistic information has been extracted from these data (see text).

SOLID PROPELLANT TRANSIENT RESPONSES

Robert L. Glick and John R. Osborn
Purdue University
W. Lafayette, IN 47907

Study addresses nonsteady interactions between flowfield in semi-enclosed duct with deflagrating walls of heterogeneous, condensed media and that deflagration process. Figure 1 illustrates basic physics and approach. Monotonically increasing flow Reynolds number leads to laminar, transitional, and fully developed turbulent flow sequence. However, deflagration produced normal flow and turbulence kinetic energy lead to unique features: inflow stabilized turbulence fronts and sequential turbulization and profile transition. As deflagration process is dependent upon pressure and fine scale turbulence close to wall and flowfield depends upon both deflagration induced flow and turbulent kinetic energy, flowfield/deflagration coupling is also unique. Key scientific questions are roles of turbulence front, bursting turbulence, and deflagration produced turbulence in nonsteady interaction and surface population fluctuations in heterogeneous deflagration. Approach is to define nonsteady burning of heterogeneous media and turbulent kinetic energy production experimentally with local, optical remote sensing technique; flowfield to be defined with combination of analysis, gross profile measures, and cold flow measures in another program; coupling to be defined experimentally at macro (transfer function) level in semi-enclosed duct apparatus forced into axial mode oscillations. All studies are unique to this program; local burning rate technique will open way to greatly improved understanding of same thru two point correlations.

Key accomplishments were concerned with the semi-enclosed duct apparatus and flow field analysis. Magnetic velocimeter design was thoroughly reviewed; field coil design was improved; circuit constraints needed for good bandwidth were developed. Similarity solution obtained for nonsteady, two-dimensional flowfield near velocity antinode in porous and semi-porous ducts showed significant normal velocity effect; acoustic boundary layer on blown surface is thickened. For blowing Reynolds numbers $> 10^4$ (typical) acoustic layer fills duct while acoustic velocities become independent of viscosity and lead mean acoustic velocity roughly $\pi/2$ near blown wall. Figure 2 illustrates magnitude of acoustic velocity for semi-porous duct (blowing Reynolds number 20,000; frequency Reynolds number 2×10^5 ; permeable wall at nondimensional distance 0). Note damped oscillatory character of the acoustic velocity field that fills the duct and overshoot near wall. Acoustic layer on impermeable wall is that expected on blown surface showing clearly that utilization of this thickness as small parameter for flowfield/deflagration studies is bad physics. Out of phase acoustic velocity near transpired surface implies reverse flow (inflected velocity profiles) at amplitudes far below those for mean flow reversal. Therefore, potential for energy transport from mean to nonsteady flow seem probable; may be mechanism for strong, non-linear wall heat flux/flowfield coupling observed by Brown. Analysis of near wall region shows these effects can be expected in tangential mode oscillations and that pressure coupling can modify phenomena.

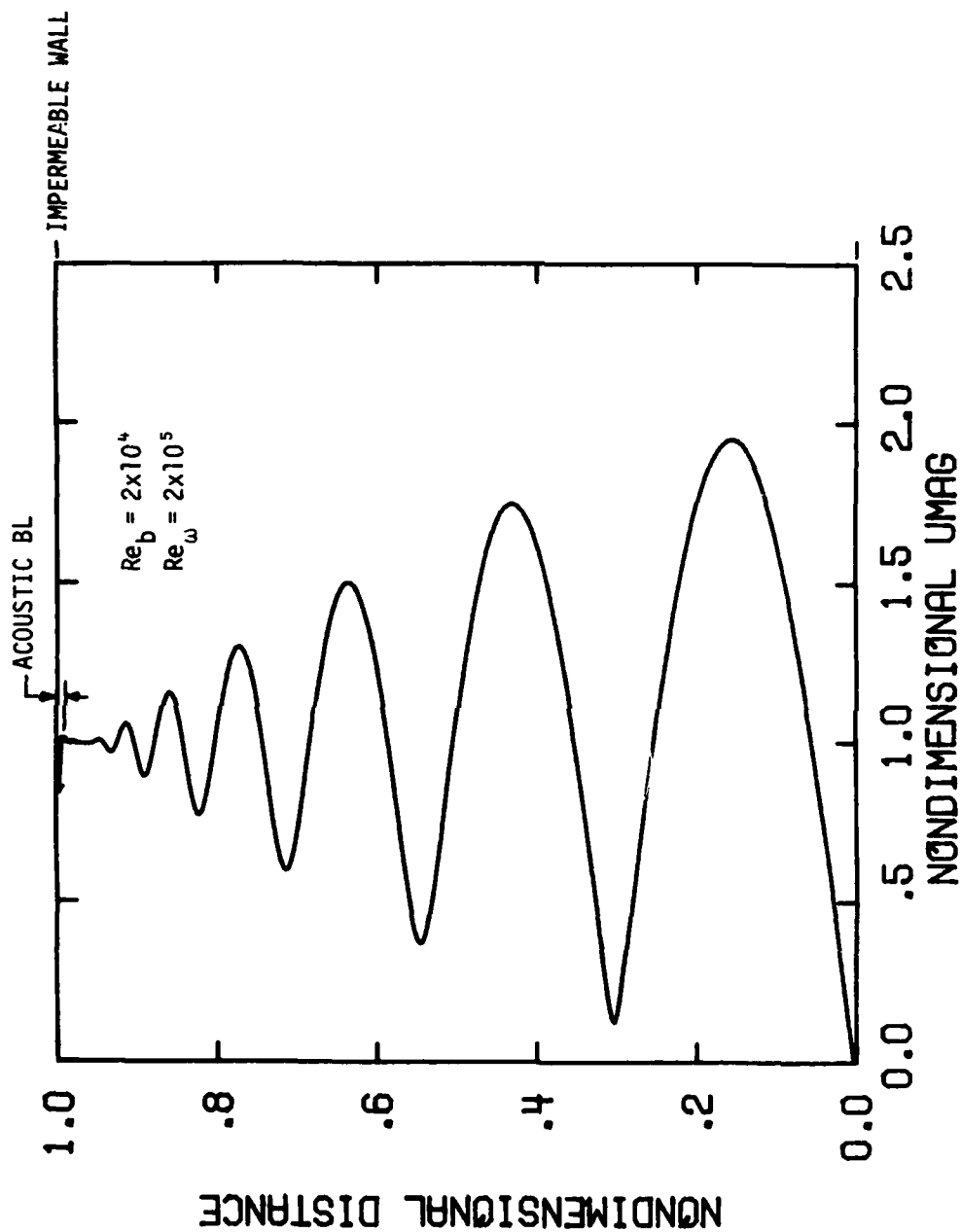


Figure 2. Acoustic Velocity Field in Semi-Porous Duct.

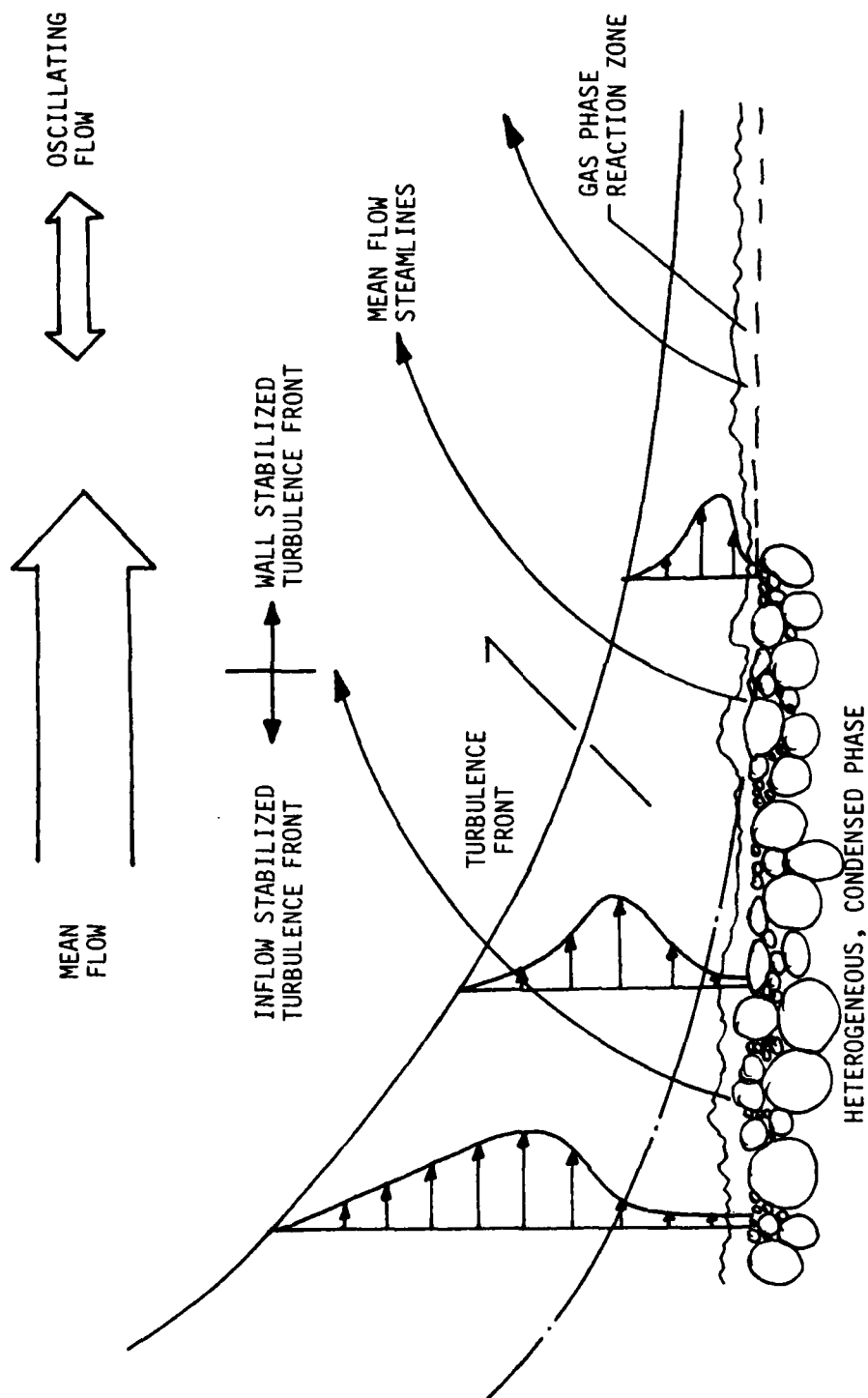


Figure 1. Schematic Illustrating Physics and Approach.

FUEL RICH PROPELLANT COMBUSTION BEHIND A BLUFF BODY

**Warren C. Strahle
Jechiel I. Jagoda**

**School of Aerospace Engineering
Georgia Institute of Technology**

The solid fueled ramjet, as with other ramjet types, requires a flame anchoring region at the head of the combustion region. This is frequently provided by a recirculation zone behind a backward facing step as shown in Fig. 1. The scientific question being posed is whether or not this flow field is predictable. The flow field is enormously complex, containing interactions between many processes, and many features of the flow absolutely require advanced diagnostics for interrogation of the field. On the other hand, there are regions of the flow field for which conventional intrusive diagnostics are superior to the non-intrusive, optical ones, so a variety of techniques are being used.

The analytical approach is currently based upon $k-\epsilon$ modelling methods. This is being carefully monitored as the experimental results come in from more and more complex flows. A modification has already been made in the treatment of pressure velocity correlation which improves the non-bleed cold flow reattachment length in comparison between theory and experiment. A unique feature of the program is the union of coworkers in both theory and experiment at the same laboratory to ensure valid modelling.

Current work has proceeded through the cold-flow, no-bleed phase. An example of the many techniques used for measurement, and their comparison with theory is shown in Fig. 2, where the mean velocity profile near the step is shown. Shown are our measurements and also those obtained at another laboratory with a highly similar configuration. Experiments compared well with the theory. More importantly, in regions of overlap of validity of the various measurement methods (near the freestream), there is very good agreement between methods; in the region where use of the laser is absolutely required (regions of reversed flow, intermittent reversed flow and near zero velocity) the ability to obtain data is substantiated.

TYPICAL TECHNICAL ISSUES

GRADIENT DIFFUSION HAS ALWAYS BEEN ILL-FOUNDED

LDV and Rayleigh scattering are being used to investigate regions of the flow where it fails and to suggest reconstructed models.

FINITE RATE KINETICS REQUIRED FOR EXTINGUISHMENT PROBLEM

Finite kinetics in turbulence require off-equilibrium modeling techniques which are now being developed.

MULTIPLE RECIRCULATION ZONES

LDV imperative for finding these by non intrusive means

BOUNDARY CONDITIONS ARE ILL-FOUNDED

Law of the wall does not strictly hold, especially near the rear stagnation point. Stagnation point solutions are being investigated.

k-ε METHODS TRADITIONALLY UNDERPREDICT REATTACHMENT LENGTH

A method of treatment of the pressure velocity correlation has corrected this for cold flow and it is being checked with bleed flow.

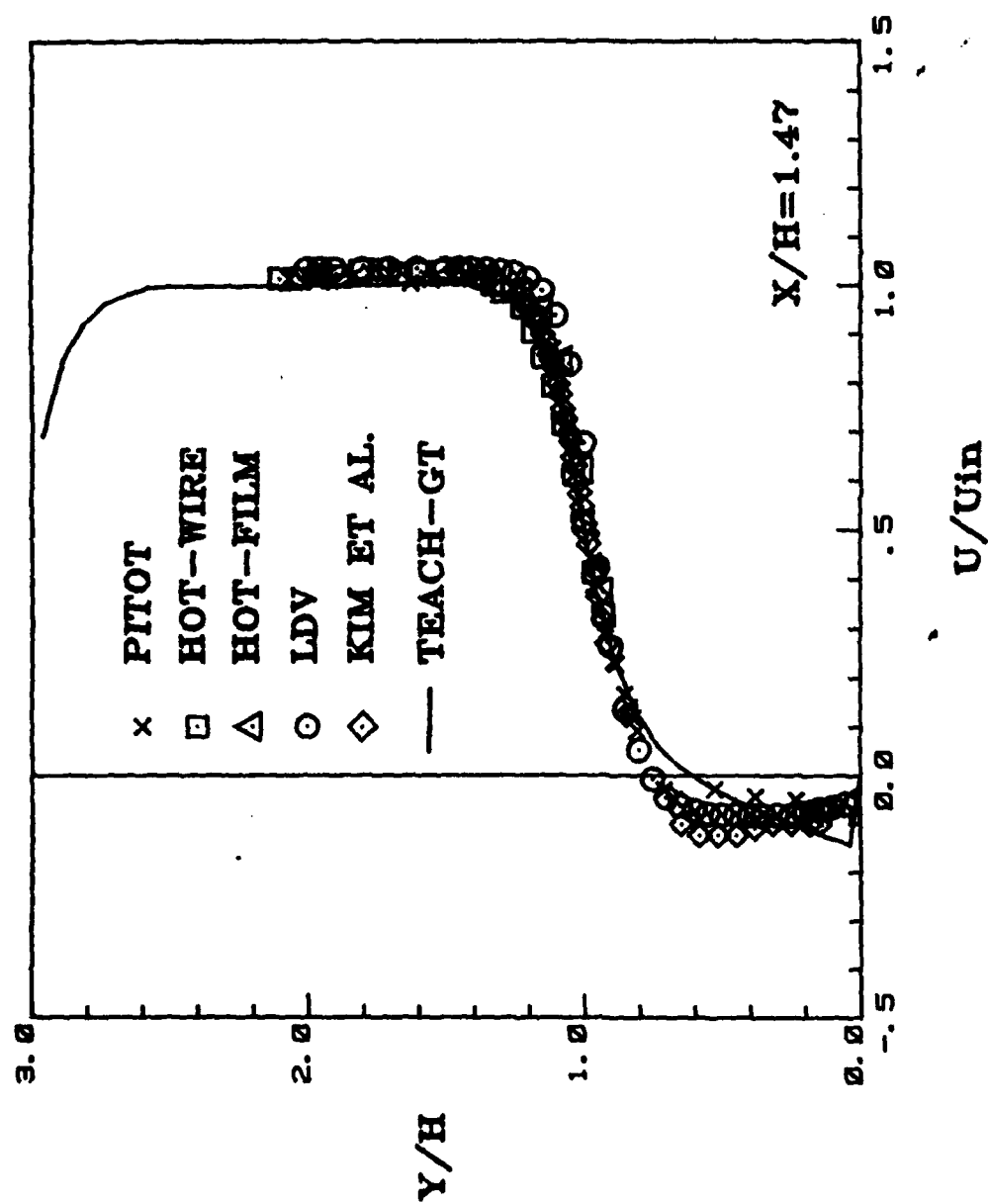
RELATIVE TURBULENCE INTENSITIES GO TO INFINITY

LDV with frequency shift is being used to counter this measurement problem.

LOW FREQUENCY RANDOM OSCILLATIONS REPORTED IN LITERATURE

Careful facility design eliminates this oscillation, suggesting many results are configuration sensitive.





MEAN STREAMWISE VELOCITY

THE SUPPRESSION OF AFTERBURNING IN SOLID ROCKET
PLUMES BY POTASSIUM SALTS

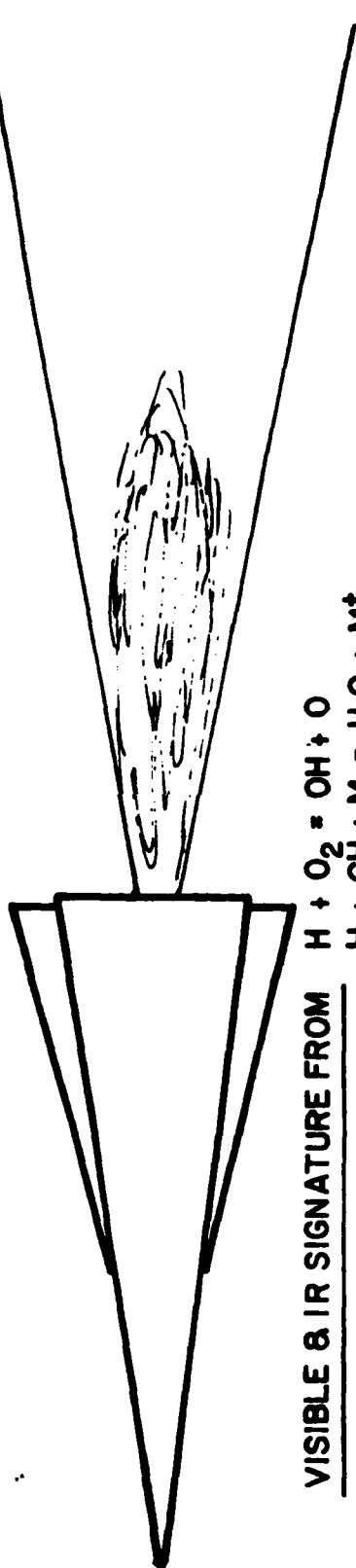
EUGENE MILLER
MACKAY SCHOOL OF MINES, CHEM & MET ENG'G DEPT.
UNIVERSITY OF NEVADA, RENO, NV 89557

In recent years, the Services have increasingly emphasized the development and use of low signature tactical solid rocket motors. Visible primary and secondary smoke have been largely eliminated by the removal of ammonium perchlorate oxidizer and most of the other energy and ballistic modifier additives from the propellant formulation - the so-called "minimum smoke" (min-smoke) propellants. The exhaust gases from min-smoke propellants however contain significant concentrations of hydrogen and carbon monoxide which when mixed with ambient air in the plume react to water and carbon dioxide producing visible flash and increased infrared radiation. Also, some of the apparent secondary smoke advantage of min-smoke propellants over reduced smoke propellants (ammonium perchlorate oxidizer with low aluminum content) is lost since the hydrogen in the plume reacts to form additional water which is available for potential condensation to smoke. The research is directed toward preventing or at least inhibiting the signatures due to afterburning.

It is known that potassium salts inhibit the reactions of hydrogen and carbon monoxide to water and carbon dioxide respectively. Potassium salts such as KNO_3 and K_2SO_4 have been added to propellant charges at a level of 1 - 3 wt pct to suppress gun muzzle flash and rocket plume infrared signature. The mechanism by which the potassium salts inhibit afterburning is controversial, but it probably involves K , KOH and possibly KO_2 reacting with H and OH radicals to break the chain reactions controlling the combustion of hydrogen and carbon monoxide. Since experimental evidence indicates that only small concentrations of the K , KOH and KO_2 are required, the amounts of salt that have been used previously in guns and rockets may have been excessive. Minimizing the amount used is important because the potassium salts increase radar signatures and the propensity for smoke formation.

The effects of potassium, KOH and KO_2 on the afterburning reactions will be studied by introducing them as a vapor into a flat diffusion flame of methane- O_2 - N_2 and scanning the flame incrementally by infrared and visible spectroscopy. It should be possible to define the conditions of gas composition and temperature for which they are effective. An opposed-jet diffusion burner and gas flow system is already being used for related afterburning research. A modified vaporizer-burner head is being built to permit the vaporization of the potassium and the salts prior to entering the flame. A Beckman IR spectrophotometer has been modified for detection of emission spectra and the scanning device is in place.

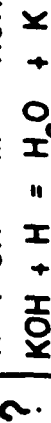
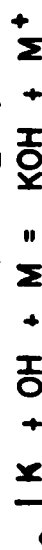
MIN-SMOKE SOLID ROCKET PLUME AFTERBURNING:



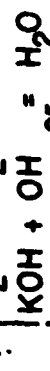
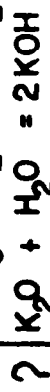
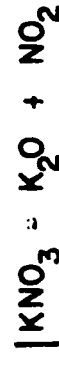
VISIBLE & IR SIGNATURE FROM



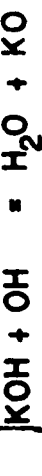
SUPPRESS w/ KNO₃ or K₂SO₄ ADDITIVES



or



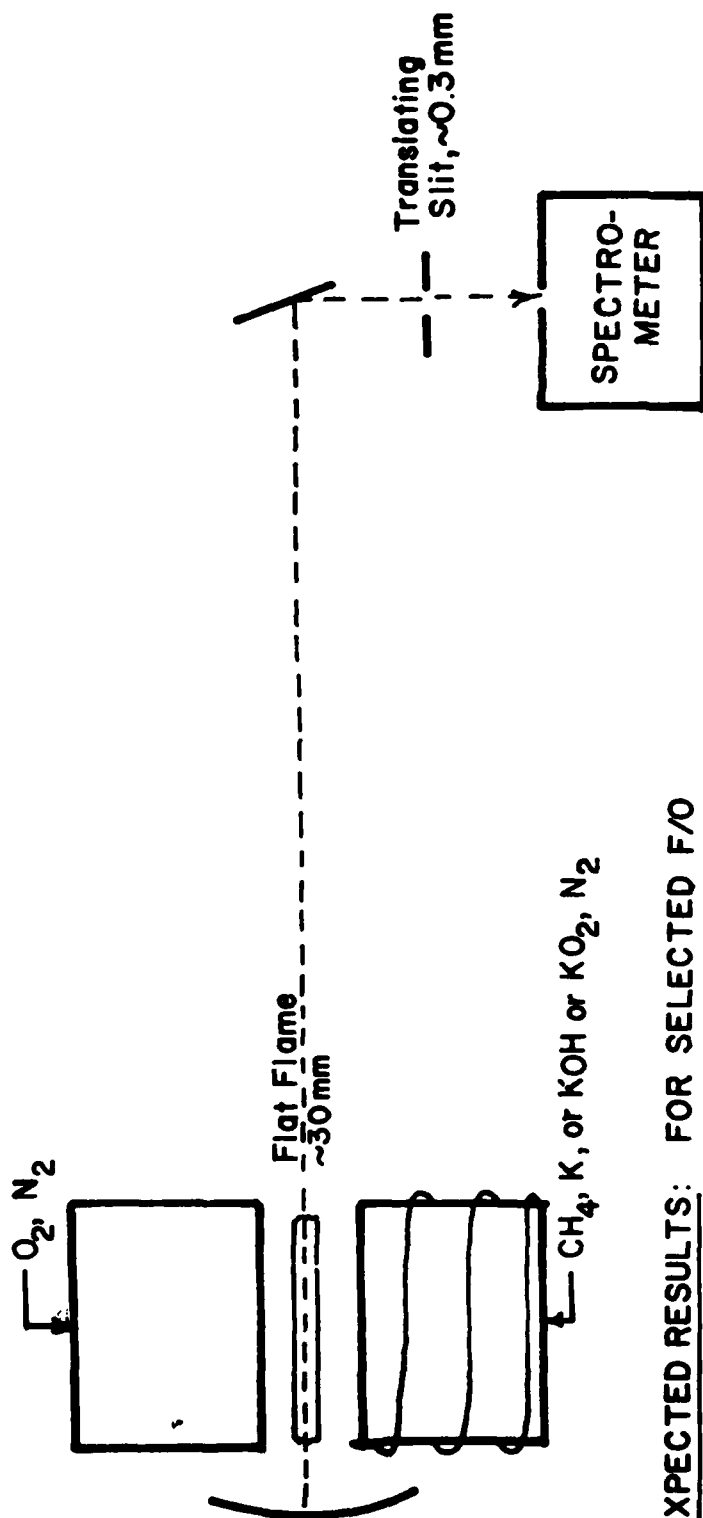
or



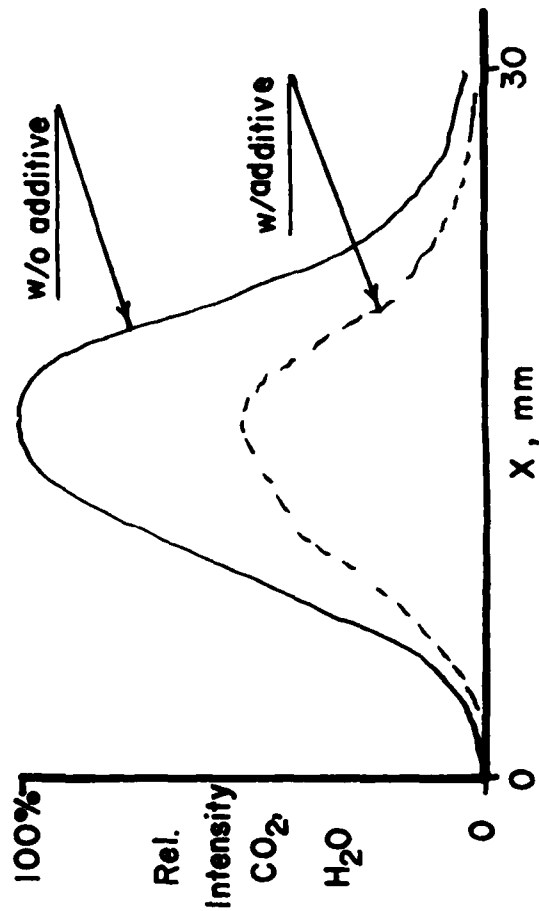
GOALS

- ESTABLISH MECHANISM & CONDITIONS REQ'D FOR SUPPRESSION
- DEFINE AS FUNCTION OF SPECIES, CONCENTRATION, F/O & T

EXPERIMENTAL APPROACH



EXPECTED RESULTS: FOR SELECTED F/O



AFTERBURING SUPPRESSION KINETICS

JAY D. EVERSOLE

**University of Dayton/ Air Force Rocket Propulsion
Laboratory, Edwards AFB, CA 93523**

Methods of reducing or suppressing rocket afterburning have been pursued largely on an empirical basis. This paper describes current research efforts to combine experimental studies of flame suppression with a computational model in order to determine conclusively the detailed chemical kinetic mechanisms for specific suppressant species.

The experimental arrangement consists of a premixed flat flame burner mounted on a motorized X-Y-Z platform. The flame is currently run at atmospheric pressure, but will eventually be enclosed in a vacuum chamber to allow operation at reduced pressures. Flow rates of the hydrogen, oxygen, and nitrogen to the burner and the temperature of the porous plug are monitored during operation. An attempt has been made to achieve laminar one-dimensional flow in the flame zone. Gas temperature and molecular hydrogen concentration profiles as a function of axial distance are determined by spontaneous Raman scattering. Hydrogen bromide has been introduced as a suppressant species into the premixed gases, and efforts are being made to introduce potassium vapor as a suppressant. Figure 1 is a schematic representation of the experimental approach. Additional diagnostic measurements will be made to determine intermediate specie concentrations.

The computational model incorporates detailed reaction kinetics with laminar one-dimensional flow. Resulting temperature and specie mole fractions are plotted as a function of axial distance. The rate constants for a basic set of seventeen elementary reactions of the hydrogen/oxygen flame are known with reasonable accuracy from previous work, and comparisons of calculated flame structure to published data and calculations have resulted in good agreement (Fig. 2). Therefore, the effect of adding a particular suppressant species to the flame may be characterized by adding a hypothesized set of reactions (and their rates) involving that species to the baseline set. For hydrogen bromide a five-reaction set has been postulated, and for potassium a two-reaction set has been considered. Comparison of predicted quantities and experimental measurements are then made for both the baseline and suppressed cases. For conclusive identification of a kinetic mechanism, agreement between the calculated and measured profiles must be achieved over a wide range of initial conditions (pressure, dilution, suppressant concentration, and stoichiometry) at the same time that any alternate reactions (or rates) do not generate the same results.

1. Dixon-Lewis, G., Proc Royal Soc London, 292, 45-99 (1979).
2. Dixon-Lewis, G., Combustion and Flame, 36, 1-14 (1979).
3. Jensen, D.E., Jones, G.A., Chem. Soc. Faraday I, 75, 2377-85 (1979).

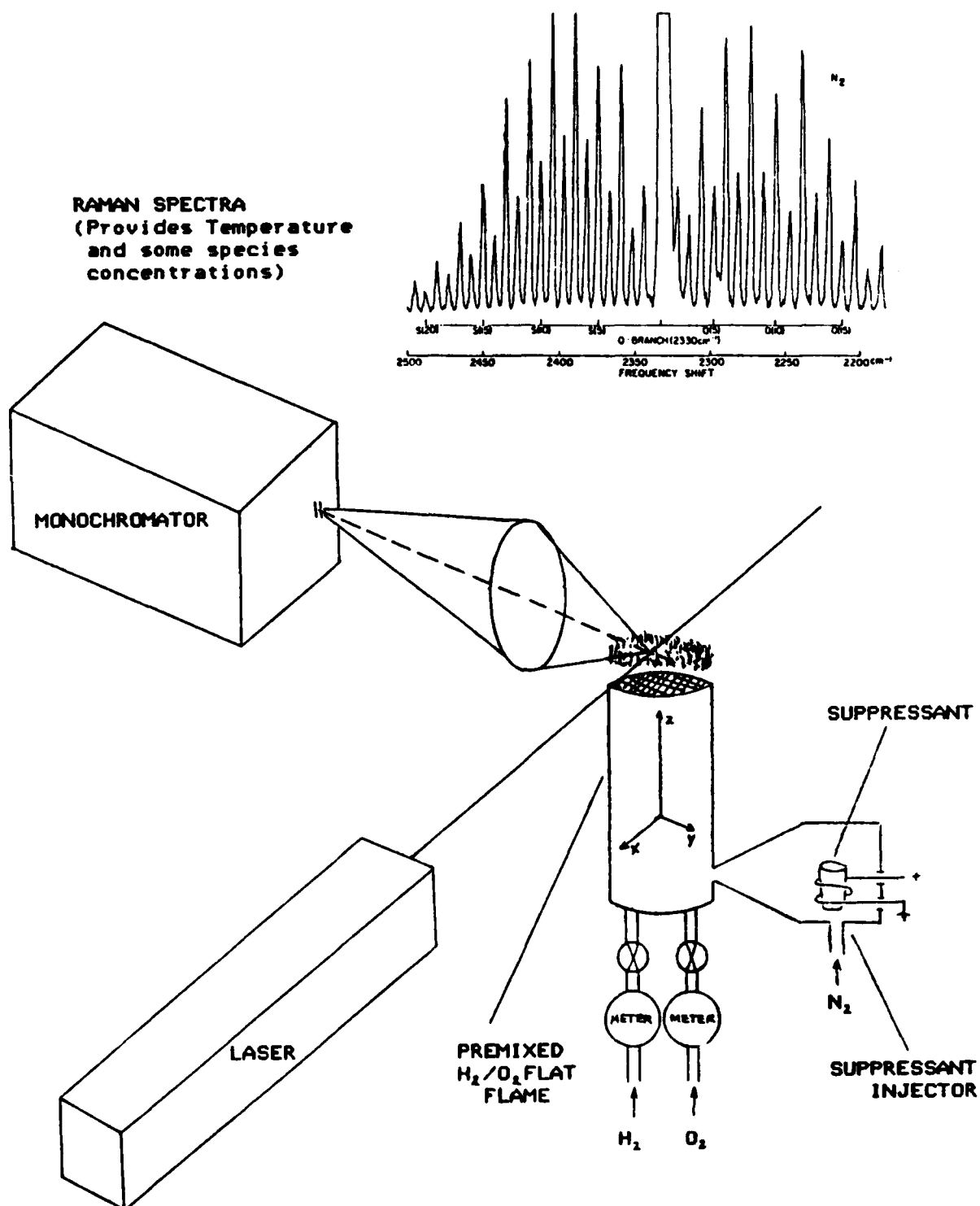


Figure 1. Schematic drawing of H_2/O_2 flat flame burner and suppressant species injector, and laser diagnostics arrangement. Spatial maps (primarily Z-axis) of temperature and species concentrations are obtained from data (Raman scattering, LIF) by translating burner.

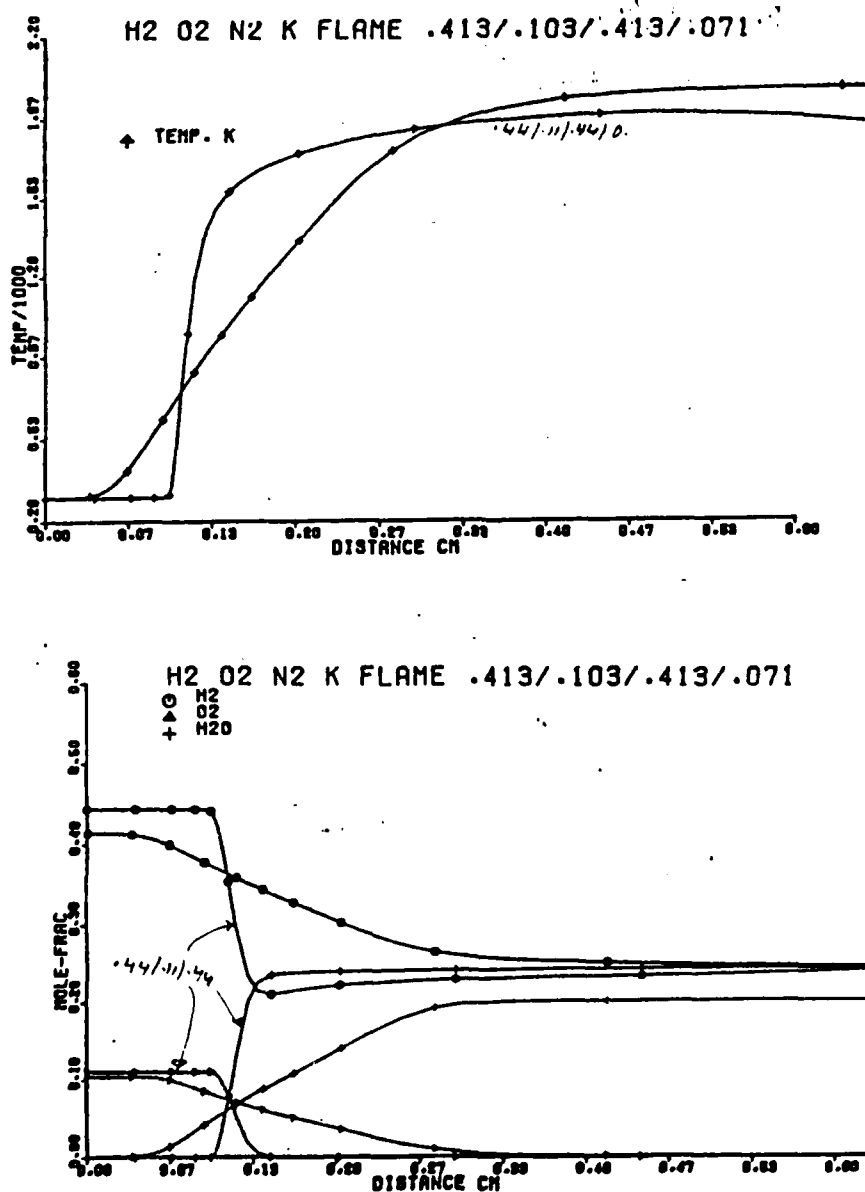


Figure 2. Shows calculated Z-axis profiles of temperature (upper curves) and major species concentrations (lower curves) for baseline and suppressed $H_2/O_2/N_2$ flame. For the baseline case the narrow flame zone is located at about 0.1 cm by the steep gradients of the profiles. When 7% mole fraction of potassium is added, the flame zone is extended by over an order of magnitude as shown by the much smaller gradient of all the profiles.

COMBUSTION KINETICS OF METAL OXIDE AND HALIDE RADICALS

Arthur Fontijn

Department of Chemical Engineering and Environmental Engineering
Rensselaer Polytechnic Institute, Troy, NY 12181

Current ability to influence combustion involving metals is severely hampered by a lack of understanding and knowledge of the ways and manner by which temperature affects the rate coefficients of individual reactions and reaction channels. While the simple Arrhenius-type equation $k(T) = AT^{1/2} \exp(-E_A/RT)$ has over limited temperature ranges been of great value, when applied to wide temperature ranges it is often not obeyed. Particularly for exothermic and slightly endothermic reactions, order of magnitude errors can be made by extrapolations based on the Arrhenius equation¹. It is the goal of the present program to provide an insight in the kinetic behavior of metallic radical oxidation reactions, as influenced by temperature, based on accurate measurements.

Figure 1 illustrates the HTFFR, high-temperature fast-flow reactor, method we are using to generate the metallic radicals and measure their oxidation kinetics. This unique tool provides accurate measurements on isolated elementary reactions in a heat bath. With traditional high temperature techniques such isolation is usually impossible to achieve; as a result, data on any given reaction depend on the knowledge of other reactions occurring simultaneously, leading to large uncertainties. Basically, the apparatus consists of two vertical high temperature reactors in series. In the upstream reactor the metallic radical is produced, BCl in the example. In the downstream reactor the relative concentration of these radicals is measured by laser-induced fluorescence, as a function of $[O_2]$, P , T and t , to determine $k(T)$. The sensitivity of the fluorescence technique² allows observations on very low radical concentrations (10^9 - 10^{11} cm^{-3}), which prevents interference from nucleation reactions.

Figure 2 shows the type of results obtained in HTFFR studies. The Al/SO_2 reaction, which is endothermic, adheres closely to the Arrhenius equation. AlO/O_2 , the only metallic radical reaction for which information is available, has a slight negative temperature dependence due to intermediate complex formation. The Al/CO_2 reaction increases with temperature much faster than Arrhenius would predict, probably due to the thermal equilibrium increase in the concentration of CO_2 in bending vibrational modes which, contrary to ground-state linear CO_2 , can react with Al at larger distances by an electron jump mechanism. This behavior of the AlO/O_2 and Al/CO_2 reactions was not predictable and indeed unexpected. By obtaining data on a number of metallic radical oxidation reactions, we anticipate to provide a basis for understanding and hence prediction.

1. A. Fontijn and R. Zellner in "Reactions of Small Transient Species. Kinetics and Energetics", A. Fontijn and M.A.A. Clyne, Eds., Academic Press, 1983, Chap. 1.
2. A. Fontijn, "The Use of Laser-Induced Fluorescence for Fundamental Gas-Phase Kinetic Measurements", Progress in Astronautics and Aeronautics, in press.

HIGH TEMPERATURE COMBUSTION KINETICS OF METALS

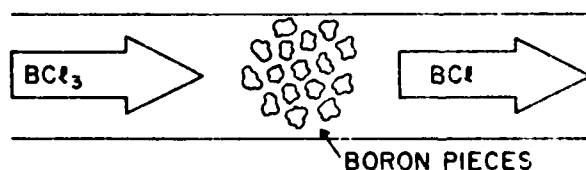
SCIENTIFIC APPROACH

GOALS

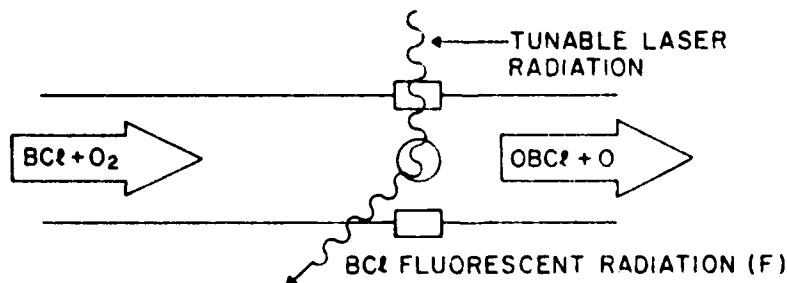
- UNDERSTAND THE MECHANISMS OF METALLIC RADICAL OXIDATION REACTIONS.
- MEASURE REACTION RATE COEFFICIENTS FOR REACTIONS IMPORTANT TO ADVANCED PROPULSION SYSTEMS:
 - $\text{BCl} + \text{O}_2 \rightarrow$ Emissions from Air Breathing Missile Plume After Burning
 - $\text{AlO} + \text{CO}_2 \rightarrow$ Combustion of Aluminized Composite Propellants
 - $\text{BO} + \text{O}_2 \rightarrow$ Combustion of Boron Slurries
 - $\text{AlCl} + \text{O}_2 \rightarrow$ Microparticulates Formation
 - $\text{AlF} + \text{O}_2 \rightarrow$ Tendency of Fluorinated Binders to Reduce Agglomeration
- OBTAIN THESE $k(T)$ DATA OVER THE 300-2,000 K RANGE. NON-ARRHENIUS BEHAVIOR PRECLUDES EXTRAPOLATION FROM NARROW TEMPERATURE INTERVALS.

TECHNIQUE

1. PRODUCE REACTANT IN HIGH TEMPERATURE FLOW TUBE



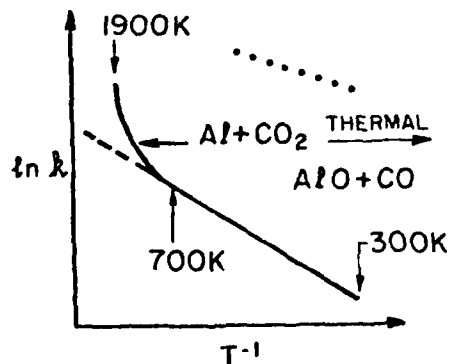
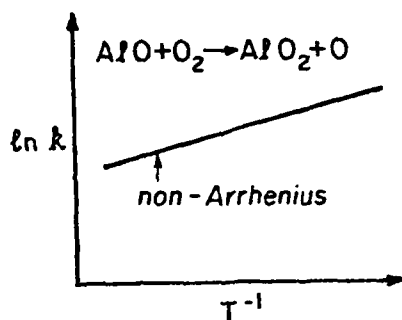
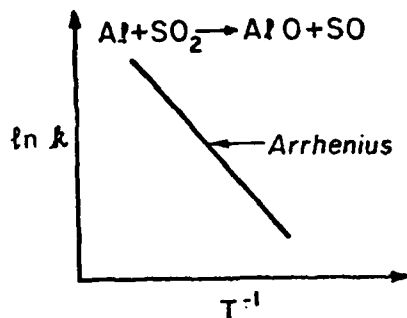
2. REACT WITH OXYGEN IN VARIABLE TEMPERATURE FLOW TUBE



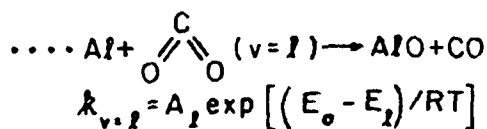
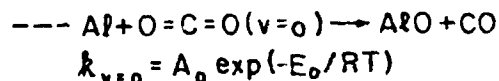
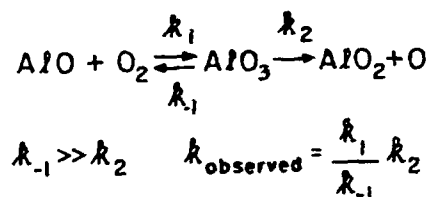
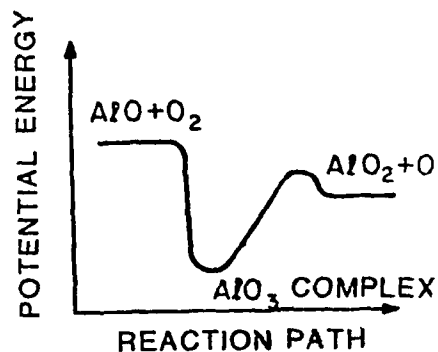
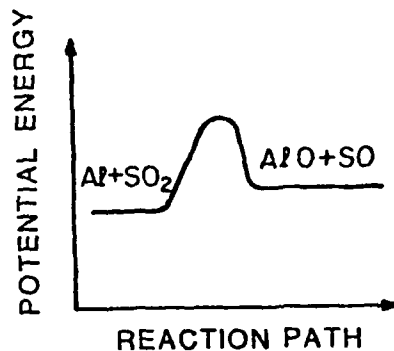
$$\ln \frac{F_{t=0}}{F_t} = k(T)[\text{O}_2]t$$

ACCOMPLISHMENTS

OBSERVATION



INTERPRETATION



$A_1 \gg A_0$, i.e. BENT CO_2
HAS MUCH LARGER REACTION
CROSS SECTION THAN LINEAR CO_2

WIDE DISTRIBUTION PROPELLANTS

Robert A. Frederick, Jr., John C. Matson and John R. Osborn
School of Aeronautics and Astronautics
Purdue University
W. Lafayette, IN 47907

Composite propellants containing a wide AP particle size distribution have exhibited unpredictable ballistic properties. Highly loaded propellants of this type do not burn continuously but show local stepwise burning patterns at the propellant surface. The propellant burns quickly for a short period of time, then "rests" for a short period of time. The increments of burning occur over distances comparable to the diameter of the coarse AP, while the rest period has been linked to the energetic properties of the binder for IPDI and DDI formulations.

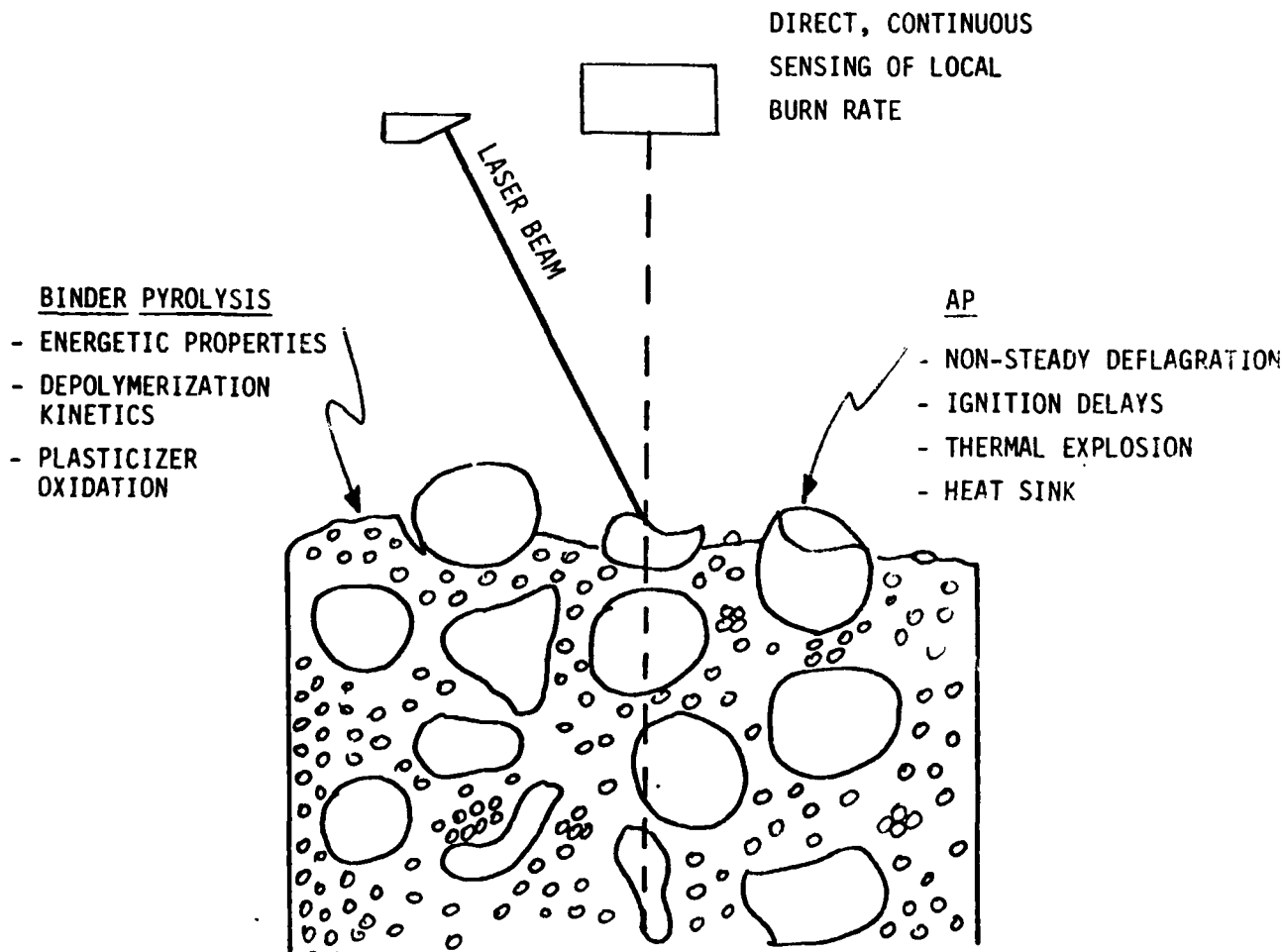
These observations challenge previous conclusions that propellant burning rate is controlled largely by the deflagration of individual oxidizer crystals and their surrounding binder. Scenarios which describe propellant combustion as strictly a time average or area average process are inadequate to describe this local intermittent combustion. It now appears possible that AP particle ignition and binder pyrolysis are controlling combustion mechanisms, at least for wide distribution formulations.

The goal of this research program is to verify that local stepwise burning of solid propellants occurs and to identify the physical processes that control the duration of the burn periods and "rest" periods. Perfecting a technique to continuously measure the local burning rate is a major task in achieving this goal. Measurements will first be completed using high-speed photography as a preliminary screening tool. The desired technique, however, is a direct measurement using a laser position detector (LPD). This LPD is being designed and developed to continuously record spatially local (40 micron diameter circle), high resolution (20 micron) distance measurements. With an adequate technique perfected, systematic composition variations will be examined to determine the roll of AP ignition and combustion properties, and the energetic nature of the binder on the local and average burning rate. Specifically, the binder curative, oxidizer modal size ratio, and pressure will be investigated as independent variables.

The significant achievement to date has been the continuous measurement of average burning rate of solid propellant burning at atmospheric pressure by sensing the position of a modulated laser beam reflected from the propellant surface. The instrument tested compensated for the variable optical properties of the propellant surface and the combustion gases.

FEATURES OF APPROACH

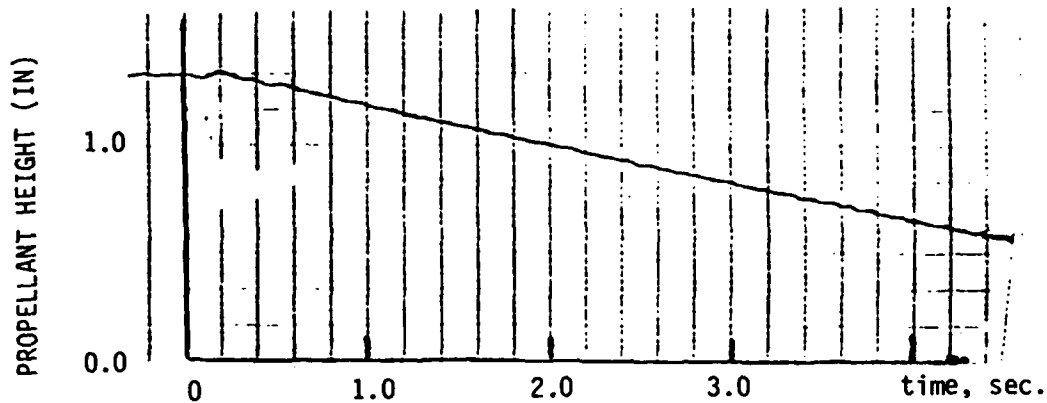
- o HETEROGENEOUS SURFACE CHEMISTRY
 - LARGE SIZE DIFFERENCE BETWEEN COARSE AND FINE AP
- o FIRST DIRECT MEASUREMENTS
 - MEASUREMENT OF LOCAL MICROSCOPIC NON-STEADY BURNING
- o SYSTEMATIC VARIATIONS
 - AP DECOMPOSITION CHARACTERISTICS
 - BINDER ENERGETICS



PRIMARY SCIENTIFIC ACCOMPLISHMENTS...

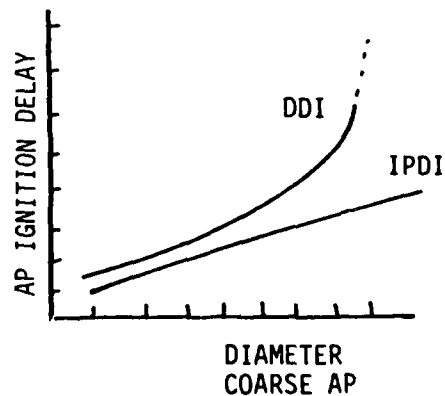
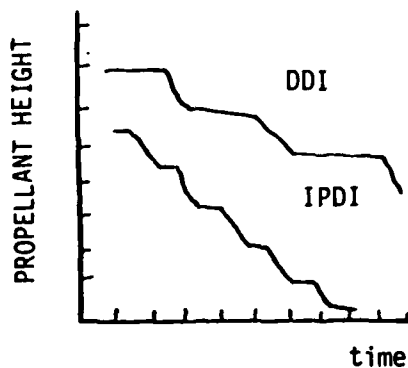
o ACHIEVED

- CONTINUOUS MEASUREMENT OF SURFACE HEIGHT AT ATMOSPHERIC PRESSURE



o ANTICIPATED

- EFFECT OF BINDER ENERGETICS ON MICROSCOPIC NON-STEADY COMBUSTION
- EFFECT OF SURFACE HETEROGENEITY ON AP IGNITION DELAYS



BEHAVIOR OF ALUMINUM
IN SOLID PROPELLANT COMBUSTION

Edward W. Price and Robert K. Sigman
Georgia Institute of Technology
Atlanta, Georgia

This research addresses the unique behavior and role of low volatility ingredients in combustion of solid propellants. Such ingredients include metal powders (fuel), ballistic modifiers, and combustion stabilizers. Because of low volatility, such ingredients tend to concentrate in varying degree on the burning surface, and their performance is strongly affected by processes that occur at the surface in the concentrate. This aspect of propellant combustion is not embodied in any combustion theory, and its importance was not generally recognized until its role in aluminum behavior forced more detailed study.

Because of the complexity of surface behavior, a variety of strategies is required to clarify underlying mechanisms, strategies ranging from thermal testing of individual propellant ingredients to combustion of specially formulated propellants (Fig. 1). In the present paper, results are presented from studies of edge-burning of "sandwiches" (laminates of two sheets of oxidizer with a binder lamina between). Combustion is observed by high speed photography and by microscopic study of quenched samples (Fig. 2). The low volatility (powdered) ingredient is contained in the PBAN binder lamina. This combustion system is used because of the extensive correlation of observable results and combustion mechanisms that has been developed on a companion project.

Tests have been run on sandwiches with several additive materials that are used as ballistic modifiers or combustion stabilizers in propellants. The materials tested can be classified (Fig. 2) in two categories that give contrasting results.

Type 1 Al_2O_3 , B_4C , ZrC , CuO : These additives do not concentrate on the burning surface appreciably, and have little or no effect on burning rate or quenched burning surfaces.

Type 2 Fe_2O_3 , $\text{Cu}_2\text{Cr}_2\text{O}_4$: These additives concentrate on the burning surface (binder). They cause increased burning rate, and modify the sample surface in a manner that has been found to result from increased proximity of the oxidizer-binder flamelets to the surface. These two ingredients are known catalysts of burning rate or propellants.

The results indicate that effective ballistic modifiers must form "catalyst beds" on the burning surface, in which the large molecular weight vapors from the polymer are broken down into more easily oxidized fuel fragments. The quenched samples indicate that the oxidizer-binder flame stands correspondingly closer to the surface, explaining the higher burning rate.

This interpretation was tested by addition of Fe_2O_3 to a specially formulated control propellant, and an aluminized version of that propellant, with results consistent with the catalyst bed, fuel-cracking interpretation.

Experimental Methods


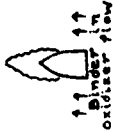


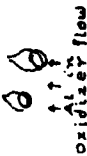
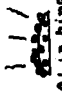



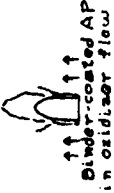


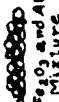
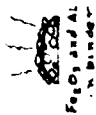



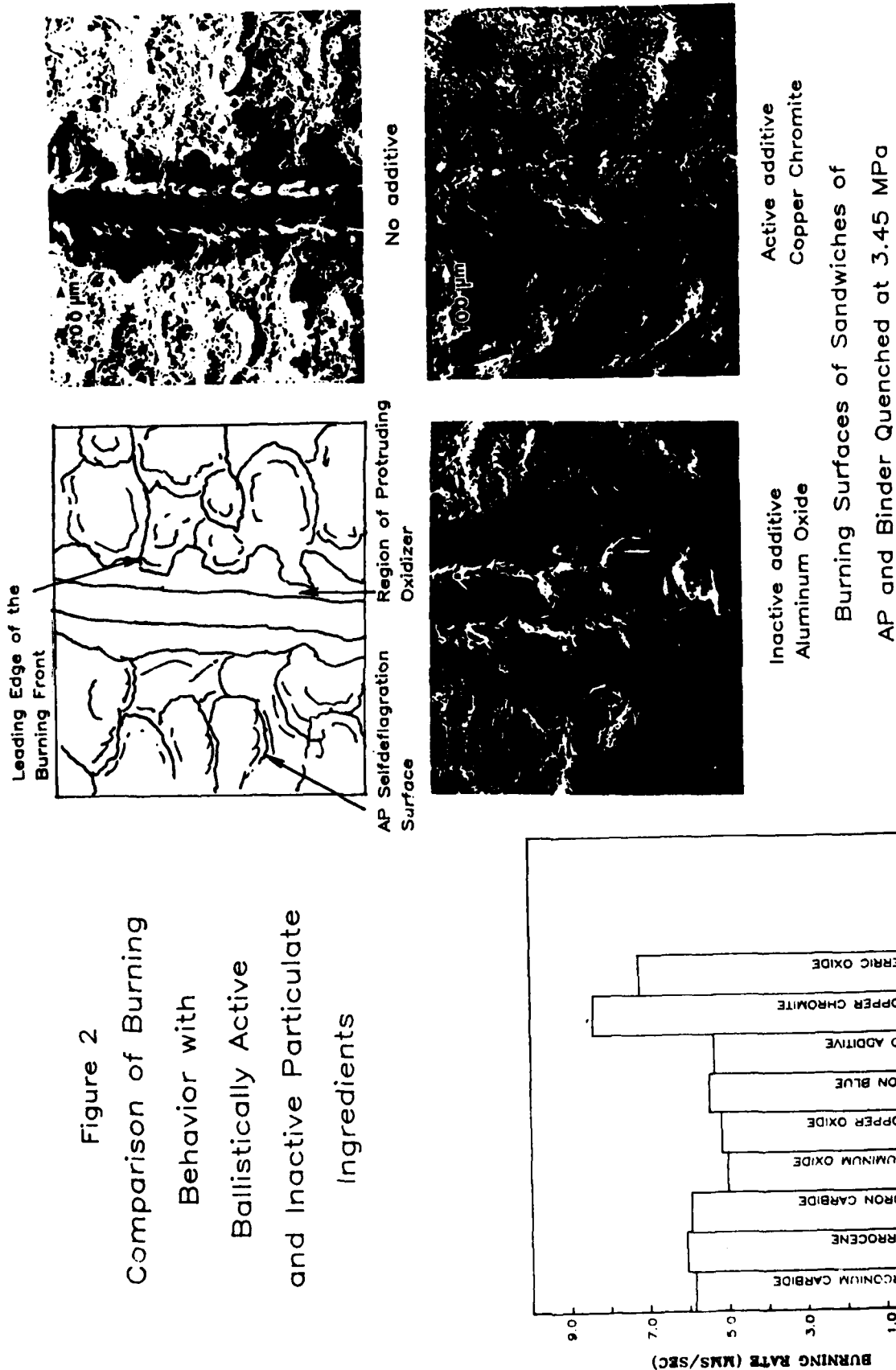
	Response to Controlled Heating	Combustion in Controlled Gas Atmosphere	Combustion of Ingredient Combinations in Geometrically Simple Systems	Combustion of Propellants
	Objective of Experiments			
Pure Ingredients Volatiles	Determine environment of concentration of nonvolatiles	Extend thermal response observations to controlled combustion zone conditions	Extend observations to propellant-like combustion system, retaining simple geometry	Test relevance of simpler tests, theory; seek additional effects
	Determine interaction of nonvolatile particles in concentrate			
Pure Ingredients Volatiles	 Binder	 binder in oxidizer flow	 deflagration	—
Nonvolatiles	 sintering	 oxidizer flow	—	—
Nonvolatile Particles in Matrix of Volatile Ingredients	 Al in binder	 Al-filled binder in oxidizer flow	 Al in AP (dry-pressed)	—
Combinations of Volatiles	 AP in binder	 binder-coated AP in oxidizer flow	 AP-Binder-AP Sandwich	 AP-Binder Propellant
Combination of Nonvolatiles	 Fe_2O_3 and Al Mixture	—	—	—
Combinations of Nonvolatiles in Volatiles	 Fe_2O_3 and Al in binder	 filled binder in oxidizer flow	 filled binder sandwich	 Propellant

Figure 2
Comparison of Burning
Behavior with
Ballistically Active
and Inactive Particulate
Ingredients



Sandwich Burning Rates at 3.45 MPa
with Various Additives

AERODYNAMIC BREAKUP - METAL DROPLETS

James E. Craig
SPECTRON DEVELOPMENT LABORATORIES, INC.
Costa Mesa, CA 92626

The breakup of Al/Al_2O_3 agglomerates in solid propellant rocket nozzles is a critical process effecting combustion efficiency and two-phase flow losses. While direct observation of agglomerate breakup has been made in subscale nozzles, the dynamics and mechanisms of breakup remain to be characterized. These phenomena for high surface tension metal droplets may differ significantly from those associated with conventional liquid droplets. Proper scientific scaling techniques must be developed to extrapolate subscale laboratory data to full scale rocket motor pressures, temperatures, and sizes. The principle goal of this investigation is to provide increased understanding of the fundamental breakup mechanisms of high surface tension liquids in aerodynamic nozzles.

Droplet breakup experiments in aerodynamic nozzle contractions have been conducted in which conventional liquids and higher surface tension liquids (Mercury) were examined. A key element of the experiment is the use of laser diagnostics. Pulsed laser holography has provided droplet and fragment observations with resolutions not previously possible. Laser velocimetry has provided droplet dynamics data revealing dramatic accelerations prior to breakup.

A series of experiments were designed to investigate the breakup mechanisms of high surface tension liquid metals. The droplet aerodynamics were determined from trajectory estimates of mercury droplets. For breakup ($We > 30$), the slip velocity requirement ranged from 270 m/s to 109 m/s for droplet diameters of 100 μm to 600 μm , respectively. For the experiments, the nozzle was operated at the sonic velocity, and the droplet diameter was varied from 190 μm to 560 μm . The droplet breakup mechanism is depicted in Figure 1. The droplets are observed to expand radially while contracting in the flow direction. As large expansions are reached (3-5X), a sphere forms in the center which is connected to the thick outer ring by a thin sheet. Much of the original droplet mass accumulates in the inner sphere and the outer ring. Since the sheet is flat and thin the aerodynamic pressure forces quickly expand the sheet downstream eventually bursting the sheet. These initial fragments are very small and move rapidly downstream from the larger primary fragments. The primary fragment takes the form of a cylinder aligned with the flow. The frontal diameter is about 30 to 40 percent of the original droplet size and deforms as higher gas velocities are reached in the nozzle. Finally, secondary breakup is observed as the primary fragment goes through a fairly chaotic failure mechanism. Hence, for metal droplets the breakup mechanism is cyclic in nature, and in these experiments two clearly defined cycles have been observed.

The droplet velocity and Weber number profiles along the nozzle contraction were obtained using double-pulse holographic imaging. The position (upstream of the throat) for the primary breakup event moved from 8 to 14 mm for the initial droplet sizes, 190 and 560 μm , respectively. The initial droplets all failed in the Weber number range of 15-20. The Weber number histories (Figure 2) for all three droplet sizes overlap when the time is normalized by the droplets first natural frequency.

METAL DROPLET BREAKUP

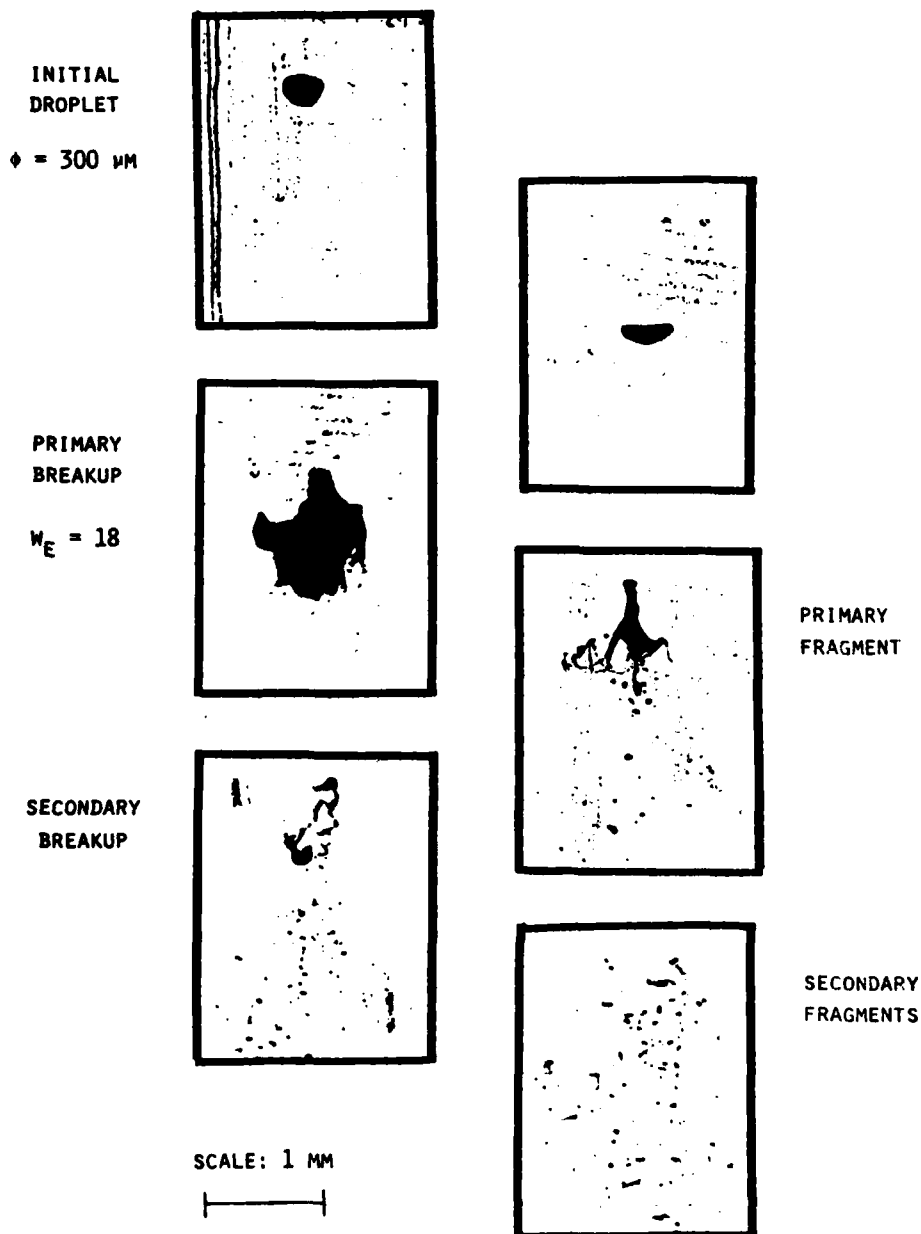


Figure 1. High Resolution Pulsed Laser Holographic Images of Mercury Droplet Breakup Mechanisms

DROPLET WEBER NUMBER HISTORIES

MERCURY

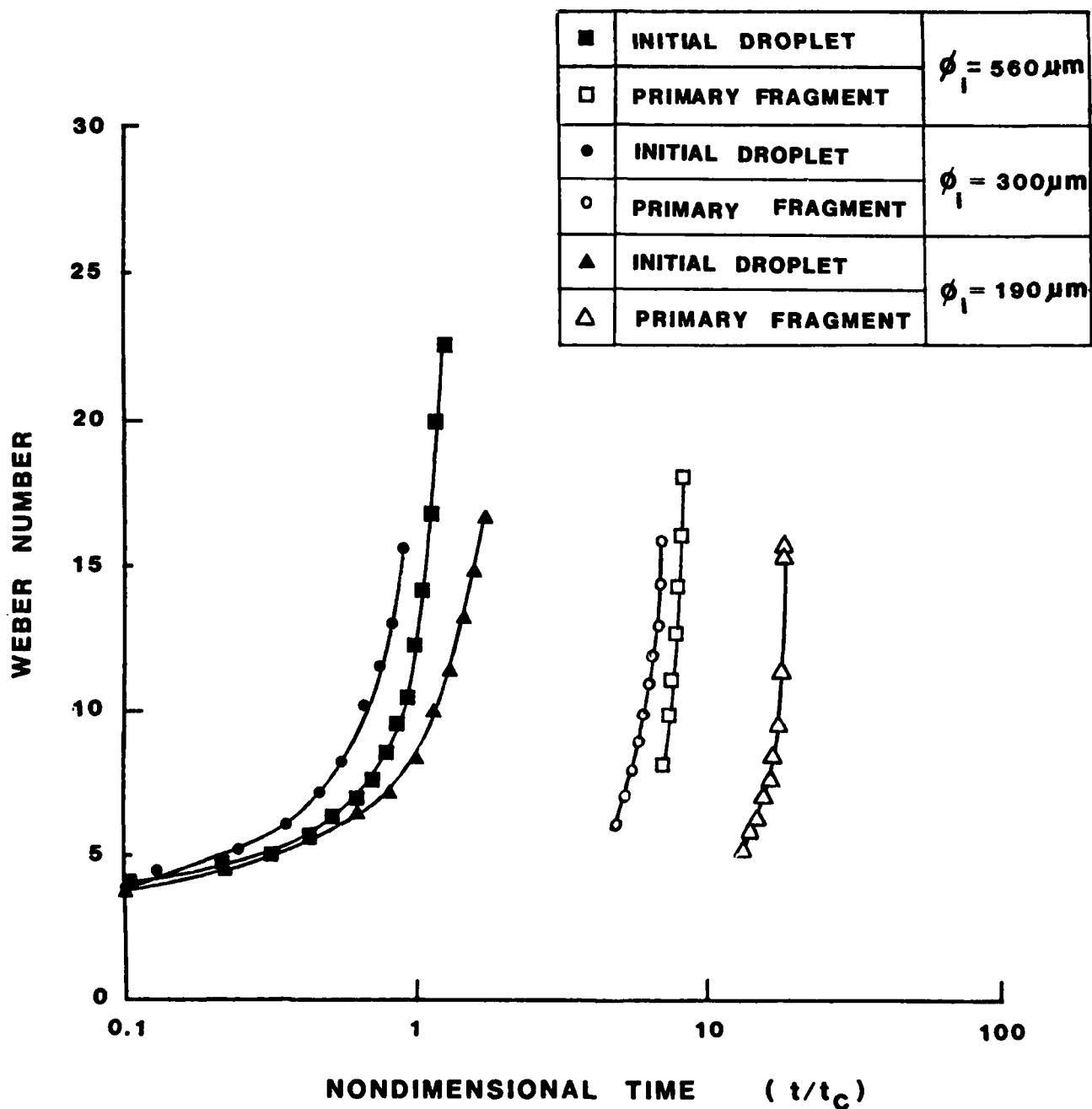


Figure 2. Mercury Droplet Weber Number Histories for Initial and Primary Fragment

AGGLOMERATE BREAKUP CONTROL
KEVIN K. NACK, ILt, USAF
AFRPL/DYC, Stop 24
EDWARDS AFB, CA 93523

Two phase flow losses are a significant loss mechanism with regard to delivered specific impulse for solid rocket motors burning metalized fuels. The primary losses occur in the rocket nozzle due to thermal and velocity lags of the metal agglomerated relative to the accelerating gas flow field. If the size of the agglomerates can be reduced, less loss would occur.

It is well known that some of the larger agglomerates break up as they enter the nozzle region. Many of them do not, however, and still cause the previously mentioned losses. Metal fuel particles accumulate on the burning surface of propellant into agglomerates 10 to 100+ times the size of the fuel particles. Surface tension of the molten metal causes accumulation at the propellant surface and inhibits agglomerate breakup in the nozzle. If surface tension could be reduced, accumulation could be inhibited and breakup enhanced both contributing to reduced two phase flow losses.

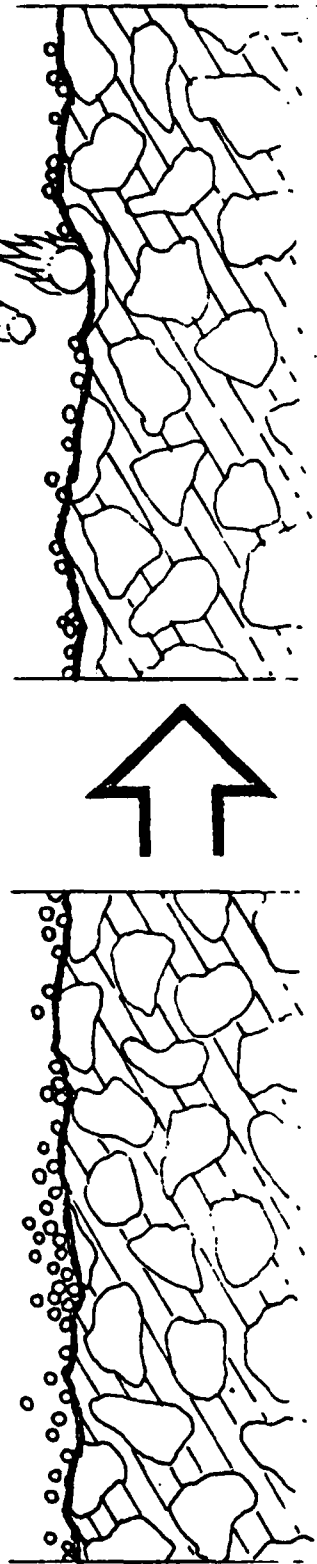
This project will use a unique approach to test the critical breakup characteristics of molten metal fuels. In addition, methods of enhancing breakup will be sought by testing breakup of metal/alloy and metal/additive combinations with more favorable breakup characteristics. The experiment will consist of an acoustic levitator, laser melter, and shock tube. The levitator will suspend an aluminum particle in a gas, the laser will melt the particle, and the shock tube will provide the flow conditions to cause breakup of the molten metal particle.

The project is currently in the build-up phase. Development work is underway on the acoustic levitator. Aluminum has been levitated, but, more work is needed to increase system reliability. The laser melting device consists of a neodymium-glass, pulsed laser and various optics. The laser has been received, but, all the optics have not and are still out on order. The shock tube is currently awaiting the construction of a support. Experiments on metallic breakup should be underway in late summer 1984.

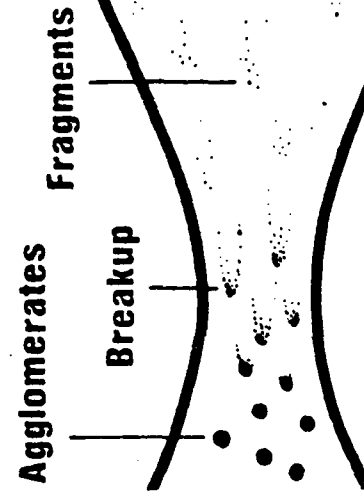
If the program demonstrates expected results. Scale rocket motors will be fired in order to demonstrate increased delivered specific impulse.

Agglomeration Process....

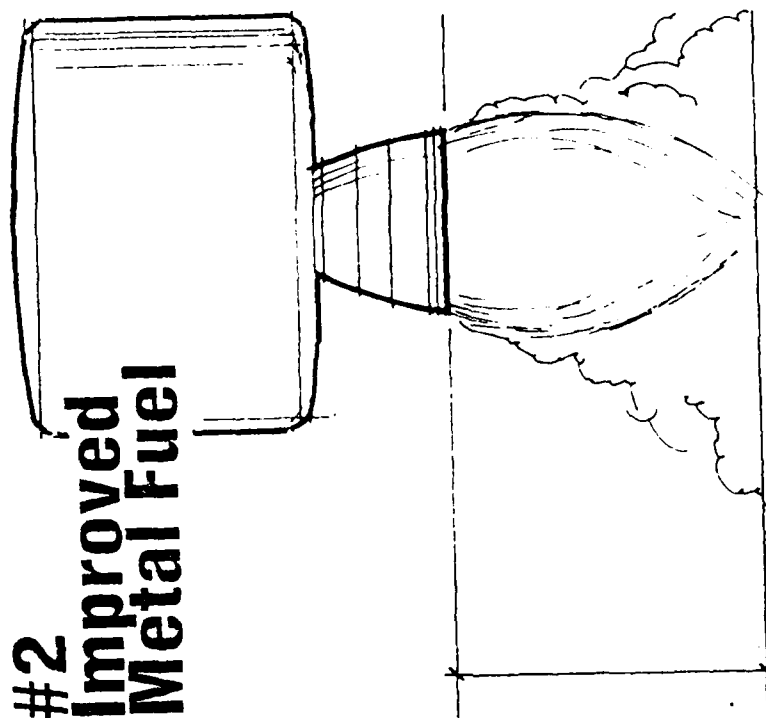
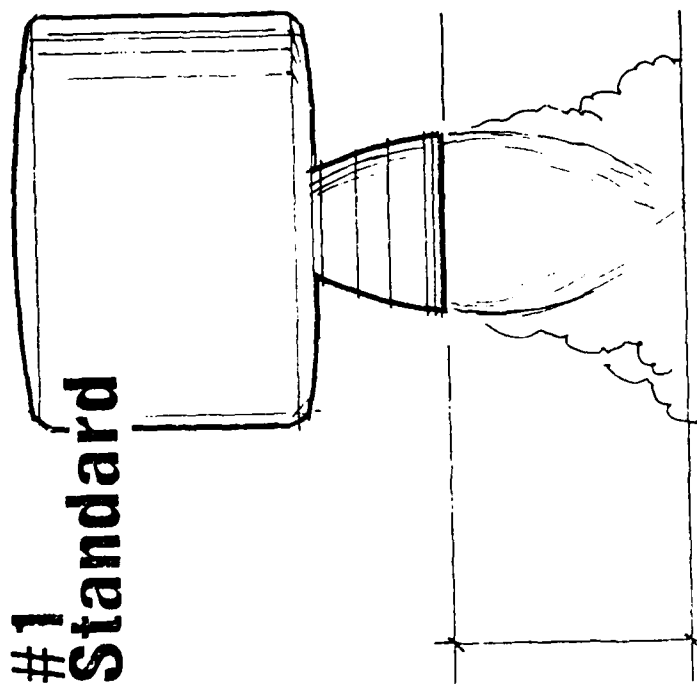
A) Burning Surface Agglomeration



B) Particle Breakup



Anticipated Result....



- Despite Identical Mass and Volume,
Motor #2 Exhibits Greater Total Impulse
due to Decreased 2-phase Flow Losses.

PULSED-LASER CINEMATOGRAPHY OF
PROPELLANT DEFLAGRATION

ROGER J. BECKER
UNIVERSITY OF DAYTON RESEARCH INSTITUTE
DAYTON, OHIO 45469

An improved understanding of the microscopic behavior of grains in deflagration is needed to model propellant performance. The temporal character of deflagration on a local scale and its correlation with the local environment is desired. High-speed photography is a local method of obtaining the desired data, but conventional cinematography is limited in resolution by motion blur, flame brightness, and illuminating intensity.

Due to the intensity and monochromaticity of the laser pulses used flame incandescence does not mask the target. Motion blur is negligible due to the 30 ns pulse width. The resolution of these experiments should be diffraction limited. Consequently, if a resolution exceeding 20 μm is to be obtained, there will be a severe depth of field problem. To meet this difficulty we have constructed a rigid frame that holds the camera, pressure chamber, and servo system together. A seven-port window bomb designed for operation at 1,000 psi has been constructed for the experiments.

The strand surface will be maintained within the depth-of-field of an electro-optic servo system. The servo circuit features a linear diode array and a proportional drive to protect against fouling of the servo windows and to maintain a smooth drive.

All tests will be made on 1/4 inch strands. The first set of experiments will be on a matrix of AP grain mixes at a series of pressures. These runs will be followed by attempts to make stereo movies, and studies of induced quenching.

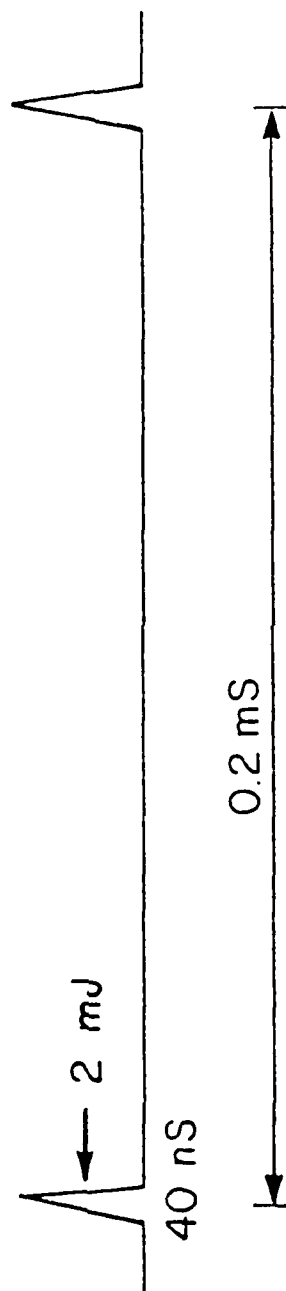
OBJECTIVES

- TIME-ORDERING OF IGNITION SITES
- GRAIN IGNITION TIMES VS. GRAIN MIX
- TEMPORAL AND SPATIAL CORRELATIONS
IN LOCAL REGRESSION RATES
- MELTING TIMES OF LARGE GRAINS
- QUENCHING BEHAVIOR

APPROACH

- IN-SITU, HIGH-RESOLUTION CINEMATOGRAPHY

TIMING SEQUENCE



- ELIMINATES MOTION BLUR
- PIERCES FLAME INCANDESCENCE
- AMPLE LIGHT FOR FINE-GRAINED FILM

SOLID PROPELLANT COMBUSTION

DIAGNOSTICS

David W. Netzer
John P. Powers

Naval Postgraduate School
Monterey, California 93943

At the Naval Postgraduate School (NPS), a continuing investigation is being conducted to obtain quantitative data that can be used to relate propellant composition and operating environment to the behavior of solid particulate (Al, Al_2O_3) within the grain port and exhaust nozzle.

These data are needed in order to (1) improve solid propellant performance predictive capabilities, (2) provide needed input related to AP-aluminum interactions for current steady-state combustion models, and (3) provide in-motor particle size distributions which will allow more accurate predictions of damping in stability analyses. The techniques employed are high speed motion pictures of strand burners and slab burners in a cross-flow environment, SEM analysis of post-fire residue (strand, slab, and motor), determination of D_{32} across the exhaust nozzle using measurements of scattered laser light, and holograms of burning propellant strands and slabs in a cross-flow environment. In addition, work has been initiated to develop automatic data retrieval methods for obtaining particle size distributions from holograms taken of the combustion of solid propellants. Once developed, these techniques/diagnostic methods could be readily employed for obtaining the needed data discussed above from a series of tests in which propellant composition, motor geometry, and operating environment are systematically varied.

Actual particle sizes of burning aluminum particles were obtained in high speed motion pictures by using high intensity rear illumination of the burning propellants to eliminate the flame envelopes surrounding the burning particles.

Measurements of diffractively scattered light were successfully made for determination of changes in D_{32} across a solid propellant rocket motor exhaust nozzle. However, to date, propellant composition and grain geometry have significantly limited the range of obtainable data.

Two-dimensional motors have been successfully employed to obtain good quality holograms of propellant burned in a cross-flow environment. Other efforts have included reduction of speckle in the recorded hologram and optimization of techniques for minimizing excessive smoke.

A Quantimet 720 has been used in an initial effort to obtain particle size distributions from a photograph taken of a reconstructed hologram. Current efforts are directed at using a computer-controlled Quantimet 720 and a computer-controlled x-y-z translation stage to obtain particle size data directly from the reconstructed hologram.

FIGURE 1 EXPERIMENTAL APPROACH

9 Specially formulated propellants: HTPB/AP/(Al, ZrC, or G), GAP/AP/Al

$P_c = 500, 1000 \text{ psia}$

1. Combustion Bomb Studies

- 5000 pps motion pictures - N₂ purged
- Particle collection - no purge
- SEM analysis of post-fire residue
- Various lighting techniques: intense back illumination, monochromatic front illumination, etc.
- + Compare post-fire and motion picture particle size data
- + Maximize resolution

Measure scattered laser power spectra to determine change in D₃₂ of particles across exhaust nozzle

2. Small End-Burning Motor

- Calibrate optical method
- + Determine utility of technique in test cell environment
- + Determine accuracy by comparison with SEM analysis of collected exhaust products
- + Conduct parametric test series for effects of propellant composition and nozzle geometry

Obtain holograms of propellants in cross-flow environment

- + Develop experimental technique for obtaining holograms in motor environment

3. Two-Dimensional Windowed Motor

- + Determine resolution limits of holocamera
- + Compare obtainable particle size data with that obtained using high speed motion pictures
- + Conduct parametric test series for effects of propellant composition

Develop practical method that can be readily used by various investigators

- + use of Quantimet 720 Image Analyzer

4. Automatic Retrieval of Particle Size Data from Holograms

- + PIP computer
- + remote control of hologram x-y-z position

Figure 2. PRIMARY ACCOMPLISHMENTS

1. High speed motion pictures of burning propellant strands
 - pressures to 1000 psi
 - 0-15% Al
 - 14 μ m resolution
 - 2500 watt rear illumination and monochromatic front illumination used to overpower flame envelopes and obtain true particle sizes
2. Holograms of burning propellant
 - strands to 1000 psi
 - 2-D motor with cross-flow to 500 psi
 - 0-15% Al
 - 11 μ m resolution
3. Particle sizing using measurements of diffractively scattered light
 - across nozzle measurements accomplished
 - technique sensitive to "contaminants" in flow
4. Automatic retrieval of particle size data from reconstructed holograms
 - Quantimet 720 used to obtain particle size distribution from photograph of reconstructed hologram
 - remote controlled positioning apparatus and computer system currently being incorporated
 - techniques for minimization of speckle currently being investigated

FUEL-RICH SOLID PROPELLANT BORON COMBUSTION (ANALYSIS)

Merrill K. King
Atlantic Research Corporation
Alexandria, VA

The analytical modeling tasks are directed at evaluating hypotheses regarding mechanisms of ignition and combustion of boron particles, agglomerates, and clouds, and delineating how they affect combustor characteristics. The uniqueness of the approach lies mainly in the development of detailed analytical descriptions of unit processes with subsequent "building-block" combination for definition of means of maximizing use of boron's high heating potential. Emphasis is placed on the fact that boron presents unusual ignition/combustion problems demanding careful attention to environmental staging.

A model of boron ignition in wet or dry atmospheres has been developed: this model is unique in its treatment of oxide-coated boron oxidation as involving series resistances associated with oxygen gas diffusion, dissolution of oxygen into the oxide film, subsequent solute diffusion to the metal/oxide interface, and finite-kinetics reaction at that interface. Evaporation of B_2O_3 and reaction of this oxide with H_2O to form $HBO_2(g)$ are both modeled as involving both kinetic and diffusional resistances. Ignition-time predictions with this model are found to agree well with the data base of Macek. In addition, a quasi-steady model of clean-particle combustion with CO_2 , O_2 , and/or H_2O with a unique finite-rate-kinetics treatment of the surface reactions of boron with these oxidizers (and other intermediates with O/B ratios > 1) has been developed and calibrated against Macek data. This model has been extended to treat unsteady-state effects and coupled with the ignition model to yield a unified ignition/combustion model. A unique aspect of this model is definition of surface gas composition and temperature versus time, with consequent identification of extinguishment conditions (occurring when $P_{B2O3,s} > VP_{B2O3,s}$).

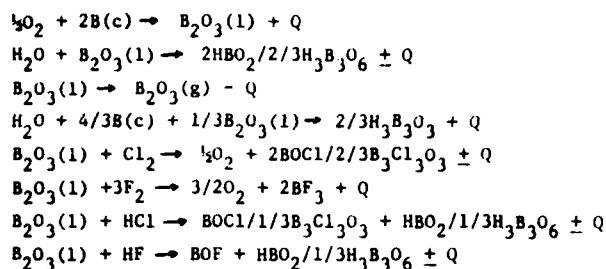
Recently the ignition model has been extended to treat possible effects of halogens, with a first-ever examination of reactions of F_2 , Cl_2 , HF , and HCl with the oxide layer. Also, a mechanism by which an outer layer of titanium or zirconium might aid ignition by providing particle heating without production of additional boron oxide to a point where the original oxide flashes off or evaporates quickly following exhaustion of the second metal, has been modeled. Finally, a unique model of the effects of LiF coatings involving the reaction of LiF with B_2O_3 to form $LiBO_2$ and BOF has been developed.

Two models of a boron slurry ramjet combustor uniquely considering the special problems associated with boron ignition/combustion through incorporation of the above analyses have been developed. Both include a well-stirred reactor (PSR), ignition zone in which the fuel and part of the air are mixed and partially reacted. In the first model, downstream addition of the remaining air is treated one-dimensionally, with user-input air addition schedule, while in the second, two-dimensional coaxial mixing is treated.

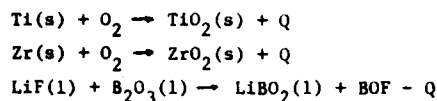
Major accomplishments of this effort include identification of several approaches to enhancing boron particle ignition (Fig. 2 - Item I), definition of approaches to proper boron slurry combustor design (Fig. 2 - Item II), and delineation of causes for observed deleterious effects of low combustor operating pressure on boron-powered airbreathing systems (Fig. 2 - Item III).

I. REACTIONS TREATED IN MODELING OF SINGLE BORON PARTICLE IGNITION AND COMBUSTION

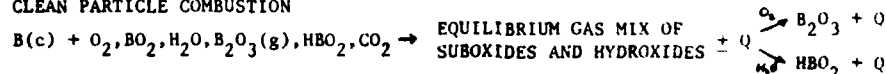
A. IGNITION IN B-O-H-N-Cl-F ATMOSPHERES



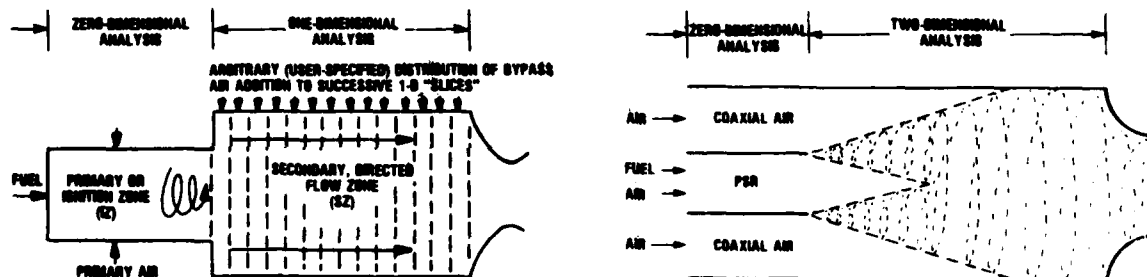
B. IGNITION WITH COATINGS



C. CLEAN PARTICLE COMBUSTION



II. SLURRY COMBUSTOR ANALYSES



ZERO-DIMENSIONAL ANALYSIS

- (1) UTILIZE MASS, ENERGY, SPECIES BALANCES OVER IGNITION ZONE
- (2) CALCULATE RESIDENCE TIME DISTRIBUTION FROM $P(\tau_R > \phi) = \exp(-\phi/\bar{\tau}_R)$
- (3) ANALYZE IGNITION/COMBUSTION OF $I \times J$ BINS OF PARTICLE-SIZE/RESIDENCE-TIME COMBINATIONS
- (4) USE FULL-UP BORON IGNITION MODEL AND CORRELATIONS BASED ON DETAILED FINITE-KINETICS COMBUSTION MODEL TO CALCULATE FRACTION VORON IN EACH BIN IGNITED AND BURNED
- (5) ITERATIVE PROCEDURE TO CLOSE LOOP ON TOTAL FRACTION BORON BURNED AND IZ TEMPERATURE/COMPOSITION

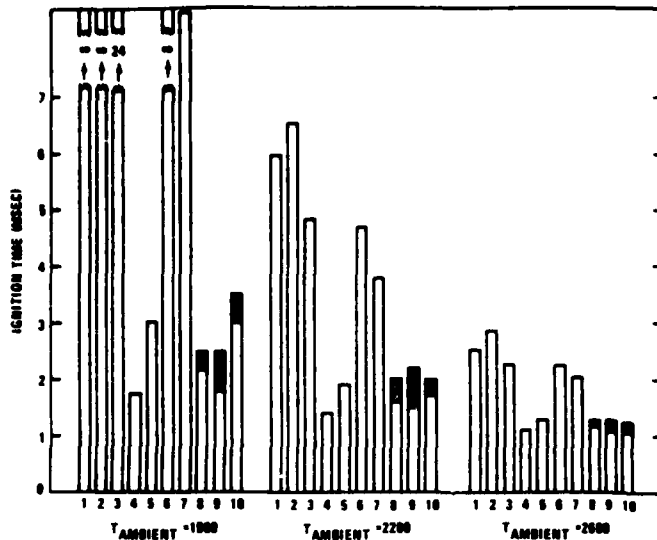
ONE-DIMENSIONAL ANALYSIS

- (1) SPECIFIED AIR ADDITION TO EACH AXIAL INCREMENT
- (2) OVERALL MASS, ENERGY, SPECIES BALANCES TO CALCULATE TEMPERATURE, COMPOSITION, AND RESIDENCE TIME IN THE INCREMENT
- (3) IGNITION/COMBUSTION MODELS USED TO CALCULATE INCREMENTAL BORON IGNITION AND COMBUSTION IN EACH BIN

TWO-DIMENSIONAL ANALYSIS

- (1) CORE-LENGTH, CENTERLINE DECAY CORRELATIONS USED TO DEFINE VELOCITY, ENTHALPY, ATOMIC COMPOSITION, AND TRANSPORT PROPERTY DISTRIBUTIONS
- (2) MASS TRANSPORT EQUATION AND CONSERVATION EQUATION FOR BORON OXIDE INCLUDING SOURCE TERM FOR REACTION USED TO DETERMINE MOLECULAR COMPOSITION OF EACH SUCCESSIVE RADIAL/AXIAL ANNULAR SLICE
- (3) ENTHALPY EQUATION USED TO CALCULATE TEMPERATURE, RESIDENCE TIME FOR EACH SLICE
- (4) IGNITION/COMBUSTION MODELS USED TO CALCULATE BORON CONSUMPTION FOR EACH SLICE

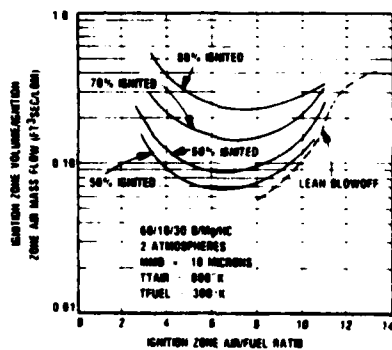
I. IDENTIFICATION OF MEANS OF DECREASING BORON PARTICLE IGNITION DELAYS



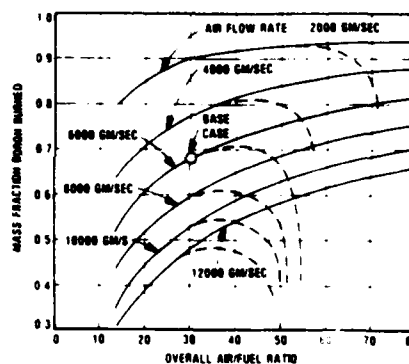
10 Micron Particle Radius, 0.2 Micron
Initial Oxide Thickness, $P = 1 \text{ Atm}$,
Initial Temperature = 300 K

- 1 Base Case $P_{H_2O} = 0.10$, $P_{O_2} = 0.10$
- 2 $P_{H_2O} = 0.00$, $P_{O_2} = 0.20$
- 3 $P_{H_2O} = 0.20$, $P_{O_2} = 0.00$
- 4 Base + $P_{F_2} = 0.10$
- 5 Base + $P_{HF} = 0.10$
- 6 Base + $P_{Cl_2} = 0.10$
- 7 Base + $P_{HCl} = 0.10$
- 8 Titanium Coating ($Ti/B \sim 0.15$)
- 9 Zirconium Coating ($Zr/B \sim 0.25$)
- 10 LiF Coating ($LiF/B \sim 0.08$)

II. IDENTIFICATION OF IMPORTANCE OF TAILORING AIR DISTRIBUTION IN BORON SLURRY COMBUSTORS

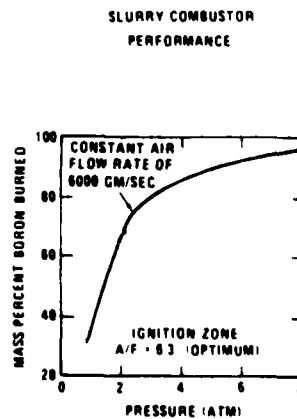
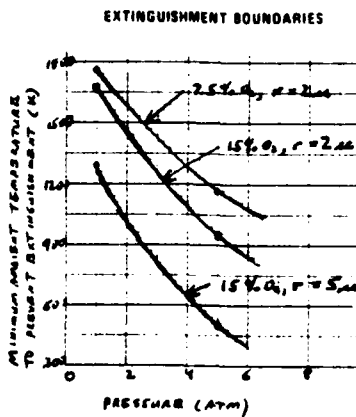
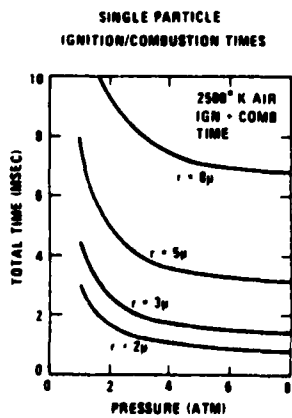


Fraction (Mass) of Boron Particles Ignited in Primary
Zone (12) as Function of 12 Air/Fuel Ratio and 12 Loading



SOLID LINES - 12 AIR FUEL RATIO HELD AT 6.0
DOTTED LINES - FRACTION OF AIR THRU 12 HELD AT 0.2

III. DEMONSTRATION OF DELETERIOUS EFFECTS OF LOW PRESSURE ON BORON COMBUSTION EFFICIENCY



**FUEL-RICH SOLID PROPELLANT
BORON COMBUSTION (Experimental)**

**James J. Komar and Ronald S. Fry
Atlantic Research Corporation
Alexandria, Virginia 22314**

This experimental research is aimed at understanding the basic physics of boron particle ignition and combustion. Experimental data are acquired on the ignition and combustion of boron particles, agglomerates and clouds, as well as combustion and ignition phenomena in consolidated fuel grains in high temperature air crossflow. This research is vital to identifying means of using the full potential of boron fuels.

Current efforts in the single particle combustion investigations are being directed towards the measurement of boron-oxide reaction rates, utilizing small single beads of boron oxide mounted on micro-thermocouple substrates. Determination of size changes as functions of time, operating conditions and initial particle sizes are being made with microoptical pyrometry, diode array photography, particle size interferometry, and photographic recording. These reaction rates are not well known and the simultaneous diagnostics approach is unique in that self-consistent measurements are possible during the course of the experiments. Representative scanning electron micrographs are shown of oxide particles of varying stages of reaction completion.

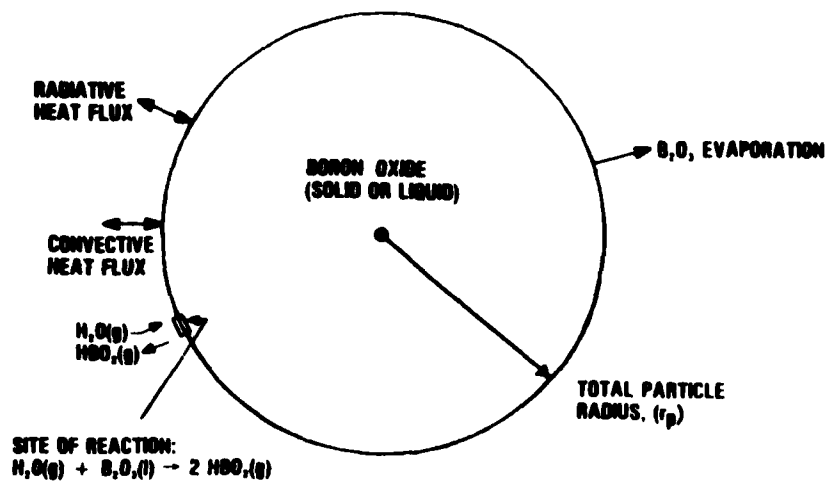
Combustion of consolidated boron fuel grains in a high temperature air crossflow involves stabilizing a flame within the turbulent boundary layer above the ablating grain surface. Mechanisms fundamental to the problem include grain surface ablation characteristics, ablated material physical properties and dynamics, radiation feed-back to the fuel surface from burning particles in the main stream and mean and fluctuating properties of the main stream and boundary layer regions.

Investigation of these mechanisms are conducted in a unique two-dimensional windowed combustor whose design comprises two facing slab grains to allow examination of radiative coupling. Flame structure dynamics are studied with high framing rate color and Schlieren photography. Particle size interferometry is being employed in an effort to characterize particle size distributions of the ablated material released from the fuel surface. The radiation thermal distribution and its interaction with the convective flow above the fuel surface is studied using a Reticon diode array camera. Details of the fuel grain conductive thermal distribution and ablation behavior is studied with embedded high response thermocouples and fiber optic probes. One component laser velocimetry is employed to characterize the mean flow field.

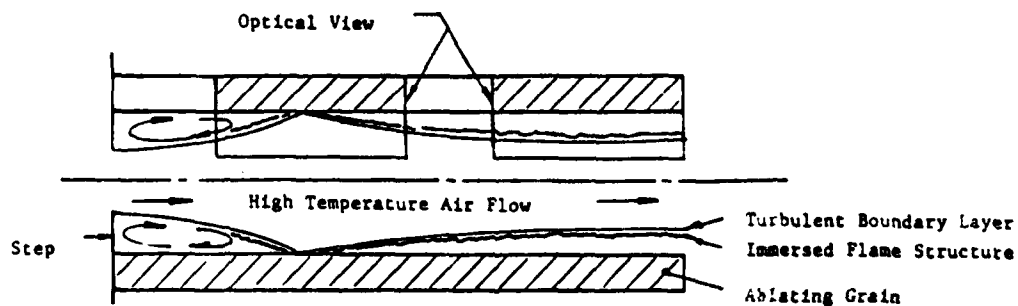
During this period, the experimental apparatus and diagnostics were checked out through air-only flow and hydrocarbon fuel combustion testing. Study of the combustion details of boron-containing fuels is ongoing. Preliminary criteria for flame stability in 2-D combustor were established. Definition of overall flow structure is possible from available data. Detailed features of the combustion dynamics, identified as program needs, are being sought.

BORON COMBUSTION DYNAMICS APPROACH

BORON OXIDE KINETICS



BORON GRAIN FLAME STRUCTURE



PROBLEM

- Physics of boron combustion in high temperature in cross-flow are not understood.
- Modeling the complex interaction between kinetics and mixing limited phenomena is intractable without experimental data
- Prior research employed diagnostics inadequate for obtaining essential data.

APPROACH

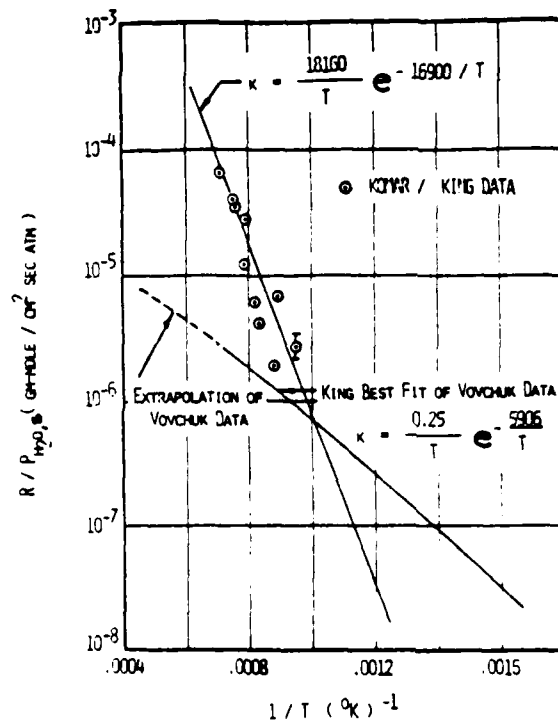
- Unique combination of experiment design and diagnostics to examine boron combustion in high temperature air cross flow.
- Laboratory scale combustion testing in uniquely suited 2-Dimensional windowed combustor.
- Application of advanced non-intrusive optical diagnostics and data processing.

SUMMARY OF ACCOMPLISHMENTS

BORON OXIDE KINETICS



SAMPLE BORON OXIDE BEAD ON
PLATINUM THERMOCOUPLE

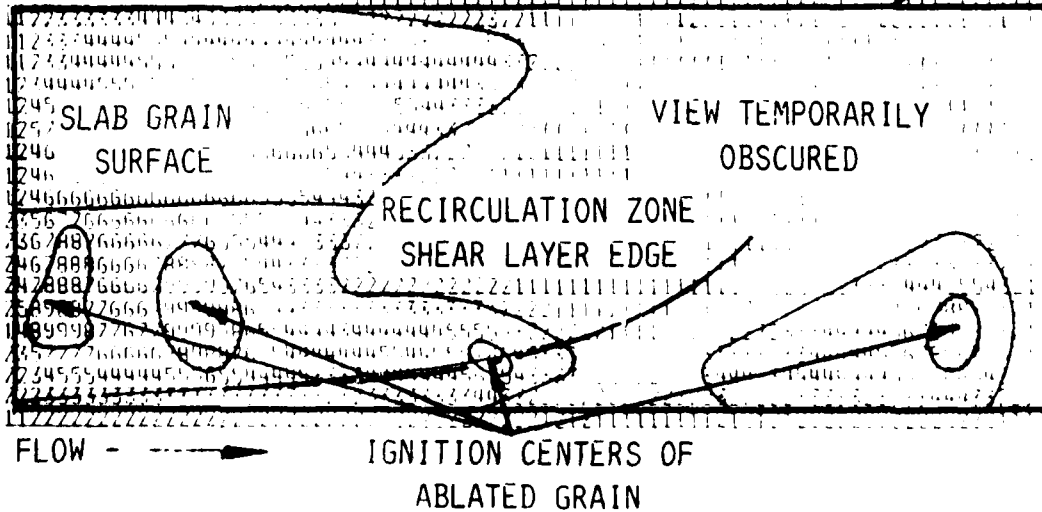


BORON OXIDE REACTION RATES WITH WATER
AT ELEVATED TEMPERATURES

SLAB GRAIN BURNER

CHAMBER WALL

OPTICAL VIEW EDGE



TYPICAL VIEW OF 2-D SLAB GRAIN COMBUSTION

OVERVIEW: AFOSR INTERESTS IN ROCKET PROPULSION

Leonard H Caveny
Air Force Office of Scientific Research
Bolling AFB
Washington, DC 20332

Present and future rocket propulsion systems present critical challenges that are not addressed adequately by present technologies. Propulsion systems must undergo continuous advancements to assure that the winning edge is maintained. As the conventional propulsion technology matures, the need persists to attain yet another round of performance gains. Thus, the technology challenges become even greater since the obvious advancements have been implemented. Also, broad classes of problems (e.g., combustion instability, service life, signature, low-temperature structural integrity, light weight thermal protection) are never solved entirely and recur often as important considerations (and compromises) prior to propulsion system qualification.

Powerful motivations continue for basic research on topics such as reacting flows, energetic materials, stability, refractory materials, propulsive processes. Many phenomena, not explained adequately, are accommodated by specific designs. Periodically, this lack of understanding is the precursor to major setbacks. Clearly, rocket motor processes present scientific challenges suggesting that properly conceived research will lead to higher performance, reduced risk, lower development costs, longer service life, etc.

This meeting will be the first review of the research relating to nonconventional primary propulsion for space. Accordingly, some introductory discussion will help put portions of this research into perspective. Nonconventional propulsion concepts periodically receive attention but invariably the propulsion systems chosen have been adaptations or extensions of conventional liquid and solid rocket technology. The dominant consideration in previous years was that the missions could be performed using conventional chemical propulsion. Consequently, major initiatives to provide technology and to overcome specific barriers could not be justified. The recent emphasis on space and the reusable launch vehicle capability to low Earth orbit present new considerations for advanced propulsion for orbit transfer. Transferring the projected large payloads using conventional propulsion would impose severe limitations on the missions. For example, 75% of the mass delivered to low Earth orbit may be the chemical propulsion system required to raise the other 25% (i.e. the active payload) to geosynchronous Earth orbit; nonconventional propulsion offers the promise of reversing this ratio of propulsion and payload masses. The technology issues are necessarily complex; controversial approaches are to be expected. Much of the research is coupled at optimistic projections for technological advances by the 1995 to 2000 time period.

The Wednesday morning session treats fundamental processes related to beamed energy and solar propulsion, i.e., radiation transmission and absorption in flowing media, plasma initiation, and chamber configurations. The immediate advantage of beamed and solar energy is high specific impulses obtained by using low molecular weight working fluids heated by external power sources to temperatures greatly above combustion gas temperatures. The premise of the beamed energy approach is that suitable megawatt laser sources will be

** 1984 ROCKET RESEARCH MEETING **
Abstract 23 Pg 2

available and justified for applications other than propulsion. Recent studies support the thesis that ground based free-electron lasers operating at suitable short wave lengths will enable attractive transmission efficiencies and compact collection optics. Conversely, a scenario for using orbiting laser systems for beamed energy propulsion is considered to be premature.

The Wednesday afternoon session on electric propulsion emphasizes concepts which lend themselves to sustained operation at megawatt power levels, possibly using clusters of thrusters. This represents a major departure from millinewton thrust, pulse-mode electric propulsion considered for station keeping or planetary probes, e.g., millisecond pulses driven by a capacitor bank charged by a dedicated kilowatt power source. Present mission analyses are exploring the dual mode premise of the megawatt nuclear power supply onboard for the main mission being available for propulsion power. Thus, propulsion does not take all the weight penalty for the power source. When large total impulses are required, thruster mass is small compared to the fuel mass; thus, a premium is placed on increasing fuel efficiencies and the low thrust densities of the thrusters become unimportant. Electrode and insulator lifetimes have been identified as primary barriers to sustained, high power density operation of magnetoplasmadynamic thrusters. Accordingly a major portion of the research is directed at mass loss mechanisms and conditions leading to abusive environments and inefficient operation.

The Thursday morning session includes presentations on several of the more challenging and higher payoff approaches to space propulsion. Such a forum stimulates thinking on the basic research approaches which must accompany major advancements in space propulsion.

Ample opportunity exists for new approaches. During the last two years, several investigations into the synthesis of energetic ingredients were initiated; complementary research is needed to improve the characterization techniques for these higher energy (and more temperamental) ingredients and propellants. Good progress is being made on understanding the origins of combustion instability; more attention must be given to the mechanisms of deliberate suppression. The advent of quantitative flow visualization for turbulent reacting flows has not been accompanied by corresponding theoretical treatments to fully exploit array data, capable of revealing rapid evolution of flow structure and flame fronts. The remarkable advances in optical diagnostic techniques present new approaches to investigate plasma flows which must be understood and controlled under magnetoplasmadynamic and beamed energy thruster conditions. The research on life limiting processes which occur at the surfaces of electrodes, electrical insulators, and refractories will benefit from advances in remote sensing of surface temperatures, composition, and structure. Space missions will present entirely new autonomous operation challenges; a theoretical basis must be established to anticipate and guide the advances in sensors, adaptive control, thruster configuration options, etc. Sustained megawatt operation of space thrusters will be limited by the inability to reject heat; research is needed to enable advances in light weight radiators and thermal management systems. We will welcome discussion on these and other topics pertinent to the Air Force basic research program on energy conversion.

EVALUATION AND COMPILATION OF THE THERMODYNAMIC
PROPERTIES OF HIGH TEMPERATURE SPECIES

Malcolm W. Chase
The Dow Chemical Company
Thermal Lab
Midland, Michigan 48640

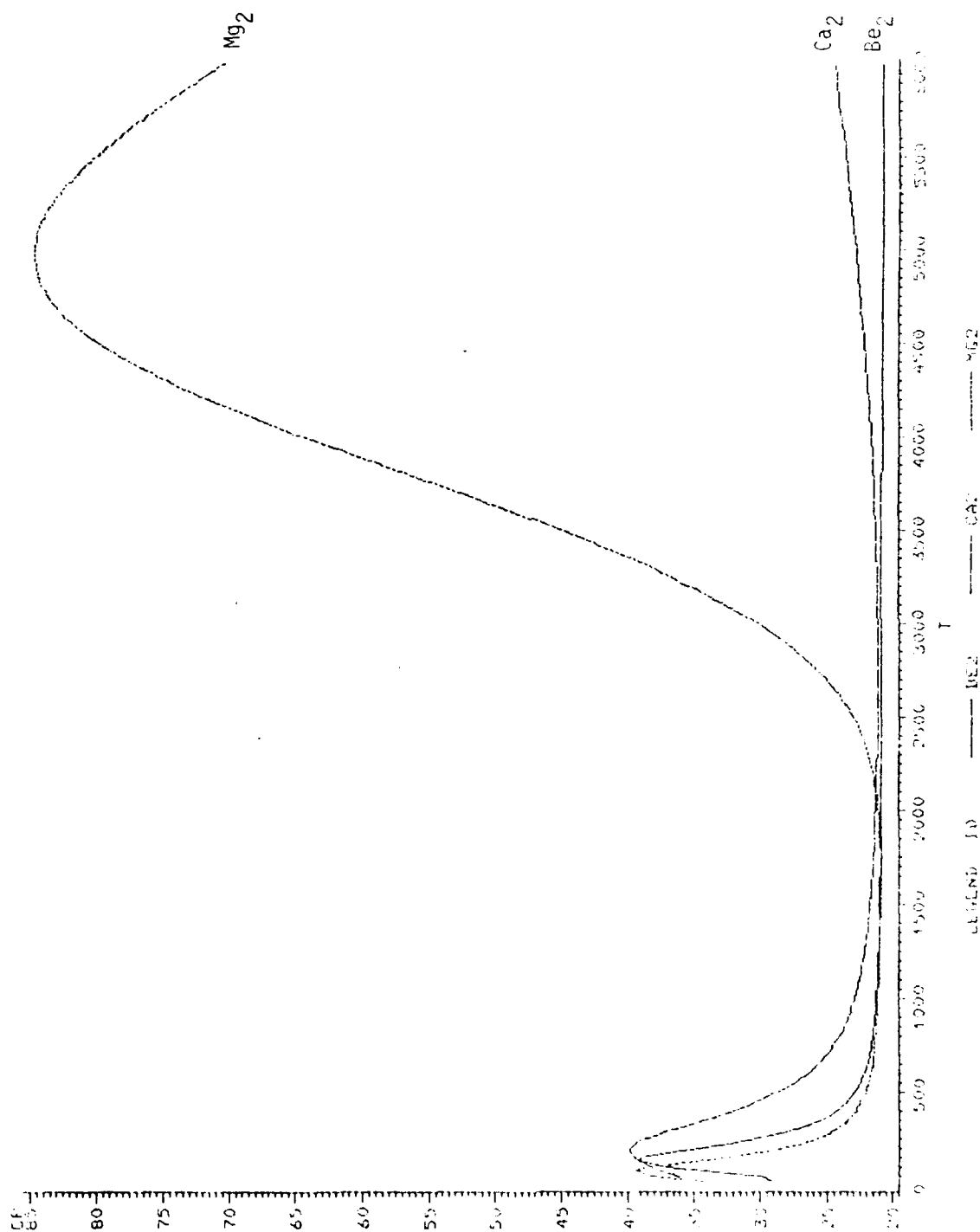
The JANAF Thermochemical Tables are a set of self-consistent thermodynamic data. These tables result from critically reviewing all literature sources, evaluating the accuracy and precision of the experimental data/theoretical calculations, calculating temperature-dependent thermodynamic functions, and publishing thermochemical tables for use in the Air Force community.

The successful application of these tables depends on the user being aware of the uncertainties in the numerical values and the possible physical and chemical phenomena peculiar to the species of interest. The quality of the tabulation is often temperature-dependent and is a compromise between the quality and extent of the available data and the calculational procedures used to generate the thermochemical tables. The effort directed towards preparing annotated bibliographies and data graphs is intended to aid the users in judging the effects of the uncertainties on the end results.

The current contract involves the re-examination of the alkaline earth metals, their gaseous dimers, oxides, hydroxides, halides, carbonates, sulfides, and sulfates. Bibliographies and data graphs are being generated for each of the 75 species; this will result in approximately 175 single- and multi-phase thermochemical tables. This analysis is revealing a significant lack of information and some potential problem areas. Three of the five alkaline earth metals are not well characterized thermodynamically. The attached graph for the low temperature heat capacity of Mg, Ca and Sr illustrates the suspect heat capacity of calcium. A similarity in the temperature dependence of these three metals is expected. A similar comparison of the heat capacities of the alkaline earth dihalides suggests that the CaCl_2 data may be in error. The alkaline earth metal dimers (gaseous) pose a different problem in that the calculational methods must be carefully chosen to properly calculate the thermal functions (see attached graph). The temperature dependence of the heat capacity of $\text{Ca}_2(\text{g})$ and $\text{Be}_2(\text{g})$ would be expected to be similar to $\text{Mg}_2(\text{g})$.

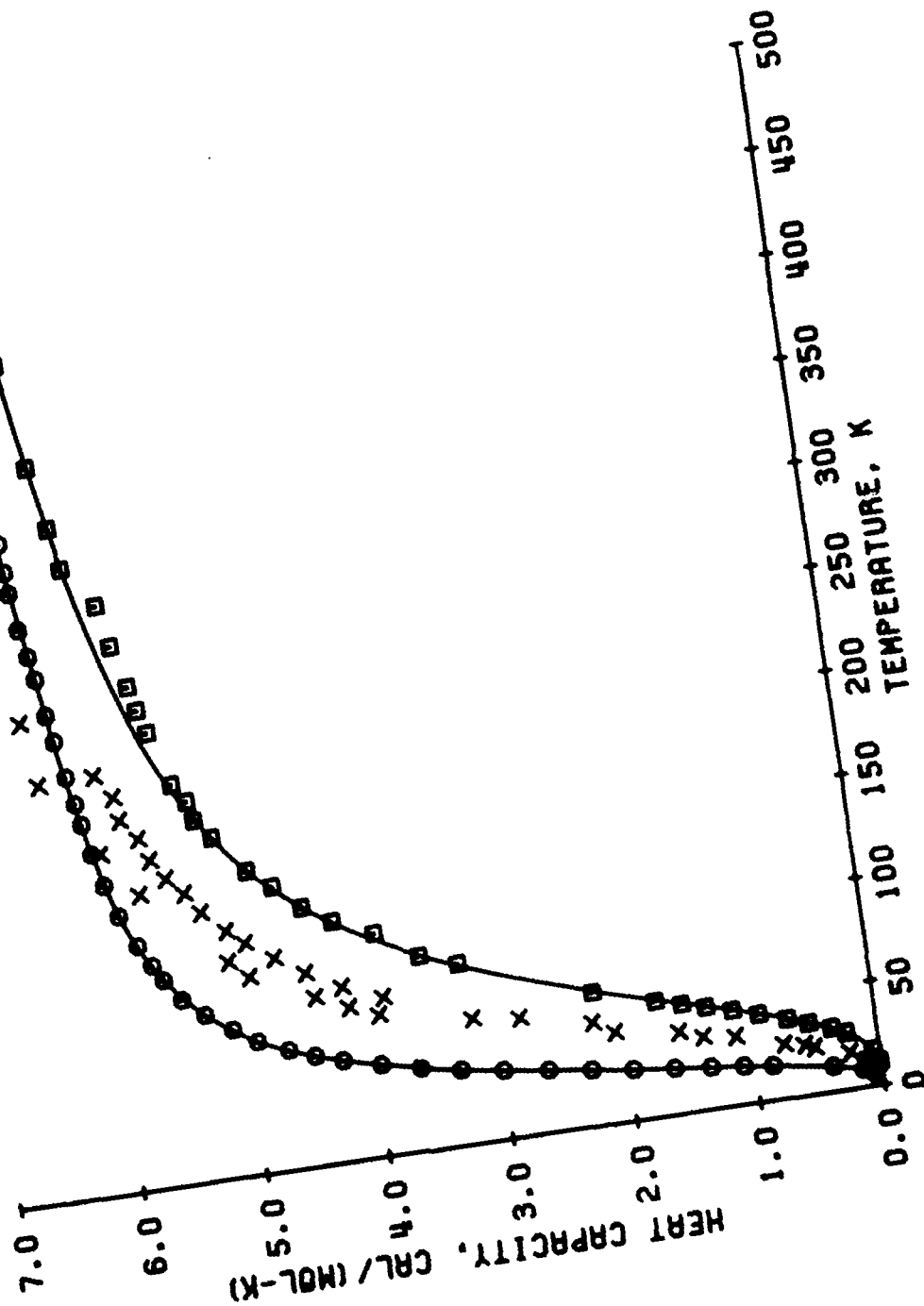
The examination of experimental/theoretical data by itself may not be sufficient to indicate potential problems whereas the examination of families of species often reveals interesting problems and discrepancies.

ALKALINE EARTH DIMER HEAT CAPACITY



LOW TEMPERATURE HEAT CAPACITIES OF ALKALINE EARTH METALS

○ STRONTIUM
× CALCIUM
□ MAGNESIUM



CRITICAL EVALUATION OF HIGH TEMPERATURE CHEMICAL KINETIC DATA

Norman Cohen and Karl Westberg
Aerospace Corporation
P.O. Box 92957
Los Angeles, California 90009

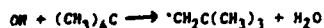
The rapid growth in chemical kinetic data, and simultaneously in the number of nonspecialists who require such data in DOD-related work, has created a need for a reliable, easy-to-use compilation of evaluated rate data and recommended rate coefficients. To answer this need, a program for the evaluation of kinetic data and for the preparation of consistently formatted data sheets patterned after the JANAF Thermochemical Tables was undertaken with the joint support of the Air Force Office of Scientific Research and the National Bureau of Standards. One such data sheet is shown in Figs. 1 and 2.

High-temperature data are of special interest to the Air Force, and this is the first data-evaluation program that routinely extrapolates rate coefficients for bimolecular reactions using methods more sophisticated than the familiar Arrhenius expression. Theory is also used to predict rate coefficients for important reactions for which there are no experimental data.

To date 35 sheets have been prepared for reactions of interest of various Air Force programs and published in a technical report. These include six reactions important in hydrogen-oxygen combustion; seven in hydrogen halide chemical lasers, fifteen in hydrocarbon oxidation, five in aluminum or boron propellant systems; and two in the oxygen-iodine chemical laser. Twenty-seven of these have recently been published in J. Phys. Chem. Ref. Data.

A series of data sheets for reactions of O atoms with alkanes (methane, ethane, propane, butane, isobutane, cyclopentane, pentane, neopentane, hexane, cyclohexane, heptane, cycloheptane, octane, 2,3-dimethylbutane, neo-octane) has just been completed and this work will be discussed. The experimental data have been reviewed and transition state theory calculations carried out for extrapolating the data to higher temperatures. Recurrent problems with the experimental data for CH_4 , C_2H_6 , neo- C_5H_{12} , and neo- C_8H_{18} include the effects of trace impurities in the hydrocarbon and the effects on the calculated rate coefficient of secondary reactions. The importance of these effects is a result of the primary reaction being so slow. The theoretical approach for reactions with such large molecules is quite different from what can be done with simple reactions, such as $\text{F} + \text{H}_2$, for which fairly reliable a priori potential energy surfaces are available.

During the remainder of the fiscal year, we will complete data sheets for reactions of O and OH with NH_3 and N_2H_4 , and for reactions of OH with a series of halomethanes.



THERMOCHEMISTRY

Thermochemical data for H_2O are taken from the second edition of JANAF Thermochemical Tables (1971); data for OH are from an unpublished supplement to those tables dated June 1977. Data for $(\text{CH}_3)_4\text{C}$ (2,2-dimethylpropane, or neopentane) are taken from Stull et al.¹ D_{298}^0 (neopentyl-H) is reported² as $419.25 \pm 4.2 \text{ kJ mol}^{-1}$, from which ΔH_f^0 can be calculated to be 35.7 kJ mol^{-1} for the neopentyl radical. S_{298}^0 for the radical was calculated³ to be $329.4 \text{ J mol}^{-1}\text{K}^{-1}$.

An analytic expression for $K(T)$ has not been calculated because the reverse reaction will never be important; at low temperatures it is too endothermic to occur, and at high temperatures the neopentyl radicals are unstable.

MEASUREMENTS

Four experimental measurements of k_1 have been reported. Greiner⁴ made observations over the temperature range of 192-493 K using flash photolysis of H_2O as an OH source, monitoring OH disappearance by kinetic absorption spectroscopy. Two room temperature measurements^{5,6} were made both using flash photolysis of H_2O and resonance fluorescence to monitor OH disappearance. In the case of one of these,⁶ the measurement was made relative to reaction between OH and $n\text{-C}_4\text{H}_{10}$. Using our own recommended rate coefficient for the latter reaction (which is about 10% smaller than that used in Ref. 6), we obtain $k_1 = 5.7 \times 10^8 \text{ L mol}^{-1}\text{s}^{-1}$. The three room temperature measurements then agree within better than 10%; the average value is $5.5 \pm 0.3 \times 10^8 \text{ L mol}^{-1}\text{s}^{-1}$. Baker et al.⁷ measured k_1/k_2 , where k_2 is the rate coefficient for $\text{OH} + \text{H}_2 \rightarrow \text{H} + \text{H}_2\text{O}$, by adding trace amounts of neopentane to $\text{H}_2\text{-O}_2$ mixtures at 703 K. Using our own recommended value for k_2 (see Data Sheet for that reaction) we obtain $k_1 = 5.2 \times 10^9 \text{ L mol}^{-1}\text{s}^{-1}$.

CALCULATIONS

Transition state theory calculations were carried out for k_1 in order to extrapolate the rate coefficient beyond the temperature range of the experimental data.⁸ $S^\ddagger(298)$ was calculated to be $388.3 \text{ J mol}^{-1}\text{K}^{-1}$ using neopentane as a model compound, giving $\Delta S^\ddagger = -102 \text{ J mol}^{-1}\text{K}^{-1}$. Vibrational frequencies were taken to be the same as for neopentane except for the removal of a C-H stretch (3100 cm^{-1}), an HCH bend (1400) and a CCH bend (1100); and the addition of the following frequencies: 3700 (OH stretch), 2200 (C-H stretch); 1000 , 1000 , 350 and 300 (deformations). The two new hindered internal rotors were assumed to have partition functions $Q_r(300) = 5.6$ and 3.9 , and barriers to rotation $V = 8.4$ and 4.2 kJ mol^{-1} , respectively. The electronic degeneracy of the activated complex, g^\ddagger , was assumed to be 2. The resulting values of $k_1(T)$ are well-described by the expression $k_1 = 6.3 \times 10^3 T^{2.0} \exp(-10/T) \text{ L mol}^{-1}\text{s}^{-1}$. This expression, derived using the experimental value of $k_1(300) = 5.5 \times 10^8$, is in good agreement with the experimental data at higher temperatures.

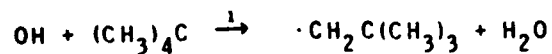
DISCUSSION

This reaction is of theoretical interest because neopentane contains only one kind of H atom (primary), so that there is only one reaction taking place, in contrast with straight-chain alkanes with more than 2 carbon atoms.

The experimental data are in good accord; the discrepancy among the three room temperature measurements is too small to suggest any real problems. Since our calculated expression agrees with all the experimental data within experimental uncertainty, we use it for the recommended expression. Thus we recommend $k_1 = 6.3 \times 10^3 T^{2.0} \exp(-10/T) \text{ L mol}^{-1}\text{s}^{-1}$, with an uncertainty in $\log k_1$ of ± 0.1 at 300 K, increasing to ± 0.5 at 2000 K.

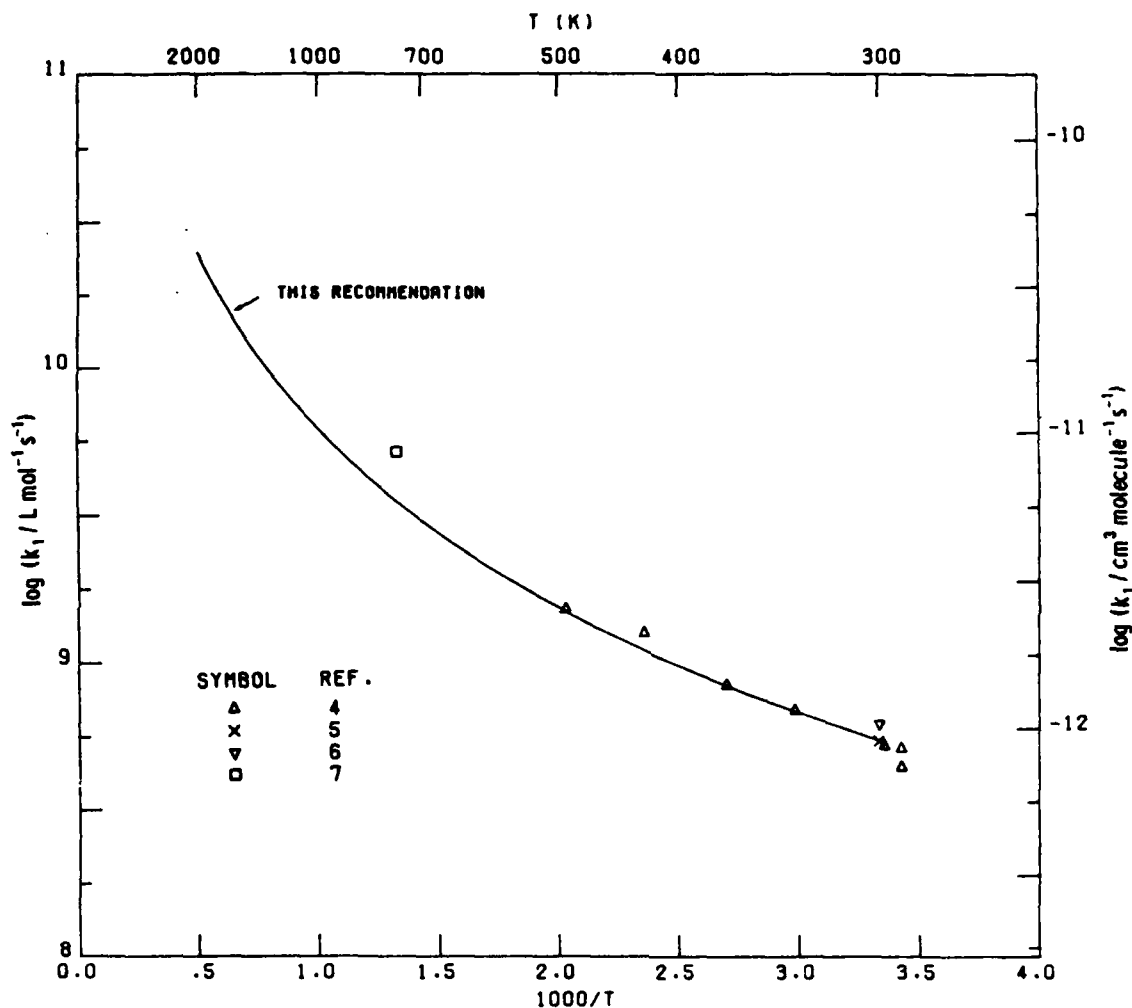
References

1. D. R. Stull, E. F. Westrum, Jr., and G. C. Sinke, *The Chemical Thermodynamics of Organic Compounds* (Wiley, New York, 1969), p. 247.
2. C. W. Larson, E. A. Hardidge, and B. S. Rabinovitch, *J. Chem. Phys.* **50**, 2769 (1969).
3. H. E. O'Neal and S. W. Benson, "Thermochemistry of Free Radicals," in *Free Radicals*, ed. J. K. Kochi (Wiley, New York, 1973), p. 275.
4. M. R. Greiner, *J. Chem. Phys.* **53**, 1070 (1970).
5. C. Paraskevopoulos and W. S. Nip, *Can. J. Chem.* **58**, 2146 (1980).
6. K. R. Darnall, R. Atkinson, and J. N. Pitts, Jr., *J. Phys. Chem.* **82**, 1581 (1978).
7. R. R. Baker, R. R. Baldwin, and R. W. Walker, *Combust. Flame* **27**, 147 (1976).
8. M. Cohen, *Int. J. Chem. Kinet.* **14**, 1339 (1982).



$$\Delta H_{298}^\circ = -79.1 \pm 4.2 \text{ kJ mol}^{-1} (-18.9 \text{ kcal mol}^{-1})$$

$$\Delta S_{298}^\circ = 28.4 \pm 4 \text{ J mol}^{-1} \text{ K}^{-1} (6.8 \text{ cal mol}^{-1} \text{ K}^{-1})$$



RECOMMENDED RATE COEFFICIENTS

<u>k</u>	<u>k(T)</u>	<u>Range</u>	<u>k(298)</u>	<u>Units</u>
k_1	$6.3 \times 10^3 T^{2.0} \exp(-10/T)$	300-2000 K	5.5×10^8	$\text{L mol}^{-1} \text{s}^{-1}$
	$1.1 \times 10^{-17} T^{2.0} \exp(-10/T)$		9.1×10^{-13}	$\text{cm}^3 \text{molecule}^{-1} \text{s}^{-1}$

Uncertainty in $\log k_1$: ± 0.1 at 298 K, increasing to ± 0.5 at 2000 K. Because the reverse reaction is unimportant at any temperature, values for $K(T)$ and k_{-1} are not recommended.

(December 1981)

LASER THERMAL PROPULSION

Dennis Keefer
The University of Tennessee Space Institute
Tullahoma, Tennessee 37388

The principal objective of this research investigation is to determine experimentally the effects of a forced convection environment and optical geometry on the stability, fractional power absorption, plasma structure, and fluid mixing in a laser sustained plasma (LSP). A continuous, 1.5 kW, axial flow, carbon dioxide laser is used to create the LSP in a cylindrical quartz flow channel. The convection flowfield surrounding the plasma is controlled by the volume flow through the test chamber, and the optical geometry is determined by the focal length of the lens. Digital images of the plasma in selected narrow wavelength intervals are obtained using a calibrated, CID digital camera and a VICOM digital image processing computer. These images are then Abel inverted to give a spatial plasma emission coefficient which is used to determine the spatial distribution of the plasma temperature. The measured temperature field of the plasma is used to determine the spatial distribution of the plasma absorption coefficient for the plasma, and permits a spatially resolved calculation of the balance between energy absorbed from the laser beam and the energy lost from the plasma through radiation, convection, and thermal conduction. Data have been obtained for argon plasmas at a nominal pressure of two atmospheres and four different bulk flow velocities from 0.4 to 2.9 m/s. The temperature isotherms for these four cases are shown in Figure 1. Note that the plasma forms upstream of the focal point of the laser beam. The distance between the temperature maximum and the focal point changes as the flow velocity changes, and is extremely important in determining the fractional power absorbed from the laser beam. As the flow velocity increases, this distance decreases, but the temperature isotherms become more elongated and move into a region of greater laser intensity, thus producing an overall increase in the optical depth of the plasma. Figure 2 shows the volumetric power absorption of the plasma as determined from the measured temperature field. Note that the maximum volumetric power absorption occurs at a position downbeam from the plasma temperature maximum, an effect which is caused by the focusing properties of the converging laser beam. Detailed examination of the complex interactions of the various energy absorption and loss mechanisms will lead to a more complete understanding of the processes which control plasma stability, fractional power absorption and mixing in the laser sustained plasma.

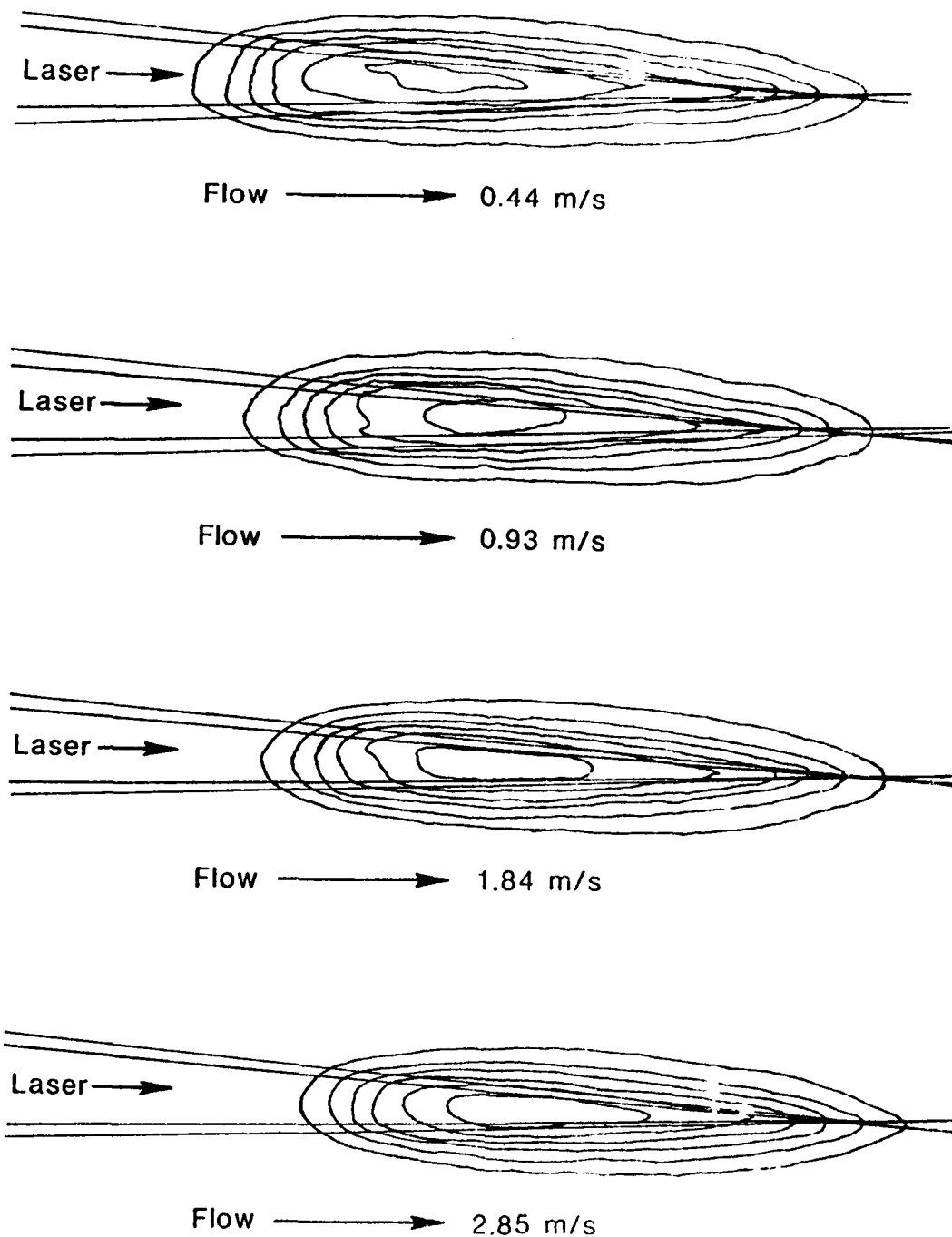


Figure 1. Anticipated isotherm profiles for an argon plasma at a nominal pressure of two atmospheres and the indicated bulk flow velocities.

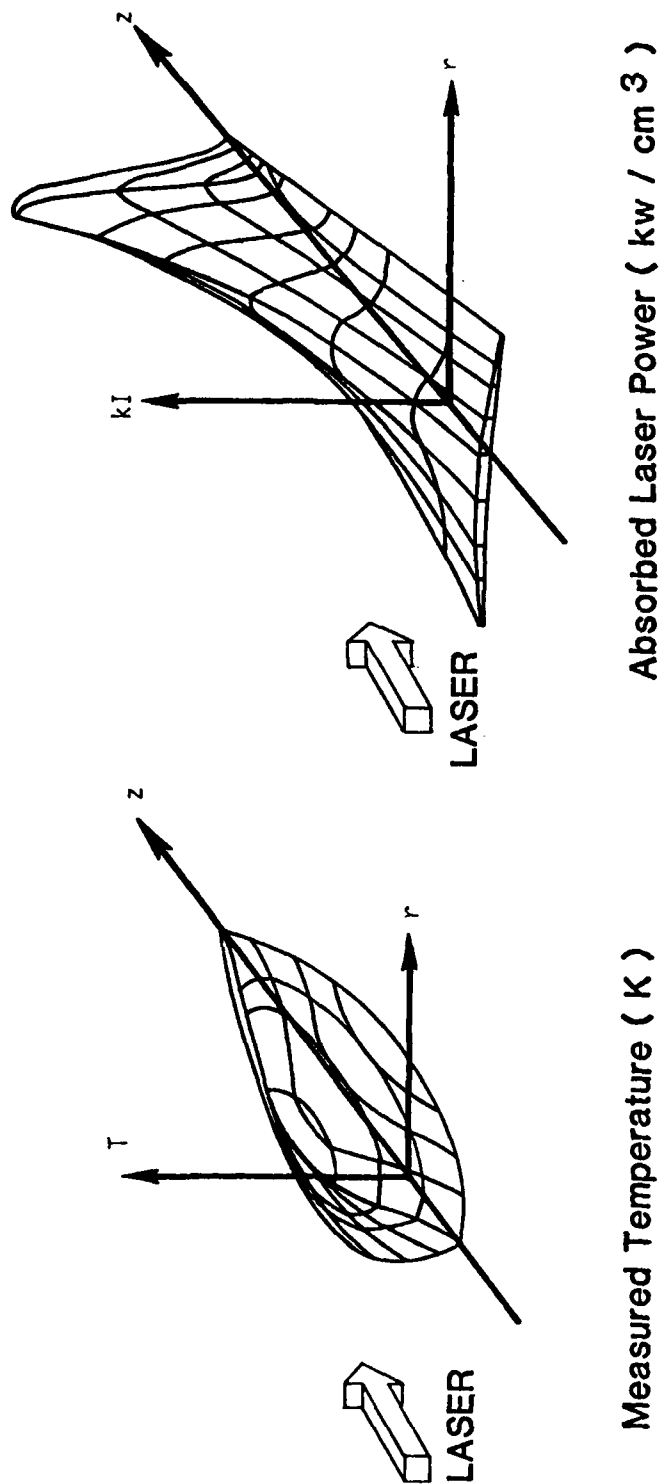


Figure 2. Anticipated results for absorbed laser power determined from measured temperature fields.

RESEARCH STUDIES IN SUPPORT OF A PULSED LASER-HEATED
THRUSTER - LASER-INDUCED GAS BREAKDOWN IN THE VISIBLE/UV

DAVID I. ROSEN AND GUY M. WEYL

Physical Sciences Inc.
Research Park
Andover, MA 01810

In the RP thruster concept shown in Fig. 1, parabolic nozzle walls focus the incoming beam to yield propellant breakdown at the focal point of the parabola. Depicted schematically in Figs. 1a-1d are the various stages in the thrusting sequence: breakdown, laser absorption, blast wave expansion, and late time expansion (when the flow becomes nearly 1-D). Past experimental studies using CO₂ lasers have demonstrated the validity of the laser heated thruster concept. Shorter wavelength lasers, however, are advocated because of the smaller optics required for propagation over large distances.

We have carried out experiments to determine threshold laser intensities required for stages a and b - ignition and absorption - to occur. We used the laser facilities of the MIT NSF regional laser center: a Nd-Yag laser beam of pulse energy $E < 0.75$ J and $\tau_p = 15$ nsec in conjunction with a frequency doubler and tripler to generate 0.53 and 0.35 micron radiation. Thresholds, I_{th} , were measured in Ne, Ar, Xe, and N₂ gases, either pure or with easily ionizable contaminants, as a function of pressure p . I_{th} was defined as the lowest I for which a visible spark was observed in the gas together with significant absorption, $\alpha > 0.05$, of laser energy.

Breakdown is associated with electron density growth through two main mechanisms: multiphoton ionization (MPI) of the atom/molecules in the intense laser field and cascade breakdown due to electron impact ionization of the gas or electron impact excitation followed by photoionization of the excited states. We have modeled both processes using known MPI cross sections and using a Boltzman code to solve for the electron distribution and calculated excitation and ionization rates. Comparison of theoretical and experimental results indicate that breakdown as defined above is associated with cascade ionization and not MPI.

The measured thresholds are plotted in Fig. 2 as a function of ionization potential, ϵ_I , of the gas. They show that I_{th} increases with ϵ_I , with N₂ showing an anomalous behavior. These thresholds are to be compared with those at 10.6 μ m also plotted in Fig. 2. The data for Ne were obtained by scaling to 10.6 μ m the microwave breakdown measurements of Kuston and Fuja¹ the data for Xenon was taken from Generalov et al.², N₂ from Weyl³, Ar from our previous work,⁴ and the data for He from Yablonovick.⁵ PT scaling was used to reduce the results to $p = 3$ atm, $\tau = 15$ nsec. For breakdown dominated by cascade ionization, one would expect the thresholds to scale as the inverse bremsstrahlung absorption coefficient, i.e. as λ^{-2} . Though such a scaling from 10.6 μ m to 0.53 μ m is nearly obeyed by Neon, thresholds are found to be much lower for most gases with smaller ionization potential. This is because excited states of these gases become rapidly photoionized at short wavelength.

1. R. Kuston and R. Fuja, J. Appl. Phys. 47, 498 (1976).
2. N. Generalov, V. Zumakov, G. Kozlov, V. Masyukov and Y. Raizer, JETP Lett, 11, 228(1971).
3. G. Weyl, J. Phys. D, Appl. Phys. 12, 33(1979).
4. DiRosen et al. PSI TR-184 (undated).
5. E. Yablonovick, Phys. Rev. Lett, 32, 1101 (1974).

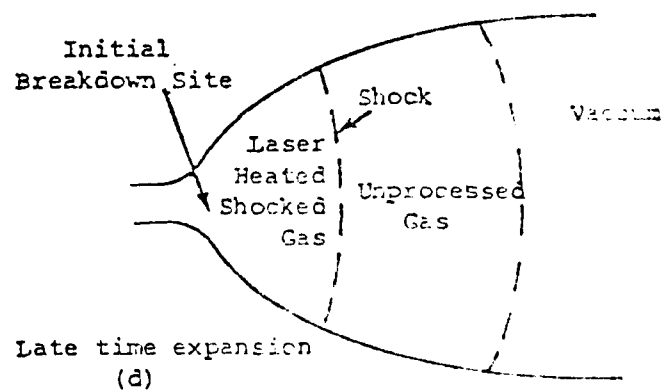
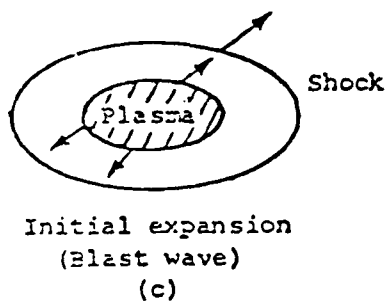
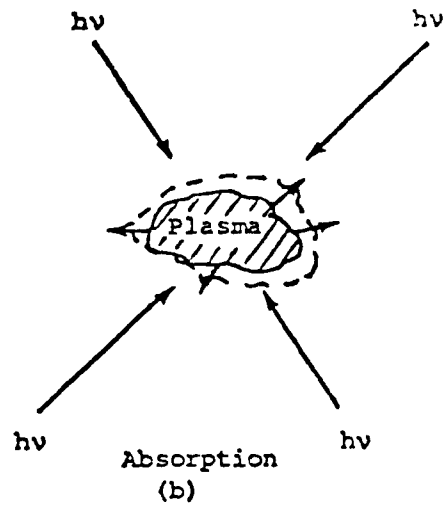
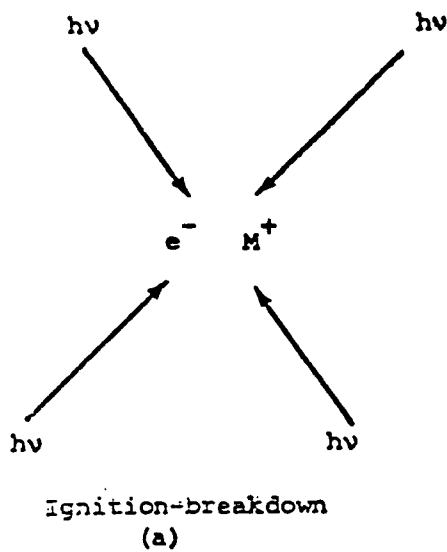


Fig. 1 Different stages in pulsed laser thruster. (Sequence a-d is repeated after initial gas has expanded out of nozzle and fresh gas enters.)

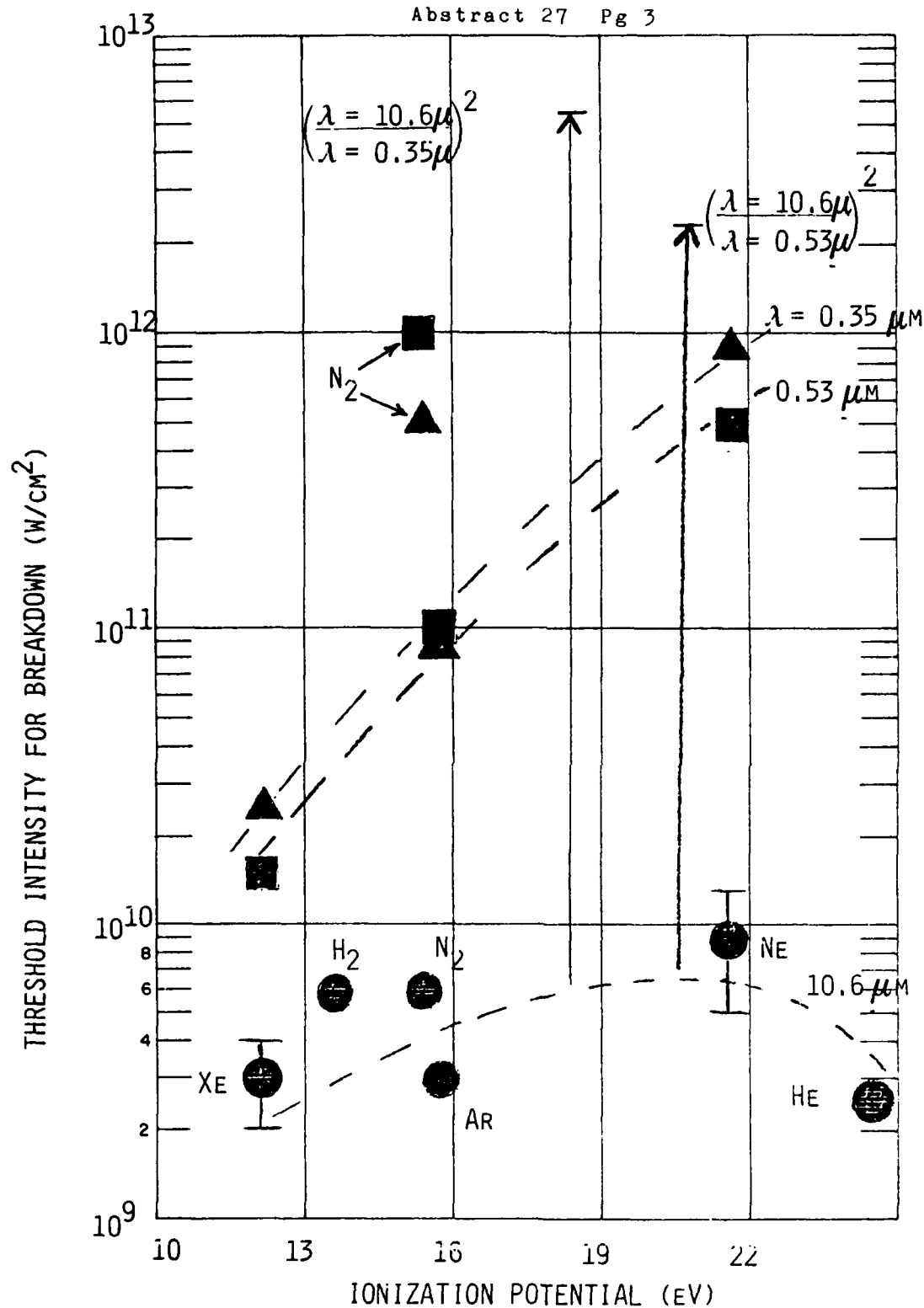


Fig. 2 Breakdown thresholds measured in simple gases showing dependence on wavelength and ionization potential. The data plotted are for $p \approx 0.05$ atm.

HIGH TEMPERATURE MOLECULAR ABSORBERS FOR CW LASER PROPULSION

David I. Rosen
David O. Ham and Lauren M. Cowles
Physical Sciences Inc.
Research Park
Andover, MA 01810

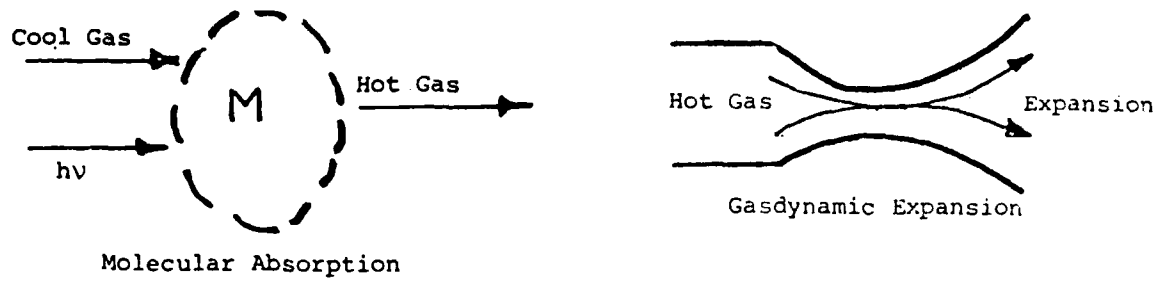
The physical processes involved in heating the working fluid of a rocket engine with a high power CW laser beam are diagramed in Fig. 1. Gas is injected into the absorption zone at a temperature most probably determined by regenerative cooling requirements. As the gas flows toward the throat, it is heated by absorption of laser radiation. With hydrogen as the primary propellant constituent, the equivalent of nine $10.6 \mu\text{m}$ photons per molecule must be absorbed to reach a stagnation condition that yields a specific impulse of ~ 1000 seconds.

The absorption scheme originally considered required the laser-induced breakdown of the H_2 "fuel" followed by the formation of a stable laser-supported combustion (LSC) wave. The principal absorption mechanism in this case is inverse electron bremsstrahlung, which requires significant ionization levels in the carrier gas. It has been suggested that the introduction of alkali seeds, which will begin to thermally ionize at temperatures of ~ 3000 - 3500 K, would allow operation at temperatures of ~ 6000 K, well below the temperature required for ionization in pure hydrogen. It remains to be shown, however, that stable LSC waves can be formed at such low temperatures.

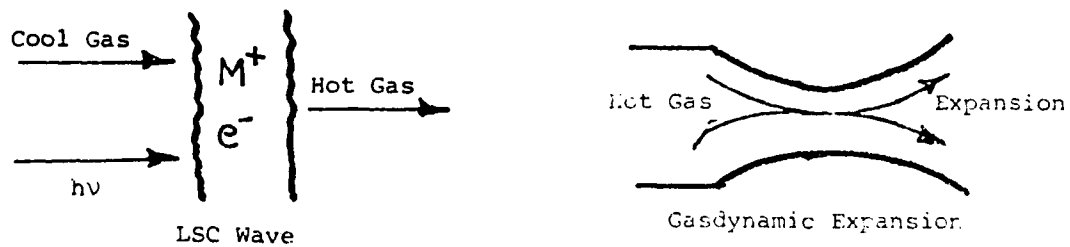
Although the use of alkali seeds appears promising, a technique, such as laser-induced breakdown, is still required to heat the gas to $T \sim 3000$ - 3500 K (to initiate alkali ionization). One alternative is to use "seed" molecules to absorb the laser radiation via vibration-rotation band transitions. Such absorbing molecules can provide for gas heating to temperatures of ~ 3000 - 3500 K, so that heating from the initially "cold" gas to stagnation conditions can be continuous rather than via laser-induced breakdown. Furthermore, if such species can absorb to $T \approx 4500$ - 5000 K, then specific impulses of 1000 - 2000 s can be achieved without the need for ionization (and thus alkali seeds).

The high resolution absorption properties of potential absorbers for this approach are not well known at temperatures exceeding 1000 K. Important absorption paths at elevated temperatures involve hot band transitions which have not been studied. Furthermore, most molecules will dissociate in the temperature range of interest, so that they no longer provide effective absorption.

We will report experimental results for the absorption of CO_2 laser radiation by the three most promising candidate absorbers in the $10 \mu\text{m}$ region, NH_3 , H_2O and CO_2 . Measurements were made in the low intensity, unsaturated absorption regime using several lines of a line tunable, CW CO_2 laser. Absorption profiles versus time were obtained in both the incident and reflected shocks for very dilute mixtures of the absorbers in Ar, shock heated to temperatures of 600 - 4000 K and pressures of 0.5 - 120 atmospheres. Curves drawn through our experimental data points are shown in Fig. 2 for the P(20) CO_2 laser line at $10.59 \mu\text{m}$. The absorption coefficients plotted in Fig. 2 are calculated per amagat of the absorber as if none of the absorber dissociates. Any dissociation appears in the measurements as reduced absorption unless dissociation fragments also absorb. The high temperature fall-off of the absorption coefficient for NH_3 is extremely sensitive to heating rate. Rapid heating allows continued absorption up to the temperature where the dissociation rate is comparable to the heating rate. These small signal results indicate that with rapid laser heating, adequate absorption to heat a thruster gas to above 4000 K can be attained by seeding with an H_2O - NH_3 mixture. Saturation effects in absorption by these species at high laser intensities will be investigated in subsequent work.

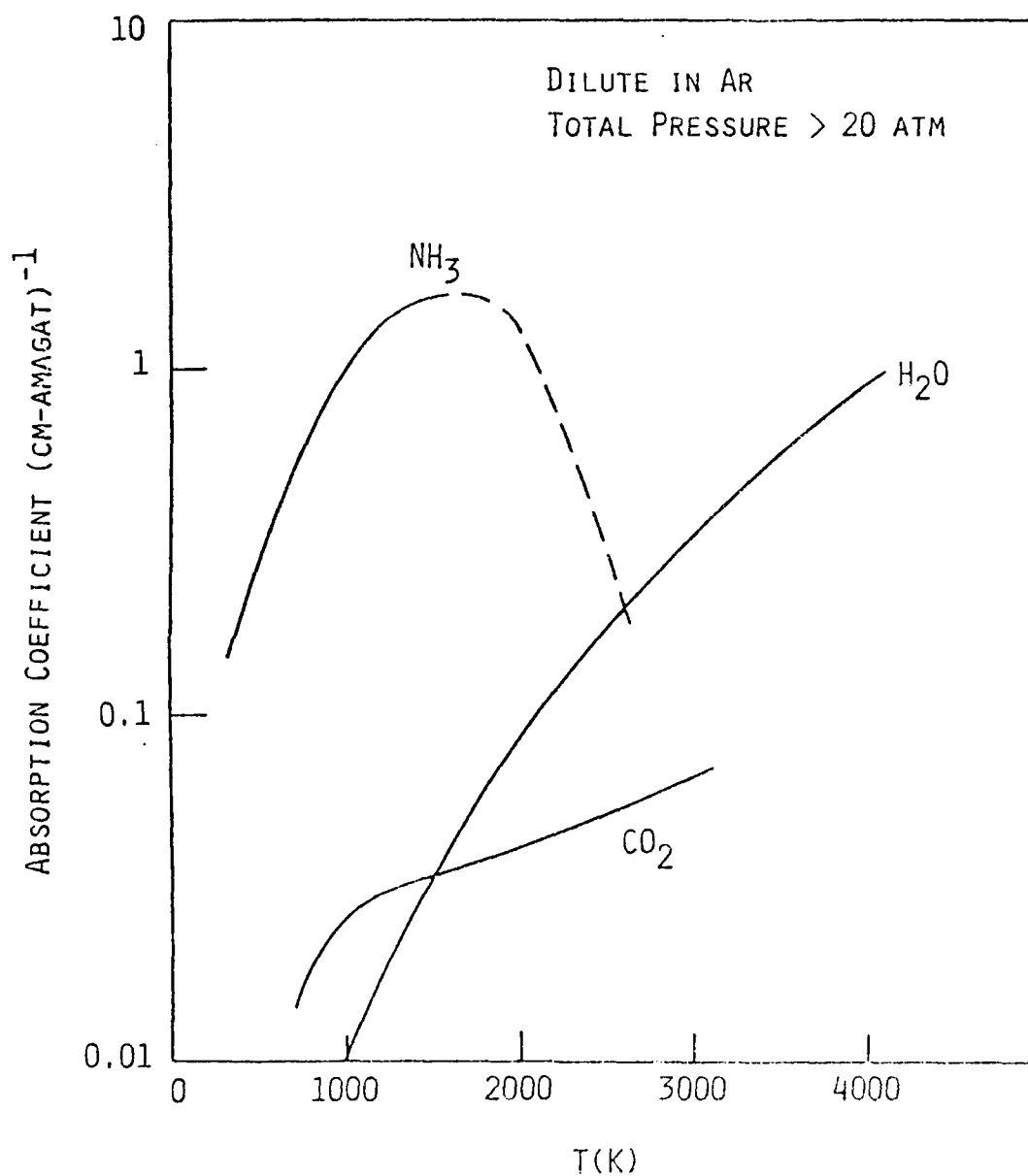


a) Continuous Absorption Mode



b) Laser-Supported Combustion Wave Absorption Mode

Fig. 1 Two possible modes of operation of a CW laser-heated thruster.



- NH₃ absorption depends on heating rate/dissociation rate (dashed region)
- Adequate absorption can be attained by seeding with an NH₃-H₂O mixture

Fig. 2 Measured low intensity absorption coefficients for 10 p P(20) CO₂ laser line.

Propagation of Laser Supported Plasmas
in Flowing Media

Charles L. Merkle and Thomas M. York
The Pennsylvania State University
University Park, PA

The absorption of electromagnetic energy in a laser thermal thruster is shown schematically in Fig. 1. An incoming collimated beam with a gaussian intensity distribution is focussed inside the nozzle. The energy absorption is determined by a strongly coupled interaction between the nozzle flowfield and the radiation. This interaction is being modeled in a detailed manner using both one-dimensional and two-dimensional analyses. The one dimensional analysis is useful for understanding such fundamental phenomena as the propagation mechanisms of the laser absorption volume and their sensitivity to the shape of the absorptivity-temperature curve. Propagation mechanisms being considered include conduction, radiation, and non-equilibrium effects, individually and in combination. Sensitivity to the absorptivity-temperature curve is to be found both by parameterizing in terms of a power-law dependence on temperature and density, and by using specific absorptivity-temperature variations corresponding to selected H_2 and H_2 -seedant mixtures.

One-dimensional results to date have indicated that the behavior of the absorption process inside a choked nozzle is considerably different from that in a constant area duct. Some representative results of this nature are given on Fig. 2.

Although such one-dimensional analyses are invaluable for obtaining initial understanding and establishing trends, they cannot be expected to yield better than order of magnitude predictions. More realistic predictions must take into account the many strong two-dimensional effects noted in Fig. 1. The effects of parameters such as beam convergence, radial intensity gradients, radiant heat loading on the walls, mixing between the hot central core and cool outer gases, and variations in the size and shape of the absorption volume cannot even be estimated from one-dimensional results. In particular, the two-dimensional formulation allows tradeoffs between the size and the peak temperatures of the absorption volume to be made. Realistic modeling of the propagation mechanisms also becomes possible in two-dimensions. Some preliminary two dimensional results which have been obtained to date are also shown on Fig. 2. These results are for beam absorption in an unchoked, subsonic nozzle. The beam convergence, Mach number and temperature contours are presented.

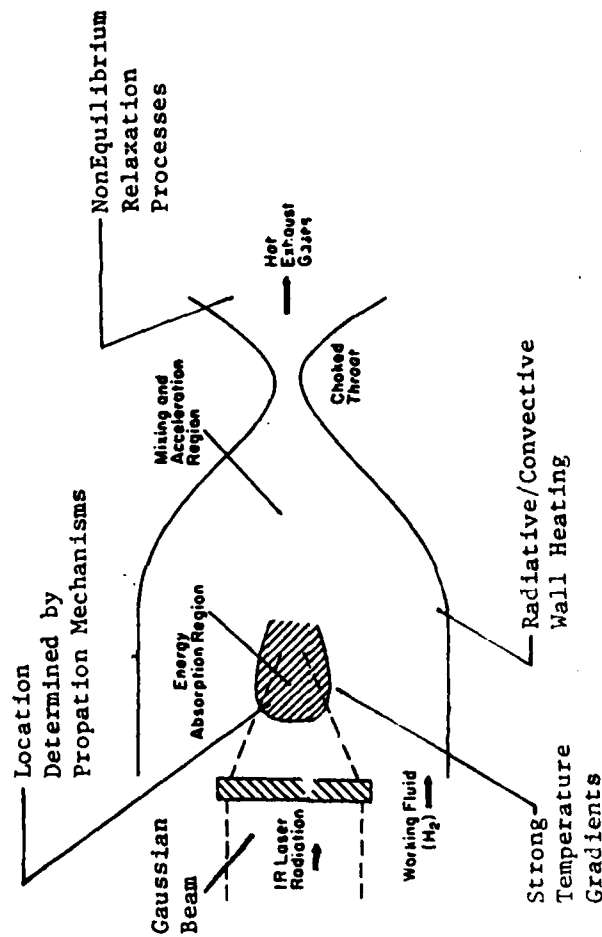


Figure 1. Schematic of Laser Thermal Thruster
 Showing Key Mechanisms which Determine
 Thruster Performance

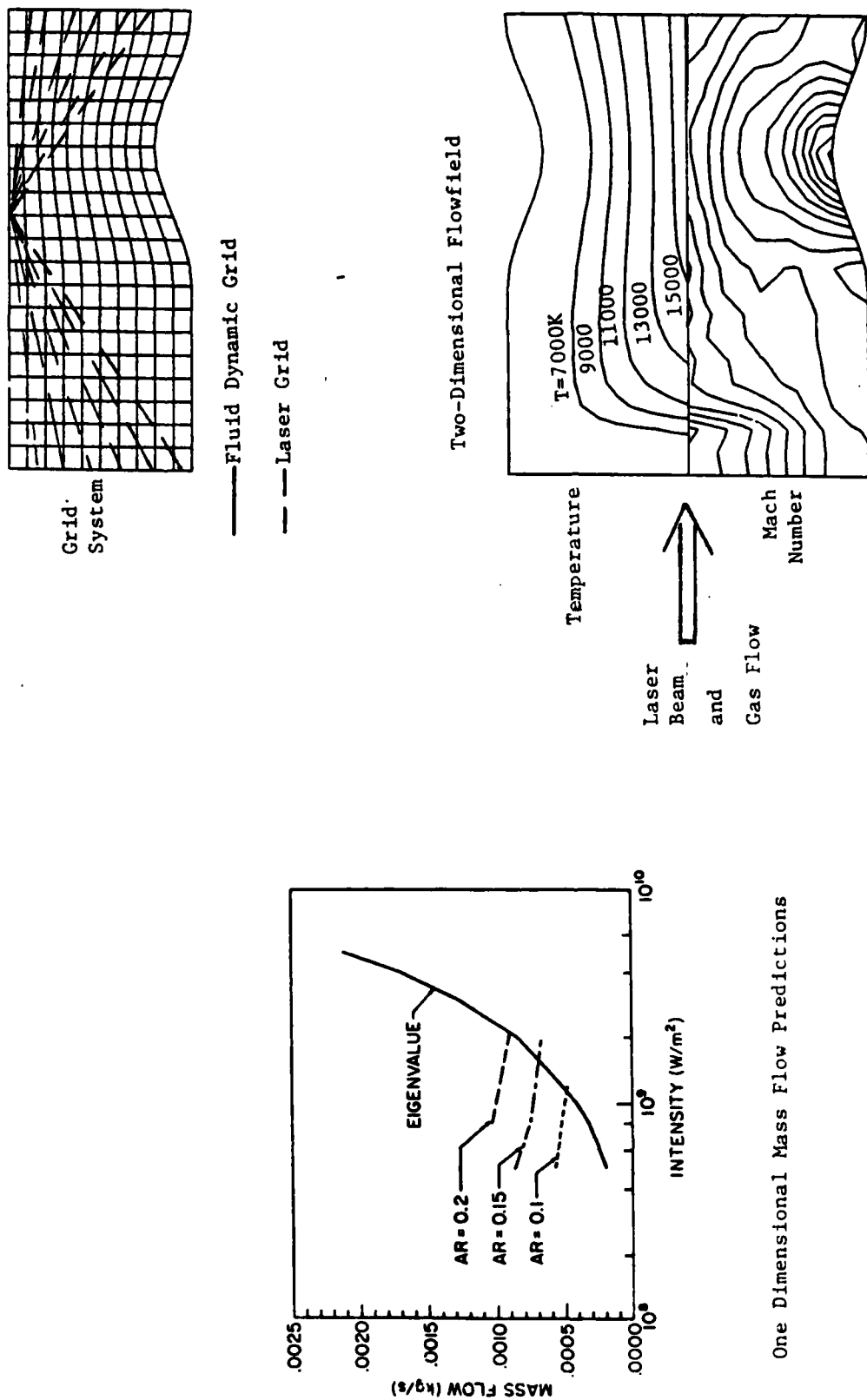


Figure 2. Characteristics of Radiation/Gas Dynamic Interaction in Nozzles

**A HIGH POWER Nd-GLASS LASER INSTRUMENT
FOR ADVANCED PROPULSION AND DIAGNOSTICS**

Charles L. Merkle and Thomas M. York
The Pennsylvania State University
University Park, PA 16802

A high power short wavelength ($1.06\mu\text{m}$) source is being developed by adding two Nd-glass amplifiers to an Nd-Yag oscillator as shown in Fig. 1. The source is to be used in radiation absorption studies for laser propulsion applications, and for advanced optical diagnostics. A short wavelength source is attractive for laser propulsion because it is near a transmission window in the atmosphere and because it allows smaller collector optics. The Nd-glass instrument also promises to be a more flexible laboratory tool than typical gas lasers.

The integration of the oscillator and the two high gain amplifiers must be accomplished with extreme care because of the near-ultimate loading in the rods and amplifiers. The combined two-stage amplifier has a gain of nearly 10^4 , and spurious triggering caused by uncontrolled feedback will destroy the amplifiers. The maximum power delivered will be dependent on achieving a high degree of effective isolation between the amplifiers. This isolation will be accomplished by means of a Faraday rotation device. Precise control of beam nonuniformities generated by the pump lamps and by rod doping must also be maintained to prevent amplifier damage. The concept described here is also being tested at Los Alamos National Laboratory, but run time requirements for the present application require an order of magnitude extension. A maximum run time of 10ms is being used as a goal.

The oscillator-amplifier system has two distinct duty cycles. In the first, the instrument operates in a quasi-CW mode as outlined in Fig. 1. In this duty cycle, the oscillator is operated mode-locked, producing a 100 nJ pulse in 100 ps every 10 ns. The output goal after amplification is to deliver 800 J in 10 ms in this mode, an average power of 80 KW. This energy delivery represents a quantum jump over presently available systems. As shown in Fig. 2, the individual pulses in this wave train will be so closely spaced in time that gas molecules have no time to move between pulses and hence see an effectively continuous radiation input.

The second duty cycle is also shown on Fig. 1. Here, the oscillator is Q-switched to produce a pulsed output at frequencies up to 50 KHz. These signals are again amplified to produce a high power repetitively pulsed output, although net gains in the pulsed mode are expected to be lower because of the higher instantaneous intensities. This repetitively pulsed output may be of interest in pulsed laser propulsion, but also offers promise for advanced instrumentation concepts. In such applications, frequency doubling to $0.53\mu\text{m}$ will probably be required. The frequency doubling can also be accomplished in the first duty cycle, and in addition wavelength doubling to $2.12\mu\text{m}$ can be performed.

HIGH POWER Nd-GLASS LASER BEAM SOURCE

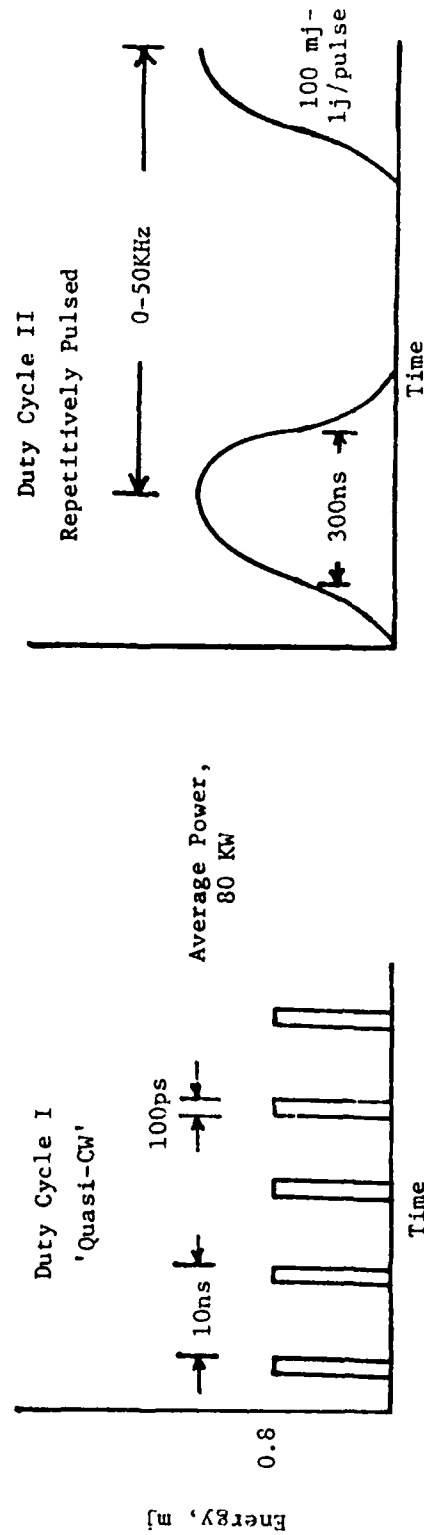
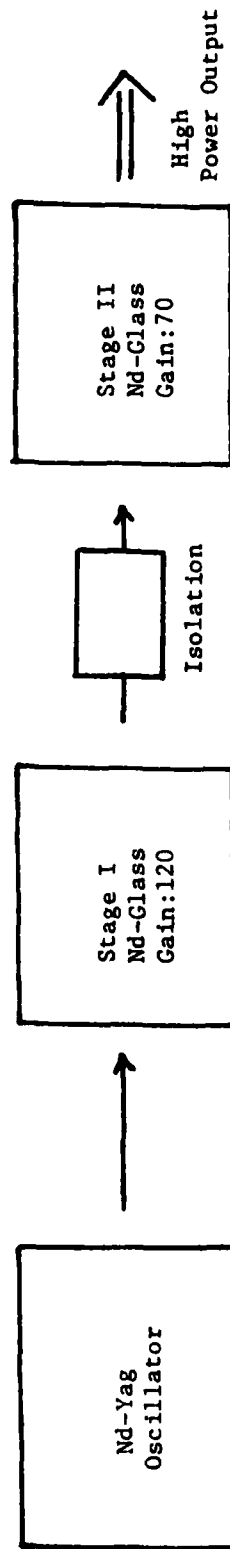


Fig. 1 High Power Short Wavelength Source and Duty Cycles

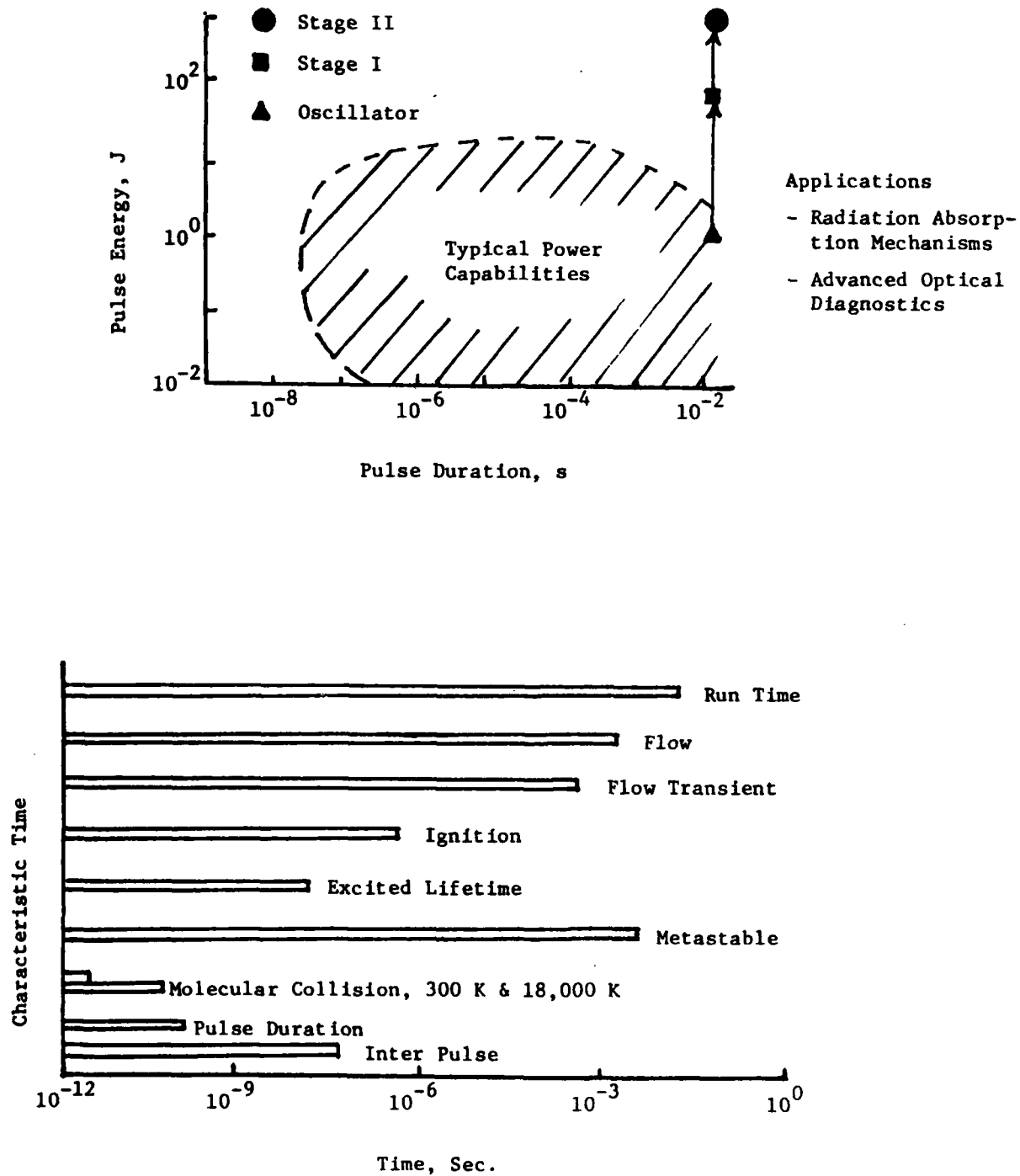


Fig. 2 Power Output Goals in Quasi-CW Mode
and Use for Absorptivity Measurement

PLASMA INITIATION MECHANISMS
FOR CW LASER PROPULSION (AFOSR #83 - 0041)

Herman Krier and Jyoti Mazumder
University of Illinois at Urbana-Champaign
Department of Mechanical and Industrial Engineering, Urbana, IL 61801

Successful utilization of laser propulsion requires a thorough understanding of laser-sustained plasmas; most of the fundamental processes found in such plasmas are summarized in Figure 1. A high energy (10 kW CO₂) laser is used to provide high flux densities ($>10^6$ W/cm²) to a gas inside a pressurized flow-through chamber. Many important questions remain, particularly in regard to plasma initiation and stability, plasma properties, convective mixing, and energy losses. It is our intention to resolve these questions by 1) investigating plasma initiation using targets and seedants, 2) producing detailed temperature and density measurements in the plasma core, 3) extending the temperature data downstream to define mixing behavior, using infrared thermography, thermocouples, and laser-induced fluorescence (LIF), and 4) estimating global absorption, using a high-flux calorimeter. Figure 2 summarizes some of the quantitative data we plan to collect in the near future; each graph represents a current analytic estimate.

During the past year, our efforts have focused on the design and construction of a pressurized flow chamber to enclose the plasma, and on installing diagnostic equipment. Our first experiments are planned for early April, '84. The chamber has been designed for maximum flexibility in data acquisition, permitting studies of plasmas under high-pressure (up to 10 atm) steady-state flow conditions. Considerable attention was given to the optical system that will focus the laser beam into desired locations inside the chamber in order to initiate the plasma. A wide range of flow velocities are possible, and the five-inch diameter allows complete study of downstream mixing. The laser optics permit precise focusing in the range $2.2 < f < 3.4$ to test for stability effects.

To measure plasma temperatures, an EG & G OMA-2 (spectroscope) system is being purchased to analyze spectral line broadening and relative line intensities. Work is now underway to correlate spectroscopic output with temperature. At lower temperatures, we will be using an infrared thermography system to examine mixing behavior. This system has recently been calibrated to 3500 K, but an even higher upper limit appears likely. We also plan to purchase a tunable dye laser to induce LIF in the gas, allowing accurate temperature resolution in the crucial 2,000 - 10,000 K range.

With the data we obtain in the PIFC (Plasma Initiation Flow Chamber) it will be possible to accurately determine the processes of plasma heating including the loss mechanisms, information required as input into our two-dimensional steady-flow computer model. Clearly the data will show whether the theoretical absorption coefficients used in the model are valid in the flowing system required for propulsion application.

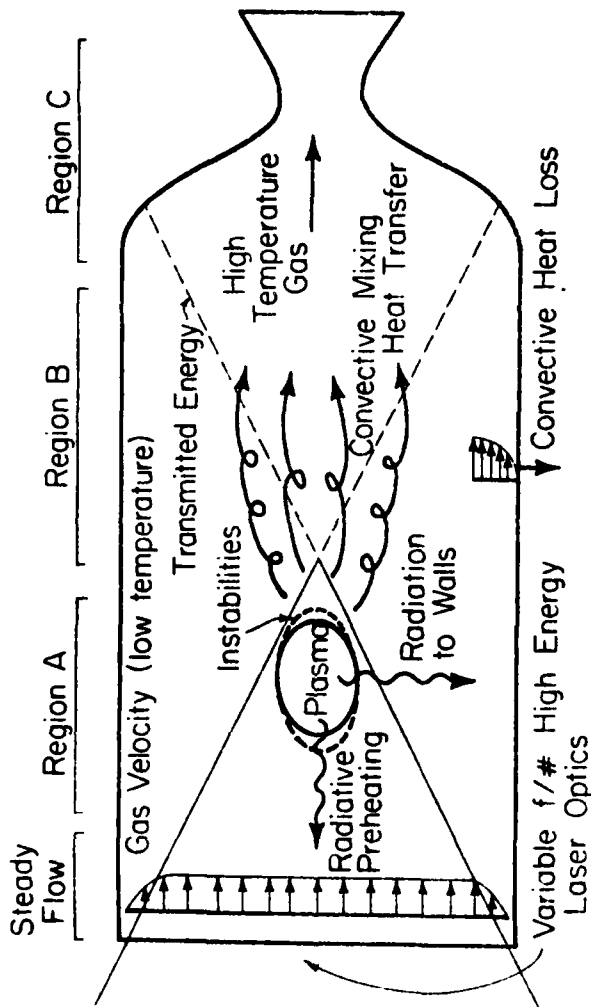
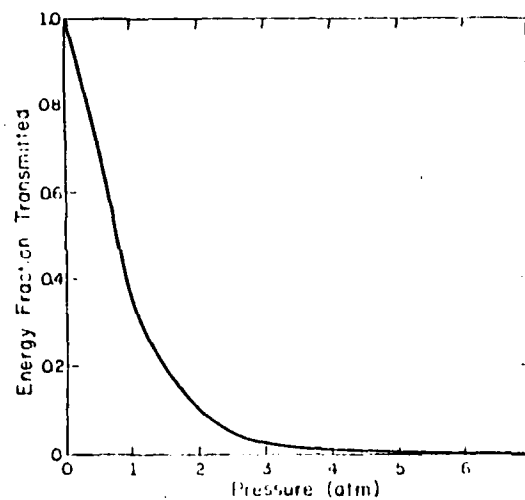
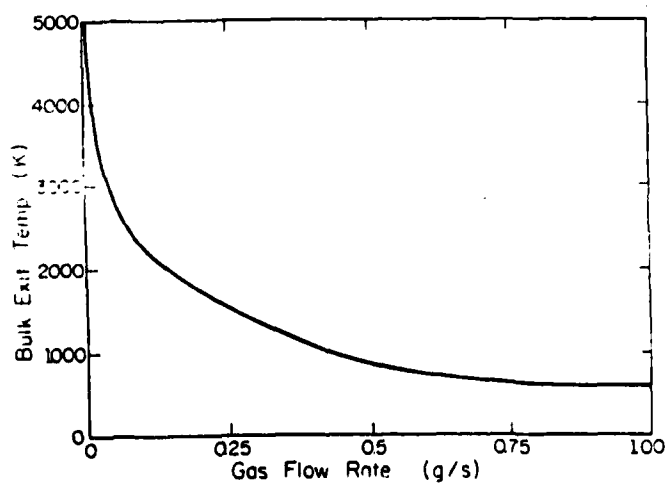
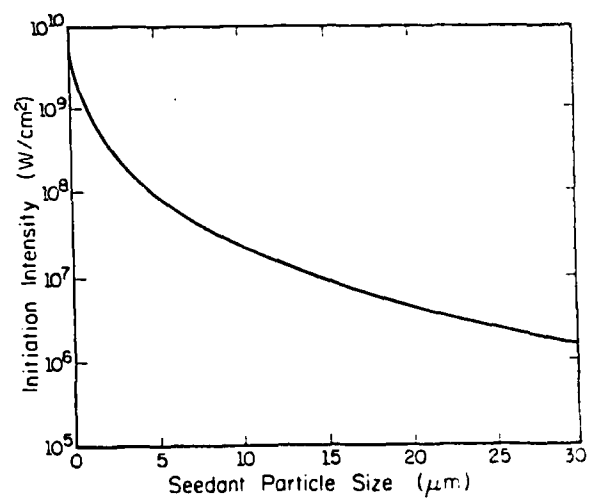
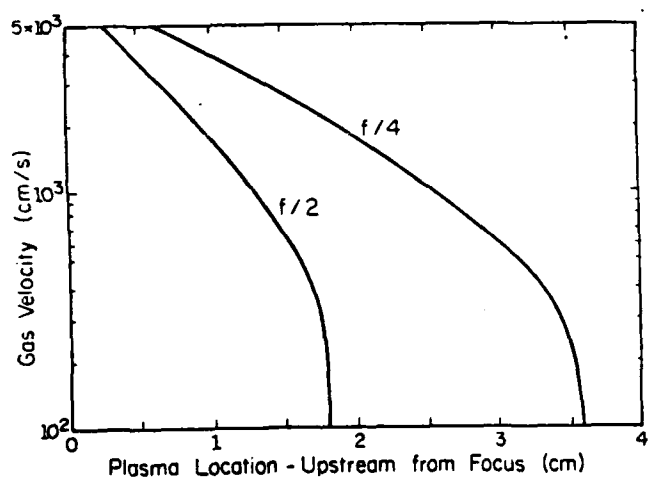
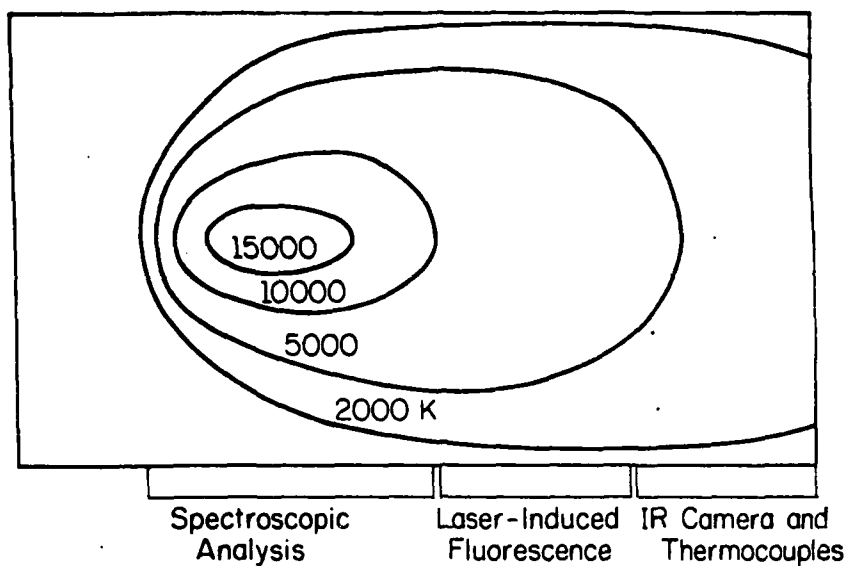


FIGURE 1
PHYSICS OF BEAMED
ENERGY PLASMA
HEATING

UNIVERSITY OF
ILLINOIS AT
URBANA-CHAMPAIGN

- HIGH-TEMPERATURE PLASMA IS HEAT STATIONARY IN A CONVERGING BEAM.
- PLASMA PROPERTIES VARY WITH FUNCTION OF INTENSITY JUST MATCHES
- THE FLOW LOCATIONS AT THE FOCUSED PLASMA LOCATION.
- PLASMA IS INITIATED BY COLLIMATED BEAM OF FREE ELECTRONS (THE FOCUSING OF TARGETS, FOLLOWING A PULSED LASER).
- PLASMA MAY EXHIBIT HIGH-TEMPERATURE INSTABILITIES AND ABSORPTION IN INSTABILITIES.
- PLASMA BEHAVIOR DEPENDS ON FLOW VELOCITY, PRESSURE, F/R OF OPTICS, ETC.
- IN REGION A:
 - HIGH-TEMPERATURE TURBULENT LOW-RE-FRASE CONVECTIVE FLOW REGIME
 - HUGE DENSITY GRADIENTS AND SIGNIFICANT BOUNDARY EFFECTS
 - UPPER-AN RADIATIVE PREHEAT ZONE
 - COMPLEX LOCALIZED BEAM PLASMA
 - VERY HIGH LEVELS OF RADIATIVE HEAT TRANSFER TO WALLS
- IN REGION B:
 - EXACTLY THE SAME MAY NOT BE THROUGHOUT MIXEL (MIXED) FLOWS AND INSTABILITIES
 - EXACTLY THE SAME MAY NOT BE IN VIBRATION/ROTATIONAL EQUIVILIBRIUM
 - LIMITED ABSORPTION OF TRANSMITTED LASER ENERGY
 - TRANSMITTED LASER ENERGY MAY BE MEASURED USING A CALORIMETER
 - PEAK TEMPERATURES MAY BE MEASURED USING A CALORIMETER
 - OVERALL EFFICIENCY MAY BE MEASURED BY USING SEVERAL
- IN REGION C:
 - MODERATE-TEMPERATURE MIXEL FREE/FORCED CONVECTIVE FLOW REGIME
 - TURBULENT UNSTEADY SHEAR LAYER MIXING ZONE
 - LIMITED ABSORPTION OF TRANSMITTED LASER ENERGY
 - LIMITED ADDITIONAL HEATING DUE TO RADIATION FROM PLASMA
 - CONVECTIVE HEAT LOSS TO WALLS



AN EXPERIMENTAL STUDY OF LASER SUPPORTED HYDROGEN PLASMAS

T. D. McCay, D. M. VanZandt and R. H. Eskridge

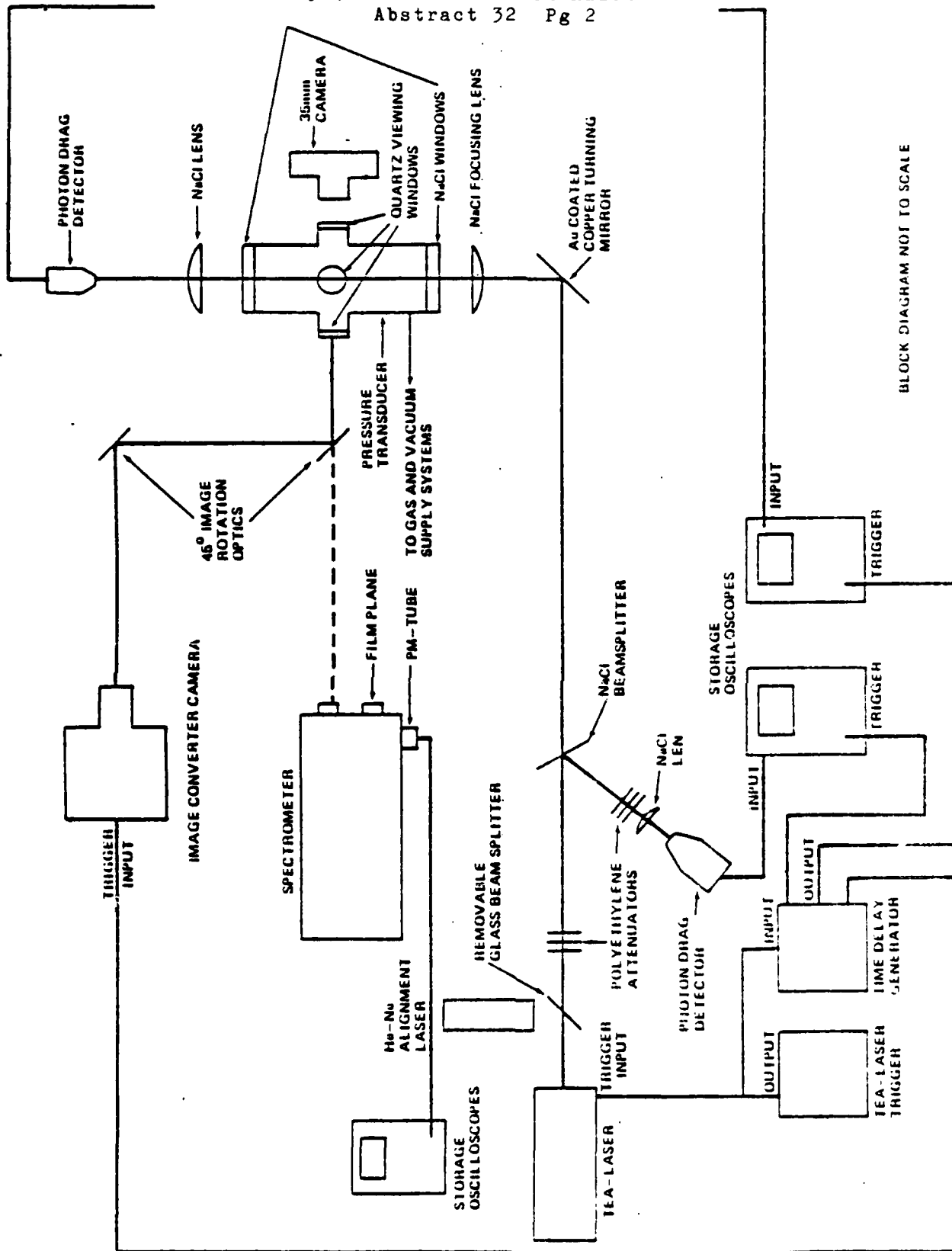
Turbomachinery and Combustion Devices Branch
Structures and Propulsion Laboratory
NASA, George C. Marshall Space Flight Center
Huntsville, Alabama

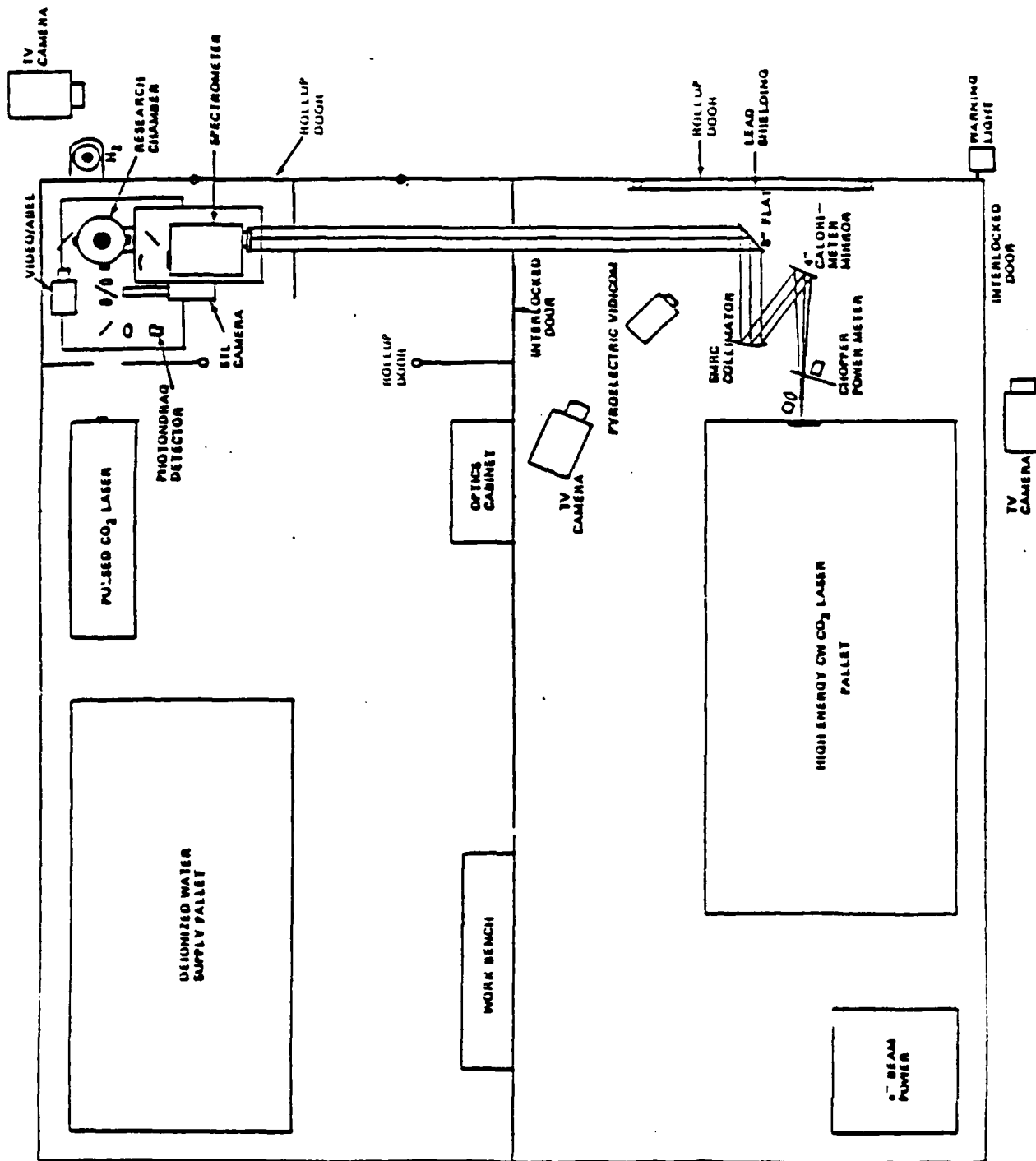
ABSTRACT

A research program has been underway since 1981 at the Marshall Space Flight Center to develop an understanding of the physical processes pertinent to a laser supported hydrogen plasma. A comprehensive experimental program has been undertaken which uses a 30 kilowatt continuous wave(cw) CO₂ electric discharge laser to produce laser supported plasmas (LSP) in air, argon and hydrogen. A pulsed laser spark ignition scheme has been developed to permit an initial highly ionized plasma to be produced at the focus of the cw laser and thus initiate an LSP. The spark breakdown scheme which uses a 6 Joule per pulse Transverse Excitation Atmospheric (TEA) CO₂ laser has been thoroughly documented. The temporal behavior of the plasma spark emission, its absorptivity, and the behavior of the breakdown threshold with pressure have all been examined. Very limited data on hydrogen laser breakdown has previously existed and this small amount of available data compares favorably with the current measurements. A breakdown intensity threshold of 10 Gigawatts was measured for one atmosphere hydrogen for the 100 nanosecond pulse length typical of the TEA laser used. In addition, the mode locking behavior of the TEA laser was found to significantly affect the character of the spark, a finding which disagrees with some previous work.

The experiments which document the transition of the laser spark into a sustained plasma supported by the 30 kw continuous wave laser have only recently begun, but data which documents the transition and also the steady state properties of the plasma should be available for inclusion in the paper. This data would include fast frame and streak photography of the transition process, spectrographic surveys, and temperature maps obtained using a video camera system with automated digitization and Abel inversion data reduction schemes. Details of the diagnostics and the results of the study, especially the parametric studies of plasma absorptivity will be highlighted in the article. Schematics of the simple spark experiments and the overall laser supported plasma experiment are attached.

The ultimate goal of this line of research is to develop a sufficient data base from which to design a thruster which would employ this concept for propellant heating. Based on concurrent chemical kinetics studies of such a system it appears specific impulse values as high as 2000 seconds at thrust levels of hundreds of pounds could be obtainable using such a concept.





EXPERIMENTAL SET-UP - LASER EXPERIMENTS

AFRPL SOLAR-THERMAL ROCKET ACTIVITIES

C. C. Selph
AF Rocket Propulsion Laboratory
Edwards AFB CA 93523

ABSTRACT

Earth orbital maneuvers, particularly orbit raising, provide the most important and extensive propulsion tasks in space and are not ideally served by either chemical rockets with their comparatively low I_{sp} or electric rockets with their low thrust. For several years the Air Force Rocket Propulsion Laboratory (AFRPL) has investigated solar thermal propulsion as a potential way of filling this gap in propulsion capability. The concept makes use of concentrated sunlight to heat propellant to temperatures approaching 5000 Deg R for expansion through a converging-diverging nozzle. Typically the propellant is hydrogen, although ammonia might be used where long term storage is more important than ultimate I_{sp} . No oxidizer is needed, so molecular weight is low, and I_{sp} values of 870 seconds for H_2 and 500 seconds for ammonia are believed reasonable goals. More advanced thrusters might add two hundred seconds more. The most characteristic feature of the propulsion system is the pair of large, paraboloidal mirrors, which collect and concentrate the sunlight several thousand fold into the absorber (Fig. 1). The collectors are 45 degrees off-axis parabolas, capable of tracking the sun by rotating around an axis perpendicular to the thrust axis, and also by rotating the vehicle around the thrust axis as necessary. They are envisioned as inflatable structures to save weight.

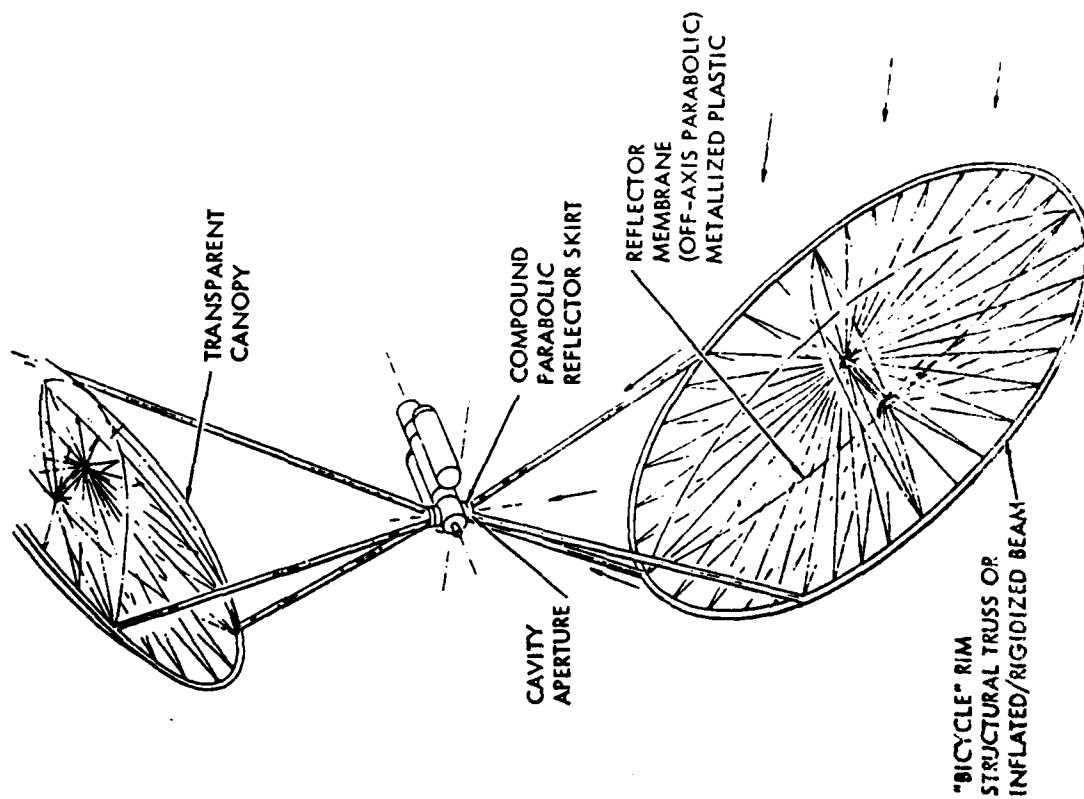
A combined contractual and in-house study was launched to provide a demonstration and evaluation of the concept within the limits of a ground test facility. The design and fabrication of a nominal one pound thrust solar rocket was contracted out, and an in-house facility was initiated to design and build a facility for testing the solar engine. In addition the analysis of alternative thruster concepts has been accomplished.

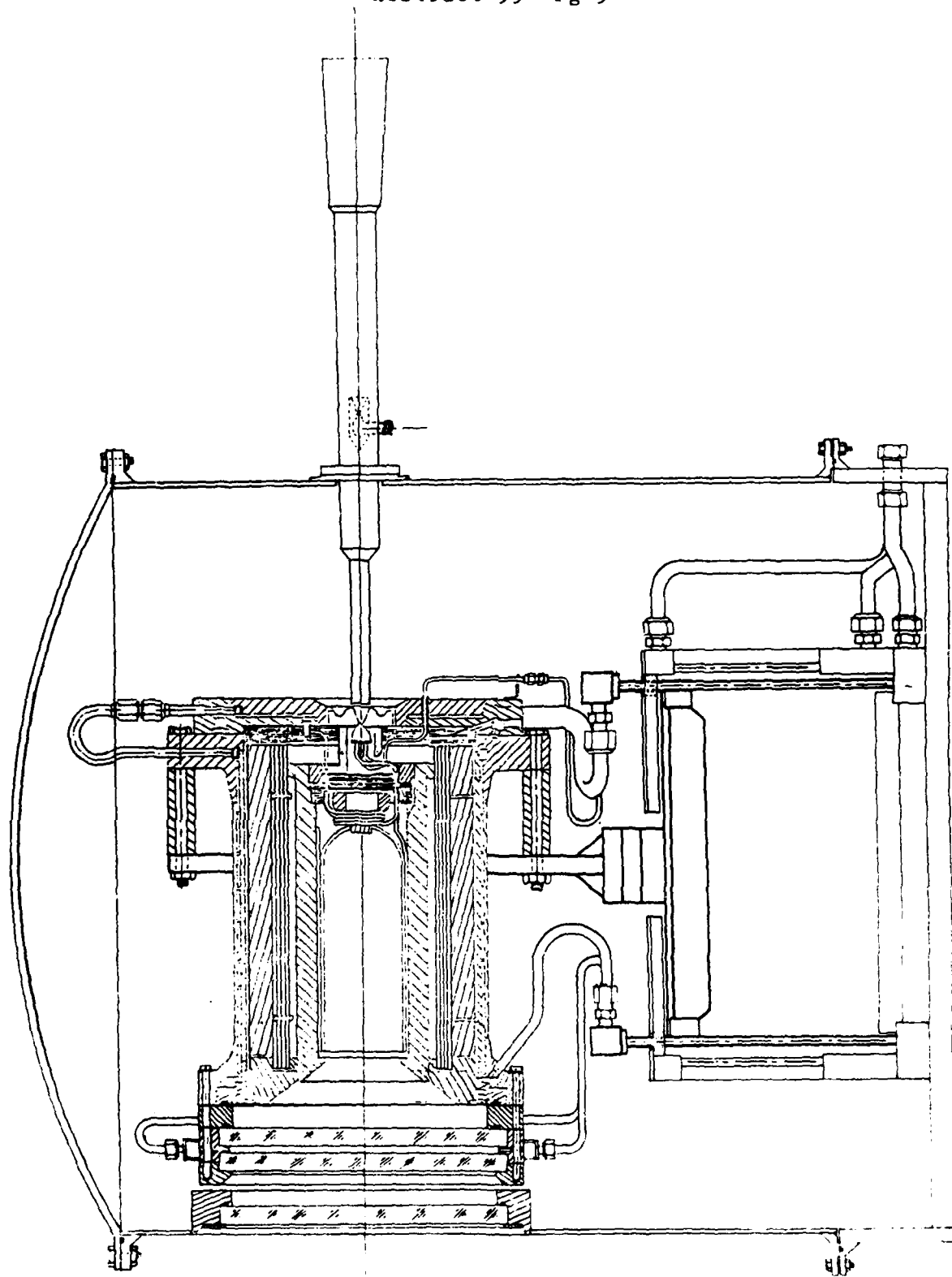
The ground test thruster design and thrust stand facility is shown in figure 2. The thruster is composed of a cavity and heat exchanger formed by windings of rhenium tubing, and a chamber and nozzle, also of rhenium. Other than facility windows to enable vacuum operation the thruster may be classified as "windowless". The main research issues are the durability of rhenium parts at these operating temperatures, and heat loss control.

Alternative thruster designs for possible future improvements include the rotating bed thruster and solar plasma thruster. These are windowed thrusters, and may require improvements in window materials over what is available today. They share concerns with the rhenium thruster in terms of heat loss control, particularly the rotating bed, since there are bearings and seals to protect. Greater understanding of the coupling of sunlight via plasmas is being sought.

NON-RIGIDIZED INFLATABLE CONCENTRATOR

FIGURE 1





BASIC PROCESSES OF PLASMA PROPULSION

Herbert O. Schrade and Michael Kirschner

Institut für Raumfahrtantriebe der Universität Stuttgart

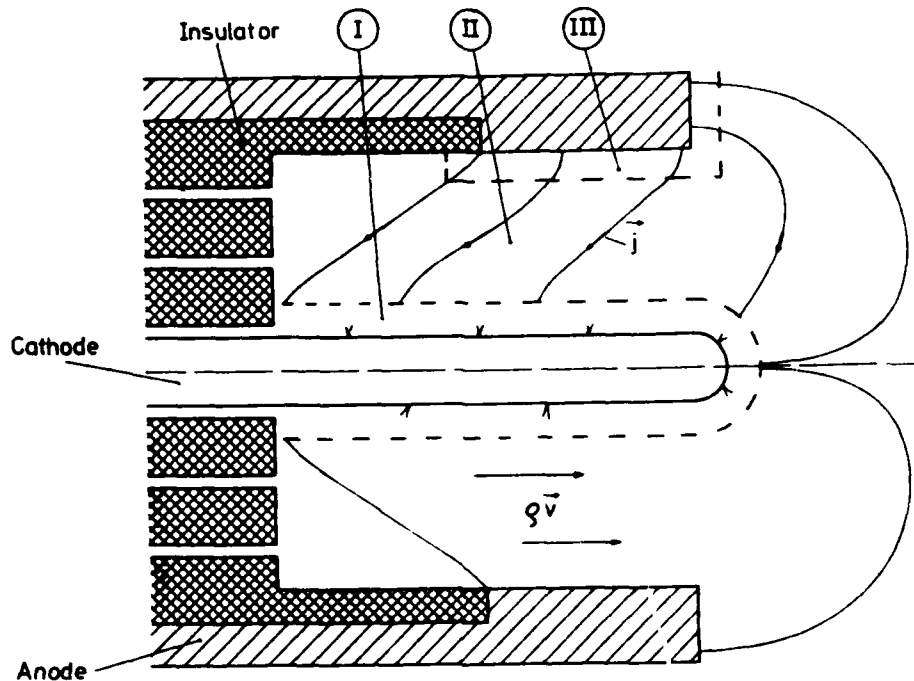
The fundamental understanding of magneto plasmadynamic arc thrusters is still incomplete. In order to assess the applicability of these thrusters for space propulsion purposes, and in order to improve their performance, a continuous, rigorous analytical and experimental investigation, together with a profound knowledge of related and competent literature is required.

This research addresses itself to the two mechanisms involved which are of great concern in these thruster devices: 1) the arc electrodes with their erosion mechanisms and 2) the flow arc discharge mechanism with its stability behavior. Recently a unique analytical approach has been developed and so far successfully applied to both problem areas. This work will be continued and extended, first, in order to gain deeper insight into the very complex physics of the electrodes and the midstream flow discharge regimes, and second, in order to come up with a realistic analytical model which predicts not only the thruster performance limits, but also allows development of design criteria for improved thruster types.

The scientific approach towards that goal is shown in Fig. 1 and is based on the following conception. According to today's understanding, the arc cathode attachment consists of one or more plasma-channels of high current densities ($\geq 10^{12} \text{ A/m}^2$) which electrically connect one or more microspots with the main interelectrode plasma body. These channels or microspots are highly nonstationary; they propagate and disappear and, depending on the electrode material (oxidized surface layer, surface chemistry), surface roughness, overall temperature, and type and pressure of the gas, these micro discharges cluster together to macrospots of different sizes with different erosion rates. It is very likely that even a so called thermionically emitting cathode of fairly large overall emitting site consists of many highly nonstationary micro discharges.

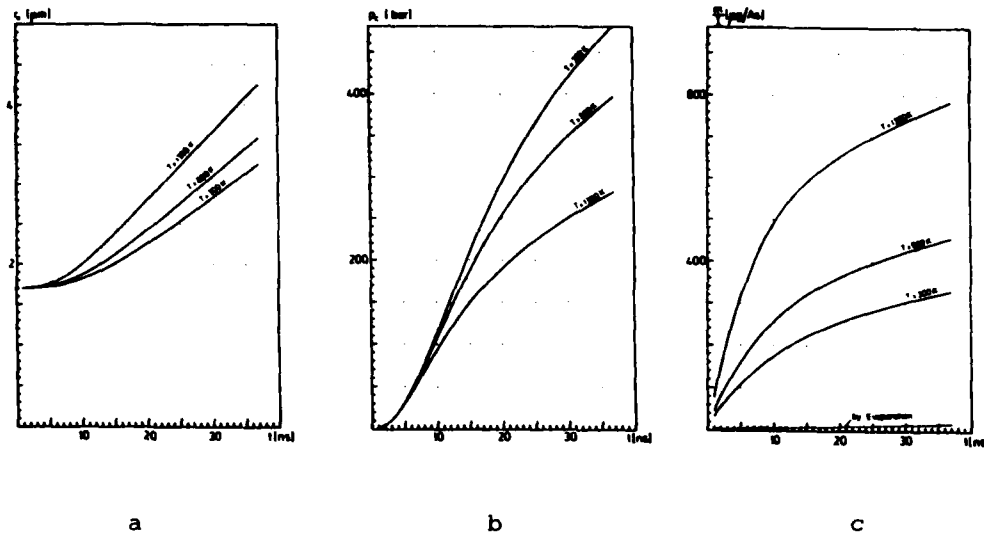
The main plasma body which extends from the cathode to the anode attachment area is confined on the upstream side by the higher pressure cold gas and ends down stream in the jet plume. The conditions within this midstream flow discharge region can be considered likewise unstable or turbulent despite the overall discharge area assuming a time averaged quasi steady configuration. At first the overall discharge area will be discussed by means of our new stability theory. Secondly a simplified turbulence model based on local stability considerations shall be developed and implemented into a two-dimensional axial flow discharge calculation.

In Fig. 2 certain initial results of an analysis about a single micro spot discharge occurring on the cathode surface of a copper electrode are shown.



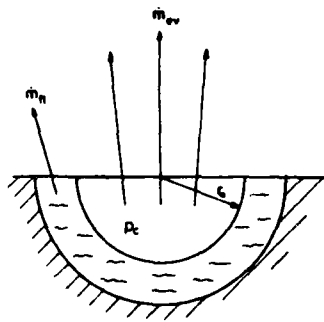
- I Arc Cathode Attachment consists of highly non-stationary micro discharges
 - Step 1 : Calculate life cycle of spot, spot splitting, spot motion, erosion rate, etc.
 - Step 2 : Develop phenomenologic approach by integration over all spots
- II Midstream Flow Discharge Region
 - Step 1 : Investigate stability of overall discharge configuration
 - Step 2 : Develop code for a turbulent two-dimensional axial flow model considering a two component approach (electrons, heavy particles)
- III Arc Anode Attachment
 - Step 1 : Discussion of discharge transition from diffuse to patches and spots

Fig. 1: Scientific Approach



- a) Crater Radius
- b) Crater Pressure
- c) Erosion Rates

as function of time for 3 different initial cathode temperatures
at a current rate of $2.667 \cdot 10^9$ A/s



Hemispherical Crater Model which
Accounts for Losses of Evaporated
and Fluid Material

Fig. 2: Primary Accomplishments.
Initial Arc Cathode Spot Calculation for Copper

MPD THRUSTER PERFORMANCE

R. Joseph Cassady, R. J. Vondra, and W. M. Schmidt

School of Aeronautics and Astronautics
Purdue University
West Lafayette, Indiana 47907

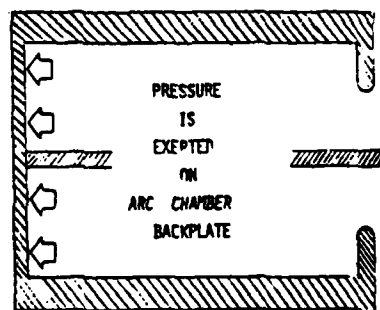
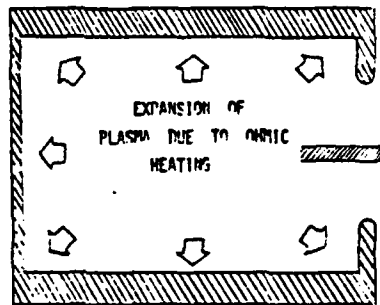
Air Force Rocket Propulsion Laboratory
Edwards AFB, CA 93523

The thrust delivered by the Magnetoplasmadynamic (MPD) thruster is comprised of two components, the electromagnetic and the electrothermal. While research has been conducted on the electromagnetic component, the electrothermal contribution to thrust has remained largely neglected. Depending on the operating parameters of the thruster, the electrothermal component may account for between 10 percent and 50 percent of the total thrust. Therefore, it is desirable to determine the pressure distribution upon the backplate of the thruster arc chamber thereby determining the electrothermal contribution to the thrust.

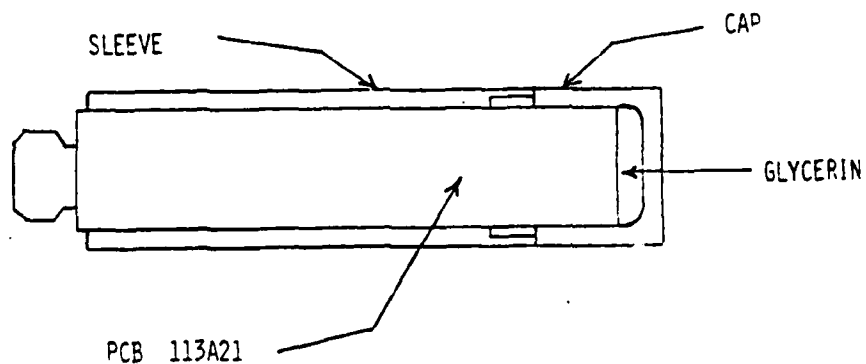
In order to measure the pressure exerted by the expanding plasma during the short (1 millisecond) pulse, a piezoelectric pressure transducer was selected as the primary diagnostic device. To overcome the difficulties of acoustic and electromagnetic noise associated with such a high energy discharge, a nylon cap and sleeve arrangement was used to protect the transducers from the plasma. The cap was designed with a cavity separating it from the transducer diaphragm. This cavity was filled with glycerin to act as a transmission medium for the pressure pulse. The front face of the cap was mounted flush with the backplate surface and capped with backplate material. This will be the first time such a pressure sensing device has been utilized at this location within the thruster arc chamber. These measurements will provide investigators modeling the arc chamber physics with fundamental data on the arc chamber pressure.

The effort was comprised of two phases. The experimental portion was performed at the AFRPL electric propulsion laboratory. Analysis of the AFRPL data was performed at Purdue University. A Benchmark geometry MPD thruster was modified to accept the pressure transducers in July 1983. Transducer modifications were completed in August, 1983. Initial pressure data were gathered in September, 1983. Analysis was performed at Purdue from September 1983, to December 1983. The conclusions drawn from the initial data prompted further measurements. Difficulties with magnetic interference in the transducer electronics cast some doubt on the precision of the pressure measurements.

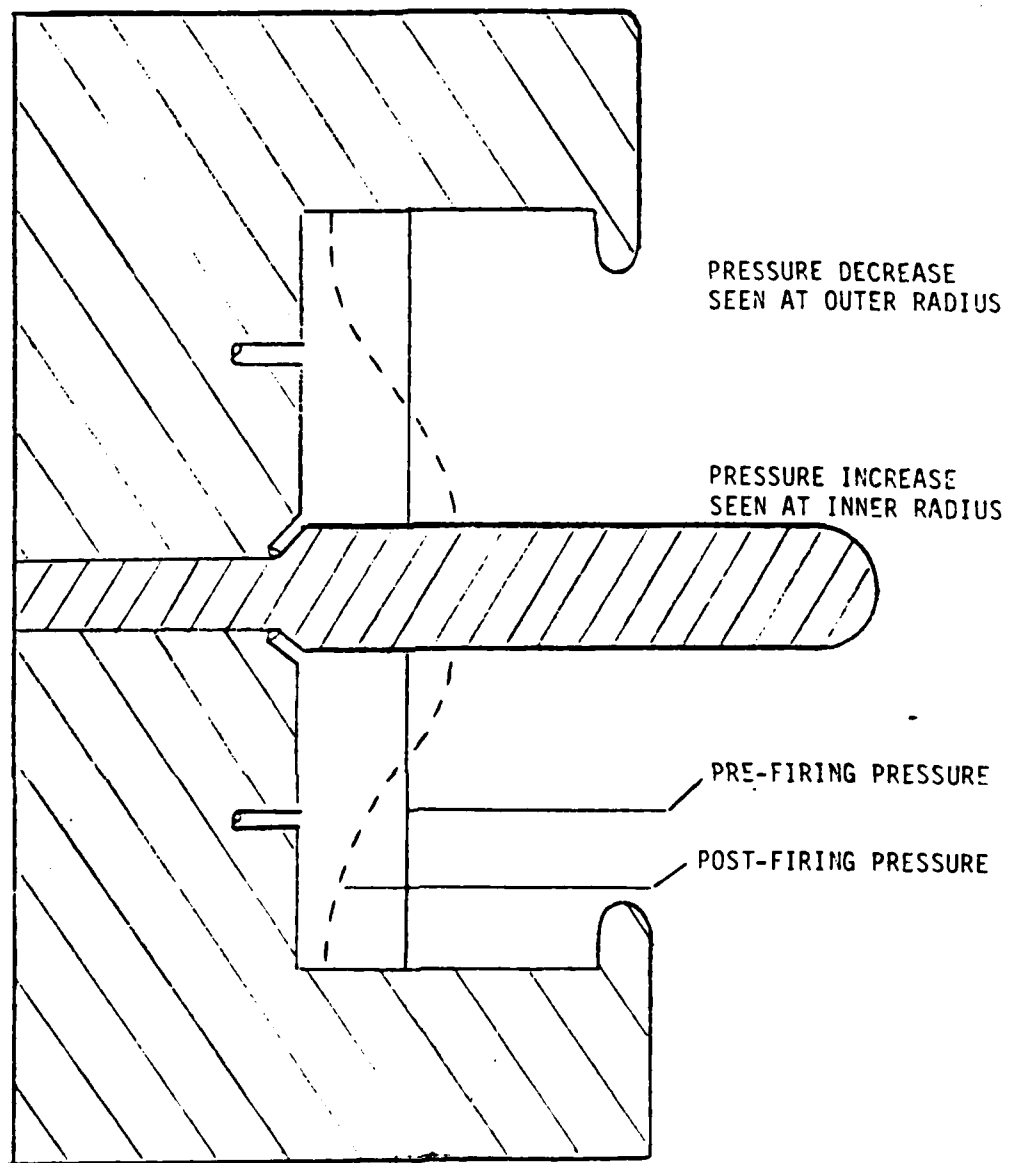
Future plans call for shielding the modified transducers with Mu - metal magnetic shielding and repeating the pressure measurements. Additionally, B-field measurements and Kerr cell photographs will be taken to supplement the pressure data.



Origin of Electrothermal Thrust



Method of Measurement



Pressure Distribution on Backplate

MAGNETOPLASMADYNAMIC THRUSTER EROSION RESEARCH

David Q. King
Jet Propulsion Laboratory
California Institute of Technology
Pasadena, California

Magnetoplasmadynamic thruster (MPDT) lifetime at sustained multi-megawatt power levels is unknown but will be limited by plasma erosion of thruster surfaces. Before the thruster can be developed for an orbital propulsion application the physics of the erosion mechanisms must be studied. The research proposed herein addresses the following key questions that must be resolved in order to understand erosion:

- 1) What are the erosion mechanisms involved and what are the quantitative rates for each mechanism?
- 2) What are the cathode emission mechanisms and heat transfer rates?
- 3) What are the surface temperatures?
- 4) How does the work function of the cathode change with time and what effect does this have on erosion?

The approach is unique in that it aims at developing an understanding of the erosion of the electrode and insulator surfaces by conducting experiments on a scaled-down electrode configuration or model, which is under construction. The most significant physical parameters are electrode current densities and attachment mode (spot or diffuse), surface temperatures, electron densities and temperatures close to the surface and total erosion rates for each surface (Fig. 1).

The design and fabrication of a pyrometer has been completed. Testing of this instrument using a known temperature source shows that temperature measurements in the range 1600-2800°K have a maximum error of +9% -2% with the biggest uncertainty being that of the spectral emissivity.

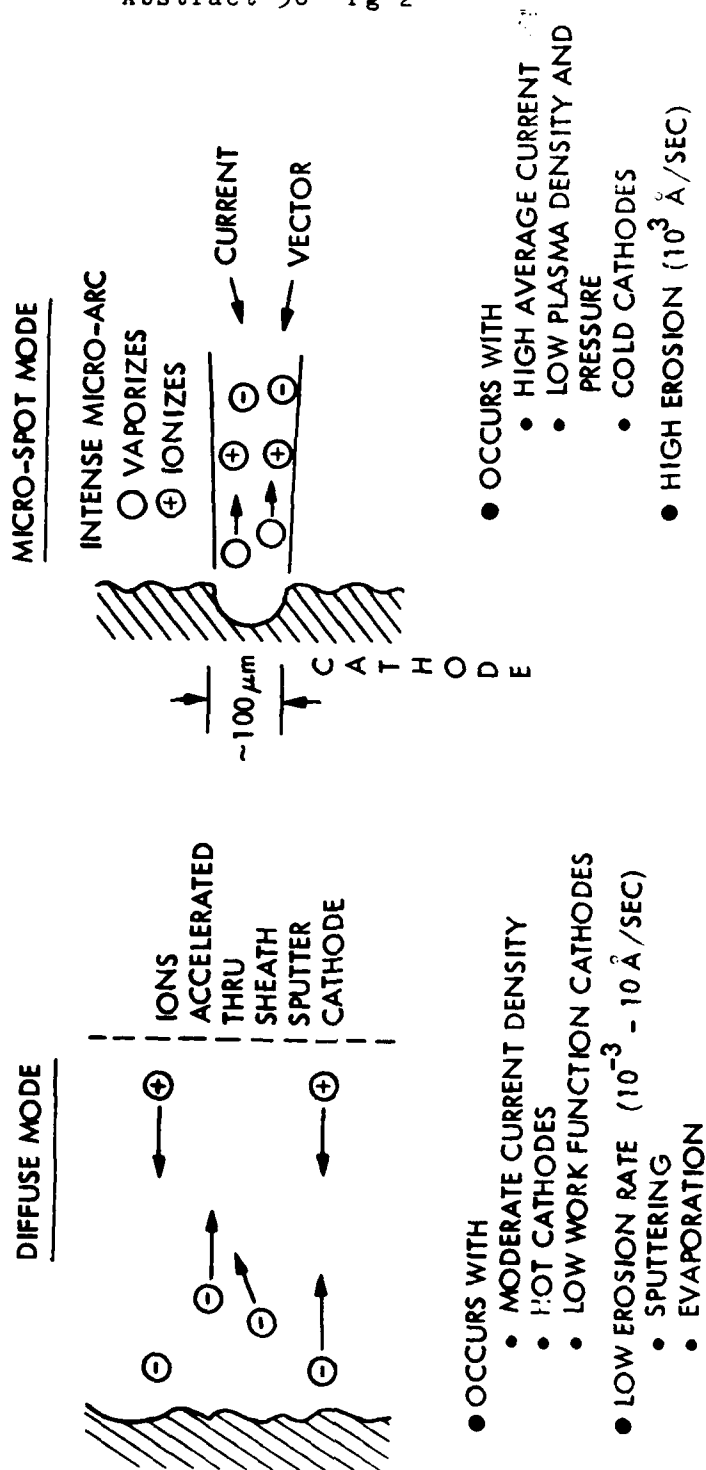
A simple, first-order model for heat transfer/electron emission at the cathode has been developed. Despite its simplifying assumptions from it one can make the following important conclusions: 1) The surface temperature and work function are key parameters, and 2) electron cooling due to thermionic emission is significant and at densities greater than $10^{15}/\text{cm}^3$ radiation cooling can be neglected.

Most importantly, the model combined with measurements of the surface temperature and the electron density close to the cathode can be used to calculate the cathode-fall voltage and ion current density. These parameters are vital in determination of the electron emission mechanisms. Measurement of the surface temperature is critical in that the evaporation rate, thermionic-emission/electron-cooling and sputtering rate all show an exponential dependence on temperature; in addition surface temperature plays a major role in the overall heat balance of a radiation-cooled cathode.

Similarly, since electron cooling and thermionic emission show an exponential dependence on work function experiments will be conducted using both pure tungsten and thoriated tungsten (W-Th) which have work functions of 4.5eV and 2.63eV respectively. Under the same operating conditions (mass flow and total current), measurements of the temperature and erosion rate for these materials will yield important results on cathode erosion (Fig. 2). Thorium depletion in the W-Th cathode will be systematically studied using surface chemical analysis and correlated with changes in work function, temperature and erosion rates.

FIGURE 1 - TECHNICAL APPROACH

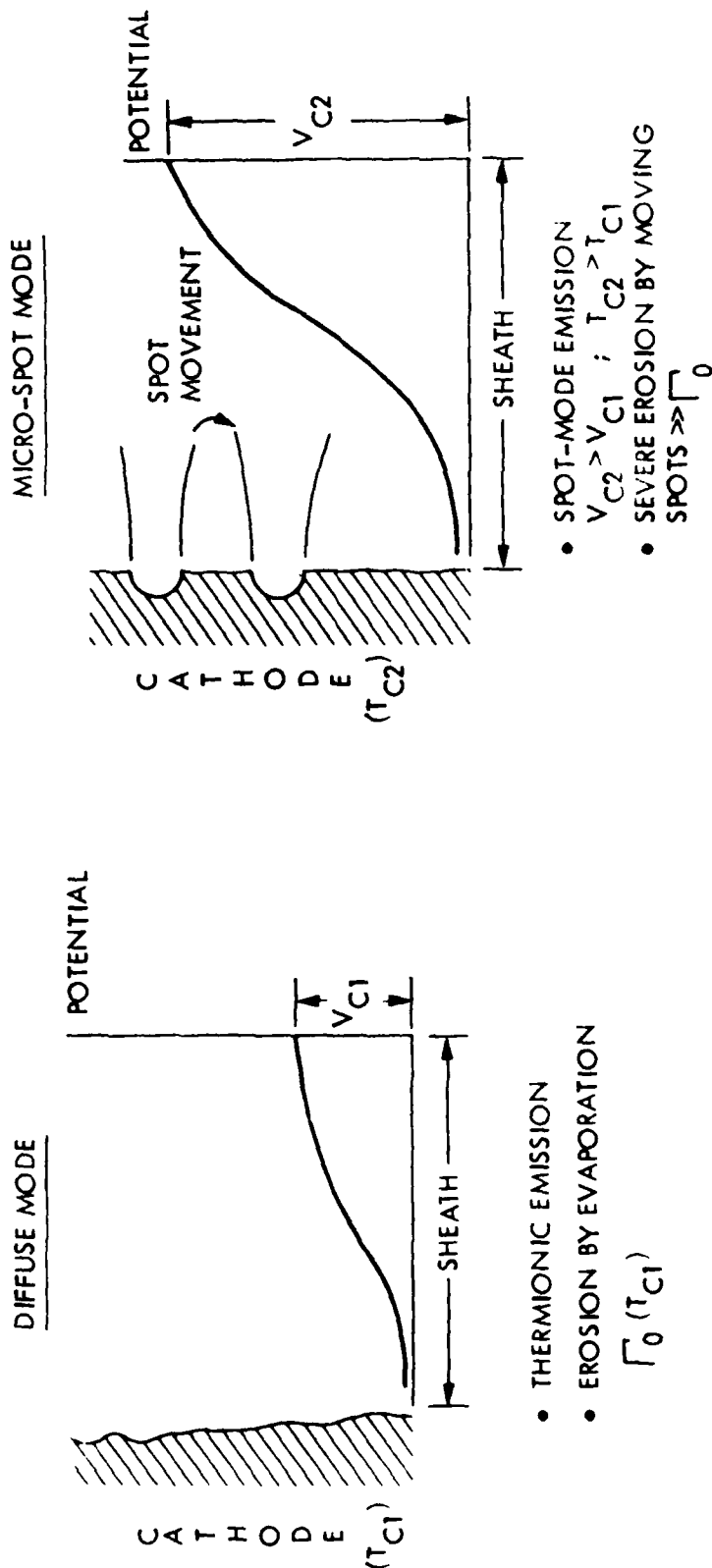
APPROACH: OPERATE SCALED-DOWN ELECTRODE MODEL TO DETERMINE
CONDITIONS CAUSING MICRO-SPOT-MODE OR DIFFUSE MODE CURRENT
EMISSION, AND CATHODE TEMPERATURE



MODE DEPENDS UPON AVERAGE CURRENT DENSITY, PLASMA DENSITY,
CATHODE TEMPERATURE, AND FIELD ENHANCED WORK FUNCTION,
NONE OF WHICH HAVE BEEN QUANTIFIED.

FIGURE 2 - EXPECTED RESULTS

- MEASURE CATHODE TEMPERATURE TO DETERMINE 1) HEAT BALANCE, 2) RATE OF THERMIONIC EMISSION, 3) EVAPORATION RATE, 4) INFER SHEATH PROPERTIES
- CATHODE TEMPERATURE AND SHEATH PROPERTIES ARE A FUNCTION OF CURRENT EMISSION MODE



Erosion and Onset Mechanisms in Magnetoplasmadynamic Thrusters

John L. Lawless
Carnegie-Mellon University
Pittsburgh, Pennsylvania 15213

Although erosion is a major concern in MPD thruster design, very little is presently known about it. To minimize erosion, it is desirable to operate in the diffuse as opposed to spot mode of current conduction. The goal of this work is (1) to determine the limits of diffuse mode operation and (2) to quantify its erosion rates. Since, at present, there are no theories to answer either question, this work is unique. Also, it is hoped to clarify the relationship between erosion and the experimental phenomenon of 'onset.'

Erosion is believed to be due to evaporation and sputtering. Evaporation is a serious concern with tungsten electrodes if the surface temperature reaches 3000K, as it might in steady-state operation. The surface temperature is determined by a heat transfer problem involving the plasma, the sheath structure, and the electrode cooling mechanisms. The importance of sputtering is determined by the rate with which energetic ions strike electrode or insulator surfaces. The major unknown here is how such high energy ions are created. One hypothesis, due to Kuriki and Onishi, is that they are created in a high voltage region of the anode sheath. Another possibility is that they are created by thermal means within the plasma. The relative importance of these two mechanisms, is determined by the mean free path for energetic ions and the plasma temperature. The above considerations are illustrated in figure 1.

Before erosion can be quantified, more information on the bulk plasma flow is needed. To this end, a flow model is being studied. This model includes the effects of pressure gradients, magnetic forces, ohmic heating, and convection in a quasi-one-dimensional approximation similar to that of King et. al.(1981). Various assumptions about the thermodynamic functions have been considered. To understand erosion, this model is being extended to yield more information on plasma conditions near the electrodes.

The primary scientific accomplishment to date has been the prediction of a new onset mechanism. This mechanism predicts that the back emf rises rapidly enough to limit the current to some critical value. This is illustrated in figure 2. This mechanism is distinct from the anode sheath failure mechanism analyzed by Baksht et. al.(1974) among others. It should be possible for experiments to distinguish between these two mechanisms. The Baksht mechanism would be observed as a rapid increase in the voltage drop of the anode sheath near the exit as onset is approached. The proposed new mechanism would be observed as a rapid drop in current density in the middle of the thruster. The preliminary evidence exists to support the existence of both mechanisms but is inconclusive about which occurs first under different flow conditions.

**** 1984 ROCKET RESEARCH MEETING ****

Abstract 37 Pg 2

In the Kuriki-Onishi mechanism, high energy ions which are created in the anode sheath may travel to the cathode and cause sputtering.

Plasma conditions near the electrodes may be affected by thermal, viscous, and compositional boundary layers

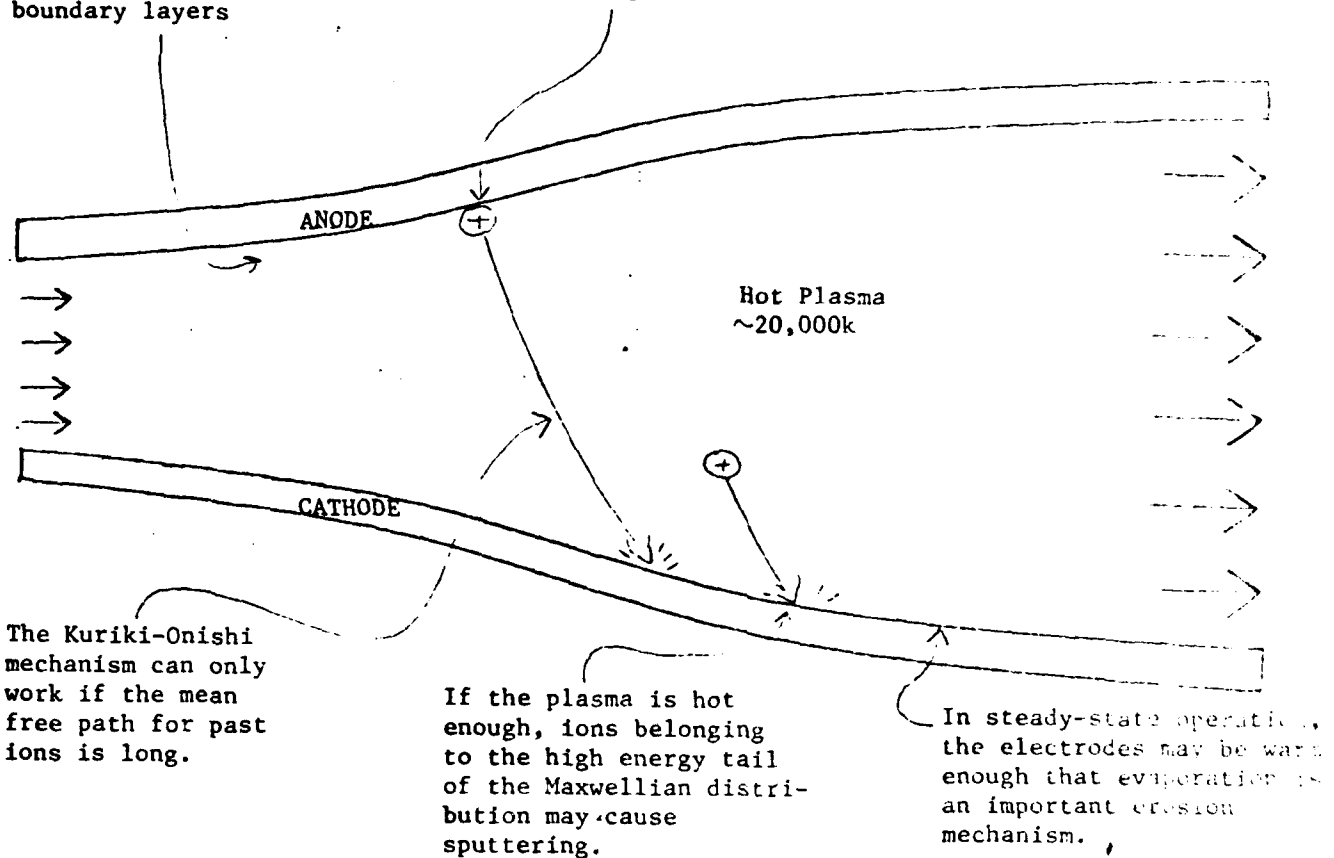
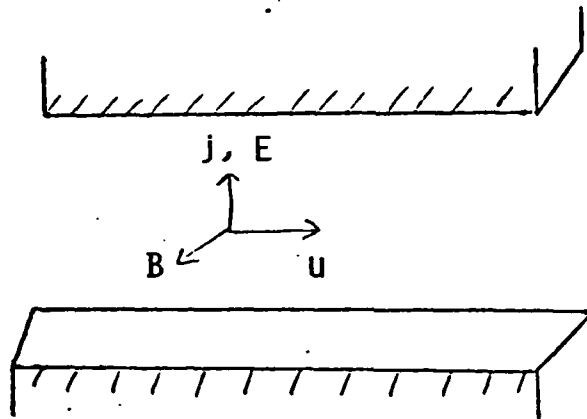


FIGURE 1

The lifetimes of MPD thrusters are limited by electrode erosion. Scientific questions related to quantifying erosion are illustrated.

OHM'S LAW

$$\vec{J} = \sigma(\vec{E} + \vec{u} \times \vec{B})$$



$$J = \sigma(E - uB)$$

Electric field
drives the current
in an MPD Thruster

The back EMF opposes
current flow in a thruster

FIGURE 2

For a smooth solution it is necessary that $uB < E$.
Flow modeling predicts that uB rises faster than E . This
may be a cause of onset.

Performance-Limiting Factors
for MPD Thrusters

Research Abstract
for AFOSR Rocket Propulsion
Research Meeting, Lancaster, CA
March 12-15, 1984

by

M. Martinez-Sanchez
Massachusetts Institute of Technology

Both self-field and applied-field MPD thrusters are subject to destructive instabilities at high currents and low flow rates. Several plausible correlations exist for the onset condition for these instabilities, but they tend to be too sweeping and lack enough mechanistic detail to allow design modifications aimed at avoiding or delaying this onset. Our research has as one primary goal the clarification of the onset mechanism(s) by means of relatively simple models of the plasma flow. A second goal is the extension of these models to a computer program that can be used as a design and data reduction tool, and as a means to study the tradeoffs between various thruster configurations.

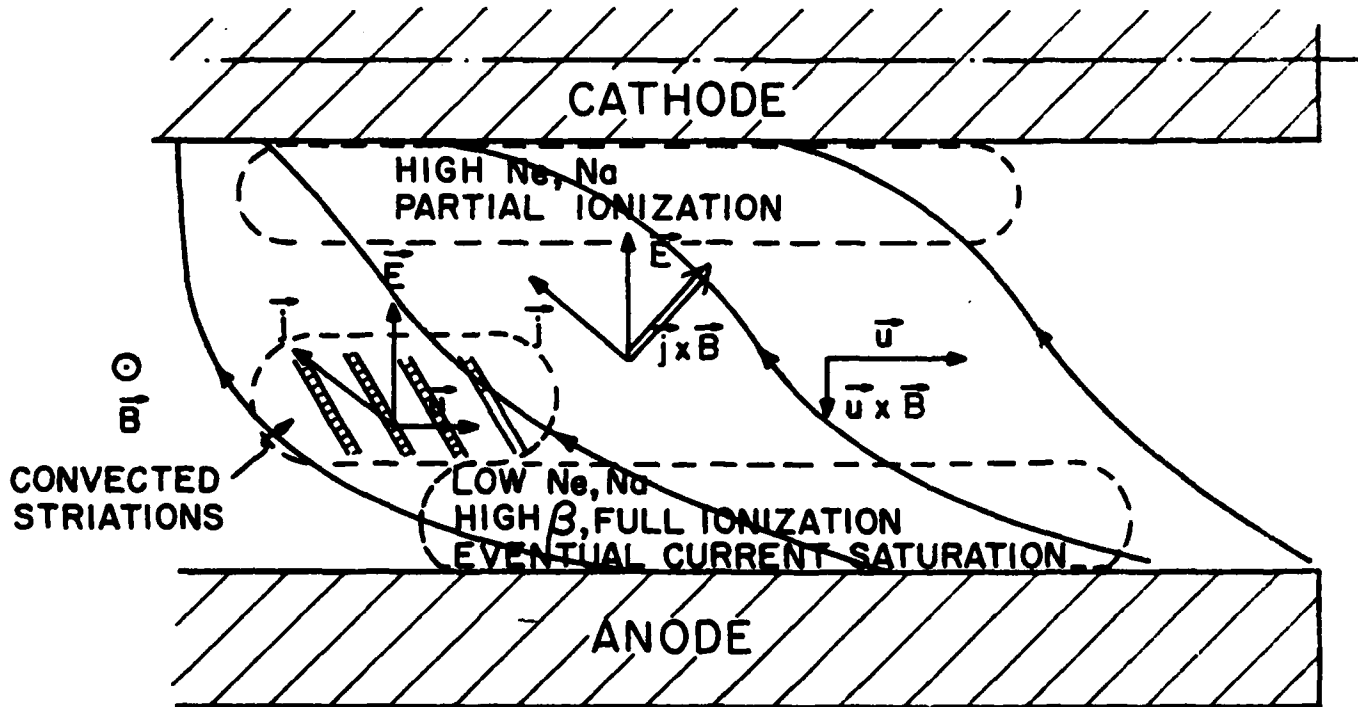
In the course of this year we have considerably extended the formulation of a quasi-two-dimensional model (Bakhst et al.) which had had some success in describing onset. This model was restricted to fully ionized gas, and relaxing this restriction has entailed addition of equations to describe ionization rate, ambipolar diffusion and electron energy balance. The computer program embodying this extended model is still being refined, but the major convergence difficulties have been overcome and results are expected within this month. These results will consist of predicted onset currents for given flow rates, type of gas and major geometrical parameters, and, in addition, predicted distributions of current, velocities, densities, etc., within the channel.

We have also performed plasma local stability analyses at various levels of detail. Results for partially ionized regions show the high Hall parameter instability, with little attenuation due to the strong magnetic interaction. Extension to regions near full ionization is under way.

We also plan to present at the meeting a detailed proposal and plan of action for the establishment of an MPD data base. We envision this work as a series of cycles, the first of which will be the systematization of data in the literature into something like a loose-leaf data book. Next will probably come a computerized version of this; finally, a mechanism for updating, maintenance, and access will be devised.

SCIENTIFIC APPROACH:

MODELING PLASMA DYNAMICS AND PHYSICS

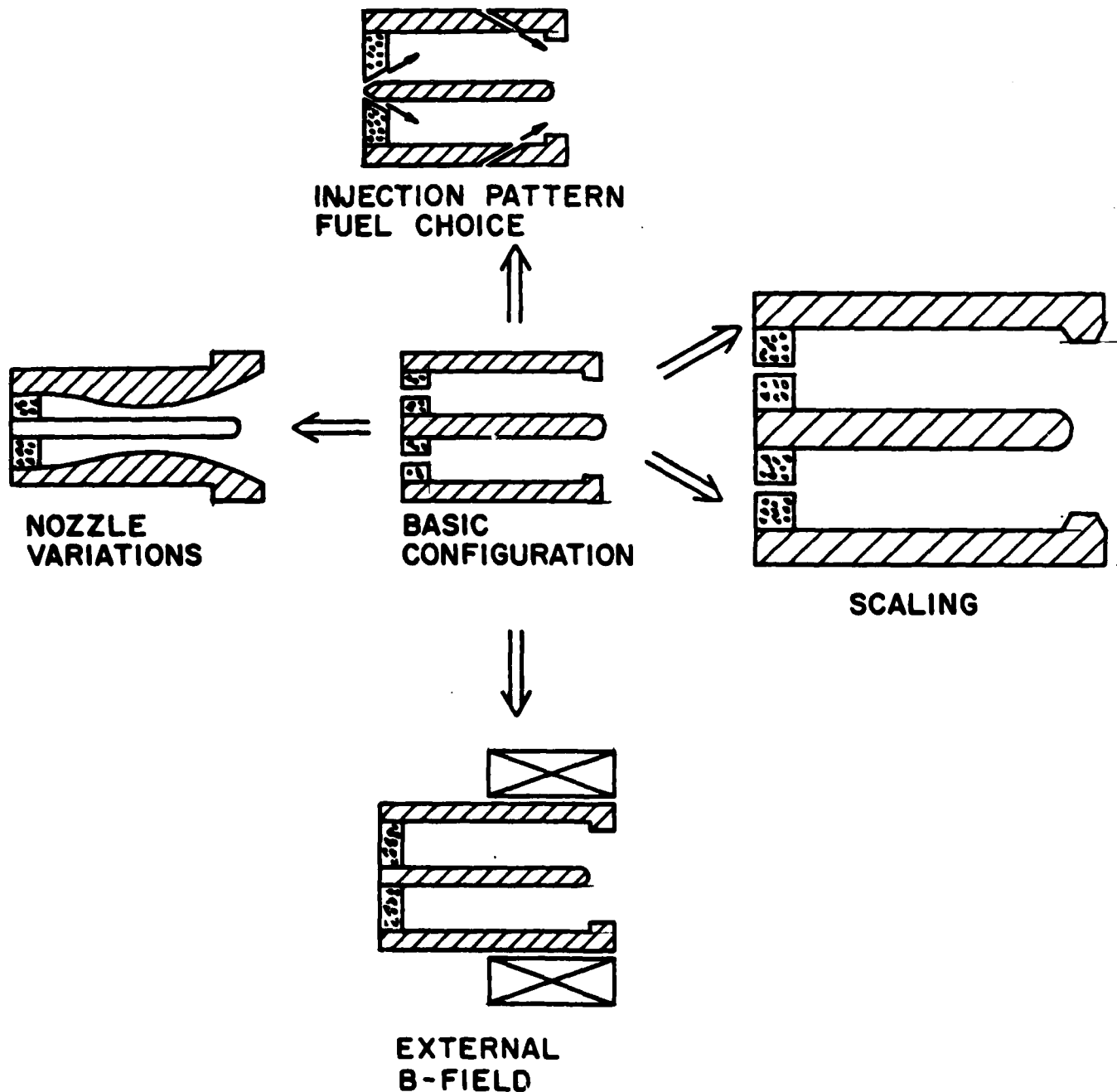


APPROACH:

- (A) EXTEND CLASSICAL MODEL OF BAKSHT TO INCLUDE
 - PARTIAL IONIZATION
 - SELF-CONSISTENT T_e
 - PRE-ONSET REGIME
- (B) STUDY LOCAL STABILITY IN HIGH HALL PARAMETER, PARTIALLY IONIZED REGIONS
- (C) INCORPORATE SAME PHYSICS INTO NEW 3-D CODE, INCLUDING
 - GEOMETRY EFFECTS
 - EXTERNAL B-FIELD

EXPECTED ACCOMPLISHMENTS

ANALYTICAL/NUMERICAL PREDICTIONS OF CONFIGURATION EFFECTS:



FIRST YEAR'S EFFORT DEVOTED TO

- (A) CLARIFYING PHYSICS
- (B) DEVELOPING NUMERICAL CODE

PULSED INDUCTIVE ENERGY TRANSFER

Peter Mongeau and Henry Kolm
Electromagnetic Launch Research, Inc.
625 Putnam Avenue
Cambridge, MA 02139

Electromagnetic induction is useful for converting stored electrical energy to the kinetic energy of a conductive propellant. Energy stored in a pulsed power device, such as a capacitor, is discharged into a high performance pulse coil. The rapidly varying magnetic field induces a current in a tightly coupled conductive reaction mass. The two currents are magnetically repelled thus producing thrust (see figure 1).

Magnetic induction is particularly efficient when used with solid metals for reaction mass such as aluminum. The combination of high electrical conductivity and density of such materials enables efficient operation in the 500 - 1500 second specific impulse range while demonstrating a force density usually associated with chemical propellants. The reaction forces are generated with no direct electrical or mechanical connection between the driving pulse coil and the exhaust mass.

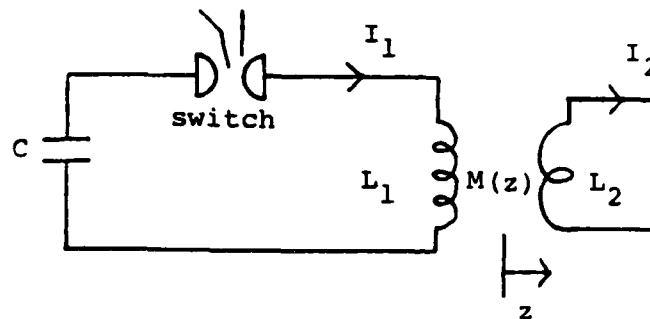
Overall performance is especially sensitive to the geometric matching of the drive coil with the reaction mass. Induction analysis has shown that both the energy transfer efficiency and thrust are maximized for thin annular coils. In this case the reaction mass is a foil ring placed directly on top of the drive coil. During the acceleration impulse induced currents in the reaction mass generate substantial ohmic heating that can lead to melting and ultimately vaporization during the discharge. The enthalpy in many metals, notably aluminum, is sufficient to permit exhaust velocities to beyond 10 km/sec before vaporization is reached (see figure 3).

The operating voltage of metallic induction reaction engines limits the maximum thrust, and consequently exhaust velocity, that can be generated while the reaction mass remains in the optimum magnetic coupling region of the drive coil. Unfortunately, as higher velocities are reached the temperature rise in the exhaust mass resistively damps the induced current, thus degrading performance (see figure 4).

Initial experiments have been conducted in a glass vacuum chamber (see figure 2). Six inch diameter drive coils of various configurations have been used in conjunction with a 90 uF, 20 kV capacitor bank. Induced melting has been demonstrated in 0.0002 inch thick aluminum foil at 600 m/s.

PULSED INDUCTION ENERGY TRANSFER

Figure 1



► Force = $I_1 I_2 \frac{dM}{dz}$

► Maximum Ideal Transfer Efficiency =

$$\frac{\text{Reaction Mass Kinetic Energy}}{\text{Initial Stored Energy}} = \frac{M^2}{L_1 L_2}$$

Figure 2

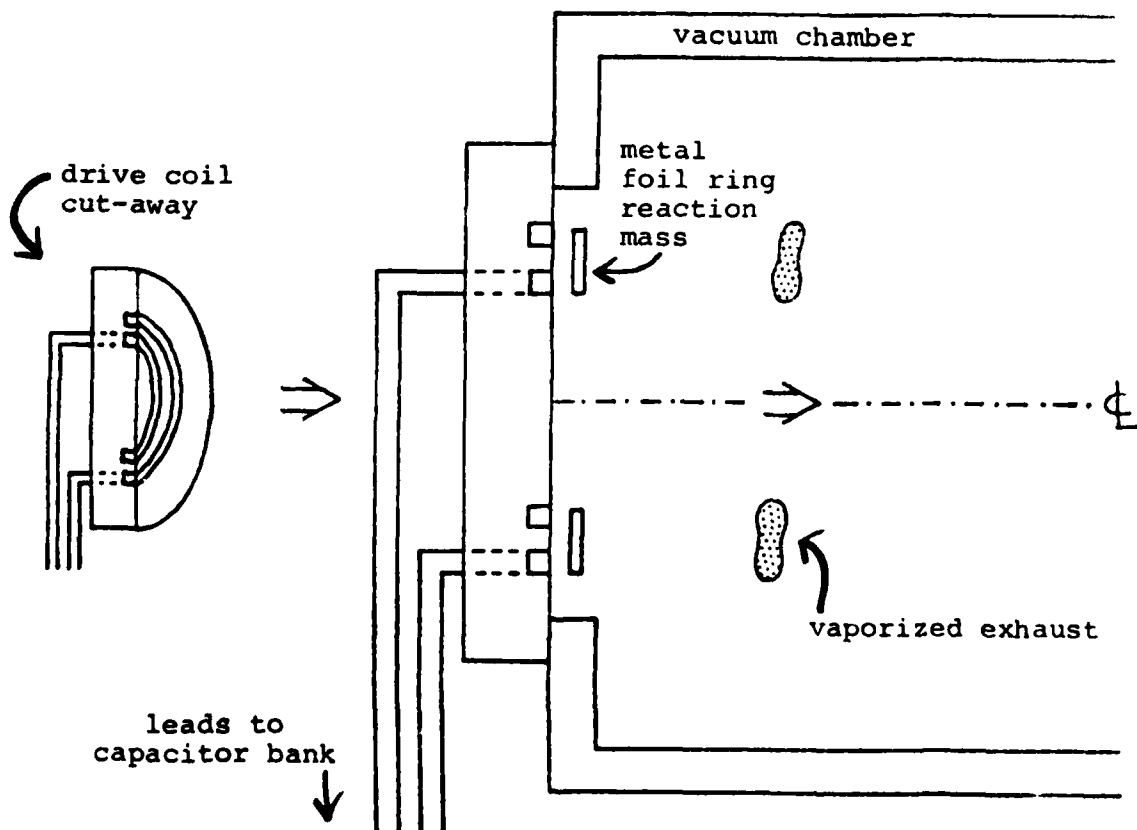


Figure 3

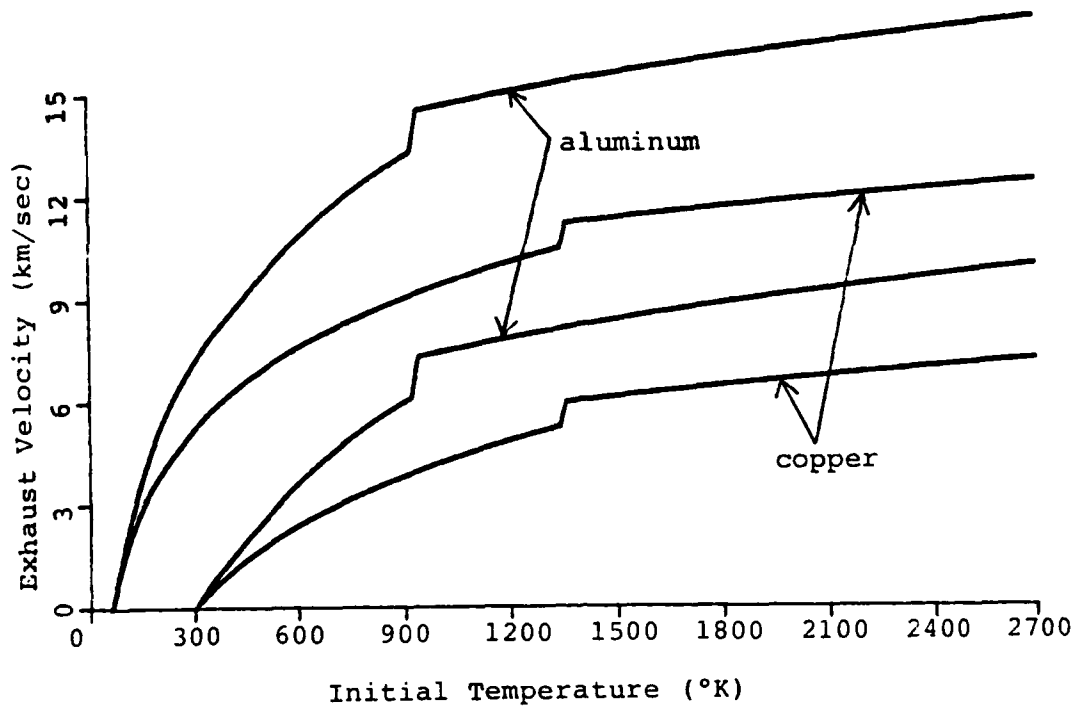
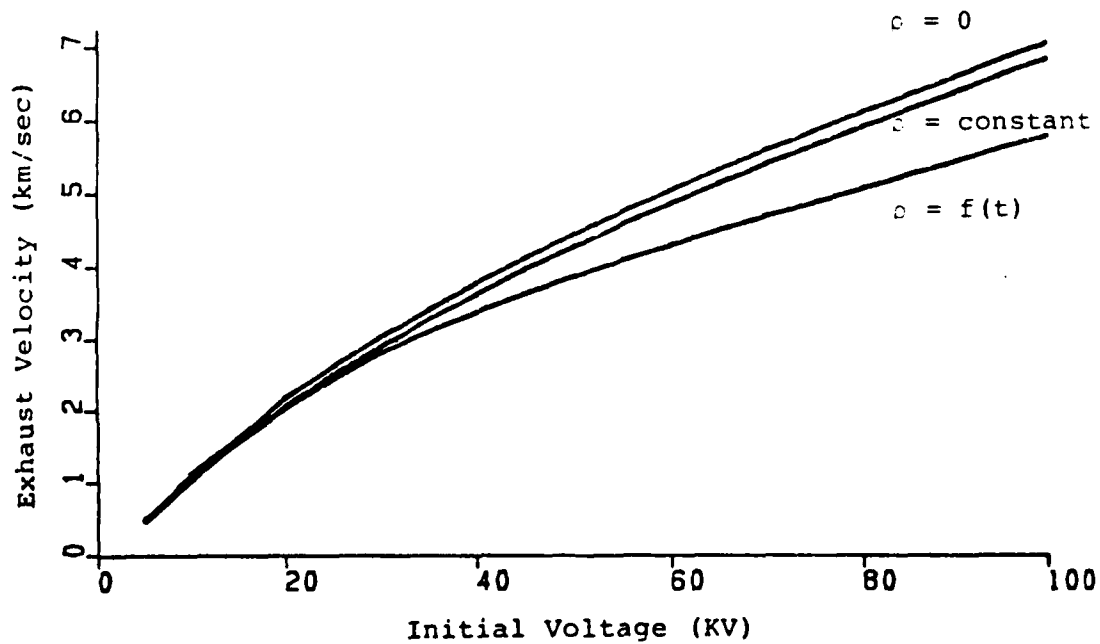


Figure 4



**UNIFIED STUDY OF PLASMA-SURFACE INTERACTIONS
FOR SPACE POWER AND PROPULSION**

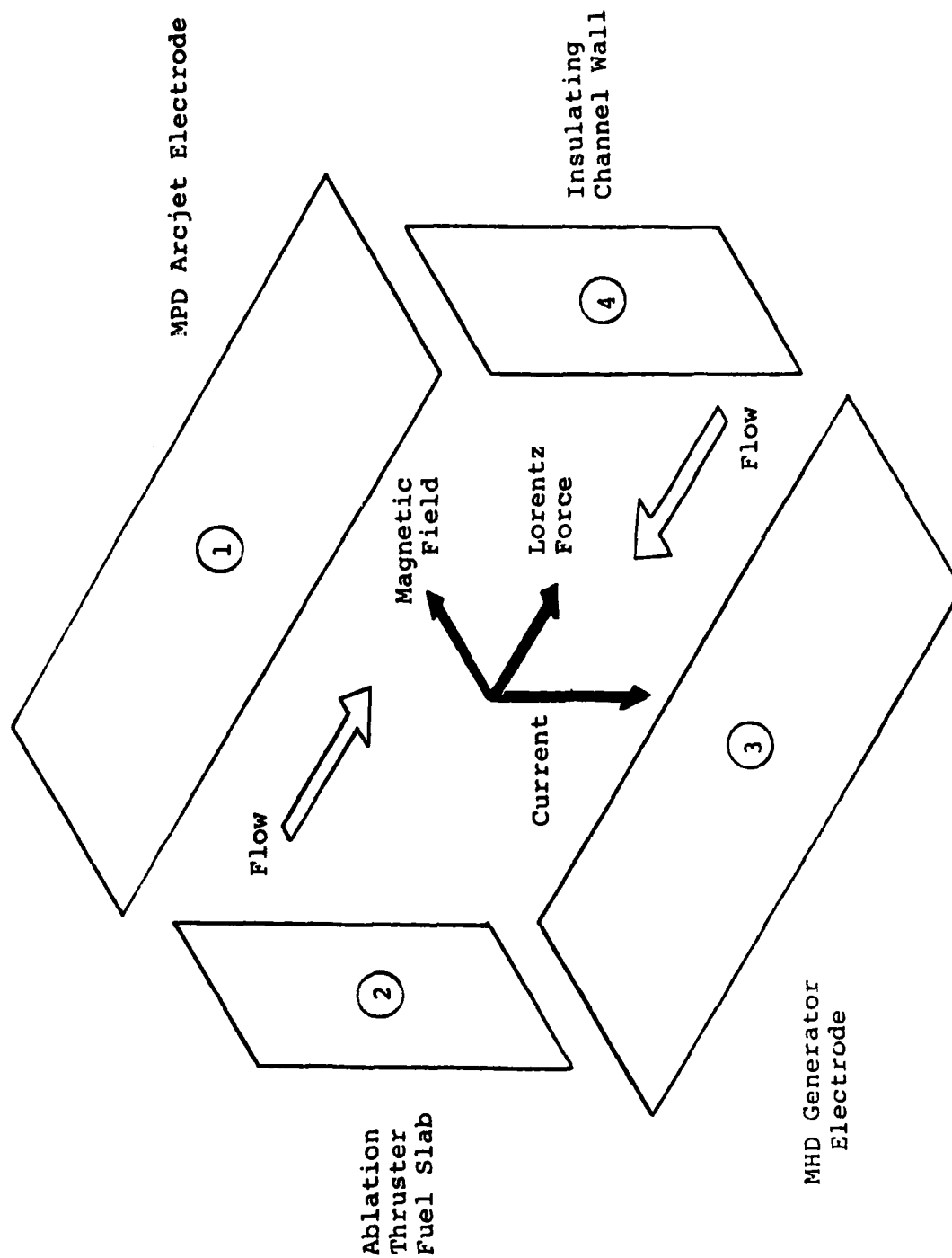
P.J. Turchi

**Washington Research Laboratory
R & D Associates
301A S. West St.
Alexandria, VA 22314**

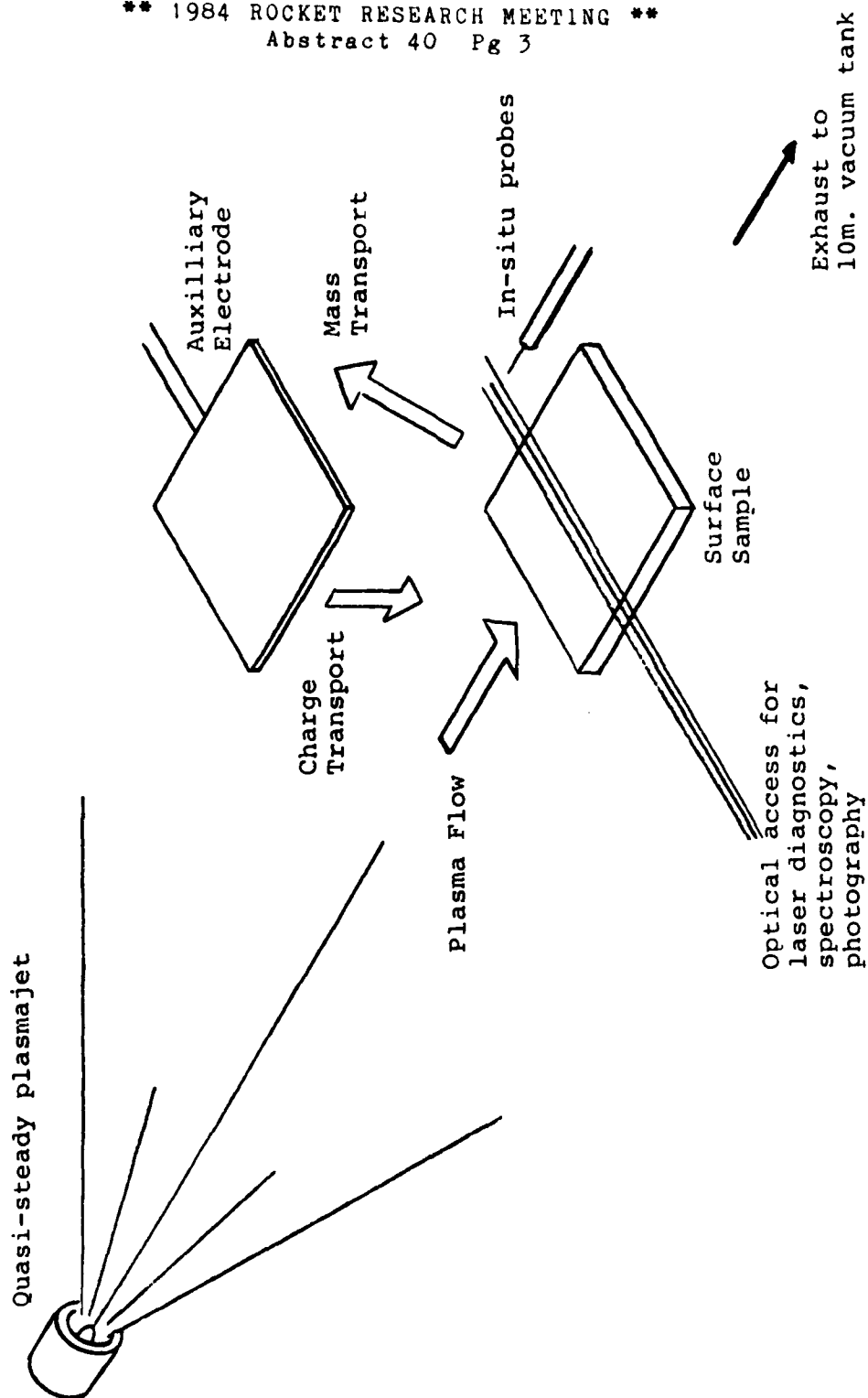
Control of working fluids in high specific power and high specific impulse devices often involves plasmas in contact with solid surfaces. A three-year basic research effort is being pursued in which plasma-surface interactions important in space power and propulsion systems will be examined. A matrix of experimental tests has been suggested that will allow a broad range of operating parameters to be considered in a systematic fashion as indicated in Fig. 1. Measurements will include both optical techniques (e.g., spectroscopy, combined laser-schlieren, -interferometry, -absorption) and probe methods (e.g., electrostatic, magnetic, piezoelectric probes), to determine densities, temperatures, potentials, and flow conditions near electrically conducting and insulating surfaces. The use of a consistent set of idealized experimental arrangements will provide detailed understanding of processes found in a variety of high specific power devices, such as MHD generators or MPD arcjets. As shown in Fig. 2, low temperature (~ 0.5 - 10 eV) plasma is established adjacent to metal and dielectric surfaces, in the absence of flow and conduction, with flow, and with both flow and conduction. The experiments use geometries that are more accessible for diagnostic techniques and more tractable for modelling than arrangements typically developed based on performance optimization for mission needs.

During the first six months of the program, the basic apparatus was assembled, including a 0.6×6 m. vacuum system and a 20 kJ pulse forming network (PFN). Preliminary tests, performed in conjunction with related work for AFRPL, created a low temperature plasma flow ($T \sim 1$ eV, $u \sim 1$ cm/ μ sec) by discharging the PFN across a Teflon surface separating two brass electrodes. The PFN current pulse time was 150 μ sec with a level that was varied from 4-10 kA. Magnetic probes indicate that about half the total current remains along the Teflon surface and the rest propagates to the downstream end of the channel. Time-integrated, spatially-resolved spectra of the plasma near the cathode show several lines of copper and zinc that diminish in relative intensity by different degrees with increasing distance from the electrode. A rather uniform carbon and fluorine (intensity) distribution is indicated across the channel. Time-resolved spectroscopy is planned using a micro-channel-plate image-intensifier system (vs. present rotating-mirror framing-camera photography that suffers from inadequate exposure levels) in order to monitor the motion of surface material into the freestream. Understanding of fundamental requirements for charge and mass transport at the interfaces between solid surfaces and low temperature plasmas should lead to improved efficiencies (e.g., lower electrode falls in MHD and MPD devices), and greater performance life (i.e., less electrode erosion and insulator degradation).

**UNIFIED STUDY OF PLASMA-SURFACE INTERACTIONS
ORIENTATION OF SURFACE RELATIVE TO FLOW AND
ELECTROMAGNETIC VECTORS PROVIDES EXPERIMENTS
FOR DIFFERENT APPLICATIONS**



SCHEMATIC OF PLASMA-SURFACE INTERACTION EXPERIMENTS
PLACEMENT AND ORIENTATION OF THE SURFACE SAMPLE IN A QUASI-STEADY
PLASMAJET EXHAUST PROVIDES A RANGE OF PLASMA AND FLOW VALUES



NONCONVENTIONAL ELECTROMAGNETIC PROPULSION CONCEPTS

Michael M. Micci

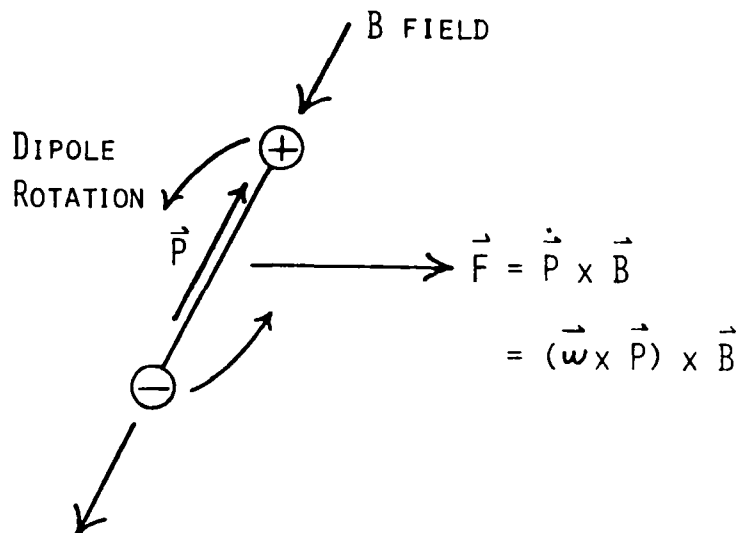
**The Pennsylvania State University
University Park, PA**

The electromagnetic acceleration of a nonionized dipolar gas by means of the force produced by the cross product of a magnetic field and an alternating polarization was analyzed to assess its feasibility as an advanced propulsion concept. Experimental evidence was found in solid dielectrics which verified both the existence and magnitude of the force. Using benchmark values of 1000 seconds of desired specific impulse with a 0.5 meter long acceleration length, the required product of rotational frequency and magnetic field strength, ωB , was calculated for several types of propellants. Water has the highest naturally occurring permanent dipole moment to mass ratio of any atom or molecule and gives a value of ωB of $5 \cdot 10^{11}$ Tesla/s to obtain the specified performance. However such an alternating field would induce an electric field three orders of magnitude greater than the field ionization limit for water, thus, destroying its dipolar nature. Use of light gases with high ionization limits such as helium was examined. The acceleration of helium to exhaust velocities of 10^4 m/s was found to be achievable before ionization breakdown would occur, however, the required product of ωB would still be quite high. Electronically excited or Rydberg atoms or molecules were studied as potential propellants due to their extremely large dipole moments, thereby lowering the ωB required for a given exhaust velocity. It was found, however, that the increased dipole moments are accompanied by a greater decrease in the ionization field strengths. Since the maximum acceleration obtainable with a dipole gas is limited by the ionization of the gas, the use of Rydberg enhanced dipole moments actually decreases the performance of such a device. When compared with other electromagnetic propulsion schemes, the alternating dipole thruster was found to give gas accelerations many orders of magnitude less.

An investigation was also initiated to study the magnetic induction acceleration of electrically conducting solid phase materials. Electrical energy stored in a capacitor is discharged through an inductor which is in close proximity to the conducting exhaust material, inducing a current in the conducting material which generated an opposing magnetic field and, therefore, thrust. The coupled differential equations describing the current flows in the thruster circuit and exhaust material, the acceleration of the exhaust material and the heating due to resistive losses in the thruster circuit and exhaust material were numerically integrated to determine thruster performance. Previous analyses had not included variable temperature effects and it was found that the heating of the exhaust material degraded the potential performance. A theoretical analysis of the acceleration process was undertaken to examine the coupling of electrical to kinetic energy. A simple analysis shows that exhaust velocity is proportional to initial capacitor voltage and experimental evidence supports this with a constant of proportionality of 0.1. A more detailed analysis indicates that the constant cannot be increased more than a factor of 2. Another concern is the state of the material after it is exhausted from the thruster. If the exhaust material is heated to its melting temperature by the acceleration process a vapor pressure can be obtained such that the material will evaporate. The vacuum evaporation process was examined and coupled to the numerical model to determine the conditions required to resistively heat the exhaust material until complete evaporation occurs.

Finally, the heating of a high pressure (> 1 atm.) gas by means of microwave radiation was examined. A literature search showed that the vast majority of the research in this area has been conducted in the Soviet Union. Both analytical and experimental studies indicate that this may be a very efficient means of adding energy to a working fluid.

ACCELERATION OF DIPOLAR GASES



TO ACHIEVE $10^4 \frac{M}{S}$ IN 0.5 M, ACCELERATION MUST BE $10^8 \frac{M}{S^2} = \frac{FORCE}{MASS}$

OPTIMAL NATURAL SUBSTANCE IN H_2O :

$$\frac{P}{MASS} = 2 \cdot 10^{-4} \frac{C \cdot M}{KG} \text{ THUS } \omega B = 5 \cdot 10^{11} \frac{TESLA}{S}$$

BUT $E_{INDUCED} > 10^3 \times H_2O$ IONIZATION POTENTIAL.

THUS H_2O IONIZES BEFORE SUFFICIENT ACCELERATION.

OPTIMAL NONIONIZING SUBSTANCE IS He:

$$\frac{P}{MASS} = 2.7 \cdot 10^{-16} E \text{ THUS } \omega B = 2.7 \cdot 10^{12} \frac{TESLA}{S}$$

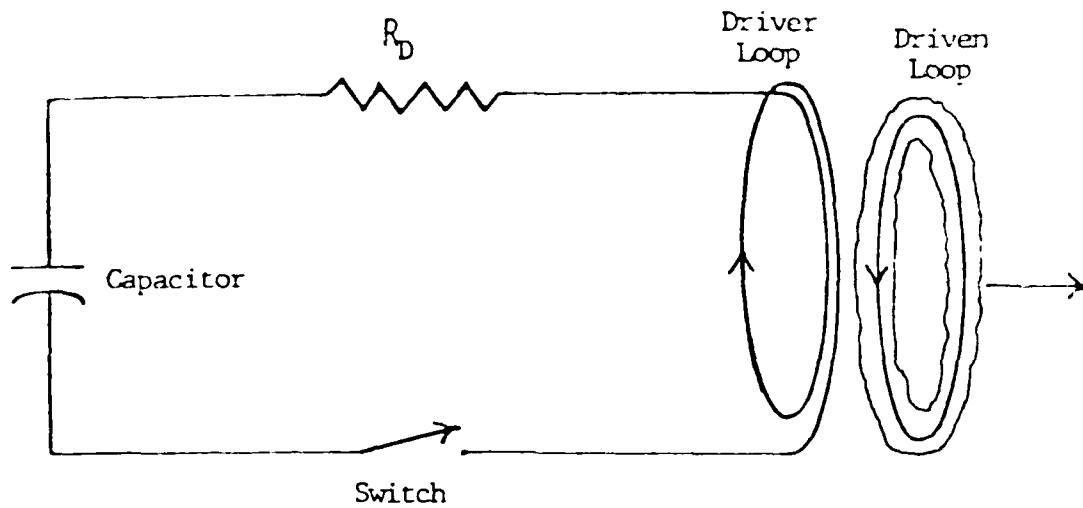
AND $E_{INDUCED} \approx He$ IONIZATION POTENTIAL.

ACCELERATION MIGHT BE POSSIBLE BEFORE ACCELERATION.

CONCLUSION:

$\frac{P}{MASS}$ IS TOO SMALL FOR SUFFICIENT ACCELERATION.

MAGNETIC INDUCTION THRUSTER



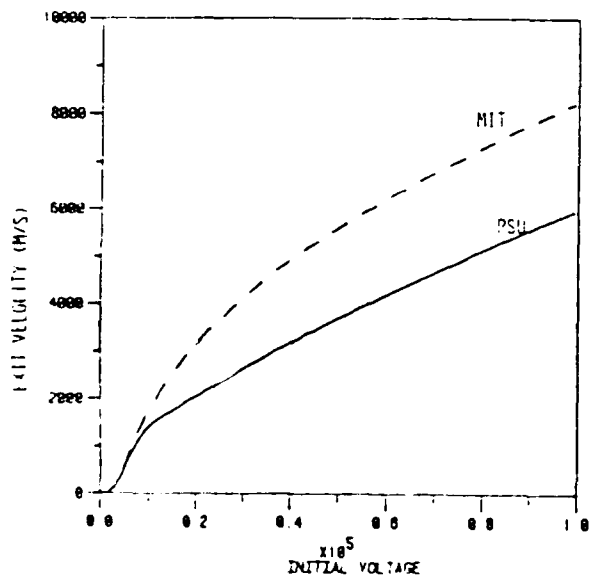
UNIQUE RESULTS OBTAINED:

EXHAUST VELOCITY PROPORTIONAL TO INITIAL VOLTAGE.

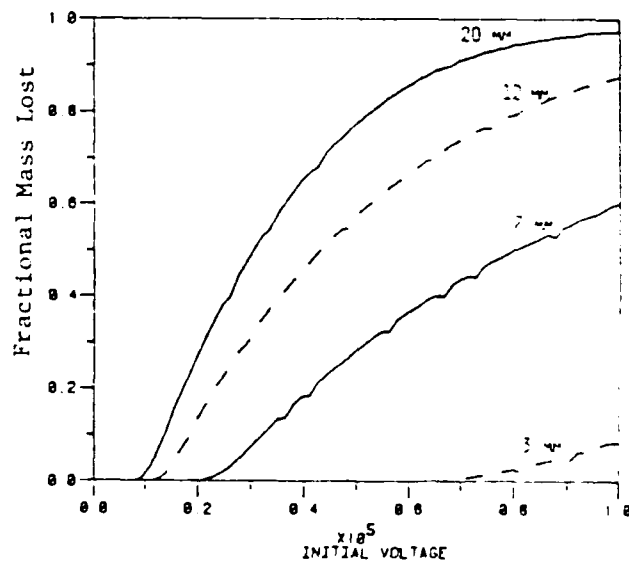
$$U_E \approx 0.1 V_0$$

THERMAL HEATING DEGRADES PERFORMANCE.

EXHAUST MASS CAN BE DRIVEN TO EVAPORATION.



COMPARISON OF DATA OBTAINED FROM
NON-THERMAL (MIT) AND THERMAL (PSU) ANALYSIS



MASS LOST VS. INITIAL VOLTAGE FOR SEVERAL RADII
(Constant Mass)

CLOSE-SPACED TEMPERATURE
KNUDSEN FLOW

John B. McVey
Rasor Associates, Inc.
253 Humboldt Court
Sunnyvale, CA

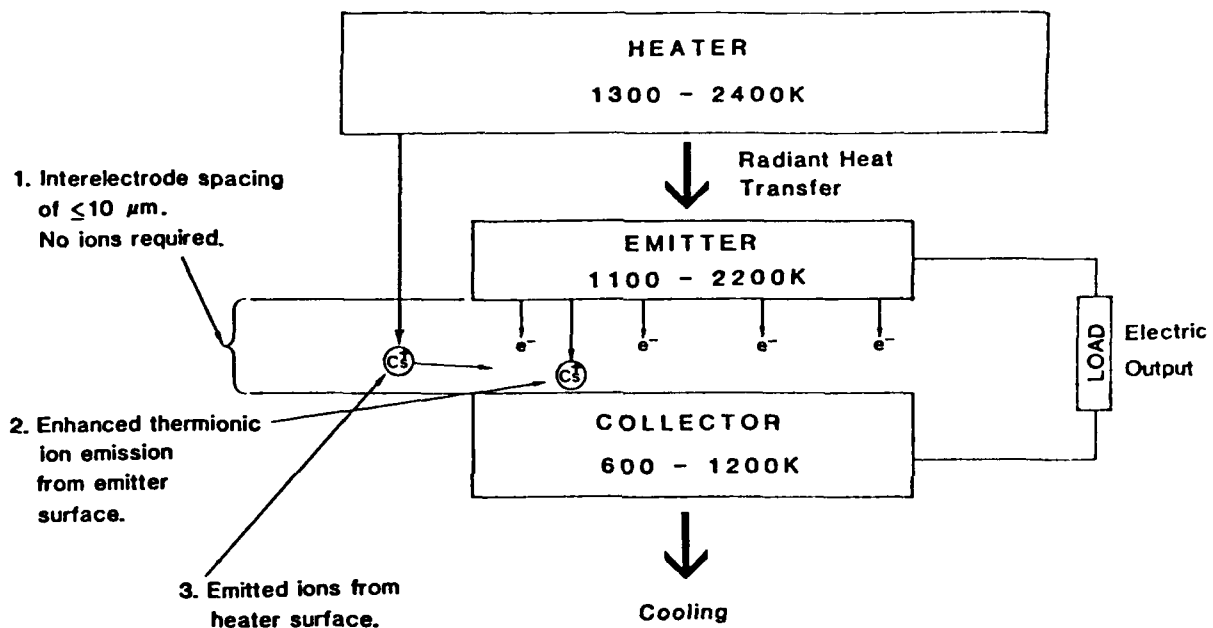
The objective of this research is to investigate and improve methods for reducing space-charge in collisionless (Knudsen Mode) cesium-vapor thermionic energy converters. The reduction of the space-charge due to thermionically emitted electrons is essential for efficient generation of electric power by such converters. Three approaches will be investigated both experimentally and by computer simulation. These are illustrated in Fig. 1. They are:

1. Very close interelectrode spacings (10 microns or less).
2. Enhanced thermal ionization of cesium on the emitter surface. This enables the interelectrode gap to be much larger (25-300 microns). Soviet researchers (Babinin, Mustafayev, Sitnov, and Ender; 1975) have indicated that this is possible by using structured emitters. The theoretical basis for the enhancement is not well understood, however. Addition of barium or cesium oxide vapor may be necessary.
3. Externally generated cesium ions. In our experiment, we plan to use radiant emitter heating. This heater can then act as a source of positive cesium ions, producing them by thermal ionization.

Our experimental program will focus on the use of SAVTEC (Self-Adjusting, Versatile Thermionic Energy Converter) - type thermionic diodes. This is a type of converter which uses small diameter electrodes, radiant heating of the emitter, and typically, uses thermal expansion of the emitter electrical lead to obtain the interelectrode gap. Such converters have been shown in previous tests to be capable of 6-10 μm spacings.

Calculational analysis will be used to correlate the experimental data. An analytical model will be developed which can analyze the Knudsen Mode discharge, including the effects of charged particle trapping and spatially oscillating interelectrode potentials. Existing models will be upgraded to study the production and transport of cesium ions from an external source through a collision-dominated region into the interelectrode space. The interaction between the ion-producing discharge and the Knudsen discharge in the interelectrode space will be handled in an approximate way, guided by experimental results.

The expected departure of the experimental volt-ampere characteristics from the ideal, non-space-charge limited diode is shown in Figs. 2a and 2b. In Fig. 2a, the effect of decreased interelectrode spacing is indicated. For smaller spacings the curve is much closer to the ideal one. In Fig. 2b, the expected curve due to the unignited mode is shown for a spacing of 2.0 mils (51 μm). The addition of ions from an external source or from emitter structuring could probably double the output current of the unignited mode. Experimental tests will determine just how effective these ionization mechanisms are.



**Fig. 1 Some Mechanisms for Space-Charge Reduction
in a SAVTEC - Type Thermionic Converter**

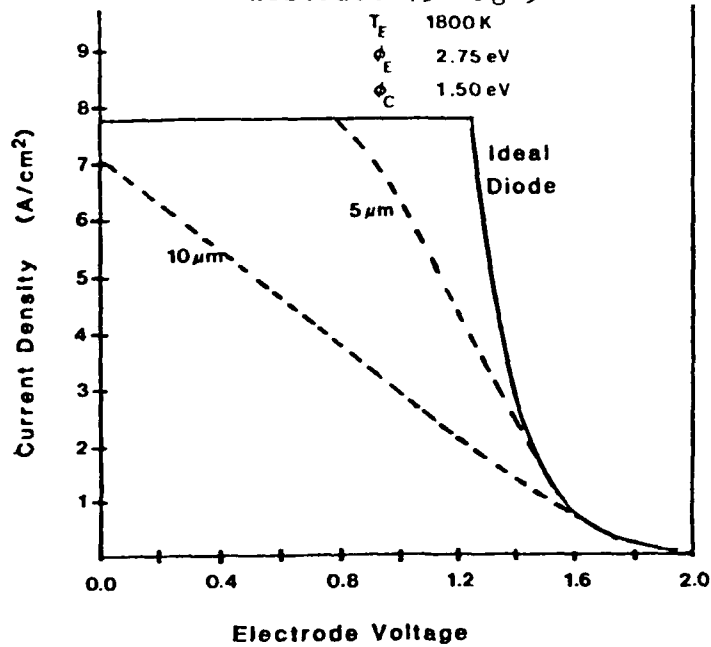


Fig. 2a Expected Volt-Ampere Characteristics for Close-Spaced Diodes

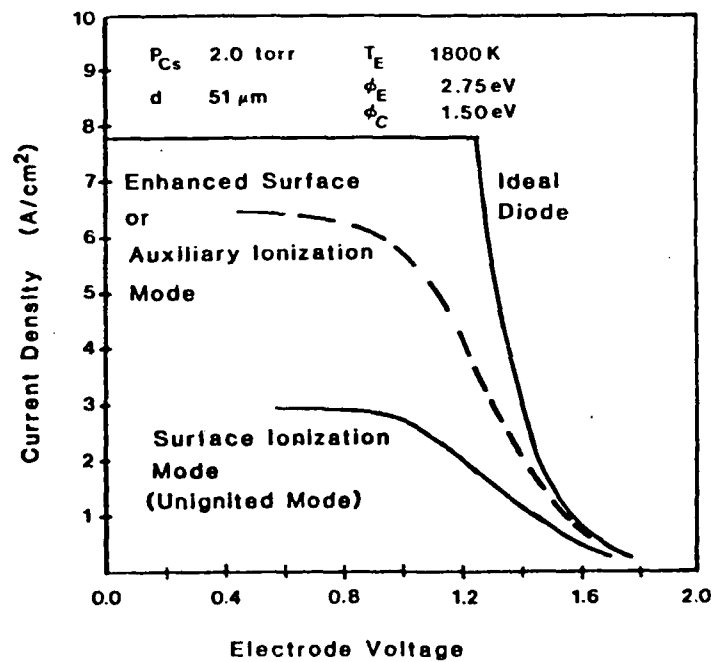


Fig. 2b Expected Volt-Ampere Characteristics for Surface and Auxiliary Ion Source Diodes

VARIABLE FIELD-EFFECTS RELATED TO
ROTATING FLUIDIZED BED SPACE POWER SYSTEMS

Owen C. Jones, Jr.
Rensselaer Polytechnic Institute
Troy, New York 12181

The overriding goal of the program is to analytically model and experimentally verify the effects of variable g-field behavior of fluidized beds in rotating systems. The initial emphasis of the program is to evaluate questions which may provide limiting or obviating conditions on the use of such systems in space power generation.

During the first six months of the program, questions relating to the coupled thermal hydraulic-neutronic stability, thermal stress, and bed expansion limits have been addressed. It has been determined that an infinitely long reactor is extremely stable with neutronic reactor period dominating the low frequency response, and propellant and fuel thermal time constants contributing at the higher frequencies. This evaluation provides a basis for research into the stability of a finite reactor when neutronics will be affected by variable neutron leakage due to the effects of propellant flow-perturbed, fluidized fuel bed thickness. Analysis of thermal stress in the blind end-plate has resolved the question regarding the importance of heat transfer characteristics from the core-zone to the plate, and focused attention on mechanisms for active cooling of this rotating cylindrical plate subjected to sharp extreme temperature difference profiles.

Finally, a simple first-principals kinematic model has been devised, based on mass conservation principals, to predict the initiation and extent of fluidization in rotating systems as pictured in Fig. 1. The model developed confirms in form a well-known empirical observation used for liquid-solid fluidization. The utility of this model for gas-solid fluidization has been demonstrated and the important scaling criteria have been identified. The model indicates that the local bed voidage α (fraction of differential volume perpendicular to the local g-field) may be related to the local volume flux of gas j_g and the local terminal velocity v_∞ of the particles by

$$\alpha = (j_g/v_\infty)^{1/n} \quad (1)$$

where n is an empirical exponent relating local relative velocity to terminal velocity through the voidage ($v_r = \alpha^n v_\infty$). Contrary to current wisdom, examination of existing data has shown that the coefficient in (2) is, in fact, v_∞ (Fig. 2a). Current controversy regarding the behavior of n has been resolved showing it to be independent of α . Data long referred to in the literature has been judged spurious in comparison with all other data (the indicated terminal velocities of hundreds or thousands of meters per second for 50-1000- μ m-sized particles being patently false). A new correlation for n given by

$$n = 5.05 [1 - 0.5 \tanh (Re_\infty/90)^{0.4}] \quad (2)$$

is shown to accurately represent the existing data for the range of terminal Reynolds numbers of $0.06 < Re_\infty < 1000$ (Fig. 2b). The data base must be extended to high pressures and larger Re_∞ .

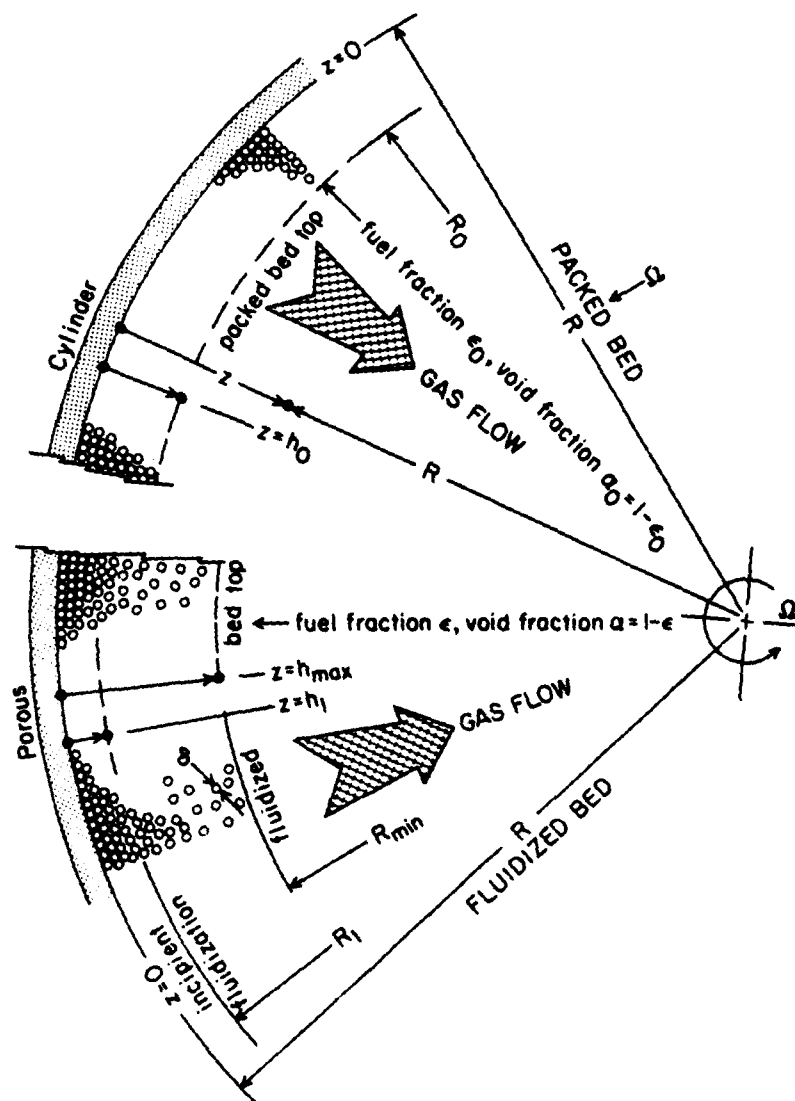


Figure 1. Schematic diagram of a rotating fluidized bed showing the packed bed with thickness h_0 in the upper half, and the same bed partially fluidized from a thickness h_1 to an overall thickness h_{max} in the lower half.

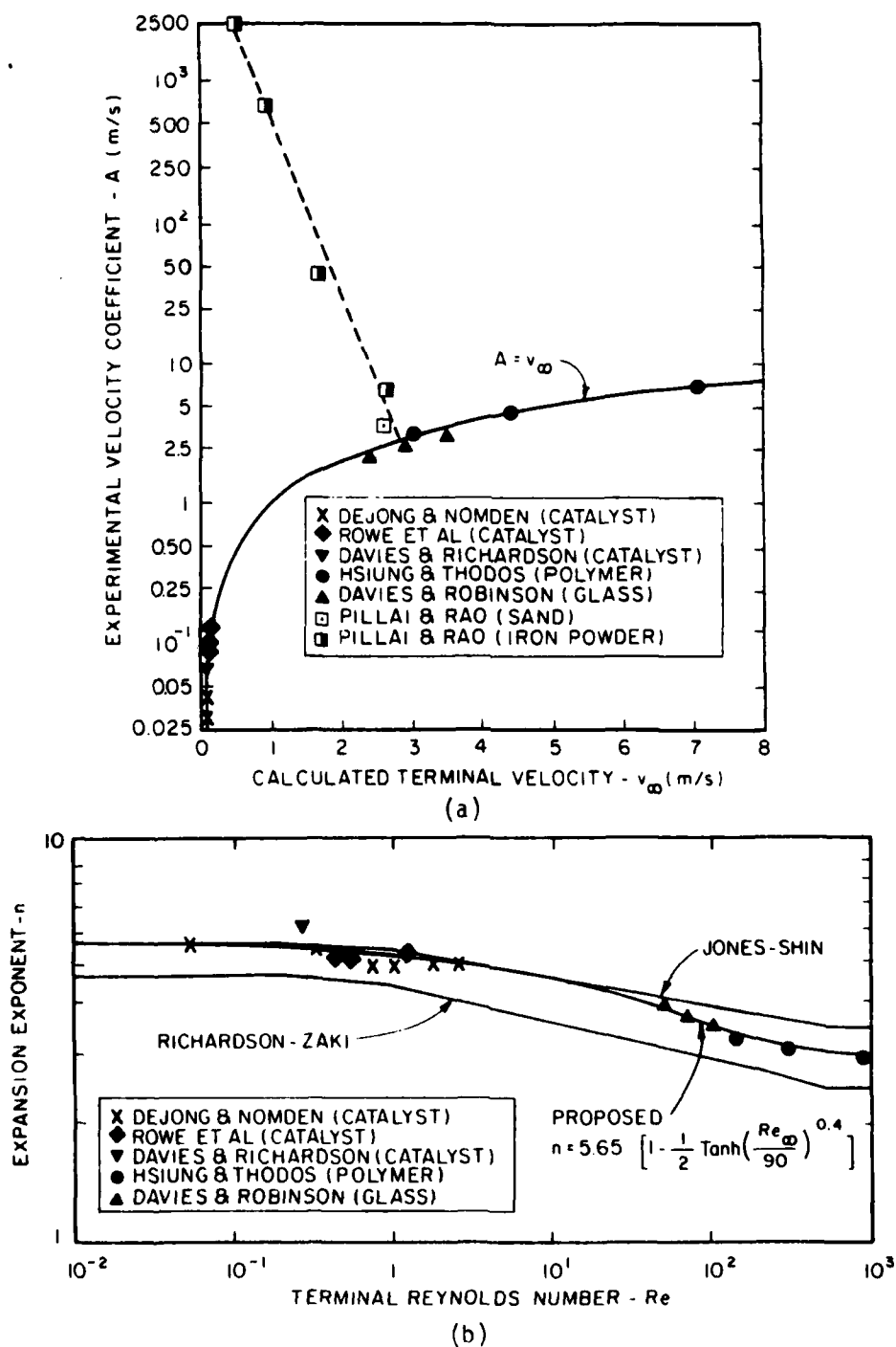


Figure 2. Comparison of fluidization coefficient (a) and expansion exponent (b) with data in the literature for gas-fluidized particulate beds.

THEORETICAL AND EXPERIMENTAL STUDIES OF STABILIZED METASTABLE HELIUM

Jonas S. Zmuidzinas
Jet Propulsion Laboratory, California Institute of Technology
Pasadena, California 91109

The general question how to stabilize metastable excited states of atoms and molecules individually and collectively in bulk is being addressed in a multiphase research program in the context of metastable triplet helium. The known long radiative lifetime, weak spin-spin and spin-orbit forces, and simple atomic structure of metastable triplet helium make it the prime candidate for studying this question. The principal objectives of the program are to acquire an understanding of the physics of bulk metastable triplet helium, to devise methods to stabilize it for long periods of time, and to create and stabilize a novel state of energetic matter, He IV-A/M, which is a bulk aggregate of spin-polarized metastable triplet helium atoms/molecules. The basic scientific question and a three-step approach to it are illustrated in Figure 1.

In the first step, the surface of superfluid helium at 1-2 K is bombarded by 50 keV electrons. Most of the excited species produced in the liquid decay fairly rapidly, the survivors being $\text{He}_2^* \equiv \text{He}_2(a^3\Sigma_u^+)$. In order to suppress the dominant destruction mechanism $\text{He}_2^* + \text{He}_2^* \rightarrow 4\text{He} + \text{VUV}$, the He_2^* are spin-polarized by circularly polarized 4650 Å CW laser light. In this manner, which is the key and unique feature of the experiment, concentrations of He_2^* may be built up much in excess of those previously achieved. Because of attractive forces between individual He_2^{*+} , microcrystals of He IV-M are expected to form at sufficiently high He_2^{*+} concentrations.

To suggest, guide, and interpret experiments, a theory of He IV is being developed, first for He IV-A and later for He IV-M. The starting point is a Hamiltonian for a system of α -particles and electrons interacting via Coulomb forces. The weak spin-orbit and spin-spin interactions are initially neglected, to be included in later stability studies of He IV. The formulation of the theory employs modern methods of quantum field theory at finite temperatures. An effective action for a system of electrons and $^4\text{He}^+$ ions has been obtained to serve as the basis for future numerical calculations on He IV. The theory is expected to be valid for a wide range of temperatures and pressures. Preliminary calculations suggest an fcc lattice structure for He IV-A.

Two key mechanisms have been identified to deexcite He IV. The second step of the approach (Figure 1) calls for devising methods to suppress or inhibit these mechanisms in order to realize long-term stability of He IV. The final step is experimental test of both theory and stabilization methods.

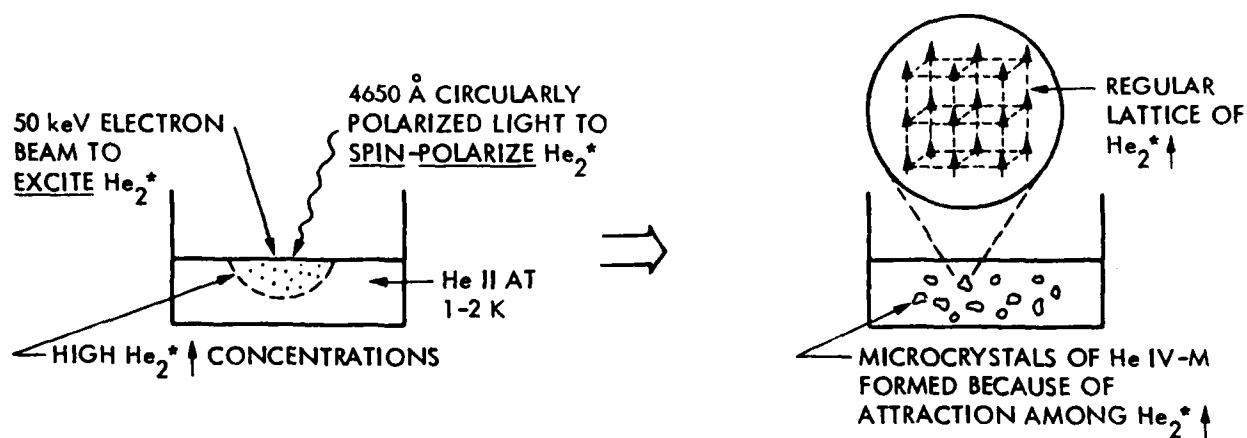
The primary scientific accomplishment expected to be realized at the end of the program is illustrated in Figure 2. One way of inhibiting relativistic magnetic-dipole radiative decay of an isolated $\text{He}^* \equiv \text{He}(2^3S_1)$ atom is by the quantum interference effect. Successful suppression of this decay mode would result in an 8-year lifetime of He^* . Suppression of the second deexcitation mechanism in Figure 2 is required to achieve long-term stability of He IV. To this end, a number of possible schemes are being explored at present by means of simple physical models which neglect complications such as lattice vibrations and imperfections.

QUESTION

- HOW TO STABILIZE He IV-A/M (BULK METASTABLE TRIPLET He* ATOMS/He₂* MOLECULES) FOR LONG PERIODS OF TIME?

APPROACH

- STEP 1 – PRODUCE HIGH CONCENTRATIONS OF SPIN-POLARIZED He₂* IN SUPERFLUID HELIUM (He II) AND CRYSTALLIZE He IV-M



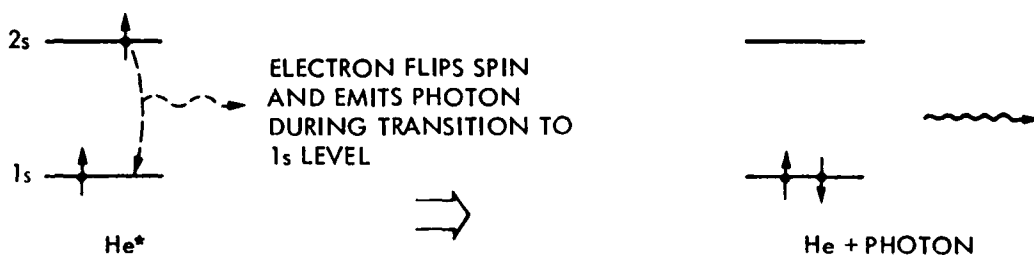
- STEP 2 – DEVELOP THEORY OF He IV AND DEVISE METHODS FOR LONG-TERM STABILIZATION OF He IV AGAINST
 - SPIN-ORBIT AND SPIN-SPIN DEPOLARIZATION
 - RELATIVISTIC MAGNETIC-DIPOLE DECAY OF He*/He₂*
- STEP 3 – TEST THEORY AND STABILIZATION METHODS IN THE LABORATORY

Figure 1. The scientific approach used in the theoretical and experimental studies of stabilized metastable helium.

SCIENTIFIC ACCOMPLISHMENT

- UNDERSTANDING ACHIEVED HOW TO STABILIZE METASTABLE HELIUM ATOMS/MOLECULES IN ISOLATION AND IN BULK AGAINST DOMINANT DECAY MODES:

- MAGNETIC-DIPOLE RADIATIVE DECAY



- SPIN DEPOLARIZATION DUE TO SPIN-ORBIT AND SPIN-SPIN FORCES WITH SUBSEQUENT DOUBLE-ELECTRON EXCHANGE ELECTRIC-DIPOLE RADIATIVE DECAY

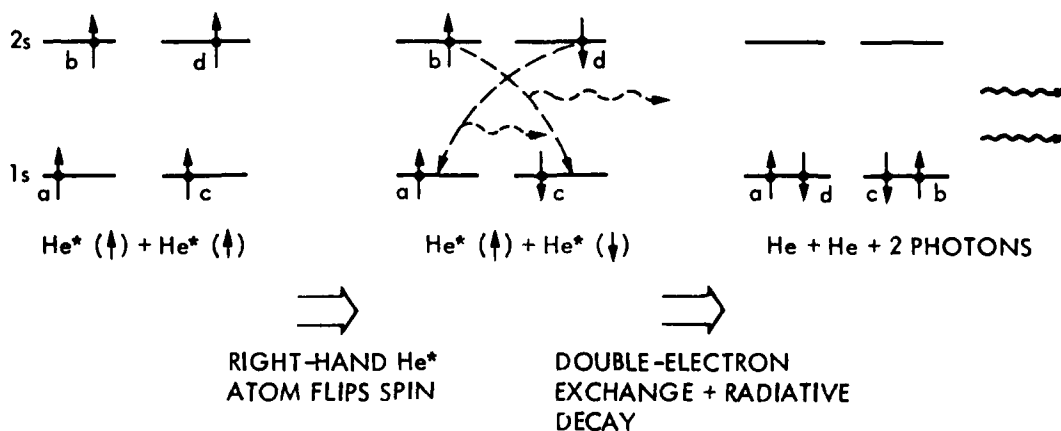


Figure 2. The scientific accomplishment expected by the end of the multiphase research program on stabilized metastable helium.

ANTIPROTON ANNIHILATION PROPULSION

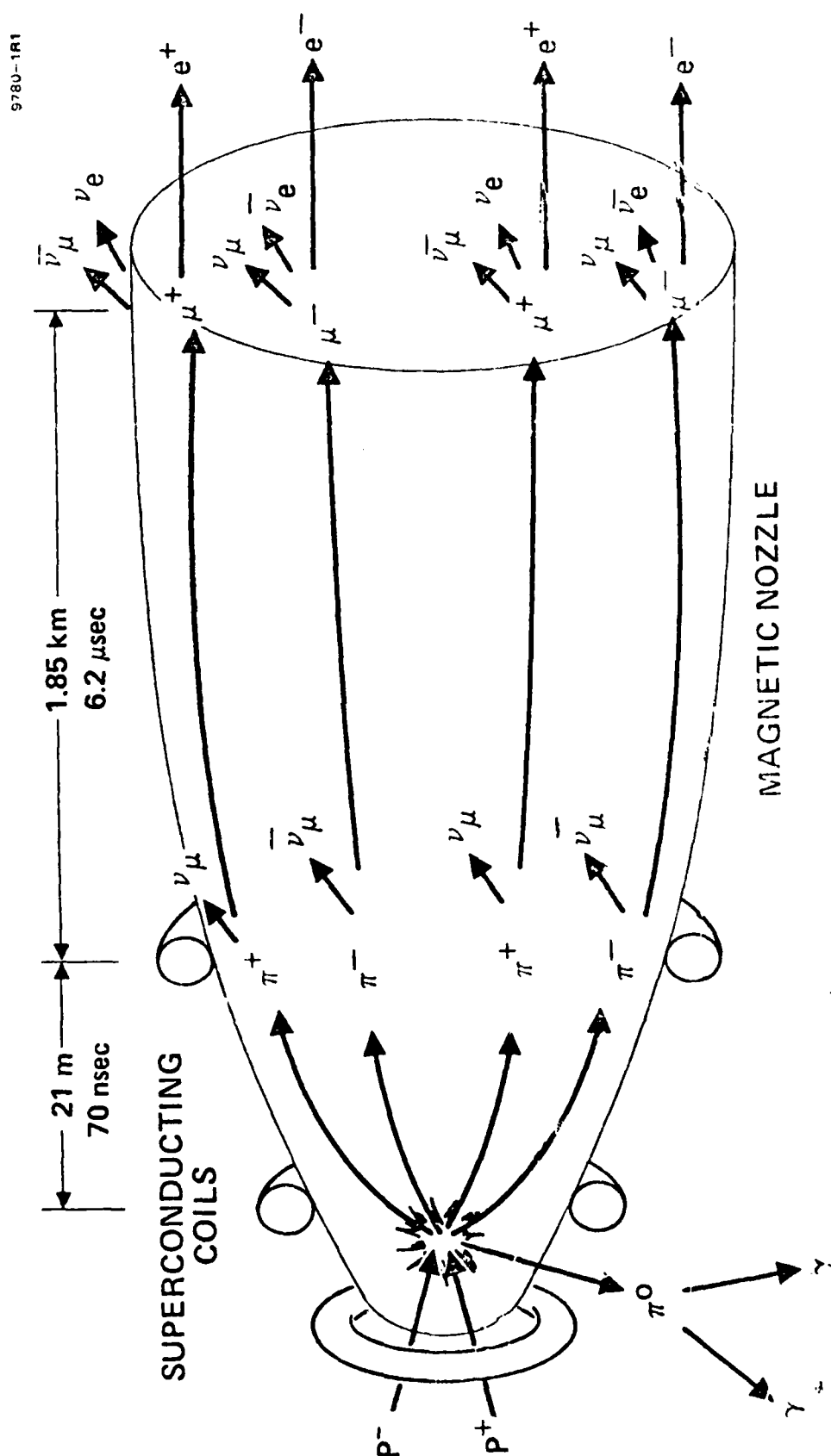
Dr. Robert L. Forward
Forward Unlimited
34 Carriage Square
Oxnard, California 93030 USA

Antimatter represents the most highly concentrated form of propulsion energy possible since the antimatter converts all of its mass to energy upon annihilation with normal matter. Antimatter fuel is a million times more energetic than chemical fuel and a thousand times more energetic than nuclear fuel. A spacecraft which uses antimatter as its source of propulsion energy could "drive" at high speed anywhere in the Solar System and even travel to the nearest stars in a small fraction of a human lifetime. A cruise missile could circle the world on the "fumes" from its superpowerful antimatter warhead.

The antimatter should be in the form of antihydrogen or antiprotons since antiprotons do not convert directly into gamma rays upon annihilation as do antielectrons (positrons.) As is shown in Figure 1, when an antiproton (P^-) annihilates with a regular proton (P^+), the annihilation energy is converted into elementary particles called pions. One third of the energy is in neutral pions, which do convert into gamma rays. The other two-thirds of the energy, however, is emitted as high energy charged pions. Although shortlived, these particles travel many tens of meters, allowing plenty of time to convert their kinetic energy into thrust by interaction with a magnetic field nozzle or a working fluid. The pions decay into muons and then electrons, all of which are charged and all of which can supply additional propulsion energy. A major portion of our initial research effort will be to determine the exact number of pions and spallation products produced as antihydrogen interacts with different nuclei such as hydrogen, helium, and heavy elements like uranium and mercury. The goal is to find a reaction that distributes the annihilation energy into a large number of low mass charged particles such as alpha particles (helium nuclei).

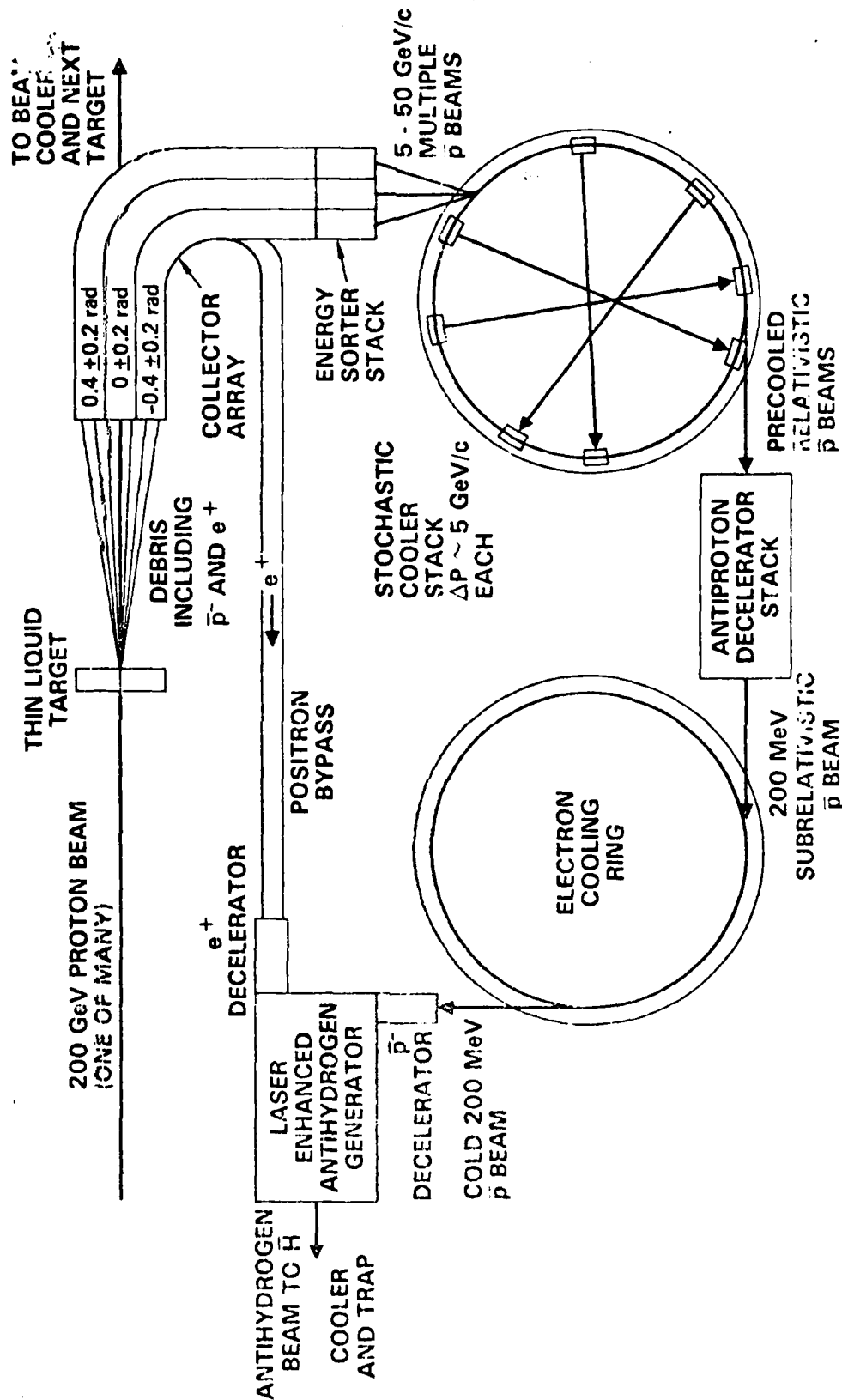
Antiprotons are already being generated, captured, cooled, and stored at a number of particle physics laboratories around the world, albeit in small numbers and with low efficiency. Figure 2 shows one concept for an antihydrogen factory based on extrapolations of the present research. Each one of the elements has already been demonstrated on a small scale. A second phase of our research is to study the physics of the present processes of generation, capture, cooling, and deceleration of antiprotons, and the formation, cooling, and trapping of antihydrogen. This basic research will lead to techniques for the efficient generation, long-term storage, and effective utilization of milligram quantities of antiprotons for aerospace propulsion.

THRUST FROM ANTIMATTER ANNIHILATION



ANTIPROTON FACTORY (ONE SEGMENT)

** 1984 ROCKET RESEARCH MEETING **
Abstract 47 Pg 3



NON-CONVENTIONAL PROPULSION

FRANKLIN B. MEAD, Jr.
AFRPL/LKCS
EDWARDS AFB CA 93523

The identification and development of new propulsion concepts is fundamental to the continued effectiveness of the U.S. Air Force as a military entity. As new concepts lead to the evolution of improved propulsion capability, new dimensions are added to strategies and operations. A properly conducted advanced concepts program can stimulate and vitalize propulsion thinking to the extent that transitions will occur at a more rapid rate than otherwise expected.

The non-conventional propulsion program at the Rocket Propulsion Laboratory is designed to seek-out and technically assess the most advanced energy and revolutionary propulsion concepts which show promise of leading to major advances for space propulsion; to identify limitations that prevent these concepts from being feasible; and to propose research programs which will scientifically attack these limitations.

Some of the most recent advancements in non-conventional propulsion occurred as a result of a study of alternate propulsion energy sources conducted by Dr Robert Forward during the calendar year of 1983. The objective of this program was to look for breakthroughs in propulsion energy sources that might lead to major advances in space propulsion in the next century. The program was conducted in two phases. Phase I, consisted of a literature search and preliminary evaluation that resulted in the selection of a limited number of concepts for indepth study in the second phase. Phase II, identified critical technical research issues and identified people or groups best qualified to attack the critical technology. As a final task, a research program plan was provided for each of the selected Phase II concepts.

The work on this program was greatly aided by a number of previous surveys and the cooperation of a large number of individuals willing to discuss their ideas with Dr Forward. Although the program itself is complete, the Air Force Rocket Propulsion Laboratory continues to search for new revolutionary concepts worthy of its support.

PERFORATED SOLAR SAILS RECOMMENDED RESEARCH PROGRAMS

OPTICAL PROPERTIES STUDY

- FABRICATE 10 TO 5000 nm ALUMINUM AND ALUMINUM COATED KAPTON FILMS WITH HOLES OF VARIOUS SIZES
- MEASURE REFLECTANCE, TRANSMITTANCE, ABSORPTANCE AND EMITTANCE vs WAVELENGTH AS FUNCTION OF HOLE SIZE, HOLE PATTERN, AND ALUMINUM OXIDE THICKNESS

AERODYNAMICS STUDY

- MEASURE DRAG OF PERFORATED FILMS IN MOLECULAR FLOWS SIMULATING CONDITIONS AT SHUTTLE ALTITUDE (SHUTTLE EXPERIMENT?)

THERMAL PROPERTIES STUDY

- DESIGN MICROSTRUCTURES TO INCREASE EMISSIVITY OF FILM BACKSIDE
- TEST FILMS WITH MICROSTRUCTURE UNDER SIMULATED SUNLIGHT
- MEASURE AGGLOMERATION POINT AS FUNCTION OF STRUCTURE TYPE AND ALUMINUM OXIDE THICKNESS

MECHANICAL PROPERTIES STUDY

- DESIGN TRUSS SUPPORT FRAMES AND PERFORATED FILMS FOR BEST STRENGTH/LIGHTNESS
- MEASURE MECHANICAL STRENGTH OF FILMS

MISSIONS STUDIES

- (AS FILM AND SUPPORT STRUCTURE DATA BECOMES AVAILABLE)

**TO SCALE
(EXCEPT FOR SAIL)**

ORBITAL RADIUS	—	40,200 km
ORBITAL OFFSET	—	7,200 km
ORBITAL LEVITATION	—	13,000 km
ORBITAL PERIOD	—	24 hours
POLAR ELEVATION	—	$9.3^{\circ} \pm 1.7^{\circ}$ (WORST CASE)

COUPLING BETWEEN VELOCITY OSCILLATIONS
AND SOLID PROPELLANT COMBUSTION

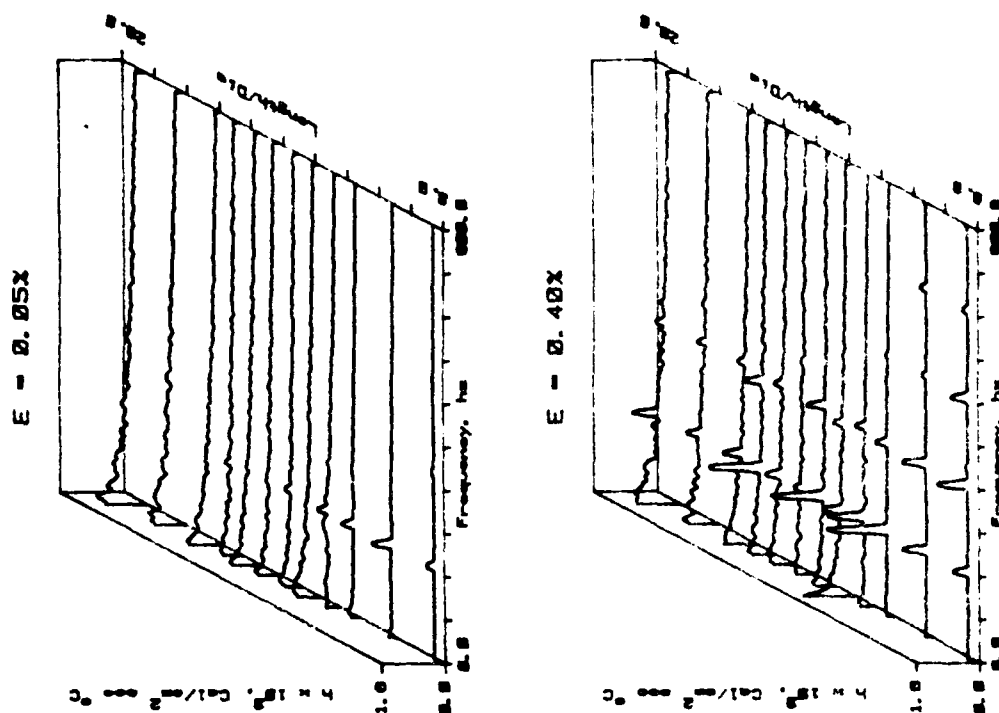
Robert S. Brown, Anthony M. Blackner, Roger Dunlap
United Technologies/Chemical Systems Division
San Jose, CA 95150-0015

Studies are being conducted to define and characterize the basic fluid mechanics and heat transfer mechanisms controlling the coupling between acoustic velocities and solid propellant combustion. The coupling produces substantial effect on the overall stability of the combustion pressure, yet substantial deficiencies exist in the current basic knowledge. Oscillatory heat fluxes and radial profile of the mean and oscillatory velocity are being measured at several axial stations in a cold flow rocket simulator.

At low acoustic pressure (ie, 0.05%), oscillatory heat fluxes are generated near the head-end of the motor, but are not discernible towards the aft-end. At the higher acoustic pressure (0.4%) nonlinearities first appear at the head-end and at the driving frequency further downstream. Velocity and turbulence profile measurements show that, at the lower acoustic pressure, the acoustic waves exist across the entire cross-section at the head-end, but downstream, are destroyed in the near wall region by the turbulence. At higher acoustic amplitudes, nonlinear flow behavior is observed near the wall towards the head-end and the linear oscillations reach the wall at the downstream location.

These data indicate when and how the heuristic models for this coupling are deficient. The principal coupling first occurs at the head-end, not the aft-end as predicted by the models. Further, the nonlinear behavior also first appears at much lower acoustic pressures than expected from the models.

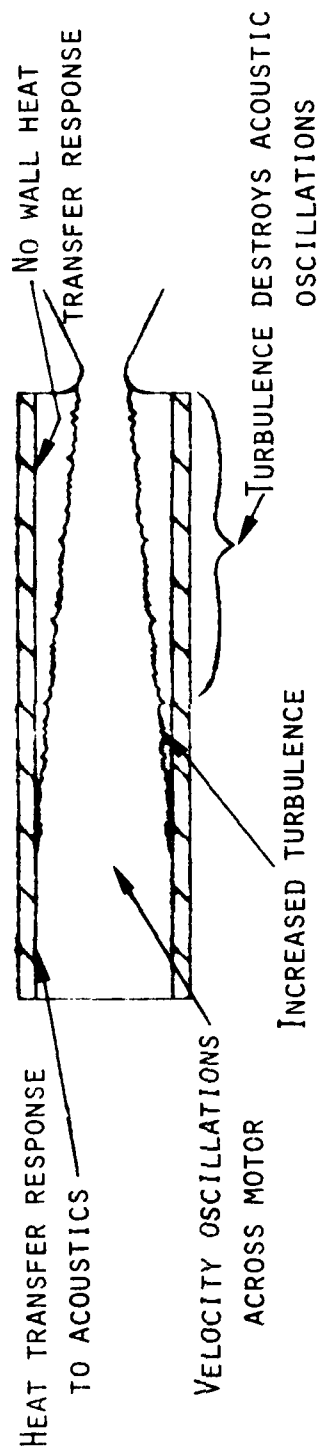
FIGURE 1. VELOCITY COUPLING WITH PROPELLANT COMBUSTION



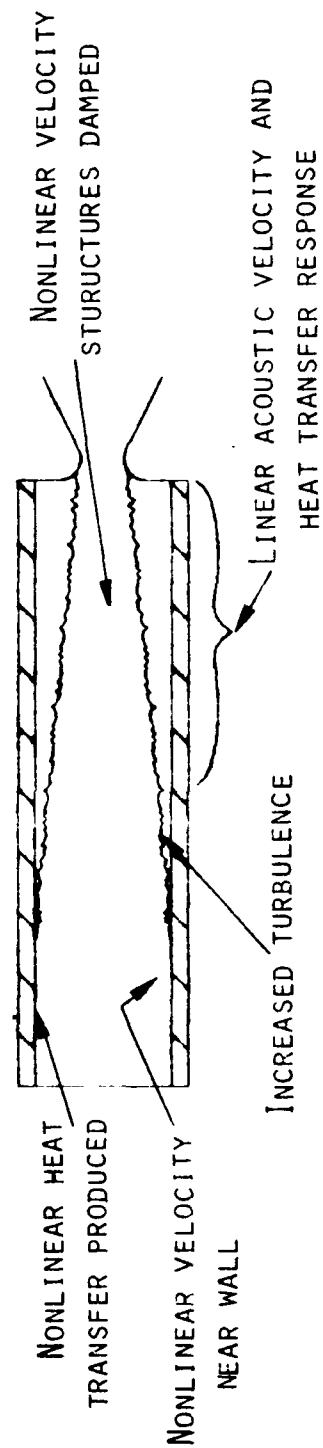
- GOAL
 - CHARACTERIZE INTERACTIONS OF ACOUSTICS
TURBULENCE AND HEAT TRANSFER TO
BLOWING SURFACE
- EXPERIMENT
 - COLD FLOW SIMULATION
- NEW OBSERVATIONS
 - VELOCITY COUPLING MODELS WRONG
 - FLOW AND HEAT TRANSFER VERY
NONLINEAR
 - STRONG TURBULENCE/ ACOUSTIC
INTERACTION
 - EVIDENCE OF TRANSITION
- FUTURE
 - COMPLETE MECHANISM UNDERSTANDING
 - DEVELOP DATA FOR MODEL DEVELOPMENT

FIGURE 2. CURRENT QUALITATIVE FLOWFIELD MODEL

LOW ACOUSTIC PRESSURES



HIGH ACOUSTIC PRESSURES



ANALYSIS OF COMBUSTION OSCILLATIONS IN
HETEROGENEOUS SYSTEMS

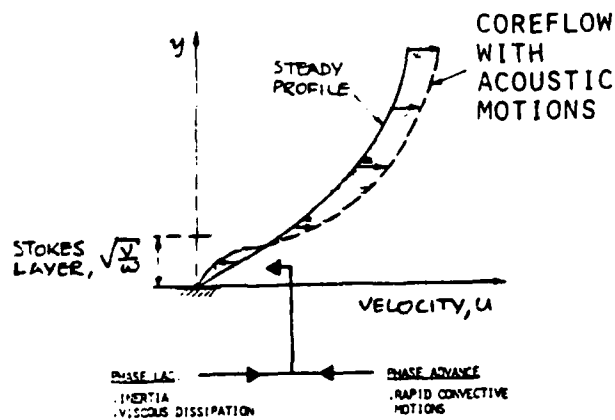
MOSHE BEN-REUVEN AND MARTIN SUMMERFIELD
PRINCETON COMBUSTION RESEARCH LABORATORIES, INC.,
MONMOUTH JUNCTION, NJ

This study is aimed at elucidation of the physical mechanisms capable of driving acoustic instability in solid propellant rocket motors, particularly of the type termed **velocity-coupled instability**. Previous studies on the coupling between acoustic oscillations and the combustion processes in solid propellant motors have demonstrated the complexity of the overall phenomenon, but have not yet defined the basic mechanisms, nor how such combustion-acoustic interactions occur under the flow conditions prevailing inside rocket chambers. The first and second tasks of this research, Critical Literature Review, and Order of Magnitude Analyses of velocity-coupling mechanisms, are now complete. The third part of the study, Analytical Simulation of the Interior Flowfield Within a Solid Propellant Grain, is near completion. The subject of the present analysis is the cold-flow simulation by Dr. Brown at UTC/CSD, in which nitrogen is injected through the porous sidewalls of a cylindrical pipe, creating an internal axisymmetric flow field. A comprehensive analytical model of the nonsteady flow processes entails a system of four partial differential equations for continuity, radial and axial momentum, and thermal enthalpy. The flowfield is considered compressible and viscous, so that all of the associated dissipative terms are included. A particular focal point of the analysis has been the thin viscous sublayer adjacent to the porous surface, where **visco-acoustic interactions** prevail. Order of magnitude analysis (based on previous theoretical works by Lighthill and Illingworth, precluding injection at the wall), as well as earlier experimental data (regarding great enhancement of wall heat transfer in pipes at the presence of a sufficiently intense acoustic field), indicate that this type of nonlinear coupling can influence the nonsteady surface heat feedback appreciably, and hence is a highly plausible velocity-coupled instability mechanism. The analytical approach to visco-acoustic coupling is summarized in Fig. 1. A singular perturbation analysis was carried out for the viscous sublayer; a simple algebraic expression for the first order axial pressure drop within the port was obtained, correlating the available UTC/CSD experimental (steady state) data excellently, demonstrating the inherent Reynolds No. effects, as shown in Fig. 2. A numerical finite-difference algorithm has been developed, using a modified (un-split) MacCormack integration scheme; the code utilizes nonuniform radial stepsize, with very fine mesh near the porous surface. Results of converged steady-state cases are currently generated. A second numerical algorithm, using a split MacCormack scheme (to accommodate for the great differences in radial stepsize, while satisfying the necessary CFL stability condition), is near completion, and will be used to simulate the nonsteady cases, where the exit flow is perturbed periodically. Results will be available in March 1984.

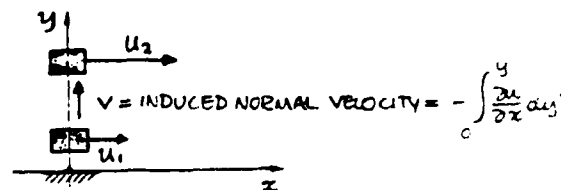
APPROACH:

ANALYSIS OF VELOCITY-COUPLED INSTABILITY MECHANISMS. ONE DOMINANT MECHANISM IS VISCO-ACOUSTIC COUPLING:

FREQUENCY-DEPENDENT SURFACE
HEAT TRANSFER (FIRST ORDER),
WITH PHASE RELATIVE TO
ATTENDANT PERTURBATION.



DC-COMPONENT: ACOUSTIC STREAMING,
WHEN u, v NOT OUT OF PHASE, NET
X-MOMENTUM TRANSFER OCCURS.
(SECOND ORDER).



ORDER OF MAGNITUDE ANALYSIS INDICATES EXPECTED EFFECTS OF
STROUHAL NO. AND MEAN FLOW MACH NO. ON SURFACE HEAT TRANSFER.
THESE INCLUDE EFFECTS OF FREQUENCY, x/D AND (IMPLICITLY)
PRESSURE.

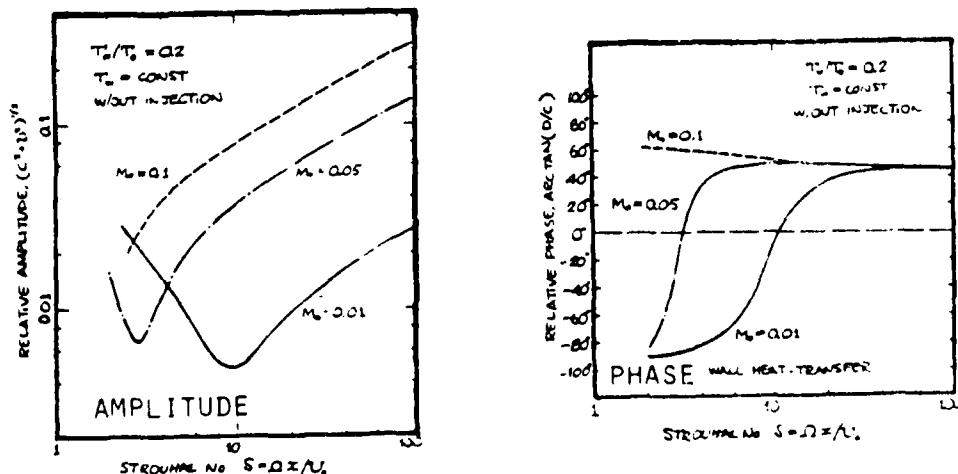
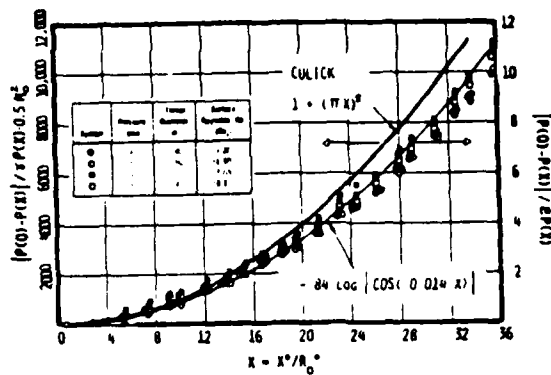
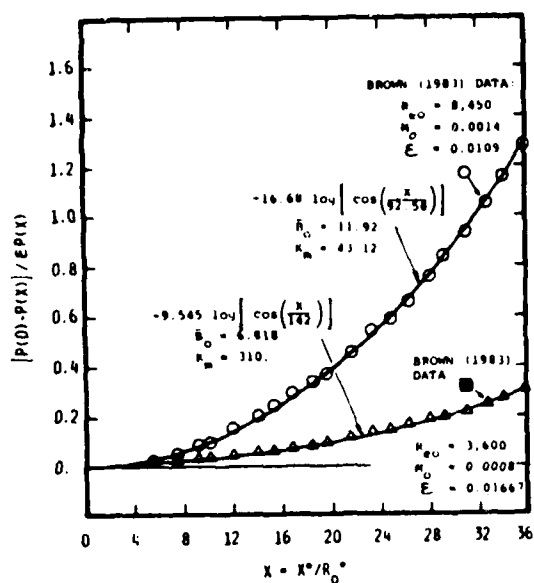


FIG. 1

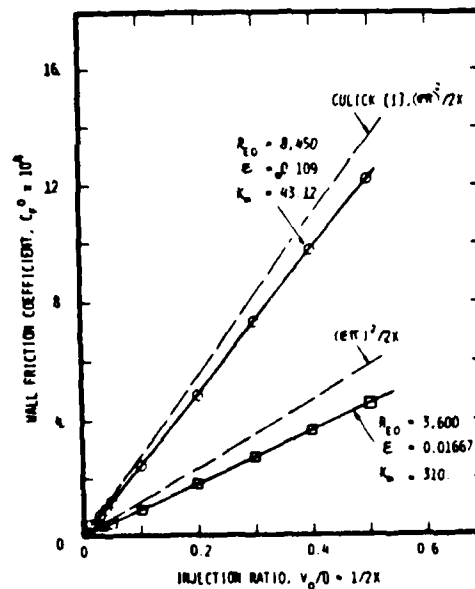
ACCOMPLISHMENTS



DIMENSIONLESS FIRST ORDER AXIAL PRESSURE DISTRIBUTION, FROM THE NEAR-FIELD ANALYSIS HEREIN. THE CURRENT RESULT IS PLOTTED OVER THE ORIGINAL FIGURE OF CSD/UTC (1982), WHICH ALSO SHOWS THE PARABOLIC FORMULA OF CULICK.



SENSITIVITY OF THE MEASURED AXIAL PRESSURE DROP TO REYNOLDS NO. (OR TO THE PARAMETERS K_m AND E HEREIN) IS DEMONSTRATED BY RE-SCALING OF TWO DISTINCT DATA GROUPS PLOTTED IN FIG. 3. EXCELLENT CORRELATIONS ARE OBTAINED BY USE OF EQ. (16).



FRICTION COEFFICIENT CALCULATED FOR THE 2 CASES SHOWN IN FIG. 4. DEVIATIONS FROM LINEAR BEHAVIOR AT LARGE VALUES OF x ARE EVIDENT, IN AGREEMENT WITH THE MEASUREMENTS OF OLSON AND ECKERT[6] WHICH WOULD NOT BE POSSIBLE WITH PURE INVISCID THEORY.

FIG. 2

SOLID PROPELLANT GAS PHASE FLAME DRIVING OF AXIAL COMBUSTION INSTABILITIES

Ben T. Zinn and Brady R. Daniel
School of Aerospace Engineering
Georgia Institute of Technology
Atlanta, Georgia 30332

This recently initiated research program consists of theoretical and experimental investigations of the interaction between solid propellant gas phase flames (to be denoted by SPGPF) and the flow oscillations in rocket motors experiencing axial instabilities. The objectives of this program are (1) elucidate the processes/mechanisms which contribute to the damping or driving of the combustor oscillations by SPGPF and (2) determine whether state of the art models are capable of describing the interaction of SPGPF with unstable combustor oscillations.

Since detailed diagnostics of actual SPGPF are presently impossible because of their extremely small dimensions, this research program investigates the characteristics of flat, premixed flames which possess some of the important features of SPGPF and are amenable to experimental probing. The proposed experimental setup, shown in Fig. 1, is designed to simulate the conditions in an unstable rocket combustor. It consists of a tube with a rectangular cross section. The investigated flame is positioned along one of the side walls to simulate the burning of a solid propellant. A second flat flame, located at one end, provides a steady flow of hot combustion products past the investigated flame. An acoustic driver at the opposite end excites a standing wave of desired properties in the tube. The expected structure of the investigated flame is shown on the bottom of the figure. Proposed diagnostics will consist of measurements of acoustic pressures, the steady and unsteady distributions of u and v , the steady state temperature distribution $T(y)$ and the injection plate admittance Y_o . The measured $T(y)$, Y_o , p' , $V(y=0)$ will be input into the developed theoretical model which will be used to predict $v'(y)$. The validity of the model will be checked by comparing the predicted and measured distributions of $v'(y)$. These studies will be conducted at various wave frequencies and amplitudes, different flame mixture compositions, different magnitudes of the mean flow \bar{u} and different locations of the flame along the standing longitudinal wave.

To date, using the boundary layer conservation equations, an approximate model of the investigated flame and an exact model of the oscillatory cold flow near the injection plate in the absence of combustion have been developed. Figure 2 presents predictions of the cold flow model for the distributions of the real parts of the normal velocities at different axial locations within that half of the combustor where p' is negative. The computations assumed that the real part of the injection plate admittance Y_{or} is negative (i.e., damping) and they show that due to viscous effects $v'(y)$ (and the damping) increase with distance from the injection plate. Furthermore, these results show that the magnitude of the damping is strongly dependent upon axial location within the combustor. Additional studies to date showed that the magnitude of the damping is a strong function of Y_{or} and a weak function of the mean flow Mach number \bar{M} . Future studies will investigate whether the presence of combustion within the acoustic boundary layer will result in net driving by the near-wall region which includes the viscous layer and the flame. Also, these studies will concentrate on identifying the SPGPF processes which exert the greatest influence upon the flame driving. The validity of these predictions will be checked by comparing them with experimental data.

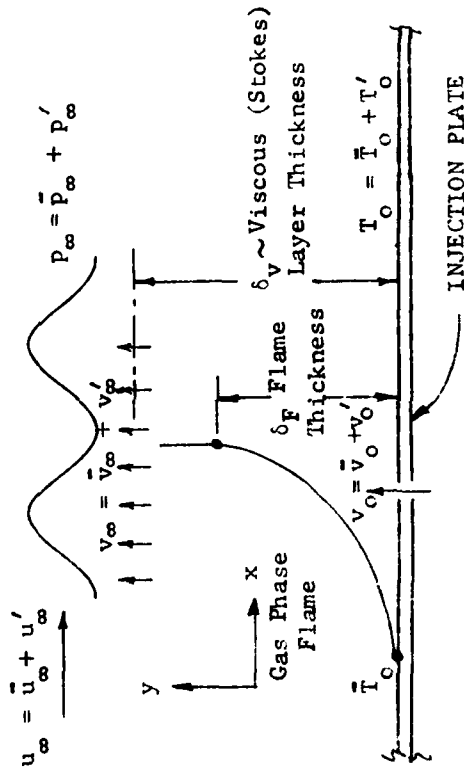


Figure 1. A Schematic of the Proposed Experimental Setup (above) and the Anticipated Flame Structure (below).

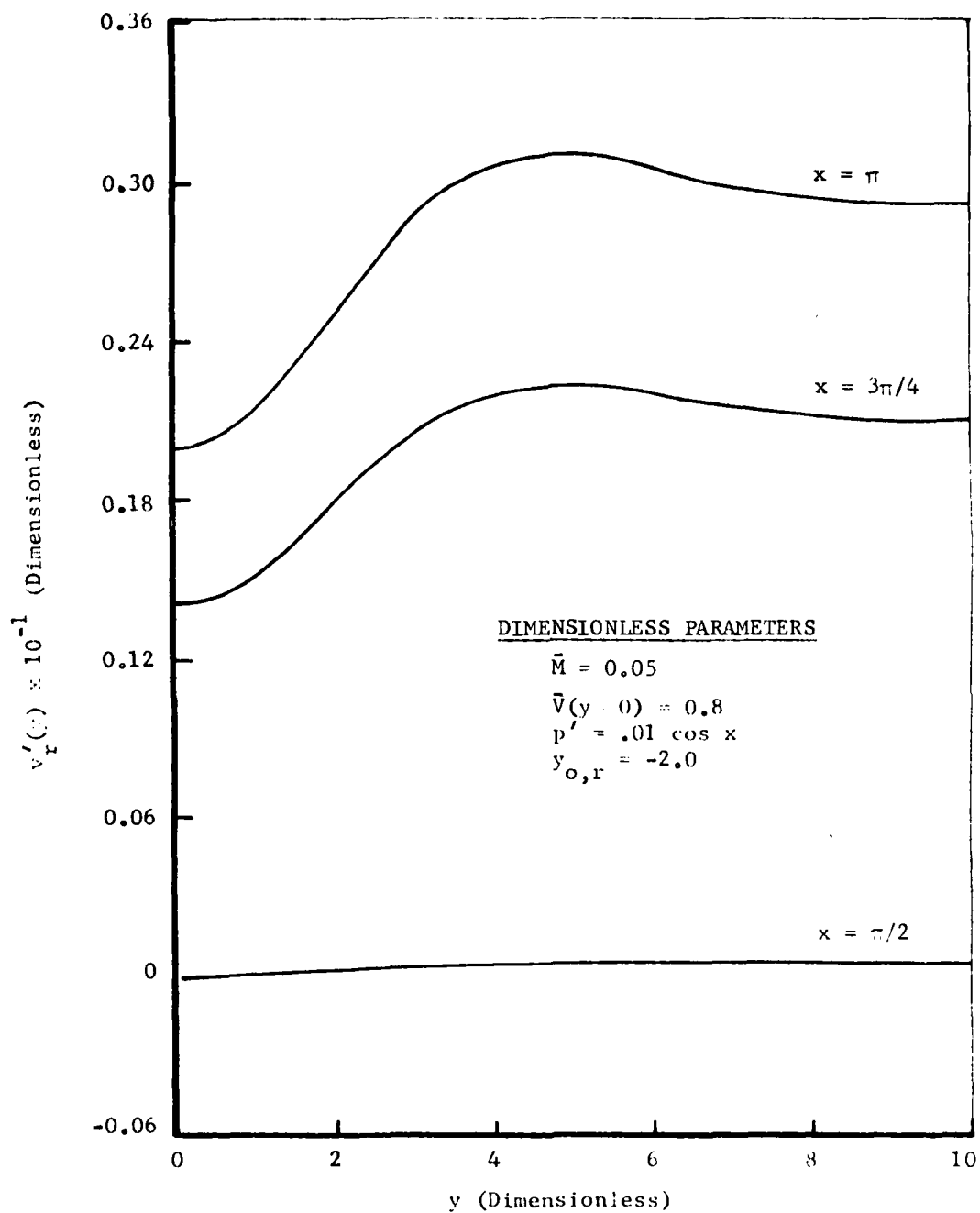


Figure 2. Dependence of Normalized Real Part of $v'(y)$ Upon Normalized Distance from the Injector Plate.

RELATION BETWEEN COMPOSITE PROPELLANT
HETEROGENEITY AND NONSTEADY BURNING

Leon Strand and Norman S. Cohen
Jet Propulsion Laboratory/California Institute of Technology
Pasadena, California 91109

Rocket motor development experience and laboratory combustion data have indicated that ammonium perchlorate particle size distribution has a major effect on combustion instability. The effect cannot be explained by classical theories which relate the combustion response of a solid propellant to its ballistics properties. This research addresses the question of why this is so, and has hypothesized that the answer is contained within the heterogeneity of the composite propellant structure. The answer is of long-range significance because combustion instability is a pervasive problem and propellant formulation adjustment is the most convenient remedy. Further, nonsteady combustion behavior and composite propellant fine structure are of interest in many other contexts.

The approach combines analytical modeling and experiments to characterize the heterogeneity of composite propellants and its relationship to the combustion response. Particularly unique features include an analysis of the combustion response to fluctuations in propellant composition, measurement of the fluctuations in composition as inherently contained within unburned propellant, and measurement of dynamic burning at constant pressure which purportedly manifests such fluctuations. Additional measurements to complete the approach, shown in Fig. 1, are of size distribution and the combustion response under oscillatory pressure conditions. It is desired to see if characteristic frequencies exist in propellants, if they appear in the course of dynamic burning at constant pressure, and if they influence the combustion response to pressure perturbations.

Theoretical accomplishments have appeared in AIAA papers 83-0476 and 83-1270, and a nonlinear analysis is in progress. The major conclusion is that the combustion response to compositional fluctuations can be relatively large. Thus if compositional fluctuations exist at the same frequency as pressure perturbations, the combustion response to the pressure perturbations will be augmented significantly (Fig. 2). The planned series of experiments have been completed and the data are being processed and studied at this writing.

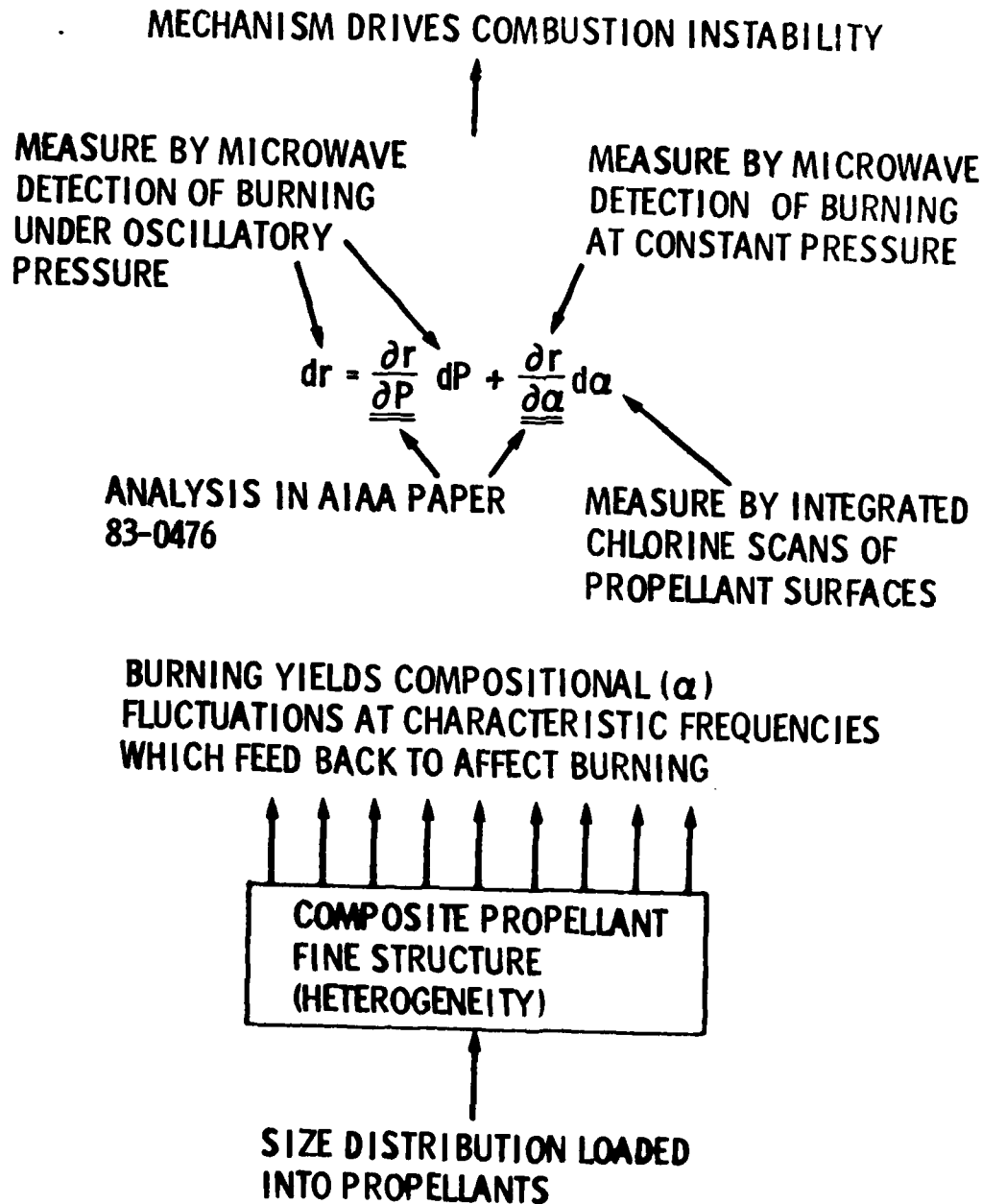


Figure 1. Nature of the approach

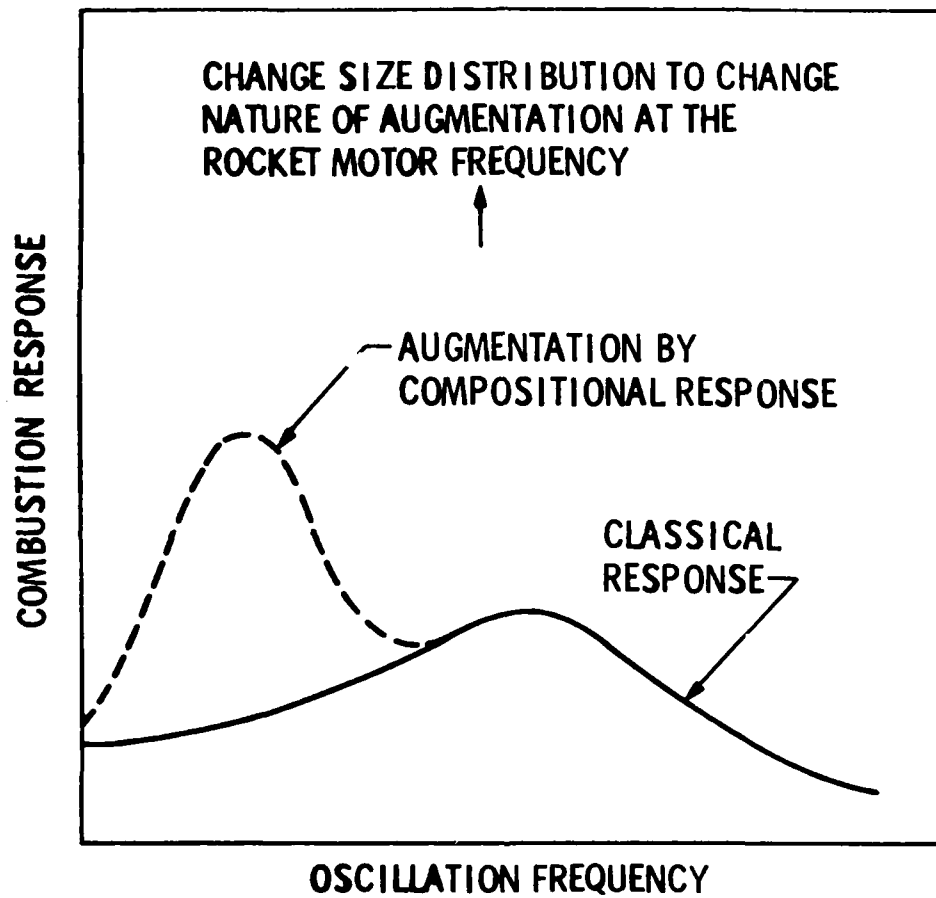


Figure 2. Nature of result of combustion response to compositional fluctuations

INTERACTION OF MULTI-DIMENSIONAL MEAN AND
ACOUSTIC FIELDS IN SOLID ROCKET COMBUSTION CHAMBERS

Joseph D. Baum and Jay N. Levine
AFRPL/DYC
Edwards AFB, CA 93523

The objective of this research program is to develop understanding of the physical mechanisms by which energy is exchanged between the mean and acoustic flow fields in a combustion chamber, specifically the mechanisms by which mean flow energy is transformed into acoustic energy through vortex shedding and the mechanisms by which energy is transferred between the acoustic field and the mean flow of combustion products entering the chamber.

A new numerical code that couples the solutions for the flow and combustion in the chamber is currently under development. The flow in the rocket combustion chamber is described via the solution of the two-dimensional, time dependent, turbulent compressible Navier Stokes equations. The transient burn rate of the solid propellant is modeled using the modified transient one-dimensional heat conduction equation utilized in the previous one-dimensional nonlinear combustion instability analysis. A algebraic grid generation procedure is incorporated in the program to provide both fine distribution of mesh points in the boundaries and in the free shear layer. The program currently includes the explicit unsplit MacCormack finite difference integration scheme. Using an explicit scheme results in a very small integration time step. Several options are currently under examination, including: (a) zonal approach, where an explicit scheme is utilized near the center line and implicit schemes at the nozzle and near the boundaries; and (b) utilizing an implicit scheme everywhere.

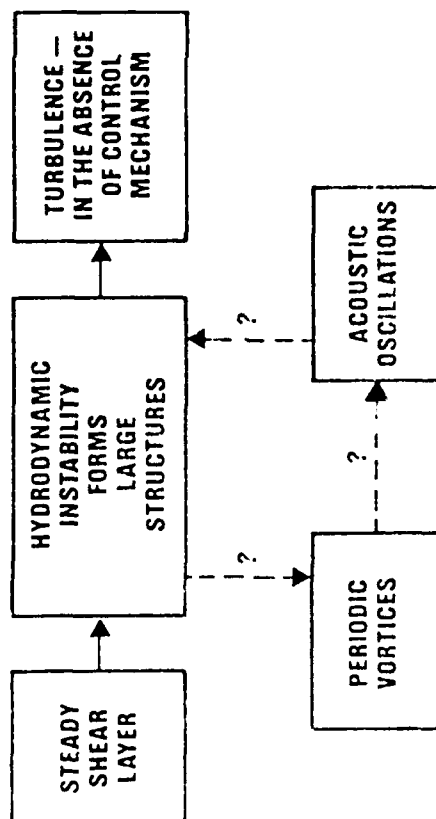
The developed code will be utilized to study the interactions between vortices shed from a sharp downstream facing edge and the acoustic field inside the chamber. Specifically, the objective is to understand the mechanisms by which vortex energy is transformed into acoustic energy and the conditions under which an acoustic field can influence the existence, frequency, and strength of vortex shedding. The program will examine the coupling between the mean and acoustic fields in a chamber in which combustion products are provided by propellant burning at the head-end, while the chamber walls are non-interacting. Several chamber geometries will be examined. The results from these numerical experiments will be examined based upon the effect of mean flow, cavity length to diameter ratio, and cavity harmonic content upon acoustic energy transfer between vortices and acoustic pressure oscillations; reflection of waves from the bottom of the cavity; reflection and amplification or attenuation of waves from the trailing wall; significance of trailing wall height; spatial and temporal propagation of large scale vortices; interaction of shear layer with reflected acoustic waves and large scale vortices; and the effect of blowing from the surface of hot combustion products upon the large-scale eddies and shear layer stability.

The developed code will be utilized to study the interaction between the mean flow of combustion products leaving the burning surface and the acoustic oscillations in the combustion chamber. Conservation of mass, momentum and energy will be calculated at several grid points close to the burning propellant surface, in order to determine the momentum and energy flux rates in and out of the cell. Following several cells across the chamber area cross-section (including cells in the acoustic boundary layer) will enable understanding and determination of the acoustic energy loss due to flow turning.

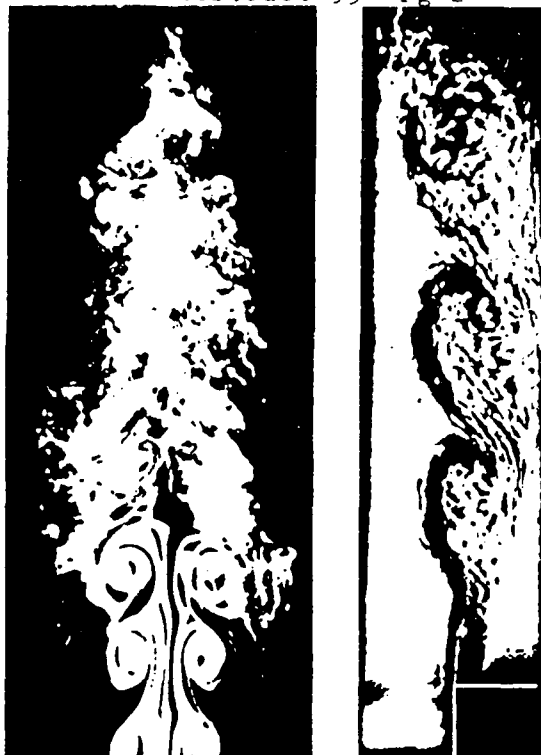
Scientific Approach — Combustion Instability....

Interaction of Multi-Dimensional Mean and Acoustic Fields in Solid Rocket Combustion Chambers

- Energy Exchange Between Mean Flow and Acoustic Fields has Significant Effects on Motor Stability



Acoustic Oscillation Generated by Hydrodynamic Shear Layer Instability



- Solution of Two-dimensional, Time-dependent, Turbulent, Navier-Stokes Equations

ISSUES BEING ADDRESSED:

- How is Vortex Energy Transformed into Acoustic Energy
- Influence of Acoustic Field on Shear Layer Instability
- Energy Exchange Between Acoustic Field and Transverse Mass Flow

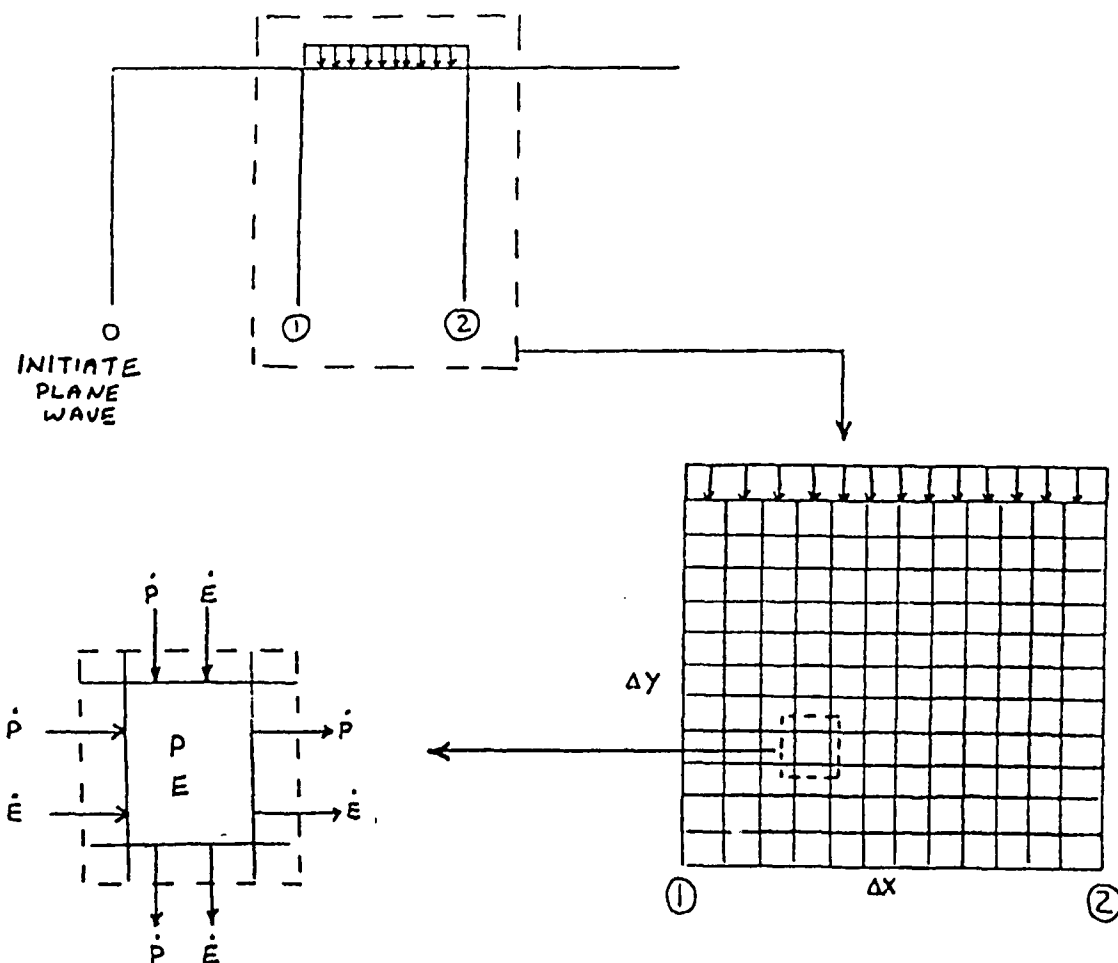


FIG. 2. A NUMERICAL FLOW TURNING SIMULATION.

FINITE ELEMENT ANALYSIS FOR COMBUSTION INSTABILITY
OF SOLID PROPELLANT ROCKET MOTORS

T. J. Chung
Department of Mechanical Engineering
The University of Alabama in Huntsville
Huntsville, AL 35899

The purpose of this research is to provide computational schemes via finite elements to analyze combustion instabilities which may occur in solid propellant rocket motors. Specifically, rigorous flow field calculations and determination of the effect of correct flow field on combustion instability constitute the most important part of the current research.

Achievements of the past year consist of (1) derivations of stability integrals which allow acoustic oscillations to interact with vortical oscillations and (2) development of computer programs to implement both the flow field equations and stability integrals. The numerical approach used is based on two- and three-dimensional isoparametric finite elements (Fig. 1) which lend themselves to efficient numerical integrations by means of Gaussian quadrature.

For irregular geometries containing inhibitors or transitions of cross sections (Fig. 1), it has been shown that there are significant interactions between the acoustic and hydrodynamic oscillations. It has also been made evident that such a study can not be performed unless accurate flow field is determined, including both mean flow and oscillatory flow fields (Fig. 2,3). Depending on a particular vortical frequency mode, the fluctuating vortical components of the velocity are expected to vary widely. The most significant aspect of the present study is the determination of the stability boundaries. Fig. 4 shows variations of hydrodynamic instability growth constants (α_H) vs vortical oscillation frequencies interacting with selected acoustic frequencies. Although these graphs indicate frequency ranges of instability, it is meaningful to show stability boundaries (Fig. 5). The general trend is that with an increase of Reynolds numbers, the stability boundaries shift to the lower frequencies, a trend similar to a flat-plate boundary layer flow. Note that multiple "islands" develop due to inhibitors. Critical Reynolds number appears to be around $Re=700$. In order to compare the acoustically interacting vortical instability with "acoustics free" hydrodynamic instability (Fig. 6), the corresponding growth constants α_v are shown in Fig. 7. It is seen that the lower frequency instabilities are absent in the lower ranges of Reynolds numbers in hydrodynamic oscillations alone not interacting with acoustics, a possibility that less stable conditions arise when vortical oscillations do interact with acoustic fluctuations. However, this trend may not be true in the case of other combinations of acoustic and vortical frequencies.

To determine the effect of flow field due to tapered cross sections with various transition angles on stability, we have analyzed an axisymmetric motor with transition angles of 30° , 45° , 60° , and 90° . Although the results are not shown in figures it was concluded that the larger the transition angle, the less stable is the motor as a result of unfavorable interactions of vortical fluctuations with acoustic fluctuations. The unstable hydrodynamic instability growth constants are positive but they are brought to negative side as summed to the acoustic instability constants.

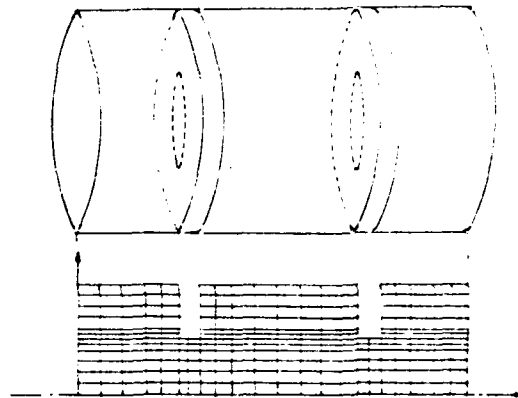


Fig. 1 Axisymmetric motor with inhibitors and Finite Element modeling

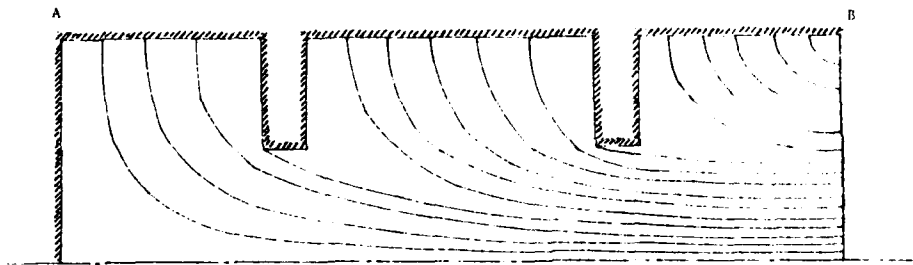


Fig. 2 Mean Flow Stream Lines, $aM_b = 10$ in/sec, 84 node system.

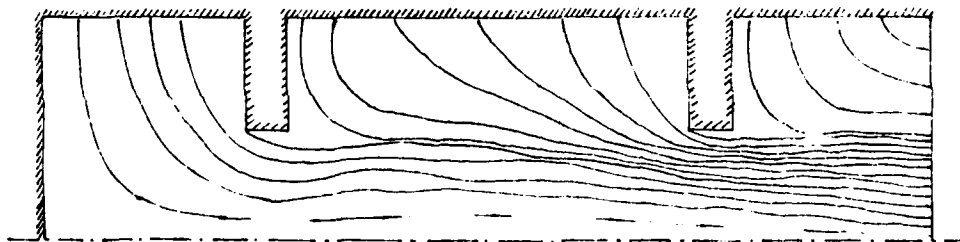


Fig. 3 Streamlines of vortical component velocity, 84 node system,
 $Re = 10^4$, $\omega_N = 102$ Hz, $\dot{\omega}_N = 61$ Hz

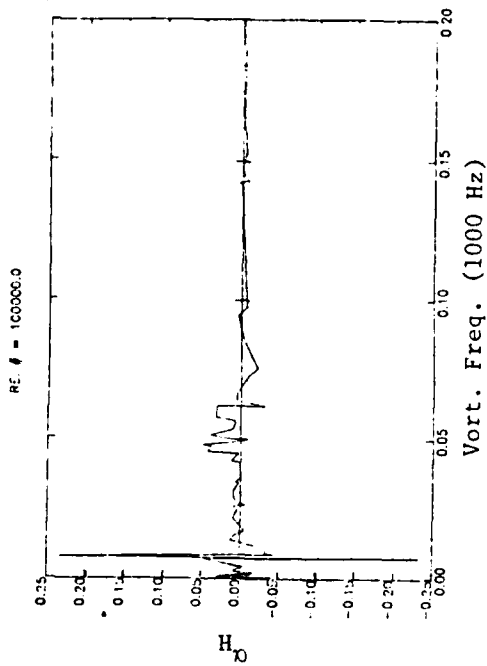


Fig. 4 Acoustically interacting hydrodynamic instability growth constants (α_H) vs vortical frequencies, $Re = 105$, $\omega_H = 102$ Hz

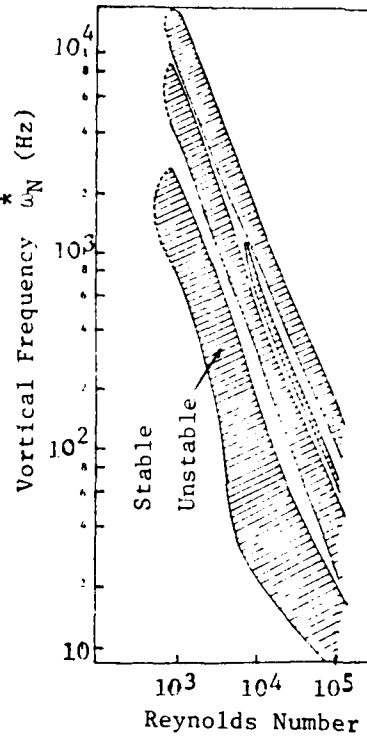


Fig. 5 Stability boundaries for acoustically interacting vortical frequencies, with various vortical frequencies versus Reynolds numbers, $\omega_N = 102$ Hz.

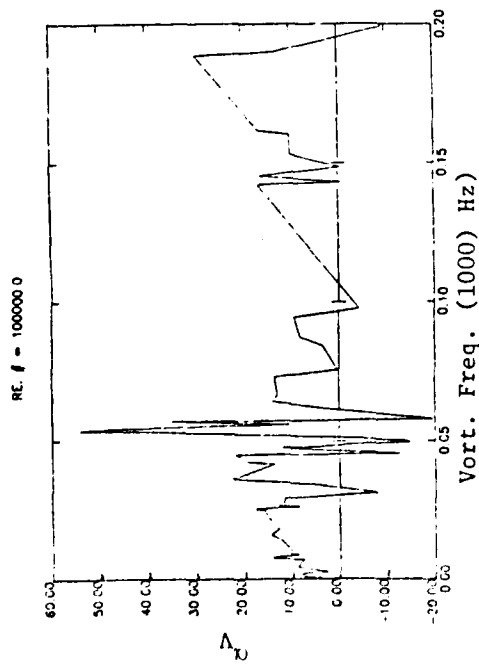


Fig. 6 Acoustically non-interacting instability growth constants (α_H) vs. vortical frequencies, $Re = 105$

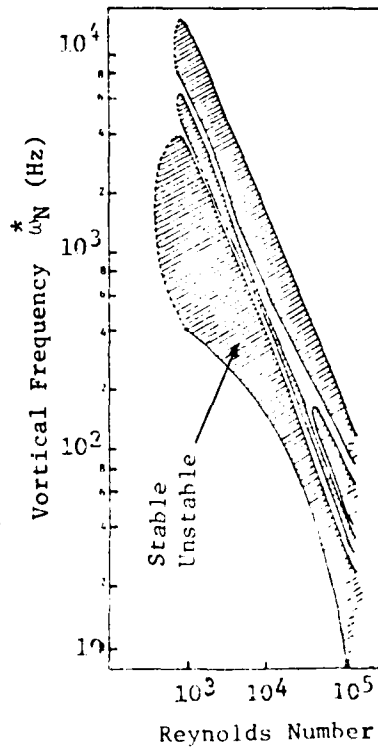


Fig. 7 Stability boundaries for various vortical frequencies vs. Reynolds numbers.

ELECTROLYTIC PREPARATION OF NOVEL AZIDODINITRO COMPOUNDS

Milton B. Frankel and James F. Weber

Rockwell International Corporation
Rocketdyne Division
Canoga Park, CA 91304

Future higher performance propellants will require new classes of more energetic ingredients. These will include new oxidizers, plasticizers, and binders. Polynitro- and azidoalkyl compounds have either been or are currently being evaluated for this purpose. Highly substituted geminal dinitro compounds [e.g., $R-C(NO_2)_2X$, where $X=CN, CH_3, F$] are of particular interest, and substitution of an azido group ($X=N_3$) will further enhance the energetics of such compounds. This should result from the fact that this substituent can contribute ~80 Kcal/group of energy to the compound without a decrease in the O/C ratio.

Only two compounds have been reported which contain the $-C(NO_2)_2N_3$ group. The approach under investigation is the synthesis of 1,1,1-azidodinitromethyl compounds, containing various functional groups, by electrochemical techniques. The program is divided into four interrelated phases: 1) synthesis, by classical means, of the requisite reactants; 2) electroanalytical studies on the reactants; 3) exploratory electrochemical syntheses of the model compounds; and 4) synthesis of the target $-C(NO_2)_2N_3$ substituted propellant ingredients. The second and third phases tend to direct the other two. The electroanalytical studies delineate suitable electrode materials, and optimum reaction (temperature, solvent, and pH) conditions and also provide mechanistic information. The model reactions direct the selection of other possible reactants and means by which the desired products can be obtained. Model reactions also yield information about optimum concentrations of substrates, order of addition, and current density.

Electroanalytical studies on the anodic oxidation of dinitrocarbanions and the azide ion in water and acetonitrile have shown both to be electrochemically irreversible and relatively insensitive to temperature (10 to 50C) and pH (6 to 11). Voltammetry also indicates a simultaneous oxidation of the dinitro carbanions and the azide ions. This means that both radicals formed are present in the reactive layer near the electrode surface and that the product is formed by a radical-radical coupling mechanism rather than a stepwise oxidation - addition-oxidation (ECE) mechanism. Although graphite appears to be the best electrode material in an electrochemical sense, its undesirable physical and mechanical properties have led to a preferential use of platinum.

Electrochemical azidization of the model compound 1,1-dinitroethane has given 1,1,1-azidodinitroethane in 40% yield. This yield was obtained by conducting the synthesis in a divided cell with substrate concentration greater than one molar, and a current density maintained at 100 mA/cm². The results obtained from the model substrate 1,1-dinitroethane are currently being applied to other dinitro compounds containing ether, ester, and acetal functioning groups. Since the target compounds contain such groups, it is of importance to understand the effects of these groups on the desired azidization reaction.

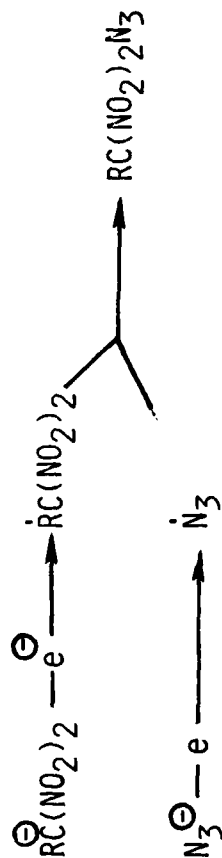
SCIENTIFIC APPROACH

- ELECTROCHEMICAL SYNTHESIS OF ENERGETIC $\text{RC}(\text{NO}_2)_2\text{N}_3$ COMPOUNDS
 - CONDUCT CYCLIC VOLTAMMETRIC STUDIES ON $\text{RC}(\text{NO}_2)_2^-$ AND N_3^- IONS
 - EXPERIMENTAL VARIABLES
 - SOLVENT
 - TEMPERATURE
 - PH
 - ELECTRODE MATERIAL
 - PERFORM ELECTROSYNTHESIS OF MODEL $\text{RC}(\text{NO}_2)_2\text{N}_3$ MATERIALS
 - OPTIMIZE
 - REACTANT CONCENTRATIONS
 - CURRENT DENSITY
 - CELL DESIGN
 - EXTEND BASIC ELECTROCHEMICAL TECHNOLOGY TO CANDIDATE PROPELLANT INGREDIENTS

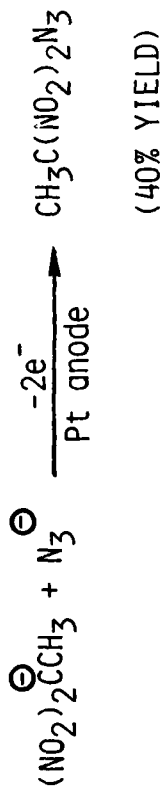
FIGURE 1

ACCOMPLISHMENTS

- ESTABLISHED IRREVERSIBILITY, AND pH/TEMPERATURE INDEPENDENCY OF ANODIC REACTIONS



- DELINEATED ELECTROCHEMICAL CONDITIONS FOR AZIDIZATION OF 1,1-DINITROETHANE



- DEMONSTRATED NON-INTERFERENCE OF VARIOUS FUNCTIONAL GROUPS ON ELECTROCHEMICAL

AZIDIZATION REACTION

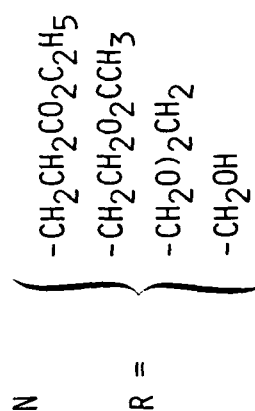


FIGURE 2

SYNTHESIS AND CHEMISTRY OF ENERGETIC METALLOTETRAAZADIENES

William C. Trogler
Department of Chemistry, D-006
University of California, San Diego
La Jolla, California 92093

The goals of our research are: 1) explore the products obtained from the reaction between organic azides and organotransition metal compounds; 2) develop new approaches to the synthesis of unsaturated (and hence energetic) metal-nitrogen ring compounds; 3) study physical, chemical and photochemical properties of the new compounds. To date there are few known organometallic compounds that contain unsaturated nitrogen ligands, and virtually nothing is known of their physical and chemical properties. Three research problems have been investigated in the last year. Our synthesis of a new ligand useful for the preparation of unsaturated metal-nitrogen ring compounds is nearly complete (Figure 1). Because the organic synthesis of unsaturated nitrogen compounds has been largely neglected since the late 1800's we have had to develop conditions for optimizing each step in Figure 1. The preparation of a series of metallotetraazadienes (Figure 2) and their chemical or electrochemical reduction to the radical anions has been completed¹. All of the radical species exhibit an isotropic epr spectrum ($g = 2.16-2.21$) in solution characteristic of cobalt centered radicals ($A^{Co} = 50-58$ Gauss). The acceptor orbital is ~50% cobalt 3d and the remainder consists of nitrogen-based $p\pi$ orbitals of the metallocyclic ring. The exploratory synthesis of early transition metal complexes has also been initiated. We have preliminary results that show $Mo(CO)_6$, $V(CO)_6$, $(\eta^5-C_5H_5)V(CO)_4$ and $(\eta^5-C_5H_5)_2V$ all react with xylal azide or methyl azide to yield intensely colored products. Characterization of these reactions will form much of the basis for next year's research.

References

- 1) Maroney, M. J.; Trogler, W. C., submitted for publication.

Figure 1: Synthesis of a New Energetic Ligand

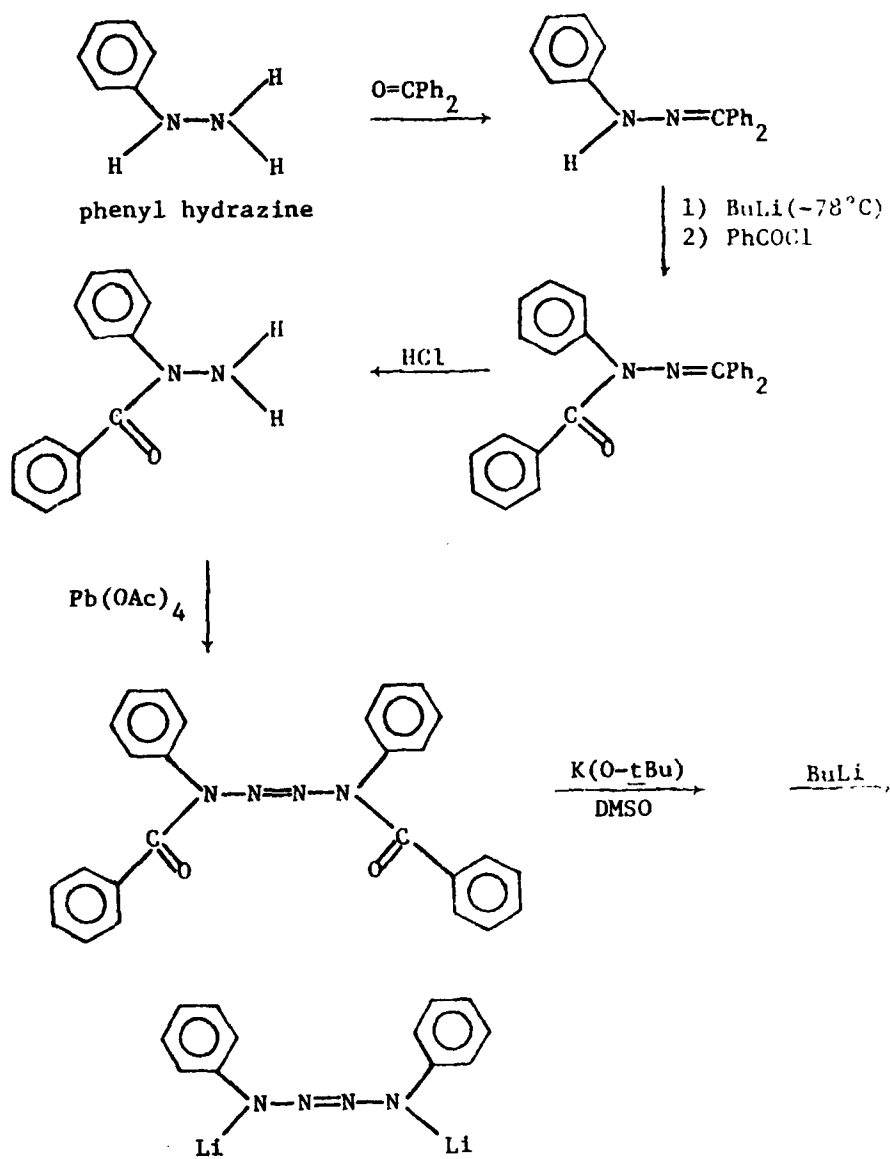
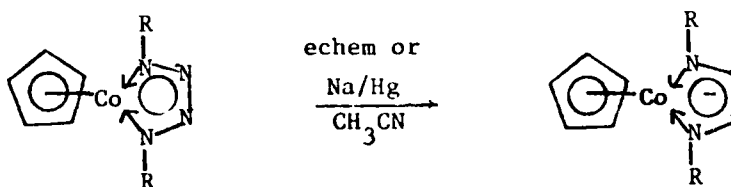
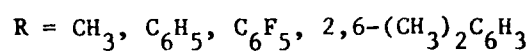
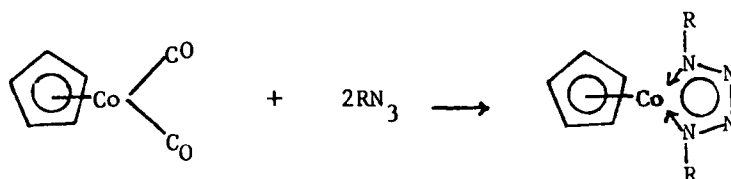


Figure 2: Preparation of Novel Metallotetraazadiene Radicals



Reduction potentials vs. NHE = $-1.53\text{v}(\text{CH}_3)$, $-1.01\text{v}(\text{C}_6\text{H}_5)$,
 $-0.71\text{v}(\text{C}_6\text{F}_5)$, $-1.31\text{v}(2,6-(\text{CH}_3)_2\text{C}_6\text{H}_3)$.

HMX COMBUSTION MODIFICATIONS

Joseph E. Flanagan, Milton B. Frankel, Dean O. Woolery

Rockwell International Corporation
Rocketdyne Division
Canoga Park, CA 91304

An understanding of the decomposition mechanisms at heating rates and temperatures similar to those experienced in actual propellants is required so that the flame chemistry can be properly altered via: 1) modification of the ingredient's molecular structure; or 2) incorporation of additives which will yield decomposition products that interact with the cyclic nitramines decomposition products.

Experimental evidence from pyrolysis decomposition studies suggests that structural symmetry of HMX derivatives must be maintained to arrive at comparable rates of C-N and N-NO₂ bond cleavage resulting in increased energy release and generation of reactive gas phase species. In addition, it has been found that structural symmetry is a key to obtaining increased melting or liquefaction temperatures.

The effort during the last year has focused upon expanding the data base for the systems which generate amidogen radicals (NH₂·) via NH₃ and the interaction of NH₂· with nitric oxide. TAGZT was the primary NH₃ source. The burning rate acceleration via TAGZT was correlated in terms of the equation

$$r = A \exp (-E/RT_f)$$

Selected experiments were carried out in which TVOPA was utilized to generate difluoroamino radicals (NF₂·) to compare the relative augmentation rates. Propellants containing TVOPA and TAGZT had higher augmentation rates than -ONO₂ plasticized systems, but the non-TAGZT containing systems burned at an equal rate for comparable flame temperature (NG vs. TVOPA). The NF₂· radicals appear to have a "catalytic" effect on the overall controlling mechanism.

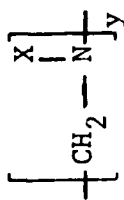
The structural modification of HMX to replace one -NO₂ group with a -CH₂N₃ group (AZMTTC) was scaled up to the 20-gram level based upon a unique reaction mechanism which employs acetyl azide. Attempts to convert AZMTTC to the corresponding amine (N₃ → NH₂) via a variety of reactions have been unsuccessful. Efforts continue in this case with the ultimate objective being the condensation of the amine with various energetic alcohols.

The bromo-precursor (BrMTTC) to AZMTTC has not been found to be especially reactive to most standard reagents. Therefore, the iodo-precursor (IMTCC) is being investigated as a potential intermediate.

Attempts to synthesize a structurally symmetrical dibromo-HMX derivative from the recently reported HMX precursor DADN were unsuccessful.

SCIENTIFIC APPROACH

CHEMISTRY



CHEMICAL
STRUCTURE
MODIFICATION
MAINTAIN SYMMETRY

a) X = CH₂N₃ (SCALED TO 20-GRAM LEVEL)

b) X = CH₂I CONDENSATION → NEW CYCLIC NITRAMINES
REACTIONS

X = NO₂

y = 4 (HMX); 3 (RDX)

COMBUSTION

HMX/RDX

+

POLYMER (INERT VS. N₃)

+

PLASTICIZER (ONO₂ VS. NF₂)

+

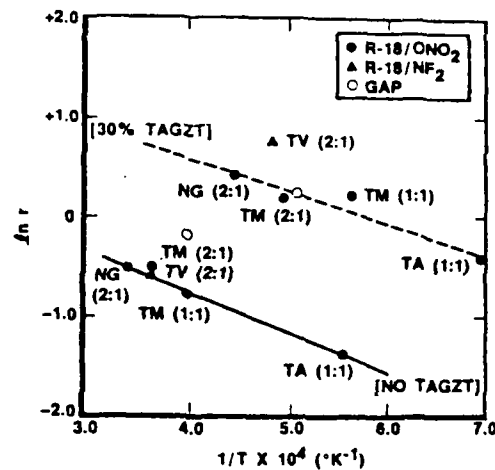
NH₂· ADDITIVE GENERATORS

RELATIVE AUGMENTATION & SUGGESTED NEW STRUCTURE

FIGURE 1.

PRIMARY ACCOMPLISHMENTS

1. CATALYTIC EFFECT OF NF_2 VS. NO



2. RDX AUGMENTED MORE READILY THAN HMX AT LOW PRESSURE DUE TO MUCH WEAKER LATTICE FORCES IN RDX VERSUS HMX, THUS ALLOWING FASTER RATE OF RDX GASIFICATION.

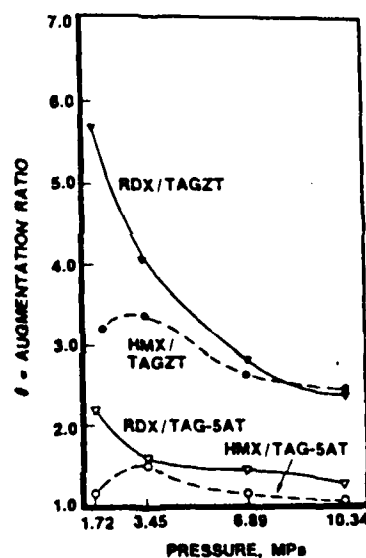


FIGURE 2.

FUNDAMENTAL STUDIES OF AZIDE DECOMPOSITION & COMBUSTION

Joseph E. Flanagan and Milton B. Frankel

Rocketdyne Division
Rockwell International
Canoga Park, CA 91304

The utilization of azide ($-N_3$) ingredients is rapidly increasing in a wide spectrum of Air Force applications. Azide materials are primarily characterized by their high, positive heats of formation, but several unique combustion features have been observed such as higher burning rates and extinguishment at pressures substantially above ambient.

This study will elucidate the decomposition and combustion characteristics of azide compounds and the interaction of the compounds with selected solid propellant ingredients. The final output from the study will be twofold:

1. Definition of the azido-chemistry, which leads to the desired end product (stop-start, higher burn rate, etc.)
2. Insight into suggested new chemical compounds (structures), which would yield the desired results and serve as a guide for future synthesis efforts

The experimental investigation will include:

1. High heating rate pyrolysis investigations at pressures ranging from atmospheric up to at least 1.38 MPa. Data analysis will be performed via mass spectrometer, gas chromatographic techniques, and isotopic labeling, to elucidate the azide-chemistry and key reactive species that control the combustion process. The following three categories of materials will be studied:
 - a. Pure azide polymers (mono and diazido types)
 - b. Azide polymers plasticized with inert or energetic materials
 - c. Solids loaded azide polymer/plasticizer systems containing oxidizers (HMX, RDX, AP, and AN)), metallic fuels, and alkali seedants.
2. Combustion investigations will be carried out in standard strand burners, windowed combustion vessels, and micromotors on each of the three categories described above to delineate:
 - a. Regions of stable combustion in both strand and micromotor conditions
 - b. Close in (less than 2 mm) flame zone characteristics (both temperature and geometry)
 - c. Fuel and seedant behavior (consumption) at the burning surface
 - d. Degree of ionization and related flow-field conductivity
3. Mechanistic descriptions of the important rate controlling and intermediate product producing reaction steps will be developed.

Sufficient data should be generated to aid the combustion modelling community in model formulation and validation.

SYNTHESIS OF DIFLUORAMINOXY-, DIFLUORAMINO- or FLUORODIAZONIUM-CONTAINING MATERIALS

Jean'ne M. Shreeve

University of Idaho
Moscow, Idaho 83843

Future rocket propulsion advances require stable high energy propellant oxidizers. The research is concerned with the synthesis of stable, highly oxidizing compounds which contain nitrogen-fluorine bonds, such as difluoraminoxy, difluoramino, or fluorodiazonium groups and the subsequent investigation of their physical and chemical properties.

Several routes to these compound types are currently under investigation or will be attempted during the next several months.

(a) The Lewis acid catalyzed introduction of $-\text{ONF}_2$ into F-olefins and functionalized F-olefins via reactions of NF_3O .

(b) Photolysis or thermolysis of N_2F_4 with hypofluorites and/or hypochlorites to form mono or bis $-\text{ONF}_2$ compounds, R_fONF_2 or $\text{R}_f\text{CF}(\text{ONF}_2)_2$.

(c) Mixed $-\text{ONF}_2$ and $-\text{NF}_2$ compounds via F-acyl fluorides and HNF_2 .

(d) Deoxygenation of N-fluoroazoxy compounds to fluorodiazonium compounds, $\text{R}_f\text{N}=\text{NF}$.

(e) Synthesis of $\text{R}_f\text{N}=\text{NR}$ compounds where R is a good leaving group which can be displaced by fluorine.

New compounds containing the N,N-difluorohydroxylamino group have been prepared by the addition of NF_3O to olefins in the presence of catalytic amounts of a Lewis acid. The new compounds R_fONF_2 ($\text{R}_f = \text{CF}(\text{CF}_3)\text{C}_5\text{F}_{11}^n$, $-\text{CF}(\text{CF}_3)\text{C}(\text{O})\text{F}$, $\text{CF}(\text{CF}_3)\text{SF}_5$, $-\text{CF}(\text{CF}_3)\text{CF}_2\text{OCF}_2\text{CF}(\text{SO}_2\text{F})\text{CF}_3$, $-\text{CF}(\text{CF}_3)\text{CF}_2\text{OCF}_2\text{OCF}_2\text{CF}(\text{CF}_3)\text{CF}_2\text{CF}(\text{CF}_3)$, $-\text{CF}_2\text{CF}_2\text{OCF}_2\text{F}$, $\text{CF}_2\text{CF}_2\text{OCF}_2\text{CF}(\text{CF}_3)\text{OC}_3\text{F}_7^n$) were obtained and characterized. The Markownikov addition products may be explained by a simple electrophilic addition of NF_2O^+ to the polar double bond, followed by fluorination of the terminal carbonium ion. The anti-Markownikov products arise from NF_2O^+ addition to the tautomeric form of the olefin ($\text{F}_2\text{C}=\text{CF}=\text{OR}_f$) in which the normal polarity of the double bond has been reversed.

Hexafluorocyclobutene and octafluorocyclopentene were reacted with nitrosyl chloride or nitrogen dioxide in the presence of KF in acetonitrile to give 80% yields of the blue heptafluoronitrosocyclobutane(I) and nonafluoronitrosocyclopentane (II), respectively. Thermal decomposition of (I) and (II) in Pyrex glass resulted in the analogous nitro compounds, $\text{CF}_2\text{CF}_2\text{CF}_2\text{CFNO}_2$ and $\text{CF}_2\text{CF}_2\text{CF}_2\text{CF}_2\text{CFNO}_2$. Cycloaddition reactions of (I) and (II) with tetrafluoroethene gave the oxazetidines, $\text{CF}_2\text{CF}_2\text{CF}_2\text{CFNOCF}_2\text{CF}_2$ and $\text{CF}_2\text{CF}_2\text{CF}_2\text{CF}_2\text{CFNOCF}_2\text{CF}_2$, and with 1,3-hexafluorobutadiene, formed the oxazines, $\text{CF}_2\text{CF}_2\text{CF}_2\text{CFNOCF}_2\text{CF}=\text{CFCF}_2$ and $\text{CF}_2\text{CF}_2\text{CF}_2\text{CF}_2\text{CFNOCF}_2\text{CF}=\text{CFCF}_2$. With tetrafluorohydrazine in metal reaction vessels, either (I) and (II) or the cycloolefins gave difluoroamines, $\text{CF}_2\text{CF}_2\text{CF}_2\text{CFNF}_2$ and $\text{CF}_2\text{CF}_2\text{CF}_2\text{CF}_2\text{CFNF}_2$. However, in the presence of Pyrex glass, N-heptafluorocyclobutyl-N'-fluorodiimide N-oxide and N-nonafluorocyclopentyl-N'-fluorodiimide N-oxide ($\text{R}_f\text{N}(\text{O})=\text{NF}$) resulted from heating (I) and (II) with N_2F_4 .

STABLE HIGH ENERGY PROPELLANT OXIDIZERS
NEW NITROGEN-FLUORINE-CONTAINING COMPOUNDS

PROPERTIES

STABLE TO HEAT, SHOCK, MOISTURE
OXIDIZING

ROUTES

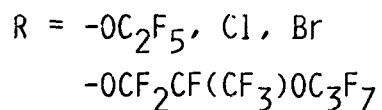
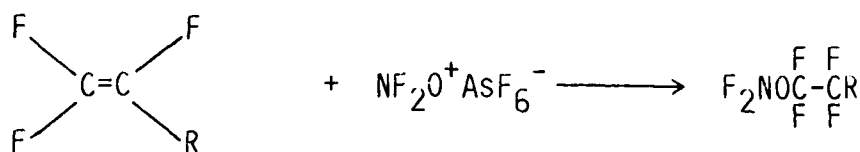
LEWIS ACID CATALYZED ADDITIONS
OF NF_3O TO OLEFINS

IN SITU GENERATION OF AN
ACTIVE FLUORINATING REAGENT

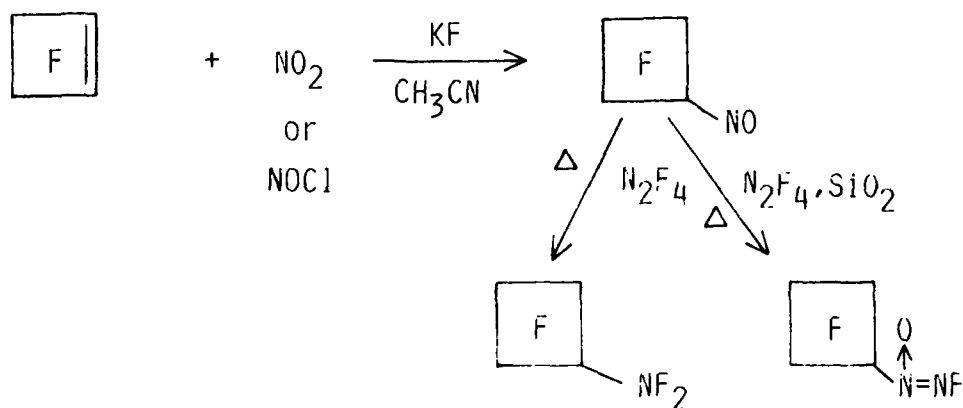
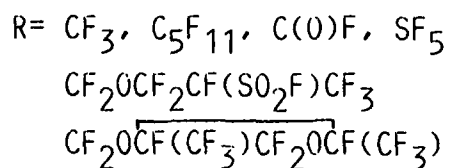
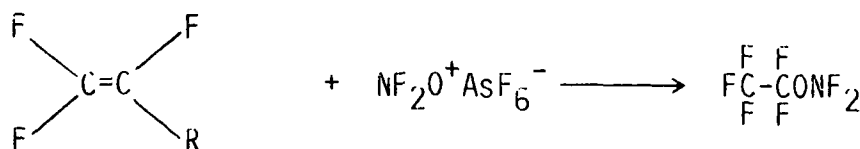
TETRAHYDRAZINE REACTIONS IN THE
PRESENCE OF SILICA

ACCOMPLISHMENTS

ANTIMARKOWNIKOV ADDITION



MARKOWNIKOV ADDITION



SYNTHESIS AND CHEMISTRY OF POLYNITROALKANES
AND POLYNITROOLEFINS

Clifford D. Bedford and Robert J. Schmitt

SRI International
333 Ravenswood Avenue
Menlo Park, CA 94025

Research programs in energetic materials synthesis and mechanisms have been hampered by the lack of general methods for synthesizing aliphatic polynitro compounds and geminal dinitroalkenes. Efforts to identify and overcome these research barriers have thus far been directed toward special situations and have met with only limited success.

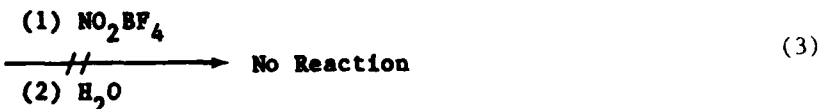
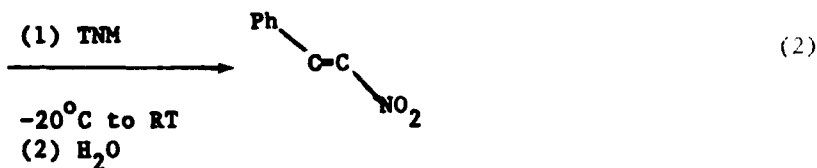
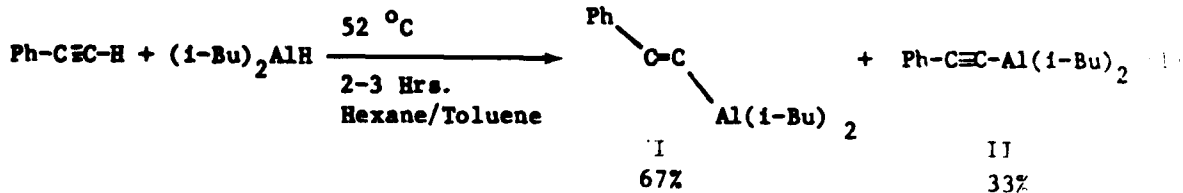
The objective of this research program is to provide a better understanding of the chemistry of polynitro and fluoronitro compounds and to lead to the design of new classes of energetic materials having the desired properties for propellant and explosives applications. Basic questions concerning the nature of specific molecular requirements and reaction conditions giving to mild nitration organic materials will be answered through the development and understanding of these new energetic unsaturated intermediates and nitration techniques.

During the first six months of this contract we have been concerned with developing new synthesis methods for preparing gem-dinitroolefins and gem-dinitroalkanes. In line with this objective, a new nitrodealumination reaction was developed for the preparation of nitroolefins. This novel reaction will lead into the more extensive area of nitrodealumination reactions.

Work to date is summarized below:

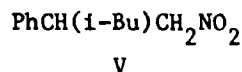
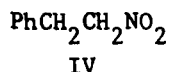
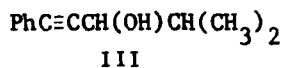
- We demonstrated the first example of a nitroolefin preparation by a nitrodealumination reaction.
- New synthesis of nitroolefins were developed using the olefin-aluminate complex in the nitrodealumination reaction.
- Electrochemical reduction of bromoalkanes in the presence of N_2O_4 leads to the alkane instead of the nitroalkane.

The vinylaluminum intermediate was prepared via a known procedure. The mixture of I and II is then treated with tetranitromethane (TNM) [equations (2) and (3)].

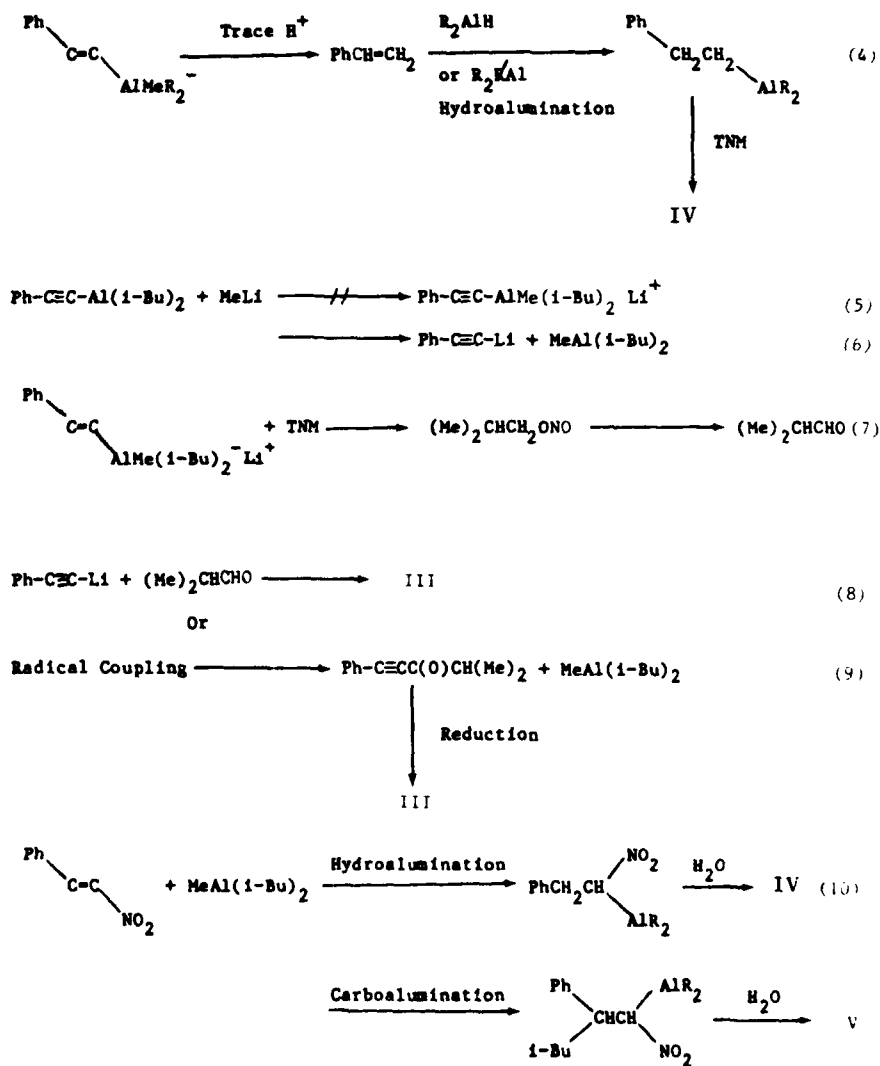


NMR and mass spectral analyses of partially purified reaction mixtures indicated the possible presence of various cross-coupled (phenyl and isobutyl groups in the same molecule) compounds containing nitro, oxime, hydroxyl, and/or carbonyl groups. Efforts are underway to characterize these interesting and unusual product mixtures. No β -nitrostyrene was evident in the product mixture resulting from the reaction with NO_2BF_4 .

Preparative gas chromatography of the vinyl aluminate salt reaction mixture afforded adequate separation of several reaction products. Combined analyses of mass spectral, IR, and NMR data of the volatile reaction products have enabled us to characterize the following compounds in addition to β -nitrostyrene:



Hypothetical mechanisms for the formation of these products are indicated in Scheme I.



SCHEME I

MODIFICATION OF PROPELLANT BINDER NETWORK
FOR IMPROVEMENT OF MECHANICAL PROPERTIES

AFRPL Contract F-4611-83-C0001

C. Sue Youn Kim
California State University, Sacramento

One of the disadvantages of energetic prepolymers such as glycidylazidopolymers (GAP) or polydinitropropyl acrylates (PDNPA) is that the fraction of the polymer chains bearing the load applied to the binder network is far less than that of conventional prepolymers such as polyethylene glycols (PEG). For example, only 40 weight % of GAP will participate in the strength and strain capabilities during deformation in contrast to 91 weight % of PEG. Hence, these energetic prepolymers usually give poorer mechanical properties than PEG when formulated into elastomeric networks.

The objective of our project was to evaluate potential improvements in the stress/strain behavior of energetic propellant binders by bimodal network formation; i.e. by blending these energetic short chains with long chain prepolymers prior to cure into rubbers. The extent of improvements of the ultimate properties were examined in terms of the chemical type, the length and the relative amount of the long chain polymers present, and also of the viscoelastic properties. The program objective and the results are summarized in Figure 1.

The extent of improvement appears to be strongly dependent on the chemical type of polymer systems. The PEG/PEG system shows negligible improvement in comparison with PDNPA/PEG systems. For example, both PEG 600/PEG 8000 and PEG 1000/PEG 8000 show little improvement at 30 weight percent PEG 8000, whereas PDNPA(M-13)/PEG 8000 and GAP/PEG 8000 systems with short chain lengths comparable to those of short chain PEG, show two- to threefold increase in strain (Figure 2). Analysis of data indicates that the differences of improvement of these systems appear to be mainly due to the degree of nonaffine deformation (lack of extension of short chains is compensated by the neighboring long chains), rather than due to the long chains acting as inhibitor of the growth of rupture nuclei. A more flexible crosslinker would allow more extensive nonaffine deformation at a given strain rate and thus further improve the ultimate properties.

Other effects such as strain induced crystallization, filler content, and strain rate are also being investigated.

Figure 1: OBJECTIVE AND RESULTS OF THE PROGRAM

Objective: Improvement of mechanical properties of propellant binder through analysis of bimodal and multimodal elastomeric network concept.

Results:

- I. GAP/PEG 8000 bimodal binder networks give significantly improved mechanical properties over monomodal GAP.
- II. PDNPA/PEG 8000 and R-45M/HTPB systems also show significant improvements.
- III. PEG/PEG bimodal systems show no advantage.
- IV. All the bimodal systems give results which are consistent with "weakest link" theory.
- V. Unfilled bimodal systems show appreciable improvements in both stress and strain properties over short chain monomodal system. As filler content increases, the favorable effect on stress tends to diminish while that on strain is retained.

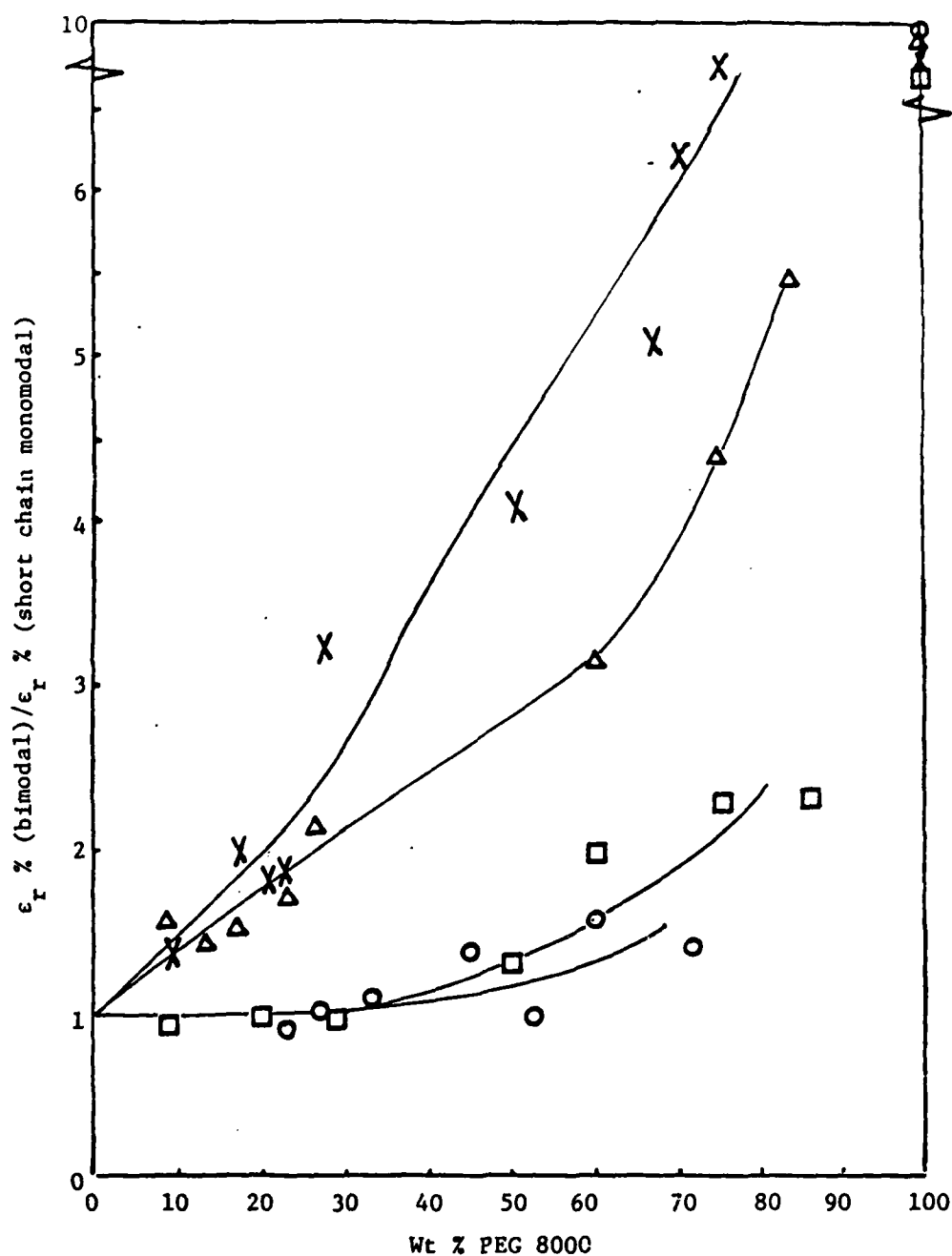


Figure 2 . Improvement of Ultimate Strain Properties of Various Polymer/PEG 8000 Bimodal Systems vs Wt % PEG 8000 at 66°C; Strain Rate 4.2×10^{-4} m/s; ○ PEG 600 (40 sk. atoms), □ PEG 1000 (70 sk. atoms), △ GAP (70 sk. atoms), × PDNPA (50 sk. atoms)

INITIAL THERMOCHEMICAL DECOMPOSITION MECHANISMS
OF ENERGETIC INGREDIENTS: DEUTERIUM ISOTOPE EFFECTS AND
ISOTHERMAL REACTION STUDIES

Scott A. Shackelford, Michael B. Coolidge,
Stephen L. Rodgers, Berge B. Goshgarian

Air Force Rocket Propulsion Laboratory
Edwards AFB, CA 93523

The thermochemical decomposition mechanism and kinetics of selected energetic ingredients are being investigated. Special attention is being given to the very early stages of the thermochemical decomposition reactions since earlier investigations with TNT revealed that key chemical steps can occur prior to detectable exothermic activity. We are using deuterium isotope effects in conjunction with isothermal thermochemical analyses to identify *in-situ* and in real time, the key chemical mechanisms and associated bond ruptures which control complex thermochemical decomposition and deflagration processes. Three tasks comprise this effort, and two are in progress.

Task 1 The thermochemical decomposition mechanism and kinetics of HMX and HMX-d₈ were investigated collaboratively with R.N. Rogers, J.L. Janney, and M.H. Ebinger of the Los Alamos National Laboratory. Isothermal DSC (IDSC) investigations were conducted 2-7°C below the melting point of HMX (553-548°C), and three distinct physical states resulted during the overall decomposition: a solid, a mixed melt, and a liquid phase. Three different deuterium isotope effects (DIE) were found depending upon which physical state predominated during decomposition. The solid phase produced a primary DIE indicating that C-H bond rupture was the rate-limiting step; the mixed melt phase produced an apparent inverse isotope effect indicating that C-H bond contractions occur as the intermolecular hydrogen bond forces are overcome during the initial melting process; and, the liquified stage afforded a value consistent with a secondary DIE caused by rate-controlling C-N bond ring rupture. While slow thermochemical decomposition in an IDSC cell produced three DIE results, isothermal pyroprobe deflagration at similar temperatures produced only a primary DIE; but, very highly confined time to explosion (Henkin) tests provided evidence that an inverse DIE operates in this thermal explosion. Preliminary evidence suggests that the rate-determining reactions in thermochemical HMX responses may depend upon the predominant physical state that results from a given type of thermochemical event (i.e., slow decomposition, pyrolysis, thermal explosion). Similar investigations will be conducted with RDX/RDX-d₆ and DNNC/DNNC-2, d₄, d₆ compounds.

Task 2 Isothermal DSC (IDSC) investigations of deuterated liquid TNT, HNBB, and HNS are being investigated to determine systematic relationships between ingredient chemical structure and thermochemical decomposition mechanisms. Earlier IDSC/deuterium isotope effect investigations at another AF laboratory (FJSRL) revealed the thermochemical decomposition of TNT and its "dimeric" analogue (HNBB) both are controlled by C-H bond rupture. HNS is an unsaturated analogue of HNBB and is significantly more thermally stable; but, its decomposition mechanism is unknown. A mechanistic elucidation with HNS should reveal how its vinyl C-H bond structure improves thermochemical stability. By employing a newly reported synthesis procedure, we successfully synthesized the deuterated HNS (HNS-d₂) needed for this study; HNS-d₂ previously was an unknown compound.

Task 3 Investigations to use elucidated thermochemical decomposition mechanisms in the modification of thermochemical rate processes are scheduled for a later start.

These three tasks address the problem of systematic thermochemical properties control via either initial molecular structural design and/or chemical additive modification of the inherent thermochemical decomposition mechanisms.

APPROACH

INITIAL THERMOCHEMICAL DECOMPOSITION MECHANISM/KINETICS ELUCIDATION → • RATE-CONTROLLING STEP

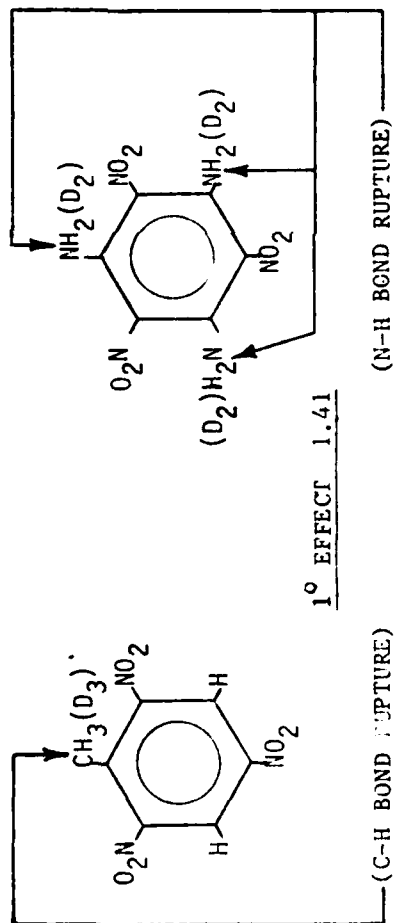
- STRUCTURE/MECHANISM RELATIONSHIPS
- RATE/MECHANISM MODIFICATION

• DEUTERIUM ISOTOPE EFFECTS (DIE) IN ISOTHERMAL DECOMPOSITION REACTIONS

- DIE is ratio between unlabeled (H) and deuterated (D) compounds

(1) Reaction Rates k_H/k_D (2) Induction Times t_D/t_H

- DIE Types (confirmed and possible)

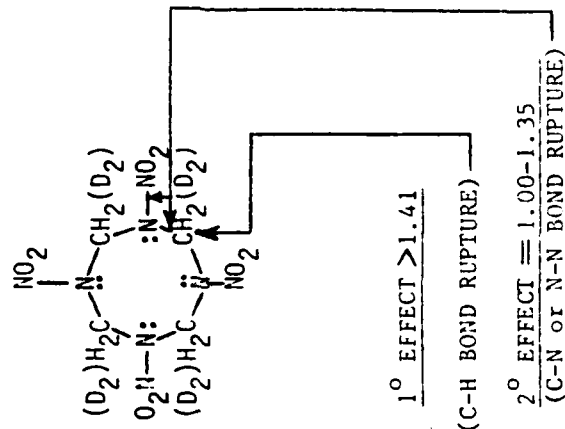


TNT

S.A. SHACKLEFORD, J.W. BOEHMANN
AND J.S. WILKES, J. ORG. CHEM.,
42, 4291 (1977)

TATB

R.N. ROGERS, J.L. JANNEY,
AND M.H. EISINGER
THE PROCHIM. ACID., 79, 207 (1980)



INVERSE EFFECT < 1.00 (C-H BOND CONTRACTION)

HNX

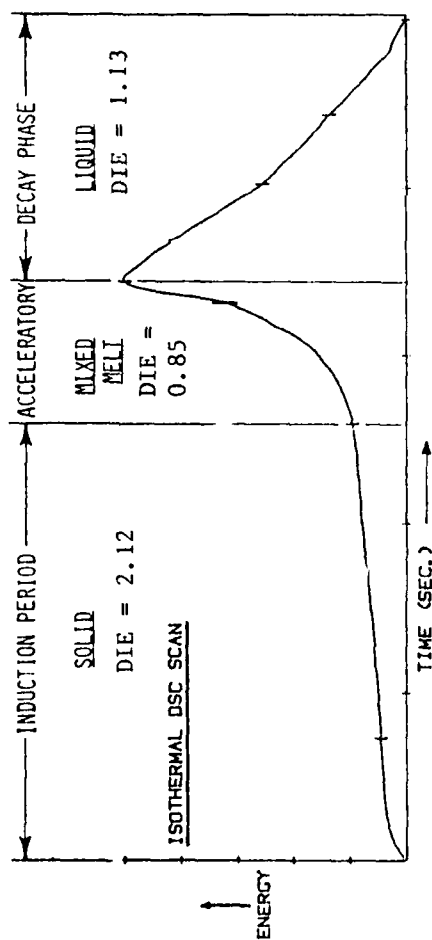
COMPLETED

(AFRPL 5-1-1977)

RESULTS

TASK 1: MECHANISM/KINETICS ELUCIDATION

- DEUTERIUM ISOTOPE EFFECTS (DIE) IN ISOTHERMAL DSC SPECTRA OF HNX & HNX-d₈

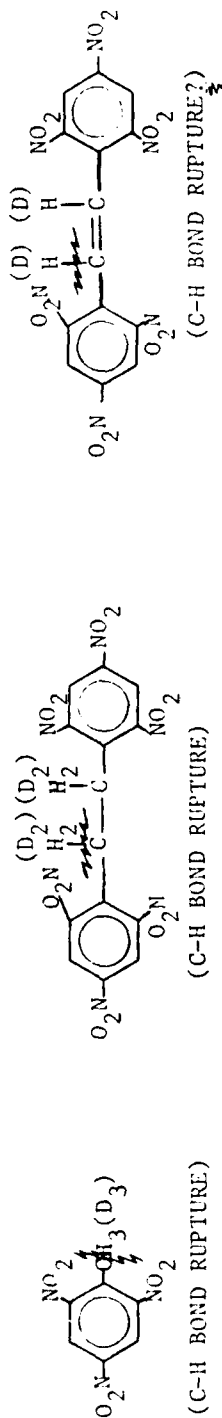


RATE-CONTROLLING PROCESSES

- SOLID PHASE: C-H bond rupture
MIXED MELT: C-H bond contraction occurs
LIQUID PHASE: C-N ring bond cleavage

- Rate-controlling decomposition process determined by predominant physical state present under a given type of thermochemical event and its conditions.

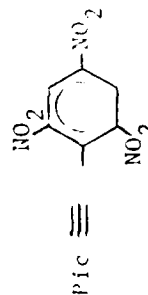
TASK 2: MOLECULAR STRUCTURE/DECOMPOSITION MECHANISM RELATIONSHIPS



SHACKLEFORD, BECKMANN, WILKES
J. ORG. CHEM., 42, 4201 (1977)
GUNZIGER, FJSRL-TM-78-1 (1978)



- HNS-d₂ HAS BEEN SYNTHESIZED:



NEW SYNTHETIC TECHNIQUES

FOR ADVANCED PROPELLANT INGREDIENTS:

SELECTIVE TRANSFORMATIONS AND NEW STRUCTURES

Scott A. Shackelford, Robert D. Chapman,
Stephen P. Herrlinger, John L. Andreshak

Air Force Rocket Propulsion Laboratory
Edwards AFB, CA 93523

New chemical transformations and methods are being investigated which potentially lead to energetic target compounds with new and novel molecular structures, or which improve synthetic routes to known compounds that are currently expensive propellant luxuries. Three of four scheduled research tasks are in progress.

Task 1 Nucleophilic substitutions of alkyl bromides with silver triflate were conducted to form precursor triflate ester compounds for conversion into key energetic ingredients. Triflate ester intermediates provide a facile and selective pathway to energetic compounds not available by direct synthetic routes. The scope and limitations of this triflate ester synthesis have not been investigated systematically, especially with dihaloalkanes. The α,ω -dibromoalkanes react much more rapidly with silver triflate than do corresponding monobromoalkanes, and unlike the monobromides, dibromoalkanes resist unwanted isomerization to 2° triflate products in CCl_4 solvent. The behavior of this is explained by an $\text{S}_{\text{N}}1$ -type reaction where intramolecular ^4Br anchimeric assistance occurs in bromoalkyl monotriflate product formation, followed by intramolecular anchimeric stabilization by the triflate group during alkyl ditriflate product formation. There is also a greater tendency to form the ditriflate product as chain length increases in the α,ω -dibromoalkanes up through 1,5-dibromopentane where this effect plateaus. Higher reaction temperatures render the intermediate triflate product unstable; decomposition with polymerization then occurs in CCl_4 solvent and aromatic alkylation results in benzene solvent.

Task 2 The reaction of alkenes, alkyl carbonyls, or organometallic compounds with energetic triflate esters could permit selective, direct syntheses of energetic alkanes or alkenes in which an overall anti-Markovnikov introduction of energetic groups is desired. Preliminary reactions between fluorodinitroethyl triflate and carbonyl compounds imply low-yield formation of energetic α,β -unsaturated ethers. Reaction between nitronium triflate and organolithium compounds showed preliminary promise as a selective non-acidic nitration technique.

Task 3 Collaborative AFIRPL/Pt Loma College (D. F. Shellhamer) studies are being conducted with alkene methoxyfluorination reactions using methanolic XeF_2 suspensions. Elucidation of this mechanism could permit an exclusive regioselective control which produces the anti-Markovnikov ether adduct. Substitution of energetic alcohols for methanol could directly produce stable, partially fluorinated energetic ethers rather than undesirable acetal-type products. Reactions with norbornene produced different fluoromethoxynorbornane isomers identified as those where the methoxy moiety exclusively added first when catalyzed by BF_3 . New isomers occurred with HF catalysis in which the F atom added first. This is consistent with our initially proposed reaction mechanism in which effecting methoxy addition first produces the desired anti-Markownikoff product. Future studies will be conducted with the energetic fluorodinitroethanol substrate.

Task IV The potential syntheses and characterization of energetic borazine compounds is scheduled for a later start.

We are addressing the necessary elements for an effective synthesis effort: (a) novel transformations, (b) improved synthetic routes, and (c) new target compound classes.

APPROACH

Task I: Reactions of triflate salts (selective intermediate syntheses)

- $\text{RCH}_2\text{Br} + \text{AgOTf} \xrightarrow{-\text{AgBr}} \text{RCH}_2\text{OTf}$
- $\text{CH}_2=\text{C}(\text{Br})\text{R} + \text{AgOTf} \xrightarrow{-\text{AgBr}} \text{CH}_2=\text{C}(\text{OTf})\text{R}$
then conversion: $\text{RCH}_2\text{OTf} + \text{EngOH} \longrightarrow \text{RCH}_2\text{OEng}$ (Eng = energetic substituent, e.g., polynitroalkyl)

Task II: Reactions of triflate esters (including nitronium triflate)

- $\text{CH}_3\text{C}(=\text{O})\text{CH}_2\text{R} \text{ or } \text{CH}_3\text{C}(\text{O})\text{CH}_2\text{R} \xrightarrow{\text{EngO}^+\text{OTf}^-} \text{CH}_3\text{C}(\text{O})\text{CH}(\text{OTf})\text{R} \xrightarrow{\text{EngO}^+\text{OTf}^-} \text{CH}_3\text{C}(\text{O})\text{CH}(\text{Eng})\text{R}$
- $\text{M}^+\text{R}^- + \text{NO}_2^+\text{OTf}^- \xrightarrow{-\text{M}^+\text{OTf}^-} \text{NO}_2\text{R}$ (selective, non-acidic nitration)

R = alkyl, alkenyl

Task III: Selective xenon difluoride fluorination

- $\text{CH}_3\text{C}(=\text{O})\text{CH}_2\text{R} \text{ or } \text{CH}_3\text{C}(\text{O})\text{CH}_2\text{R} + \text{XeF}_2 \longrightarrow \text{CH}_3\text{C}(=\text{O})\text{CH}(\text{F})\text{R} \text{ or } \text{CH}_3\text{C}(\text{F})_2\text{CH}_2\text{R}$
- Chemical catalysis \longrightarrow ionic reaction mechanism } different fluoride products
 Light initiation \longrightarrow radical reaction mechanism }
 • $\text{ROCH}=\text{CH}_2 + \text{XeF}_2 \xrightarrow{\text{EngOH}} \text{ROCH}(\text{F})\text{CH}_2\text{OEng} + \text{ROCH}(\text{F})\text{CH}_2\text{F}$
 $\text{--OEng 1st addition} \quad \text{--F 1st addition}$

RESULTS

Task I

- $$\text{Br}(\text{CH}_2)_4\text{H} + \text{AgOTf} \xrightarrow[\text{CCl}_4 \text{ (RT)}]{t_{1/2} = 78 \text{ h}} \text{TfO}(\text{CH}_2)_4\text{H} + \text{CH}_3\text{CH}(\text{OTf})\text{CH}_2\text{H}$$

(rearrangement)
- $$\text{Br}(\text{CH}_2)_4\text{Br} + \text{AgOTf} \xrightarrow[\text{CCl}_4 \text{ (RT)}]{t_{1/2} < 2 \text{ h}} \text{TfO}(\text{CH}_2)_4\text{Br} \xrightarrow[\text{AgOTf/CCl}_4]{t_{1/2} = 274 \text{ h}} \text{TfO}(\text{CH}_2)_4\text{OTf}$$

(no rearrangement)
- $$\text{Br}(\text{CH}_2)_n\text{Br} + \text{AgOTf} \longrightarrow \text{TfO}(\text{CH}_2)_n\text{Br} + \text{TfO}(\text{CH}_2)_n\text{OTf}$$

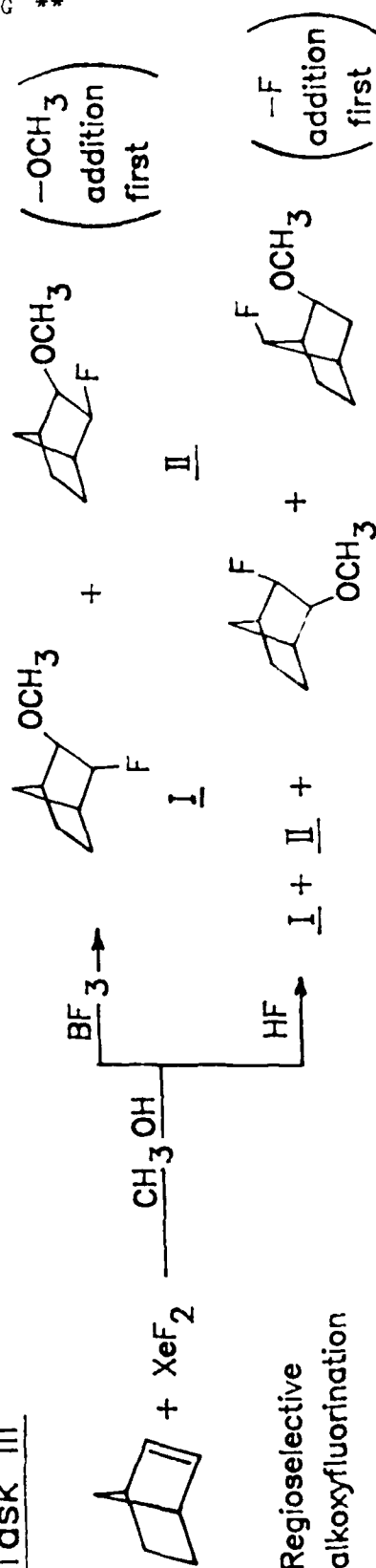
$\frac{1}{2}$ $\frac{2}{2}$ $[1]/[2] \downarrow$ as $n \uparrow$

Task II (Preliminary)

- $$\text{CH}_3\text{C}(\text{O})\text{C}(\text{O})\text{CH}_3 + \text{CF}(\text{NO}_2)_2\text{CH}_2\text{OTf} \xrightarrow[\text{Bu}_4\text{PV}]{(\text{FDNE})\text{O} \text{ O}(\text{FDNE})} \text{CH}_2=\text{C}(\text{C}(\text{O})\text{CH}_3)_2 \quad (?)$$

- $$\text{NO}_2^+\text{OTf}^- + n\text{-BuLi} \xrightarrow[\text{(xs)}]{\text{hexane}} \left[\text{C}_3\text{H}_7\text{C}(\text{NO}_2) \right]^- \text{Li}^+$$

Task III



MECHANISTIC COMBUSTION INTERACTIONS OF
ISOTOPICALLY LABELED PROPELLANT INGREDIENTS

Scott A. Shackelford

Air Force Rocket Propulsion Laboratory
Edwards AFB, CA 93523

We are elucidating in-situ and in real time the key fundamental chemical reaction mechanisms and ingredient interactions which control the global combustion process. Isotopically labeled propellant ingredients are being used to detect potential deuterium isotope effects and to determine the randomness of isotopic scrambling experienced during combustion. These approaches should provide the mechanistic chemical reaction data needed to address current technological barriers in nitramine burn-rate limitations, and scientific propellant performance tailorability. Early investigations are being conducted in a pressurized window bomb with pure pressed pellet ingredients. Mixed strand burn formulations and later micromotor firings will follow to elucidate fundamental chemical reaction mechanisms and ingredient interactions under the ballistic, pressure, and temperature conditions encountered in a rocket combustor. Two of three tasks are in progress.

Task 1 integrates the deuterium isotope effect concept directly to the combustion process. In a collaborative venture with Thiokol (D. A. Flanigan and R. E. Askins) and LANL (R. N. Rogers), HMX and HMX-d₈ pressed pellet burn rates were determined in a pressurized window bomb. Burn rate comparison of identically synthesized HMX and HMX-d₈ samples revealed a primary deuterium isotope effect at 500 and 1000 psai pressures. This strongly suggests, under these static combustion conditions, that C-H bond rupture during solid state thermochemical decomposition ultimately controls the burn rate of HMX. By applying deuterium isotope effects to the actual combustion processes, we also provided the combustion research community a new in-situ scientific method for investigating flame reaction mechanisms. Further window bomb pressed pellet experiments will be conducted with deuterium and non-deuterium labeled RDX and DNNC samples.

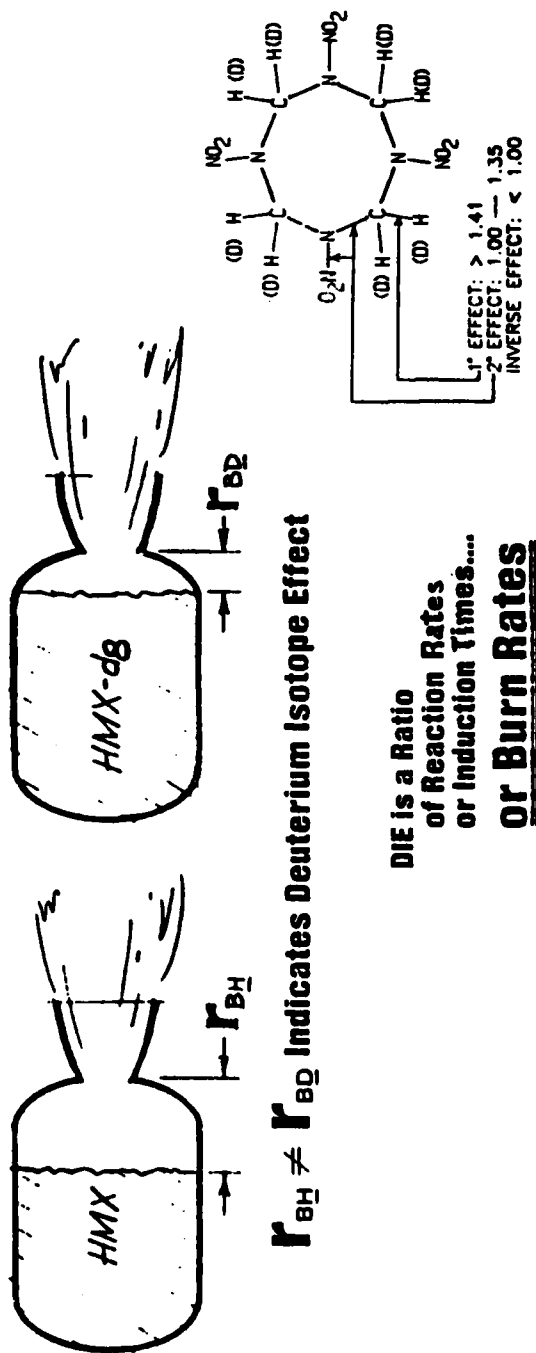
Task 2 addresses intramolecular diffusion in a rocket combustor. Individual propellant ingredients appropriately labeled with ¹³C, ¹⁵N, and/or ¹⁸O will be fired in a rocket micromotor, and the kinetically frozen products will be collected for analysis. The degree of randomness found in scrambled isotopic product labels compared to that expected if complete thermodynamic equilibrium were achieved prior to nozzle kinetic freeze out will reveal the amount of intramolecular diffusion or thermodynamic versus kinetic control exhibited by a given ingredient. HMX, RDX, and DNNC will be studied.

Task 3 will study ingredient - ingredient chemical interaction and diffusion control in mixed ingredients and formulated propellants. Initially, window bomb strand burns with mixed ingredients will be studied in which only one ingredient is deuterium labeled, and burn rates will be analyzed to detect any change in key rate-controlling processes from pure ingredients. Micromotor firings will follow with ¹³C, ¹⁵N, or ¹⁸O labeled ingredients, and collected combustion products will be analyzed. The degree of random isotopic product scrambling will be compared to that expected if a complete ingredient-ingredient equilibration is established prior to nozzle kinetic freeze-out. Bi-ingredient formulations will be built one ingredient at a time until formulated propellant samples are fired. We are initiating stand burn experiments this year with HMX and HMX-d₈ sample mixtures.

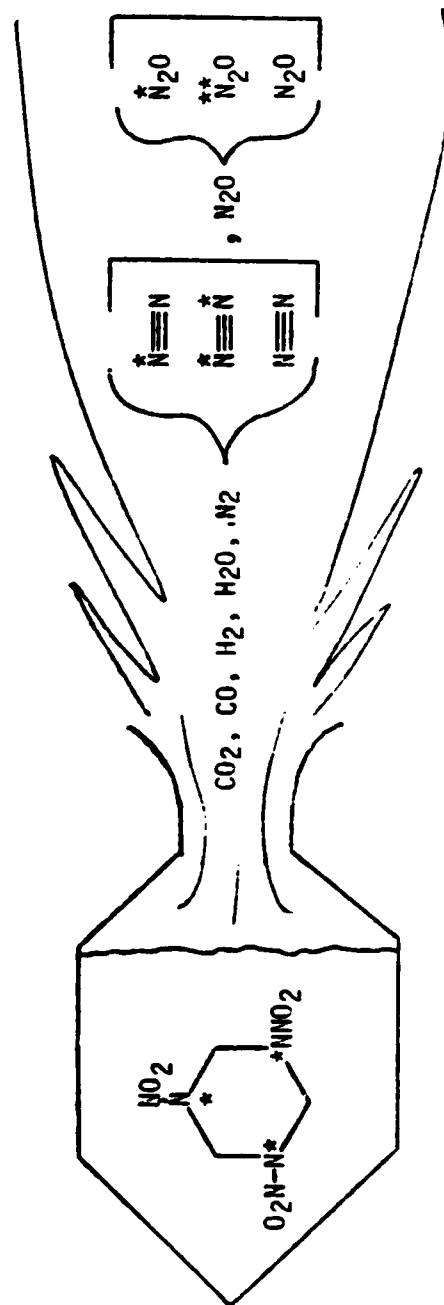
These three tasks address a mechanistic need to (a) identify rate-limiting molecular bond ruptures, (b) determine the degree of molecular kinetic vs. thermodynamic control, and (c) measure the amount of ingredient-ingredient diffusion encountered in propellant combustion.

APPROACH

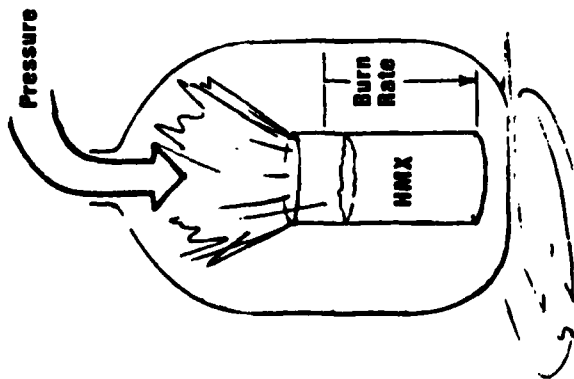
- DEUTERIUM ISOTOPE EFFECTS (DIE) TO IDENTIFY RATE-CONTROLLING BOND RUPTURE



- ISOTOPIC SCRAMBLING RANDOMNESS IN CHEMICAL COMBUSTION MECHANISMS



• DEUTERIUM ISOTOPE EFFECTS (DIE) IN CHEMICAL COMBUSTION MECHANISMS - RESULTS



WINDM BOMB EXPERIMENTAL RESULTS
WITH HMX PRESSED PELLETS

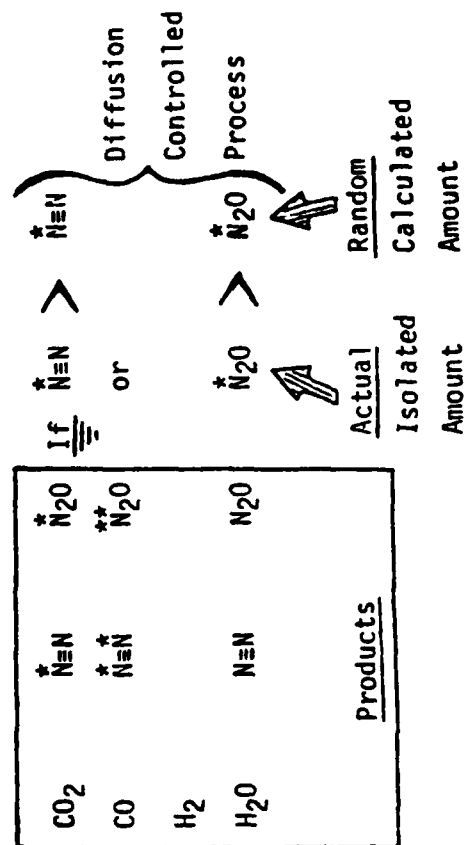
500 PSAL : $\frac{R_{H1}}{R_{HD}} = 1.34 - 1.44$
 1000 PSAL : $\frac{R_{H1}}{R_{HD}} = 1.41 - 1.61$

RATE-CONTROLLING PROCESSES

SOLID PHASE: C-H bond rupture
MIXED MELT: C-H bond contraction occurs
LIQUID PHASE: C-N ring bond cleavage

- 1° DEUTERIUM ISOTOPE EFFECT OPERATES
 - SOLID STATE C-H BOND RUPTURE
- CONTROLS COMBUSTION PROCESS

• ISOTOPIC SCRAMBLING RANDOMNESS TO DETERMINE INTRA - & INTERMOLECULAR DIFFUSION - POTENTIAL RESULT.



NEW ENERGETIC POLYMER SYNTHESIS

AND BINDER CONCEPTS

Stanley D. Morse

University of Dayton Research Institute
Dayton, OH

New polymeric syntheses and chain modification techniques are being investigated to obtain improved mechanical properties of known energetic binders, new energetic prepolymer and binder systems, and correlations of polymeric chemical structure to physical/mechanical properties. Its approach centers on new energetic polymer syntheses via cationic polymerization or by synthetic modifications of known polymers. Two tasks are active.

Task 1 seeks to improve the physical and mechanical properties of known energetic polyether polymers derived from glycidyl-substituted monomers. The modified copolymerization technique, successfully demonstrated with the PECH polymer in this project's predecessor work unit and completed during the initial stages of this work unit (J. Polym. Sci. - in press) will be used with GAP, PGN, and poly-G polymer systems to maximize stress, strain, and modulus properties. Epibromohydrin polymerizations were conducted to assess the PEBH modified polymer as a viable precursor for the aforementioned energetic binder materials; limited success resulted.

Task 2 will seek to obtain a hydroxy-terminated poly-dinitropropyl vinyl ether polymer suitable for propellant urethane curing procedures. The dinitropropyl vinyl ether monomer is obtained in a high-yield one-step synthesis and has successfully been polymerized into an energetic non-hydroxyterminated binder for pressed HMX explosive fills. Its inherent superior thermochemical stability, coupled with its excellent hydrolytic stability and chemical compatibility at elevated temperatures with HMX, makes it a very attractive energetic binder candidate for minimum smoke propellants.

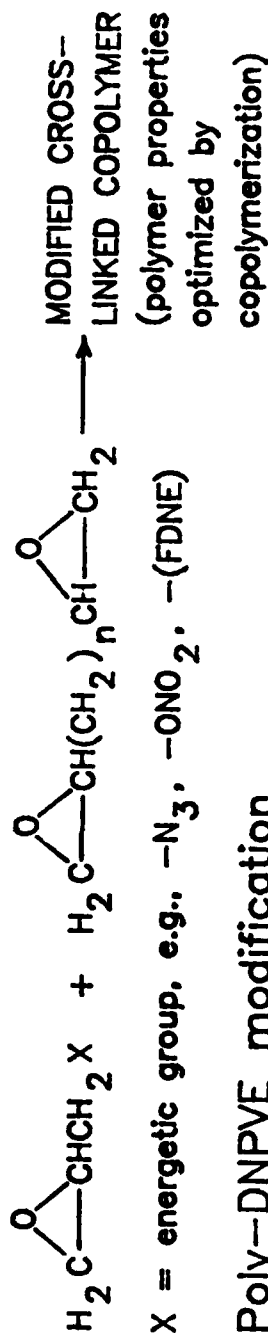
Task 3 addresses the polymerization of any new energetic monomer structures. Polymerization reactions will be conducted to characterize new energetic polymer structure, functionality, and physical properties. Urethane curing at various cure ratios will be conducted with promising new energetic prepolymers; then, mini-dogbones will be fabricated and evaluated to determine resultant mechanical properties.

Task 4 employs polymerization syntheses and techniques which provide structurally controlled polymer backbones for correlation investigations of structure and physical/mechanical properties. Unlike Task 1 which seeks to optimize the physical and mechanical properties of GAP, PGN, and poly-G via individual synthetic modification procedures, Task 4 seeks to modify only the energetic pendant substituent on an identically synthesized polymer backbone structure. Any differences in mechanical or physical properties of GAP, PGN, or poly-G samples will be caused solely by the $-N_3$, $-ONO_2$, or $-OCH_2C(NO_2)_2F$ groups themselves. Because of the ease with which a pendant triflate group could be displaced by energetic but weak nucleophiles (e.g. $-N_3$, $-ONO_2$, $-OFDNE$), a poly-glycidyl triflate ether polymer was synthesized. The isolated glycidyl triflate polymer afforded a number average molecular weight of 6100g/mole. Its synthesis so far is limited by low monomer yields. Reaction between glycidyl bromide and silvertriflate produced this monomer which was isolated and characterized by NMR, IR, and Mass Spectrometry. While yields are low to date, reaction between glycidyl bromide and silver triflate demonstrated the first triflate synthesis in which the reactant's epoxide bond was left intact. Other synthetic methods produce epoxide ring opening and destroy the glycidyl structure required for subsequent polymerization reactions.

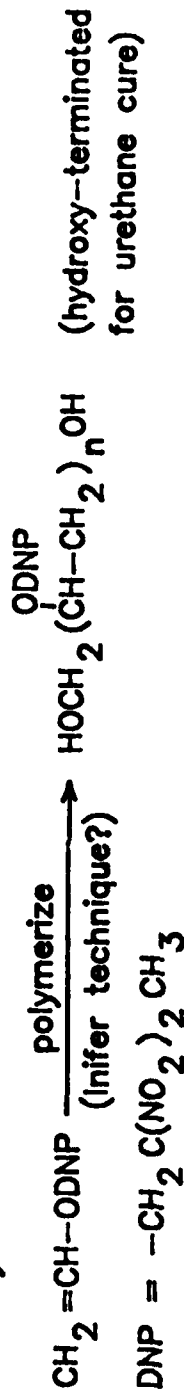
The overall goal of this project is two-fold: new improved energetic polymer/binder systems and systematic polymer structure/mechanical property correlation.

APPROACH

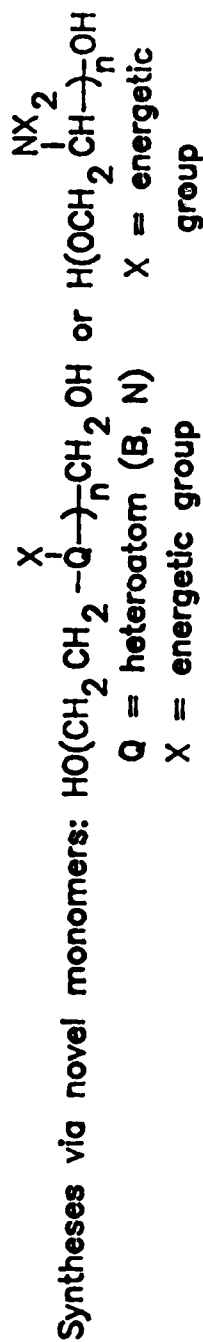
Task I: Glycidyl prepolymer chain extension/copolymerization



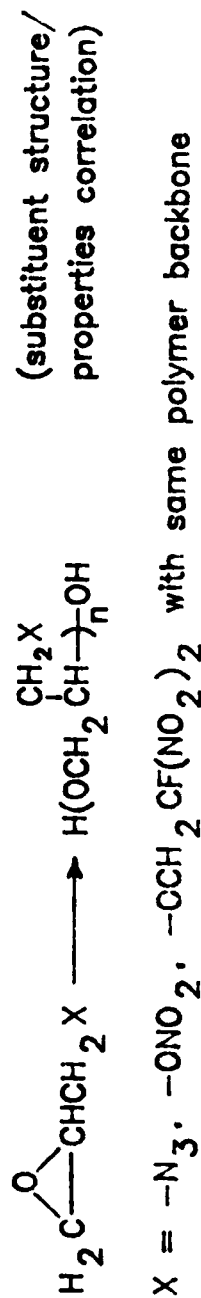
Task II: Poly-DNPVE modification



Task III: New energetic prepolymer structures

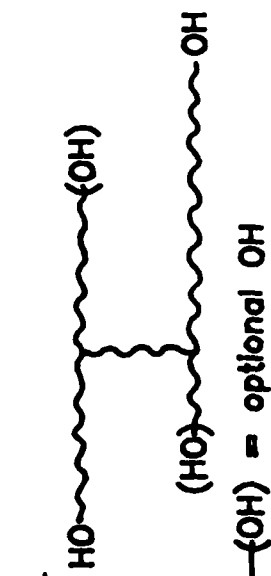


Task IV: Energetic prepolymer structure/properties correlation

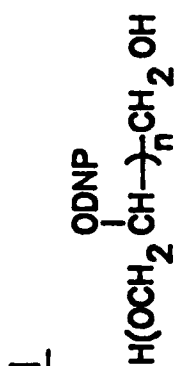


EXPECTED RESULTS

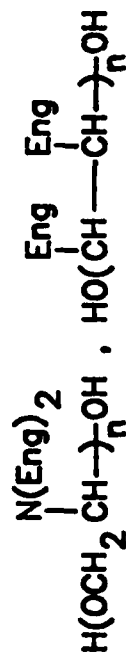
Task 1



Task II

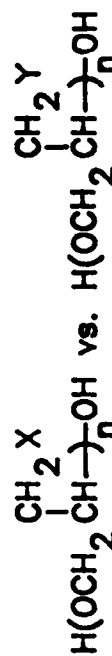


Task III



Eng = energetic substituent

Task IV



**Energetic crosslinked copolymers
with improved mechanical properties**

Thermally stable, nitramine-compatible energetic polymer for minimum smoke applications

**New energetic polymer structures/
improved energetics**

Predictable property variations from X vs. Y energetic substituent changes

PROPULSION RESEARCH GOALS

GENERAL GOALS: Research in support of rocket propulsion is directed at providing a fundamental basis for a new generation of propulsion concepts and improving the scientific understanding of phenomena associated with the generation of propulsive power. Research is needed from molecular to macroscopic scales in areas which include plasma acceleration, dynamics of rocket combustion, the behavior and synthesis of advanced energetic materials, characteristics of exhaust plume formation and radiation, and the dynamics of advanced propulsion concepts. Further knowledge is needed in these areas to meet mid-term and long-term Air Force technology goals related to improving performance, reliability, penetrability, and durability for Air Force mission applications involving space systems, ballistic missiles, and air launched missiles. However, specific provisions are also included for research directed toward scientific opportunities which cannot be related to particular mission areas at this time.

Future Air Force space missions for communications, surveillance, and weapons systems will require substantially higher power density and greatly improved propulsion for orbit raising. Research is expected to lead to improvements of 20% in propulsion efficiency with improved liquid and solid propellants and 100 to 400% with non-conventional systems such as electromagnetic plasma acceleration and energy beaming, magnetoplasmdynamics and nuclear power.

SPECIFIC GOALS:

The following topics summarize many of the current goals which are being addressed by the ongoing research programs.

Solid Propellant Mechanics To improve understanding of damage tolerant design for new materials. To investigate fatigue, damage propagation and detection, fracture, and effects of spectrum loading and sequencing. To extend the existing theories to three dimensions, including the interactions between viscoelastic behavior and damage, the micromechanics of propellant structure, and effects of temperature to obtain approaches that can predict propellant stress-strain behavior from relatively simple tests. To establish an age-life model based on chemical reactions. To establish the relationship between carbon/carbon material processing variables and the kinetics of reaction of these materials with gases representative of rocket exhausts.

Noninterfering Diagnostic Techniques To achieve sensors which will enable the adaptive control and autonomous operation of high performance propulsion systems. To achieve diagnostic techniques for measuring the gas and gas-particle flow properties representative of rocket systems including plumes. To devise diagnostic techniques to obtain rapid and quantitative spatially and temporally resolved measurements of temperature, pressure, velocity, species concentrations and densities, and particle/droplet size and distribution in optically dense, high-temperature reacting, unsteady, turbulent flowing media. To establish techniques for obtaining rate data for energetic material being heated in excess of 10^5 K/s.

Exhaust Plumes To provide mechanistic basis for analyzing, interpreting, and altering plume radiance. Establish the influence of composition and flow environment on particle formation and growth mechanisms. To verify and improve predictive models for nucleation and condensation in multi-component, multi-phase systems. To determine reaction pathways and to obtain chemical rate data for combustion chamber, nozzle, and exhaust plume flows. To improve and devise diagnostic methodology for determining the spatial and temporal distribution of important species so that rate processes can be measured. To determine the mechanism of exhaust plume ignition in the presence of flame suppression additives.

Solid Propellants and Energetic Materials To control the behavior of energetic materials during combustion. To establish relationships between molecular structure, decomposition and combustion processes. To synthesize energetic ingredients leading to tough, high energy propellants with desirable properties which include low glass-transition temperatures, high thermochemical stability temperatures, high solid loadings, and smokelessness. To improve techniques to determine polymer properties.

Combustion and Reacting Flows To understand important bond rupture and heat release mechanisms so that research to modify burning rate and combustion efficiency can be directed at specific reaction sites. To explore methods for obtaining the key reaction parameters for energetic materials being heated at rates in excess of 10^4 K/s. To determine the effects of acceleration-fields on propellant ballistics. To characterize the mechanisms leading to changes in solid propellant properties and burning modes that produce transition from normal deflagration to detonation of rocket motor grains. To increase the scope and usefulness of the JANAF Thermochemical Property Data.

Combustion Instability To improve analytical methods for interpreting, predicting, and avoiding instability behavior of solid motors through mechanistic understanding of contributions such as nozzle damping, acoustic erosivity, pressure coupling, vortex streaming, vortex shedding, distributed combustion, particle and structural damping, and high velocity effects. To account for the more significant effects of 2-D and 3-D geometries. To defeat combustion instability by purposely dissipating acoustic energy in prescribed modes. To examine more direct means of measuring acoustic admittance. To conduct verification of new combustion response measurement techniques. To investigate methodologies for measuring the unsteady velocity, pressure, and temperature components in multi-dimensional unsteady reacting flows. To visualize nonsteady, multi-phase flow and condensed-phase breakup for the purpose of understanding the role of transient processes or acoustic energy gains or losses. To determine and characterize acoustic energy gains and losses in terms of flow field parameters. To understand contributions of heterogeneous structures in composite propellants.

Metal Combustion To characterize the basic mechanisms and chemistry involved in the formation of metal oxide particulates. To experimentally determine physical and chemical processes leading to the acceleration of metal droplet ignition and combustion. To explore methods of greatly reducing the size of metal oxide agglomerates entering nozzle convergent sections. To improve methods for simultaneously measuring temperature and concentration of

turbulent flame zones of multi-phase media so that conditions leading to metal combustion under solid propellant ram-rocket conditions (particularly high altitude) can be characterized. To assess the role of fluorine in the combustion of fluorinated metallic propellants and to determine mechanisms that affect oxide particle size.

Beamed Energy To quantify mechanisms of laser energy transfer to working fluids, to assess the barriers to optical access for energy transmission, and to establish approaches to plasma confinement. To enable consideration of candidate short wavelength energy beams with hydrogen; to determine if other working fluids and fuels offer promise.

Solar Thermal Propulsion Establish the mechanisms of solar radiation energy absorption under the desired thruster conditions.

Electromagnetic Acceleration To understand magnetoplasma dynamic processes for the purposes of establishing the conditions of sustained high energy density operation and to project upper limits of power density. To establish the mechanism leading to extended electrode life. To extend operational time of electrode and contact surfaces. To produce stable magnetoplasma dynamic flows for sustained high energy density operation. To produce conditions that vaporize and disperse metallic fuels being considered for use in low Earth orbits. To overcome cooling limitations on electrical propulsion systems operating continuously at megawatts power levels. To realize more weight efficient and less vulnerable heat rejection concepts for electrodes, chambers, and nozzles.

Ultra-High Energy Density To decrease the losses in thermionic flows. To explore novel approaches to high energy density storage. To devise means of accommodating plasma temperatures greatly in excess of material limits.

1984 AFOSR/AFRPL ROCKET RESEARCH MEETING
AUTHORS - ABSTRACTS & PRESENTATIONS

ANDRUSHAK, J L	63
BAUM, J D	53
BECKSTAD, M W	5
BECKER, R	19
BEDFORD, C D	60
BENREUVEN, M	50
BLACKNER, A M	49
BRAITHWAITE, P C	5
BRANCH, M C	8
BRILL, T B	9
BROWN, R S	49
CAMPBELL, D	6
CASSADY, R J	35
CAVENY, L H	23
CHAPMAN, R D	63
CHASE, M W	24
CHUNG, T J	54
COHEN, N	25
COHEN, N S	52
COLLIDGE, M B	62
COWIES, L M	28
CRAIG, J E	17
DANIEL, B R	51
DUNLAP, R	49
EDWARDS, J T	6
ESKRIDGE, R H	32
EVERSOLE, J D	13
FLANAGAN, J E	57, 58
FONTIJN, A	14
FORWARD, R L	47
FRANCIS, G	3
FRANKEL, M B	55, 57, 58
FREDERICK, R A	15
FRY, R S	22
GLICK, R L	10
GLUMB, R J	31
GOSHGARIAN, B B	62
HAM, D O	28
HANSON, R K	41
HERRLINGER, S P	63
HOFFMAN, W P	1
HULSIZER, S C	6
JAGODA, J I	11
JONES, O C	44
KARPOWICZ, R J	9
KEEFER, D	26
KIM, C S	61
KING, M	21
KING, D Q	36
KIRSCHNER, M	34
KOLM, H	39
KOMAR, J J	22
KRIER, H	31

LAWLESS, J L	37
LEVINE, J N	53
LIU, CHI T	2
MARTINEZ-SANCHEZ, M	38
MATSON, J C	14
MAZUMDER, J	31
MCCAY, T D	32
MCVEY, J B	43
MEAD, F	48
MERKLE, C I	29, 30
MICCI, M M	42
MITTER, E	12
MONGEAU, P	39
MORSE, S D	64
MYRABO, L	46
NACK, K K	18
NETZER, D	20
OLSEN, D B	4
OSBORN, J R	15
OYUMI, Y	9
PRICE, E W	16
RAUN, R L	5
RODGERS, S L	62
ROSEN, D I	27, 28
SCHRADE, H O	34
SCHMIDT, W M	35
SCHMITT, R J	60
SEIPH, C C	33
SHACKELFORD, S A	62, 63, 64
SHREEVE, J M	59
SIGMAN, R K	16
STRAHLE, W	11
STRAND, L	52
SUMMERFIELD, M	50
TAPPER, M	45
TAYLOR, R F	7
TROGIER, W C	46
TURCHI, P	40
VANZANDI, D M	32
VONDRA, R J	35
WEAVER, D P	6
WEHR, J F	55
WESTBERG, K	25
WEYL, G M	27
WOOLERY, D O	57
YORK, T M	29, 30
ZINN, B T	51
ZMUDZINAS, J S	45

SPECIAL PRESENTATIONS AND OVERVIEWS:

HART, D	Tues PM
WEISS, R R	Tues PM
CAVENY, L H	Tues PM
BIGGERS, R A	Tues PM
ORAN, W and LABUS, T	Tues PM
MCCAY, T D	Wed AM
COCHRAN, T H and BYERS, D C	Thurs AM